Synthesis, Characterization and Properties Evaluation of Degradable Poly(vinyl-co-ester)s

Dissertation

Zur Erlangung des Doktorgrades

der Naturwissenschaften

(Dr. rer. nat)

dem Fachbereich Chemie

Der Philipps-Universität Marburg

vorgelegt von

Liqun Ren

aus Jilin V.R. China

Marburg/Lahn 2008

Vom Fachbereich Chemie

Der Philipps-Universität Marburg als Dissertation am 27.06.08 angenommen.

Erstgutachter PD Dr. Seema Agarwal

Zweitgutachter Prof. Dr. Andreas Greiner

Tag der mündlichen Prüfung am 20.08.08

Acknowledgement

First and foremost, I want to thank my direct supervisor PD Dr. Seema Agarwal for giving me this interesting topic. I would like to thank her unfailing encouragement, motivation and her belief in me from every aspect throughout the work. She has been actively interested in my work and has always been available to advise me. Without her support and guidance I could not have accomplished all in this period. I greatly appreciated her involvement and insight.

I would also like to thank Prof. Dr. Andreas Greiner for providing the lab space for my Ph.D. work. I greatly appreciate his kindness, support and many useful advices and suggestions during my work.

I am very grateful to all the members in our group for the friendly working atmosphere, the helpful discussions and the enthusiasm of involving me in every kind of activities in the group, even though I always travel to Karlsruhe at weekends. Three years staying in Germany with you have made me feel like at home. Here I have to especially thank my lab colleges: Johanna Otto, Rimpu Kumar and Yasser Asssem Elgamaly. I appreciate the cooperation in the lab, the understanding of different cultures between us and the friendship we have built up. Together with Anna Bier, Olga Dzenis, Priyanka Bansal and Thorsten Röcker, thanks very much for helping me correct my Ph.D. thesis.

I also especially owe many thanks to the members in our group, who have been helping me a lot with measurements during my PhD work.

Thanks first go to Marco Gensheimer, who gave me a lot of help on preparing bacterial suspension, showed me how to determine the antibacterial activity of the quaternary amonium polymers and helped me with IR measurement. I really appreciate his kindness and his comments during the work.

Thanks then go to Uwe Justus, Dr. Julia Getze and Norman Grabe for plenty of work with GPC measurements.

Thank Lisa Hamel for showing me handling several kinds of instruments. I also appreciate her work for the IR measurement.

Thank Katharina Kowalski for helping me with Contact Angle measurement and for the useful discussions on synthesis of monomers.

Thank our previous group member Dr. Markus Schackmann for solving the problem during DSC and TGA measurements.

Thanks also go to Martina Gerlach for helping me with DMA and Tensile Instron measurements for degradable ionomers.

I am very grateful to Shuiliang Chen in our group, together with Ping Hu in the group of Prof. Dr. Haoqing Hou in the Department of Macromolecular Chemistry of Jiangxi Normal University, for helping me with DMA measurements for ionomers.

I appreciate Dr. Michael Bognitzki and the previous group member Dr. Christian Krüger for giving me advices on monomer synthesis. Thanks for the useful discussions.

I would also like to thank the members in the group of Prof. Dr. Joachim Wendorff, who nicely helped me with spin coating of degradable cation containing polymers.

Thank the Central Analytic Department for the plenty of NMR measurements and elemental analysises. I would especially thank the previous member Dr.Oliver Happel in the group of Prof. Dr. Andreas Seubert for establishing the UV spectroscopic instrument for measuring LCST of thermo-sensitive degradable polymers.

Thank Michael Hellwig and Dr. Andreas Schaper for the measurement with Electron Microscopy.

I would also like to thank Prof. Dr. Thomas Kissel and Regina Reul in the Department of Pharmaceutics at the Philipps-University Marburg for their cooperation on determining the toxicities of the polymers.

Thanks also go to Dr. Dieter Schollmeyer in the Department of Inorganic Chemistry at University Mainz for the immediate response and plenty of ASXS measurements of ionomers without delay.

I had the pleasure to supervise and work with several students who did their “Vertiefung” work in my project and have been beneficial for the presented work in this thesis.

Finally, I owe special gratitude to my husband Wesley Wanyin Cui and my parents for continuous and unconditional support. The happiest thing happened in Germany has been getting to know Wesley and marrying him. Thanks so much for his understanding and his love.

Contents

1. Introduction and the aim of the work

One novel way to synthesize degradable polyesters is the ring-opening polymerization of cyclic ketene acetals（CKA）, which has been of great interest since 1980s.[1,2,3,4,5] Cyclic ketene acetals, due to their structure, can be polymerized by either radical[6] or cationic[7] polymerization. The tendency of ring-opening of CKAs depends greatly on the ring sizes, the substitutes on the ring and the temperature.[8] Comparing to the cationic polymerization, radical polymerization easily leads to ring-opening due to the relatively low activation energy of isomerization of cyclic free radicals. The resulting polyesters can be degradaded by hydrolysis to oligomers and later on by micro-organism metabolism.

It is, therefore, possible to bring degradability to non-degradable vinyl polymers just by ring-opening radical, cationic copolymerization of cyclic ketene acetals and vinyl monomers.[9] Vinyl monomers can provide other mechanical, optical, electrical or other functionalities. The resulting poly (ester-co-vinyl)s are therefore a class of new materials combining degradability and other interesting properties. The problem is just the low polymerization reactivity compared to many other vinyl monomers, which leads to homovinylpolymers with no ester linkage incorporated in the chain. Proper vinyl monomers and the mechanisms of copolymerization need to be found out. The structure-property correlation needs to be built up. Evaluation and improvement of the properties are also important for utilizing the new materials.

The aim of my work is to provide basic understanding of polymerization behavior of cyclic ketene acetals with different vinyl monomers and their properties evaluation.

First, functional degradable poly(ester-co-NIPAAm) is synthesized by free radical copolymerization. The copolymerization behavior is intensively analyzed. The resulting polymers are found to be hydrolytic degradable and thermal sensitive leading to a solution-suspension transition in water.

Second, the strong reactivity of cyclic ketene acetals with Brönsted acids is intensively investigated, which provides important data for synthesis, cationic polymerization of cyclic ketene acetals and their copolymerization behavior with vinyl acids.

Third, ion containing degradable polymers, including ionomers and polyelectrolytes, are synthesized by free radical polymerization and subsequent quaternization of amine in the chain. The resulting polymers obtain a variety of new properties, which can be easily tuned by changing the copolymer compositions and quaternization behaviors. Microstructures are intensively investigated by NMR, SAXA, TEM and DMA to establish the relationship between morphology and property.

2. Background

2.1. Degradable polymers

Polymers have been intensively investigated since the 1920s. The market has been booming very fast and increasing every year. Until 2003 the annual amount of plastic products of the world has been more than 200 million tons. However, most of the synthetic polymers are durable and resistant to various forms of degradation. Since 1980s an environmental concern of the so called "landfill crisis" has trigged countries and organizations to develop and engineer new degradable plastics as substitutes to eliminate the environmental crisis. Nowadays, research in the field of degradable polymers has been focused not only on plastic commodities to solve the landfill problem but also on therapeutic and biomedical uses, like drug delivery[10], tissue engineering[11, 12], and other applications[13].

2.1.1. Definition and standards for characterization

There have been several confusions and conflictions on definition of degradable polymers. The American Society for Testing and Materials (ASTM) has undertaken the development of standards, including classifications, guides, practices, test methods, terminologies, and specifications, in the area of degradable plastics.[14] According to ASTM standards, degradable polymer is polymer designed to undergo a significant change in its chemical structure under specific environmental conditions, resulting in a loss of some properties (e.g. integrity, molecular weight, structure or mechanical strength), that may vary in a period of time as measured by standard test methods appropriate to the plastic and the application.

According to the different kinds of environmental conditions, degradable plastic was further defined as (1) oxidatively degradable plastic, in which the degradation results from oxidation;[15]
(2) photodegradable plastic, in which the degradation results from the action of natural daylight;[16]
(3) hydrolytically degradable plastic, in which the degradation results from hydrolysis;[17]
(4) biodegradable plastic, in which the degradation results from the action of naturally-occurring micro-organisms such as bacteria, fungi and algae;[18]
(5) compostable plastic that undergoes degradation by biological processes during composting to yield carbon dioxide, water, inorganic compounds, and biomass at a rate consistent with other

known, compostable materials and leaves no visually distinguishable or toxic residue.[19] The definition of compostable plastic is explicit; it demands satisfactory biodegradation and must be completely safe in the environment. ASTM standard D6400-04 established specifications for plastics to be labeled compostable in the industries.

2.1.2. Degradation mechanisms

Due to the C-C backbone, most of the synthetic polymers are durable and resistant to various kinds of degradation. However, polymers containing heteroatomatic functional groups like ester, carbonate, anhydride, acetal, amide, phosphazene or hydroxyl-esters in the backbones are susceptible to hydrolysis or micro-organisms attack and confer (bio)degradability.[20,21,22,23,24,25]

The first stage of degradation is an enzymatic or a non-enzymatic hydrolysis to oligomers or even small molecules with functional groups, like carbonylic acid, or alcohol for polyesters.[26] Since it is difficult for a relatively big enzyme to diffuse into the depth of solid substrates, enzymatic hydrolysis occurs only on the surface of the solid and starts from the amorphous or relatively less-ordered area instead of the more rigid crystalline interior. After the surface has been hydrolyzed, the resulting small molecules will be washed away by water, and enzyme can attack another new layer. Therefore, the molecular weight of the substrate does not change theoretically, only the loss of weight of solid could be observed. Non-enzymatic (basic or acidic) hydrolysis also starts from the surface and prefers amorphous area. However, small basic or acidic reagent can diffuse into the solid substrate and lead to in-depth degradation. Therefore, the molecular weight of the material decreases, but the total weight of solid can not be detected very fast. The hydrolytic rate is dependent on the pH condition, the type of enzymes and the polymer structures. For a complete biodegradability it requires a second stage of degradation: metabolisation of the resulting small molecules by micro-organisms into CO_2, water and biomass.

There are some of degradable synthetic polymers with C-C backbones, like poly(vinyl alcohol)[27,28,29] and poly(vinyl methyl ether).[30,31,32] In general they contain function pendent groups in the chains, which can undergo (photo, thermo or enzymatic) oxidation and the resulting product can react further to oligomers or even small molecules (Scheme 2.1 and Scheme 2.2).

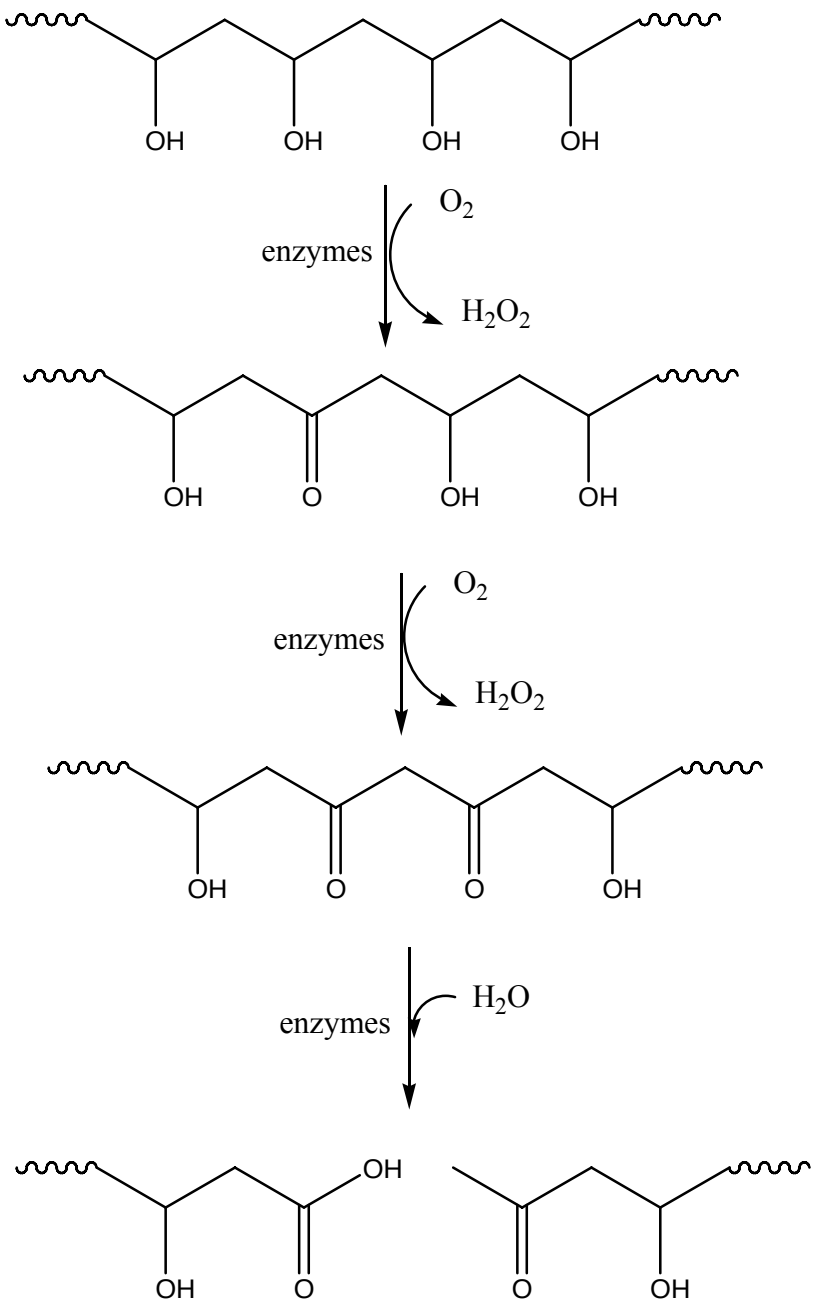

Scheme 2.1. Enzymatic degradation of poly(vinylalcohol).[28]

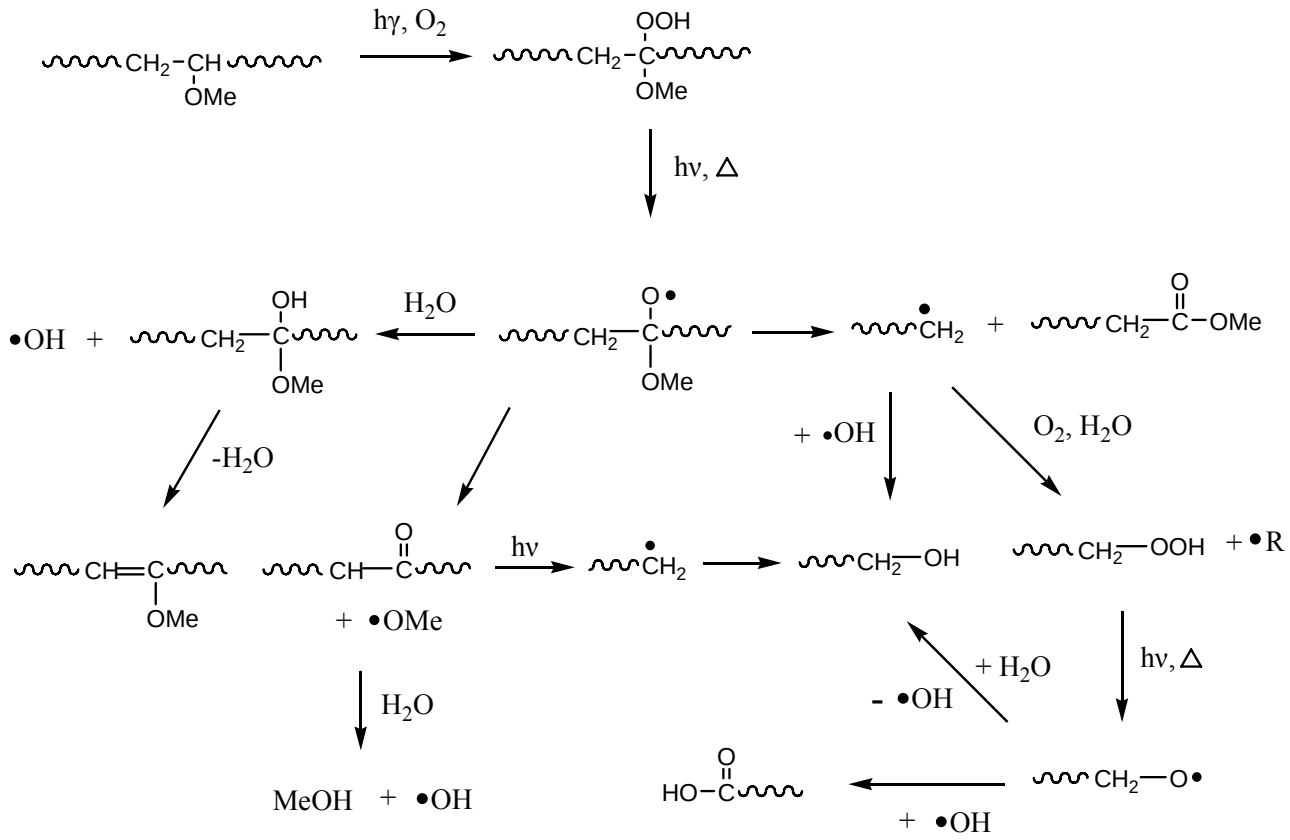

Scheme 2.2. Photooxidation mechanism of poly(vinyl methyl ether).[32]

2.2. Biodegradable Polyesters

Compared to starch based naturally occurring polymers, aliphatic polyesters are one of the promising biodegradable materials for industrial and biomedical uses with relative good mechanical properties and processability. A wide range of aliphatic polyesters can be designed by changing the synthesis recipe (like copolymerization) and synthesis conditions to meet specific requirements such as hydrophobicity, crystallinity, degradability, solubility, glass transition temperature, melting temperature, etc. Commercially available degradable polyester found their applications as flexible and tough thermoplastics. Enzymes like Lipases and PHA depolymerases cleave the ester bond of aliphatic polyesters.

2.2.1. Classification of degradable polyesters

According to the type of constituent monomers, aliphatic polyesters can be classified into two types. One type is polyhydroxyalkonate, a polymer of hydroxyl acid (OH–R–COOH). Furthermore,

hydroxyl acids can be divided into α-, β-, ω-hydroxyl acid, etc., depending on the position of OH group to the COOH group. The other type is poly(alkylene dicarboxylate), which is synthesized by the polycondensation reaction of diols (HO–R_1–OH) and diacids (HOOC–R_2–COOH). Four types of aliphatic polyesters with commercially available products are listed in Table 2.1.

Table 2.1. Classification of aliphatic polyesters[33]

Chemical structure	Biodegradability	Examples (trade mark / producer)	
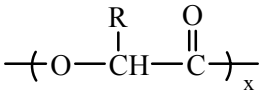	Chemical Hydrolysis	R = H	Poly(glycolic acid) (PGA)
		R = CH_3	Poly(L-lactic acid) (PLLA) EcoPLA/Cargill Lacea/Mitsui Toatsu Chemicals Lacty/Shimadzu
Poly(α-hydroxy acid)			
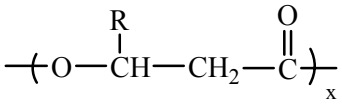	Enzymatic Hydrolysis	R = CH_3	Poly(ß-hydroxybutyrate) (PHB)
		R = CH_3, C_2H_5	Poly(ß-hydroxybutyrate-co-ß-hydroxyvalerate) (PHBV) Biopol/Zeneca
Poly(ß-hydroxyalkanoate)			
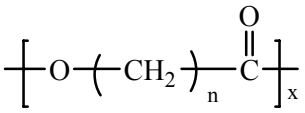	Enzymatic Hydrolysis	n = 3	Poly(ß-propilactone) (PPL)
		n = 5	Poly(ε-caprolactone) (PCL) Tone/Union Carbide Placcel/Daicel Chemical Industries
Poly(ω-hydroxyalkanoate)			
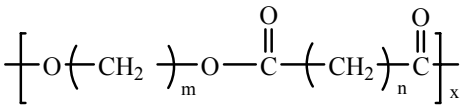	Enzymatic hydrolysis	m = 2, n = 2	Poly(ethylene succinate) (PES)
		m = 4, n = 2	Poly(butylene succinate) (PBS)
		m = 4, n = 2, 4	Poly(butylene succinate-co-butylene adipate) (PBSA) Bionolle/Showa Highpolymer
Poly(alkylene dicarboxylate)			

2.2.2. Synthetic routes for polyesters

One method to synthesize aliphatic polyesters is by condensation polymerization of hydroxyl acids (OH–R–COOH) or diols (OH–R_1–OH) and diacids (COOH–R_2–COOH) as mentioned in Chapter 2.2.1. Another conventional route is by ring-opening polymerization of cyclic esters and related compounds using a catalyst like stannous octanoate in the presence of an initiator that contains an active hydrogen atom (Scheme 2.3). Compared to condensation polymerization, ring-opening polymerization (ROP) is favored at relatively low temperature and short reaction time to get polyesters with high molecular weights.[34] In Table 2.2, the glass transition temperatures and the

melting points are listed for the most common aliphatic polyesters, which were synthesized by ring-opening polymerization (ROP) of cyclic esters.

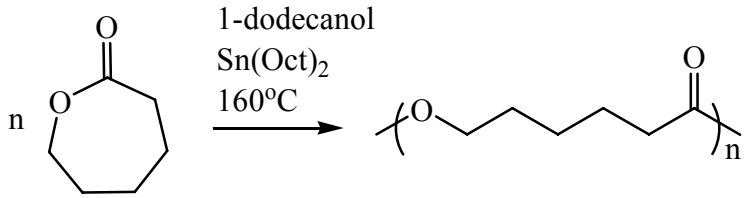

Scheme 2.3. Ring-opening polymerization of cyclic esters to synthesize poly(caprolactone) (PCL).

Table 2.2. Properties of the most common aliphatic polyesters synthesized by ROP[35]

Monomer	Polymer	T_g (°C)	T_m (°C)
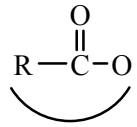	Polylactone Poly(ω-hydroxy acid)		
R = -$(CH_2)_2$-βPL, β-propiolactione	PβPL	-24	93
R = –$(CH_2)_3$–γBL, γ-butyrolactone	PγBL	-59	65
R = –$(CH_2)_4$–δVL, δ-valerolactone	PδVL	-63	60
R = –$(CH_2)_5$–εCL, ε-caprolactone	PεCL	-60	65
R = –$(CH_2)_2$–O–$(CH_2)_2$–DXO, 1,5-dioxepan-2-one	PDXO	-36	—
R = –$(CH_2$–$CH(CH_3))$– βBL, β-butyrolactone	PβBL isotactic	5	180
	PβBL actatic	-2	—
R = –$(C(CH_3)_2$–$CH_2)$–PVL, pivalolactione	PPVL	-10	245
R = –CH_2–$CH(CO_2C_7H_7)$– βMLABz, bezyl β-malolactonate	P(R,S)MLABz	25	—
	P(R)MLABz	20-25	150
	P(S)MLABz		
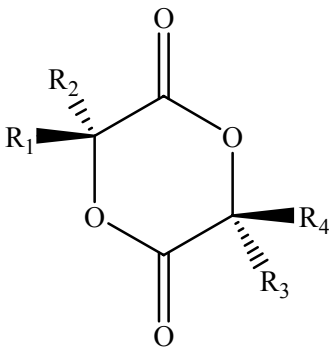	Poly(α -hydroxyacid)		
$R_1 = R_2 = R_3 = R_4$ = H GA, glycolide	PGA	34	225
$R_1 = R_4 = CH_3$, $R_2 = R_3$ = H, L,L-LA, L,L-lactide	PL,L-LA	55-60	170-190
$R_1 = R_4$ = H, $R_2 = R_3 = CH_3$, D,D-LA, D,D-lactide	PD,D-LA	55-60	170-190
$R_1 = R_3 = CH_3$, $R_2 = R_4$ = H meso-LA, meso-lactide	PmesoLA	45-50	—
D,D-LA/L,L-LA (50-50) D,L-LA, (D,L) racemic lactide	PDLLA	45-50	—

An alternative synthesis route is radical ring-opening polymerization of cyclic ketene acetals, which will be discussed in Chapter 2.3.

2.2.3. Effect of molecular structure on biodegradation

Both of the primary structure, including chemical bond, functional groups, hydrophilic-hydrophobic balance, side chain, cross-linking and degree of polymerization and etc. and the high-ordered structure, including orientation and crystallinity, affect the rate of enzyme degradation.

In order to be degraded by an enzyme, the polymer chain must be flexible enough to fit into the active site of the enzyme. Tokiwa and Suzuki found out that the flexible aliphatic polyesters were degraded by lipases, whereas heterocyclic ones were limited to be degraded and rigid aromatic polyesters are hardly degraded by lipases.[36] Among aliphatic polyesters it is generally accepted that balanced hydrophobicity and hydrophilicity in the polymer structure helps enzymatic degradations of various synthetic polymers.[37,38,39] The polymers derived from C6 and C8 alkane diols were reported more degradable than the more hydrophilic polymers derived from C2 and C4 alkane diols or the more hydrophobic polymers derived from C10 and C12 alkane diols. Molecular weight and polydispersity do not influence biodegradability, claimed by Mochizuki and Hirami. However, Doi and coworkers found out that the number of lipases capable of hydrolyzing the respective PHA sample decreases as the degree of polymerization increases.[40]

Crystallinity is the most important factor of solid state morphology that affects the rate of degradation of solid polymers such as fibers or films. Both enzymatic and non-enzymatic degradations proceed more easily with amorphous or less ordered regions, which allow enzymes or small non-enzymatic catalysts and reagents to defuse into the substrates, than the rigid crystalline regions, although the crystallites are eventually degraded from the edges inward.[41] Enzymatic degradation occurs only on the surface of the solid, whereas small non-enzymatic catalysts can rather easily diffuse into polymer system and result in an in-depth degradation. In the study of enzymatic degradation of films made from butylene succinate – ethylene succinate copolymer, Mochizuki and Hirami claimed that the dependence of degradation rate on polymeric compositions is ascribed to the degree of crystallinity rather than to the primary structure.[42] Crystalline aliphatic polyesters having a lower melting point were generally more susceptible to biodegradation than those having a higher melting point.[43]

In recent years it was shown that synthetic copolyester with proper amount of aromatic constituents also obtain biodegradability, demonstrated by Witt et al. in 1995.[44,45,46,47] Terephthalic acid ($COOHC_6H_4COOH$), adipic acid ($COOHC_4H_8COOH$) and butanediol (OHC_4H_8OH) were condense -polymerized to produce degradable copolyester with favorable use properties. The polymer structure is shown in Fig 2.1. The degradability decreases as the amount of aromatic constituent increases. Polymers with 22mol% of terephtalic acid were shown to completely degrade to monomers in 30 days incubated in the micro-organism actinomycete T. fusca.[26]

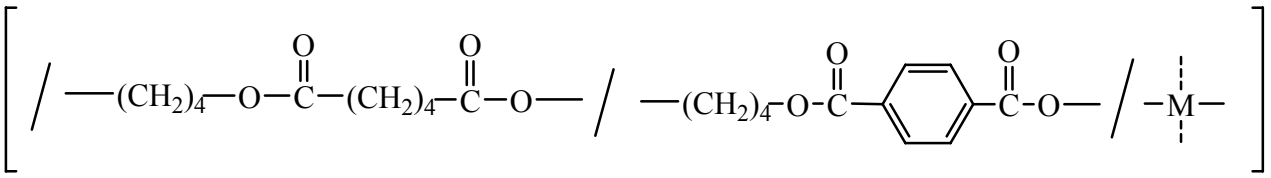

Fig 2.1. Primary structure of biodegradable copolyester with aromatic constituents.

2.3. Cyclic ketene acetals

Free radical ring-opening polymerization was first investigated in the group of Bailey in 1970s.[48,49] Cyclic ketene acetals (Fig 2.2) were found to be potential monomers to form degradable ester linkages after polymerization reactions. Since then cyclic ketene acetals became more and more interesting because of their possibility of copolymerization with vinyl monomers to introduce degradability into the non-degradable vinyl backbones.

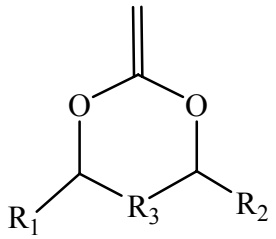

R_1, R_2, R_3 :

hydrogen, alkyl or phenyl substituents, can differ from each other

Fig 2.2. Structure of cyclic ketene acetals.

2.3.1. Synthesis of cyclic ketene acetals

In 1940s, preparation of cyclic ketene acetals was first studied by Mc Elyain and Curry.[50] The cyclic ketene acetals (IV) , were obtained by the dehydrohalogenation of the corresponding halogenated cyclic acetals (III) by potassium t-butoxide in t-butyl alcohol. The compounds (III), with the exception of the chloral cyclic acetals, were prepared by an alcohol exchange between the glycol and the methyl (or ethyl) acetals (II) (Scheme 2.4a). It was found advantageous to prepare some ethylene glycol acetals from the methyl rather than the ethyl acetals (II) because of the proximity of the boiling points of the ethyl acetals to those of the cyclic acetals (III, n is 2). The trimethylene glycol acetals, because of their higher boiling points, could be prepared from either the methyl or ethyl acetals. Chloral diethyl acetals did not undergo this type of alcohol exchange; instead higher boiling products were obtained, which appeared to have the structures $CCl_3CH(OC_2H_6)OCH_2CH_2OH$ and $CCl_3CH(OCH_2CH_2OH)_2$. The acetals of chloral, corresponding to (III), were prepared directly from the aldehyde (I) and the glycols (Scheme 2.4b).

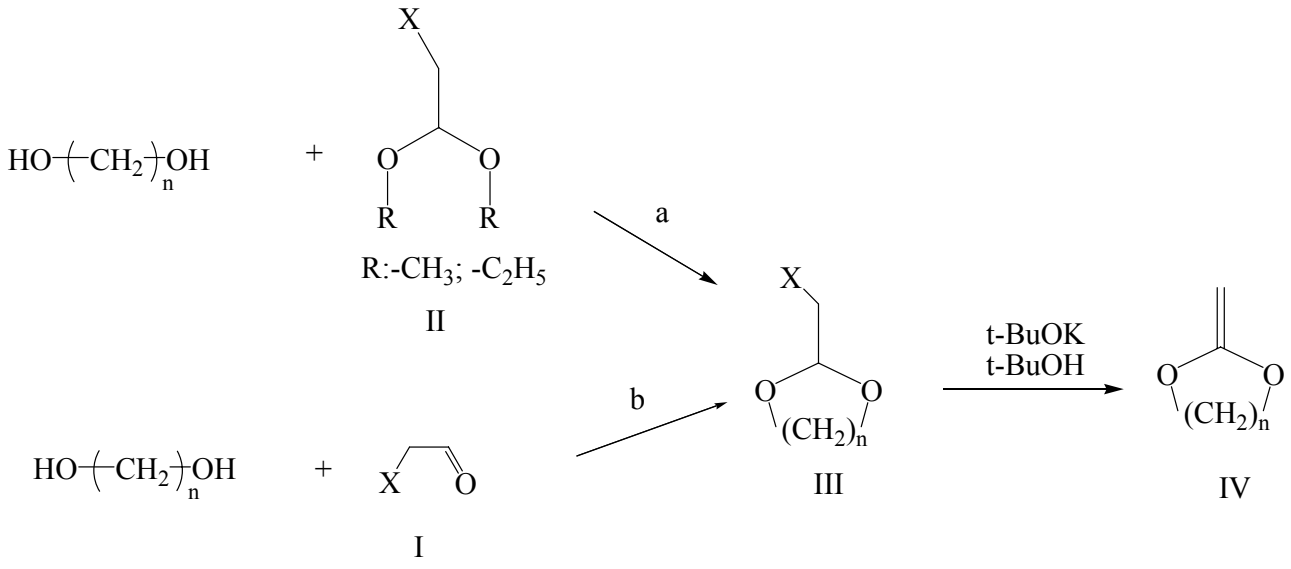

Scheme 2.4. Synthesis of cyclic ketene acetals.[52]

The striking property of synthesized cyclic ketene acetals, especially for those without substituents on the cyclic ring, is their tendency to undergo spontaneous polymerization during isolation and their sensitivity to water, alcohols and acids. It was also claimed by several scientists that when these acetals reacted with water, they are converted to the hydroxyalkyl esters (II, Scheme 2.5), probably via the intermediate ortho acid-ester (I, Scheme 2.5), or the reaction of cyclic ketene acetals with an alcohol produces the stable ortho ester (III, Scheme 2.5). With the exception of

2-methylene-l,3-dioxoane, when treated with hydrogen chloride, the ketene cyclic acetals react with this acid to yield the chloroalkyl esters (IV, Scheme 2.5). However no detail data could be provided due to the lack of the modern analytic techniques.

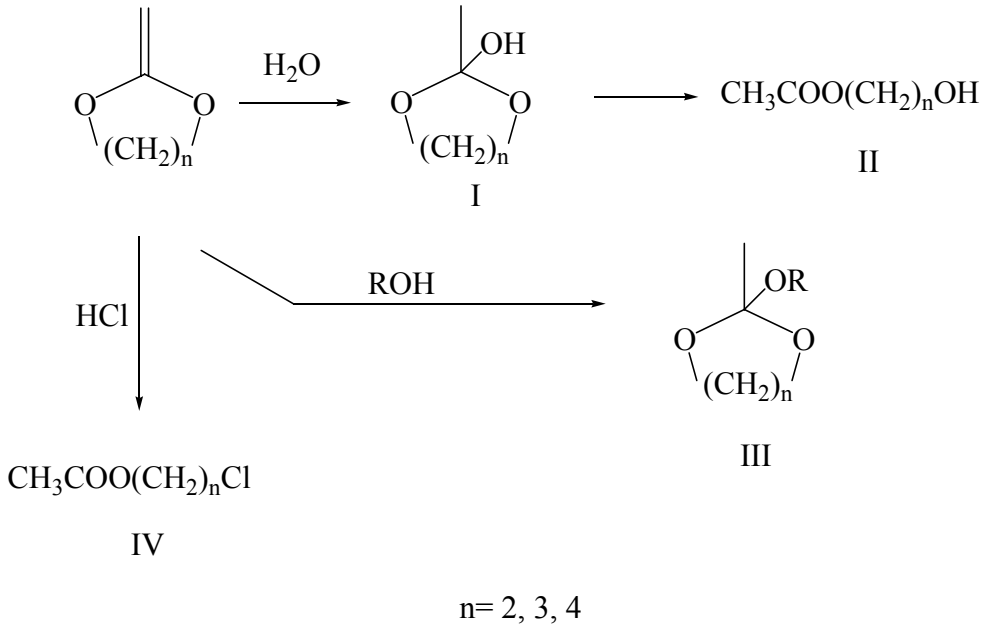

Scheme 2.5. Reaction of cyclic ketene acetals with water, alcohol or acid.[52]

Since 1980s, Bailey and his coworkers synthesized and purified a wide range of cyclic ketene acetals for radical ring-opening polymerization.[1, 2] It has been shown that 7-membered ring cyclic ketene acetals are more stable in water and acid than 5-membered ring cyclic ketene acetals. Besides, phenyl or alkyl substituents to the carbon next to the acetal group on the cyclic ring (R_1 and R_2 in Fig 2.2) can relatively stabilize cyclic ketene acetals in water and alcohols. Thus, only normal precautions should be taken to avoid acid when handling them.

2.3.2. Polymerization of cyclic ketene acetals

Radical ring-opening polymerization

Radical ring-opening polymerization of cyclic ketene acetals was first intensively studied by Bailey in 1980s.[6] For cyclic ketene acetals, there are three possible routes to undergo radical polymerizations. One is ring-opening polymerization after the isomerization of the radical (Scheme 2.6, route a_1 and a_2 if R_1 and R_2 are different) to form polyesters; another is direct vinyl addition to form vinyl polymers with ring formic substituents (Scheme 2.6, route b); the last is a mixture of the

two polymers. (Scheme 2.6, route c) The extent of ring opening of cyclic ketene acetals depends on the ring size, the substituents on the ring,[51] polymerization temperature[52] and other conditions. Voluminous substituents inhibit or prevent the polymerization.[53]

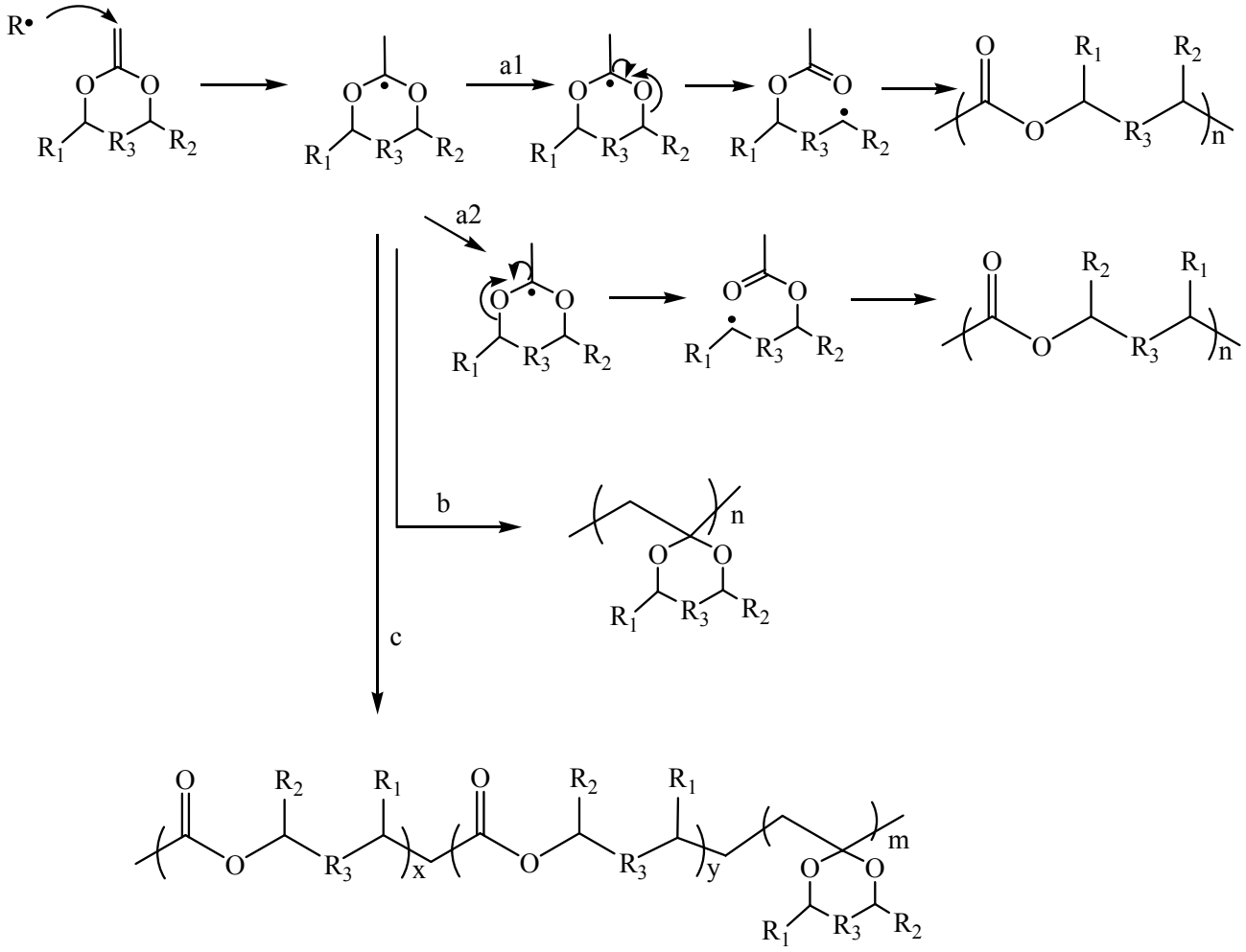

Scheme 2.6. Possible radical polymerization behaviors of cyclic ketene acetals.

Bulk radical polymerization of a 5-membered ring cyclic ketene acetal with benzyl as substituents: 2-methylene-4-benzyl-1,3-dioxelane, whereby 2-5 mol% AIBN or DtBp as initiator, underwent 100% ring-opening after isomerisation at temperatures from 60-120^{o}C and nearly complete region-selective ring-opening; which generates the more stable secondary benzyl free radical (Scheme 2.7a). The structures of the polymers were established by elemental analysis and 1D ^{1}H and ^{13}C-NMR techniques.

Superior to 5-membered ring, 7-membered ring cyclic ketene acetals and those with substituents, like 2-methylene-1,3-dioxepane（MDO）(Fig 2.3A) or 5,6-Benzo-2-methylen1e-1,3-dioxepane

(BMDO) (Fig 2.3B) were found to undergo 100% of ring-opening polymerization. The increased stability of the ring-opened radical and the increase in steric hindrance to direct non-ring-opened vinyl polymerization are believed to promote the extent of free radical ring opening during polymerization.

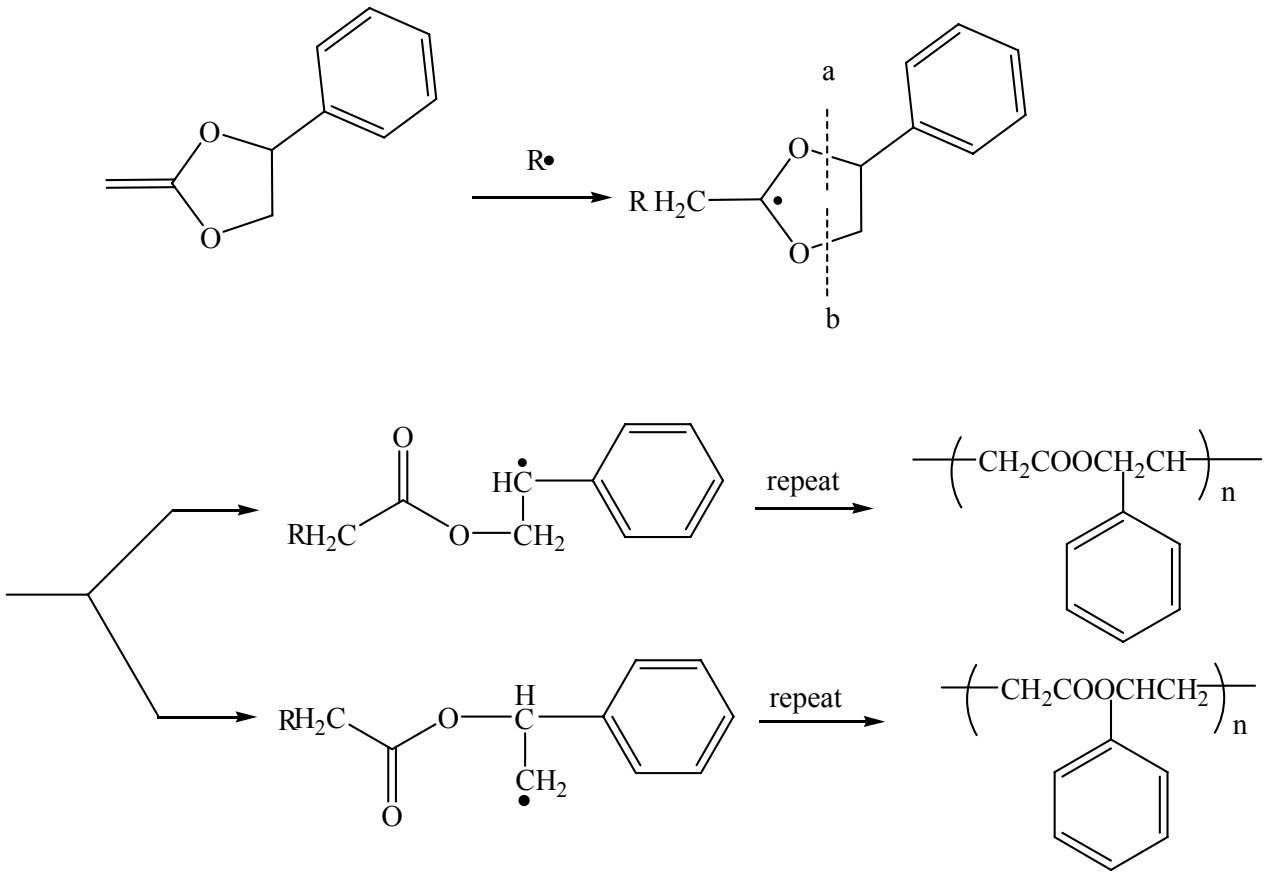

Scheme 2.7. Radical region-selective ring-opening polymerization of 2-methylene-4-benzyl-1, 3-dioxelane.[2]

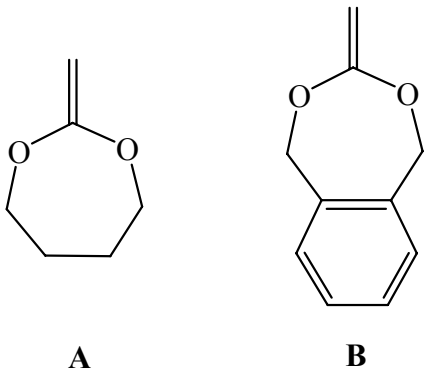

A **B**

Fig 2.3. Structure of 2-methylene-1, 3-dioxepane (MDO) and 5, 6-benzo-2-methylene-1, 3-dioxepane (BMDO).

E. Klemm and T. Schulze reviewed some of the most common classes of mono-cyclic and hetero-cyclic ketene acetals and claimed that a monomer has to meet certain structural preconditions that make them suitable for isomerisation. The combination of strain release due to ring-opening isomerization, an energy decrease in the transition state caused by the formation of carbonyl-functionalities and an appropriate stabilization of the growing chain end by steric and electronic effects may lead to clear ring-opening mechanisms.[8]

One problem of radical polymerization of cyclic ketene acetal is the slow polymerization rate and low molecular weight of the resulting polymers. It is difficult to get polyester with high molecular weight and high conversion in an appropriate reaction time. The rate of isomerization, or ring-opening process, requires energy and proceeds very slowly. This leads to a slow overall polymerization rate and much more risk of termination. It is especially true when the reaction proceeds more than 30%; the reduced active initiator concentration and the reduced monomer concentration make the initiation and propagation difficult, leading to termination.

Copolymerization behavior of cyclic ketene acetals and other vinyl monomers was first studied by Bailey and his coworkers to introduce degradability to non-degradable vinyl backbones.[52,54] It was demonstrated that many of cyclic ketene acetals still undergo 100% ring-opening when copolymerized with other vinyl monomers. However, the main feature during the copolymerization is the huge reactivity difference between the CKA and the most common vinyl monomers leading to either low molecular weight homo vinyl polymers without ester linkages or copolymers incorporating only low amounts of the comonomers with block structure.[55,56,57,58,59,60]

Among seven-membered ring cyclic ketene acetals, 2-methylene-1,3-dioxapane (MDO) (Fig 2.3A) and its analogue 5,6-Benzo-2-methylene-1,3-dioxepane (BMDO) (Fig 2.3B) are intensively investigated since 100% ring-opening polymerization of MDO is supposed to generate the same structure as biodegradable and biocompatible poly(caprolactone) (PCL), which has been widely used as biomedical material. With the help of 2D Heteronuclear Multiple Quantum Coherence (HMQC) and Heteronuclear Multiple Bond Coherence (HMBC) NMR and other techniques, it was found by Agarwal et al. and other scientists that primary radicals are very reactive and are likely to undergo intramolecular hydrogen transfer (backbiting) to form more stable radicals

(Scheme 2.8) to generate branched poly(caprolactone).[51,61]

Poly(MDO) synthesized by radical ring-opening polymerization of cyclic ketene acetal is semicrystalline. Due to the branches, degree of crystallinity is lower and the range of melting point is broader than high molecular weight poly(caprolactone), which is a tough and semi-rigid material at room temperature having a modulus between those of low-density and high-density polyethylene, synthesized from cyclic ester.

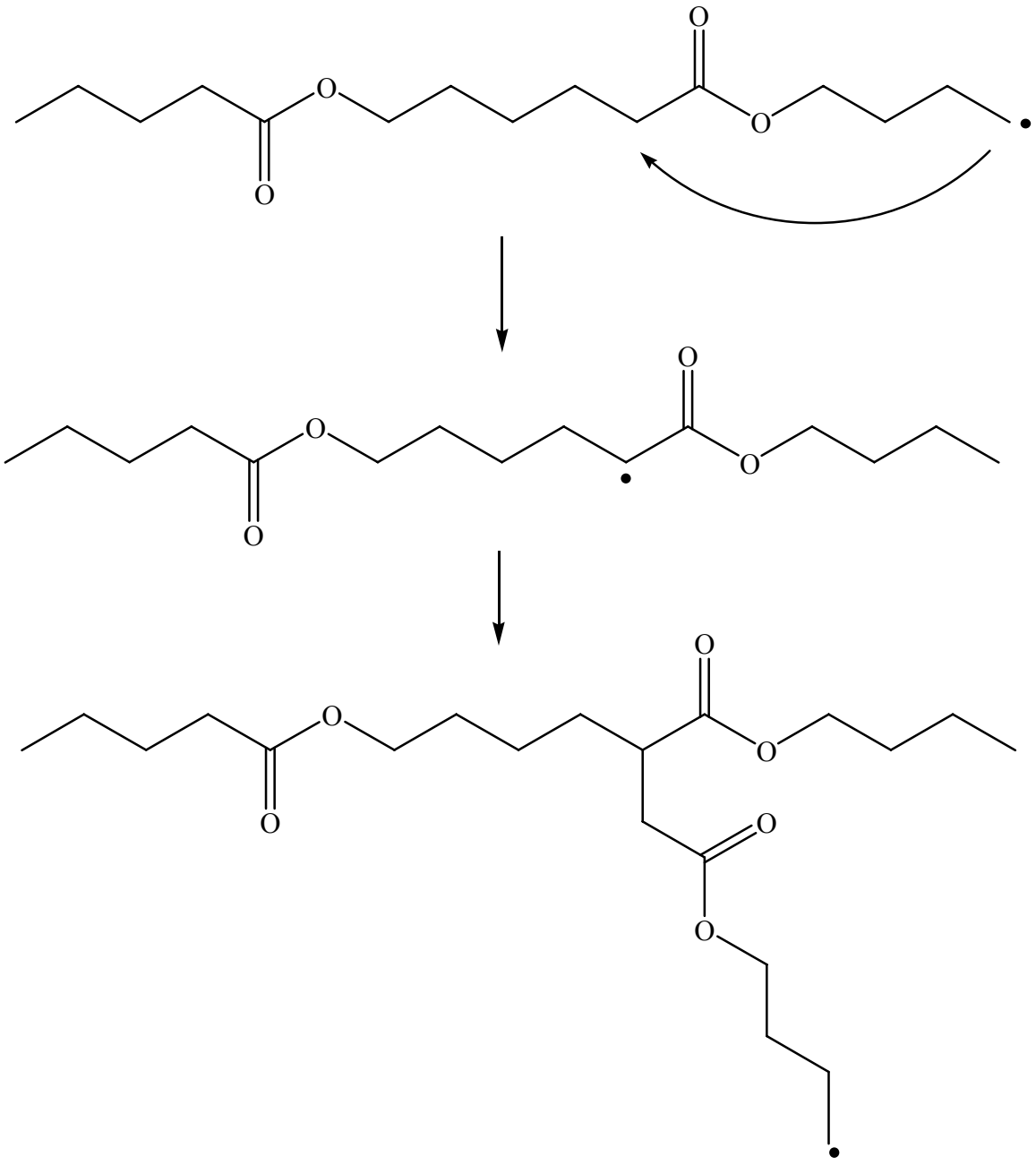

Scheme 2.8. Backbiting reaction during polymerization of MDO.[69]

In recent years, besides the conventional free radical random copolymerization, controlled free radical copolymerization, like atom transfer radical polymerization (ATRP) and reversible addition–fragmentation chain transfer (RAFT) of cyclic ketene acetal and vinyl monomers (like MMA[62] and St[9]) was investigated.

Cationic polymerization

Cyclic ketene acetals (CKAs) are extremely electron-rich vinyl monomers with a polar double bond. They become dioxonium ions when the nucleophilic exo-methylene group is protonated or reacted with an electrophile. Therefore, cyclic ketene acetals are potential monomers for cationic polymerizations. Similar to radical polymerization, cationic polymerization can proceed by three pathways (Scheme 2.9): 1,2-vinyl addition polymerization (route a), ring-opening polymerization (ROP) (route b) or a mixture of both (route c).

In route a, the propagating ring-dioxonium cation is attacked at the sp^2-hybridized carbon by the exo-methylene carbon of another monomer and a new ring-dioxonium is formed. Via 1,2-vinyl addition, poly(cyclic acetal) is obtained. In route b, the propagating ring-dioxonium cation undergoes isomerization via ring-opening and forms an ester linkage and a primary cationic polyion. The new cation then adds to another monomer. Polyester is produced by this way.

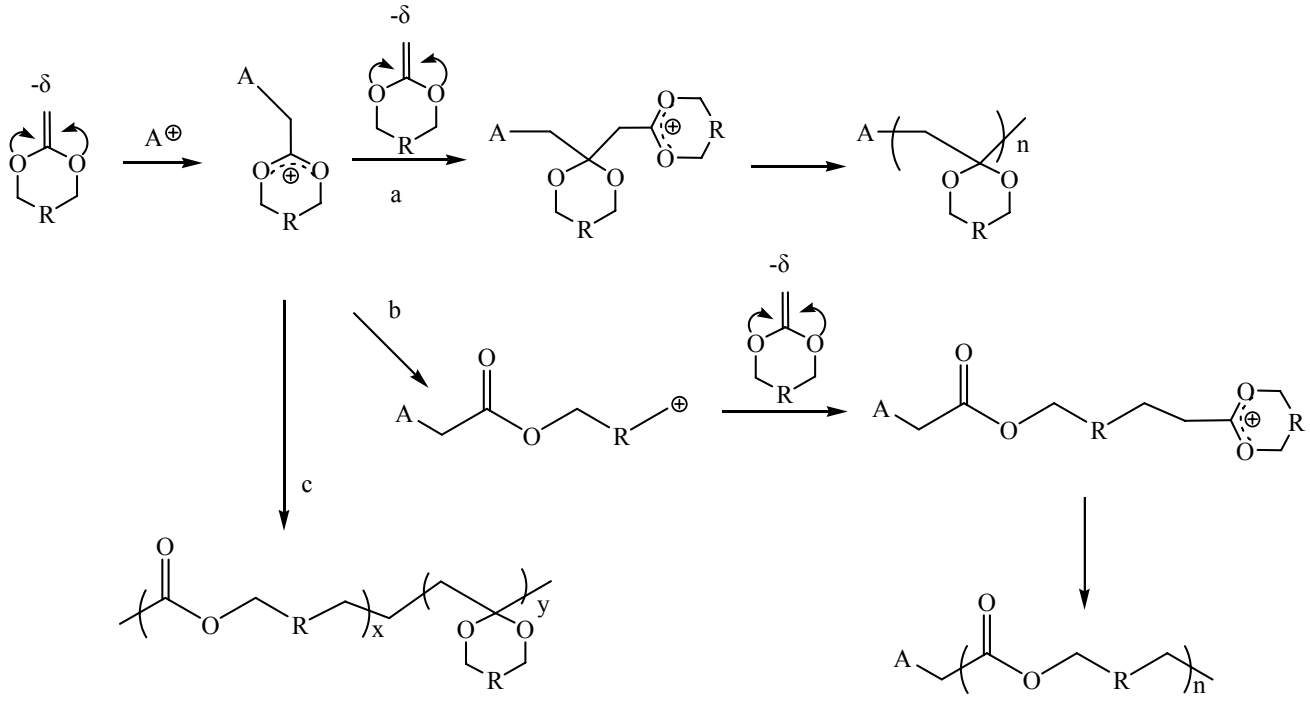

Scheme 2.9. Cationic polymerization routes of cyclic ketene acetals.

Scheme 2.10 and Scheme 2.11 show the transition energy differences between different types of radicals and cations. The transition energy difference between primary and tertiary carbon radical is around 4.5 kcal/mol, while that between primary and tertiary carbon cation is around 33 kcal/mol. Therefore, for cationic polymerization of cyclic ketene acetals, the formation of the high-energy primary cationic polyion is unfavorable, and this route may be dismissed unless the ring-opened cationic center was substituted with stabilizing groups.

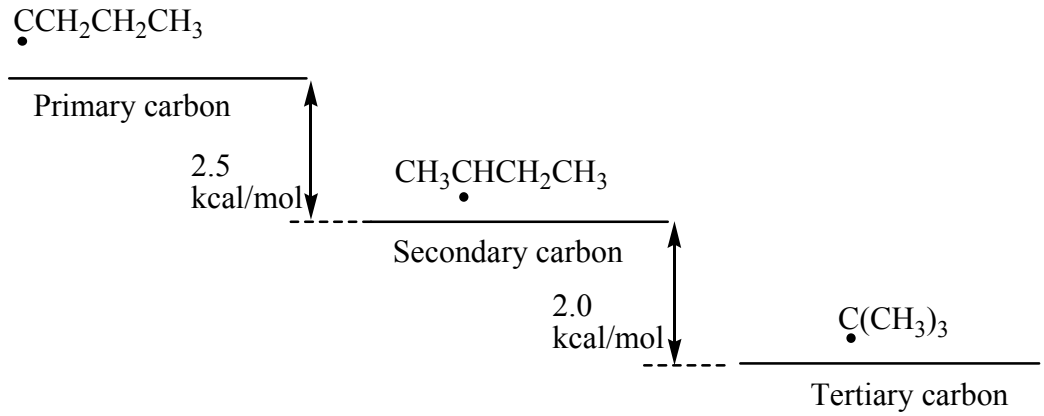

Scheme 2.10. Transition energy difference between primary, secondary and tertiary carbon radicals.

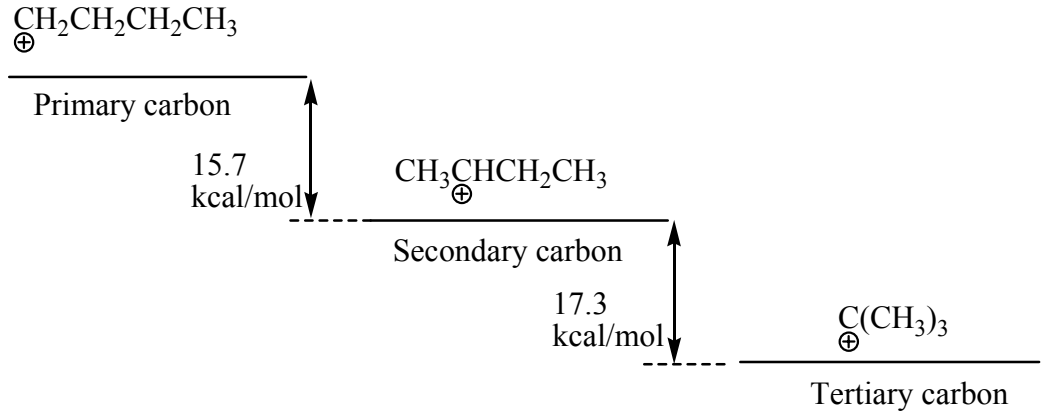

Scheme 2.11. Transition energy difference between primary, secondary and tertiary carbon radicals.

Compared to radical polymerizations, cationic polymerizations of cyclic ketene acetals have not been extensively investigated. However, a few examples have been reported. Pure or dominant

cationic 1,2-vinyl addition polymerization proceeds very fast and completes under low temperatures leading to high molecular weight poly(cyclic acetals) with $M_n \approx 10^5$ in the presence of different kinds of Lewis acids, including ($TiCl_4$, BF_3, $Ru(PPh_3)_3Cl_2$) and protonic acids, including H_2SO_4 as initiators.[63,64] The resulting poly(cyclic acetal)s are thermally stable but can be easily hydrolyzed and are likely to undergo crystallization to form insoluble cross-linked polymers in the presence of water, alcohol or acid.[65,65,66]

Zhu and Pittman found out that high temperature helped to initiate cationic ring-opening polymerization of cyclic ketene acetals, especially when the temperature was raised close to the ceiling temperature (T_c) for 1,2-vinyl addition.[7] However, high temperature also speeds up termination, which leads to low molecular weight with M_n less than 10,000.

2.3.4. Application of cyclic ketene acetal homo and copolymers

One important property of cyclic ketene homopolymers and copolymers is the biodegradability of the resulting aliphatic polyester after ring-opening polymerization.[67] Several functionally terminated oligomers were synthesized after simple hydrolysis of poly(cyclic ketene acetal-co-vinyl monomer)s.[52] Degradable polyesters poly(vinyl-co-ester)s are potential to be used for biomedical materials and compostable materials to solve the solid-waste problems.

Another property of cyclic ketene acetals is the low shrinkage or even expansion during polymerization. This is because during the ring-opening polymerization, one bond is broken for each new bond formed. This special property is intriguing with respect to applications as matrix resins or dental restoration, high-strength composites, adhesives, coatings, precision castings and sealant materials.

2.4. Ionomers

Interest in ionomer field has been continuing and growing since 1970s both in the academic and in the industrial world. The total number of papers in this field now approaches 650 per year; approximately one third of that number is patents. Ionic association in ionomers leads to their unique properties, such as thermo-elasticity, toughness, high melt strength, superpermselectivity,

etc. which therefore permits a wide range of applications in membranes and films,[68,69,70,71] plastics,[72,73] elastomers,[74] drilling fluids,[75] catalysts and catalytic supports[76].

2.4.1. Definition of polyelectrolyte and ionomer

Both polyelectrolyte and ionomer are ion containing polymers. Generally it is claimed that the difference between these two is the amount of ion content in the polymer. Currently, ionomers are defined as polymers containing a relatively low ion-content (up to around 15 mol%), while polyelectrolytes are defined as materials containing a very high ion-content, to the point of being water soluble.

Actually, the core factor to define polyelectrolytes and ionomers is in the phenomorphological point of view. Eisenberg claimed that ionomers are polymers in which the bulk properties are governed by ionic interactions in discrete regions of the material (the ionic aggregates).[77] In these materials, for example, the glass transition temperature is expected to increase as the ion concentration increases. While polyelectrolytes are polymers in which solution properties in solvents of high dielectric constants are governed by electrostatic interactions over distances larger than typical molecular dimensions. Thus, it is expected that the reduced viscosity will increase as the concentration of the polymer solution decreases. Similarly, the radius of gyration is expected to go up as the polymer concentration goes down. The fact is that some materials can behave as ionomers in bulk, and polyelectrolytes in aqueous solutions.

2.4.2. Chemical structures in ionomers

Molecular architecture of ionomers

There are several different possible molecular architectural features of regular ionomers as shown in Fig 2.4. The simplest type of ionomer consists of a single ion placed at one end or both ends of a polymer chain, which is called monochelics[78] or telechelics[79], respectively. One example is polystyrene containing a terminal carboxylate anion (Fig 2.4A). It can be synthesized using one or two functionallized initiator in the anionic polymerization of styrene, followed by termination of both ends with CO_2,[80] propanesulfone[81] or other groups.[82] The next family of ionomers is block ionomers, including AB diblock, in which one of the segments is non ionic and the other consists of

ionic repeating units.[83] One example is Poly(styrene-co-N-methyl-4-vinyl pyridinium iodide) (Fig 2.4B), which can be synthesized by living copolymerization, followed by quaternization.[84]

Simple random copolymers consisting of a nonionic material matrix (such as ethylene and styrene) with an ionogenic species (such as acrylic acid, methacrylic acid, or vinylpyridine) (Fig 2.4C) can be synthesized enormously and have been investigated most extensively.[85,86] Another class is the so-called homoblends, in which one polymer chain contains only anions, while the other chain contains only cations. These materials exhibit some of the properties of ionomers.[87,88] Graft ionomers can also be prepared. Examples include the large family of cellulosics with grafted acrylate or methacrylate chains.[89]

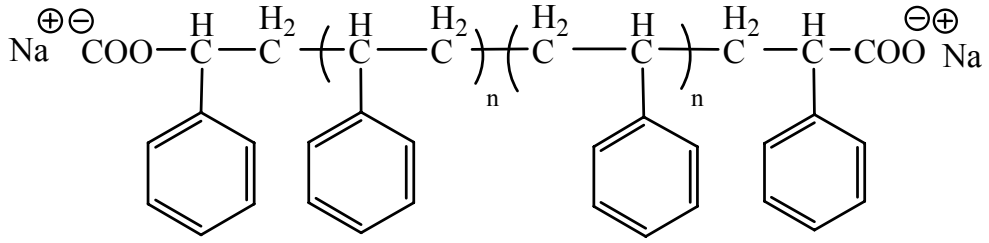

A

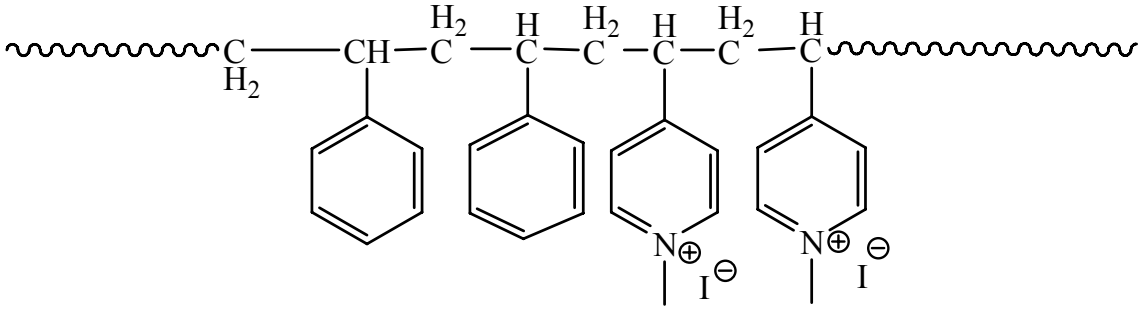

B

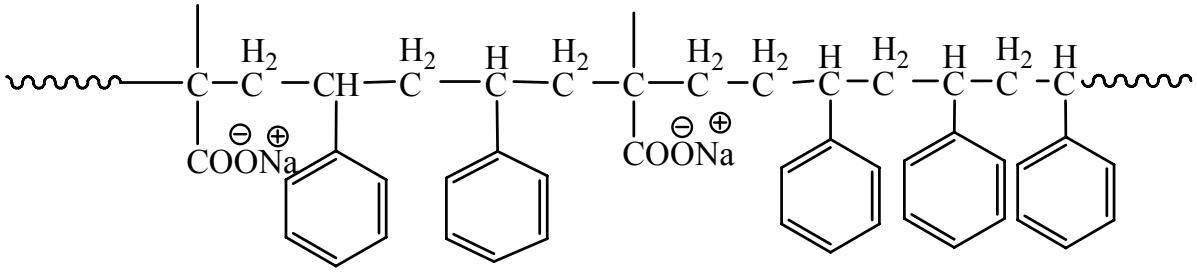

C

Fig 2.4. Example of (A) telechelics ionomer,[92] (B) block ionomer,[97] (C) random ionomer.[98]

Nature of ions

The pendent ions for the ionomers can be anions or cations. The most common pendent anions used in synthesis of ionomers are the carboxylates and the sulfonates (Fig 2.5A). Carboxylate can be introduced into the polymers either by direct copolymerization with species such as acrylic acid, methacrylic acid, maleic anhydride and many other unsaturated carboxylic acids, or via a post polymerization reaction, i.e. the carboxylation of the resulting copolymers, which is particularly suitable in the case of aromatic substitutions, like polystyrene.[90,91] Since copolymerization of

sulfonated monomers with non-ionic monomers is not easy to carry out in many cases, due to the low reactivity ratio and the limited solubility of the comonomers,[92] the more common route to sulfonation is via a post polymerization reaction of aromatic site. Nonetheless, copolymerization of sulfonated monomers with non-ionic organic monomers has been carried out successfully.[93]

The pendent cations are also quite commonly used for ionomers (Fig 2.5B). Pendent pyridine groups are among the most common examples, due to its proper copolymerization reactivity with a range of nonionic monomers.[94,95,96] Other pendent cations are also possible, such as aliphatic or aromatic amines and their salts.[97,98]

The counter ions for anionic polymers can be a wide range of metal ions, such as the alkali (Li^+, Na^+, K^+, Rb^+, Cs^+), alkaline earth (Mg^{2+}, Ca^{2+}, Sr^{2+}, Ba^{2+}), the transition metal (Zn^{2+}, Ni^{2+}, Mn^{2+}) or even organic cations, e.g. ammonium, pyridinium.[99,100,101,102] Compared to monovalent cations, multivalent cations are more difficult to incorporate. Cationic polymers have a relatively smaller range of counter ions available, including the halides (F^-, Cl^-, Br^-, I^-) and organic anions (OTs^-).[95,97,103]

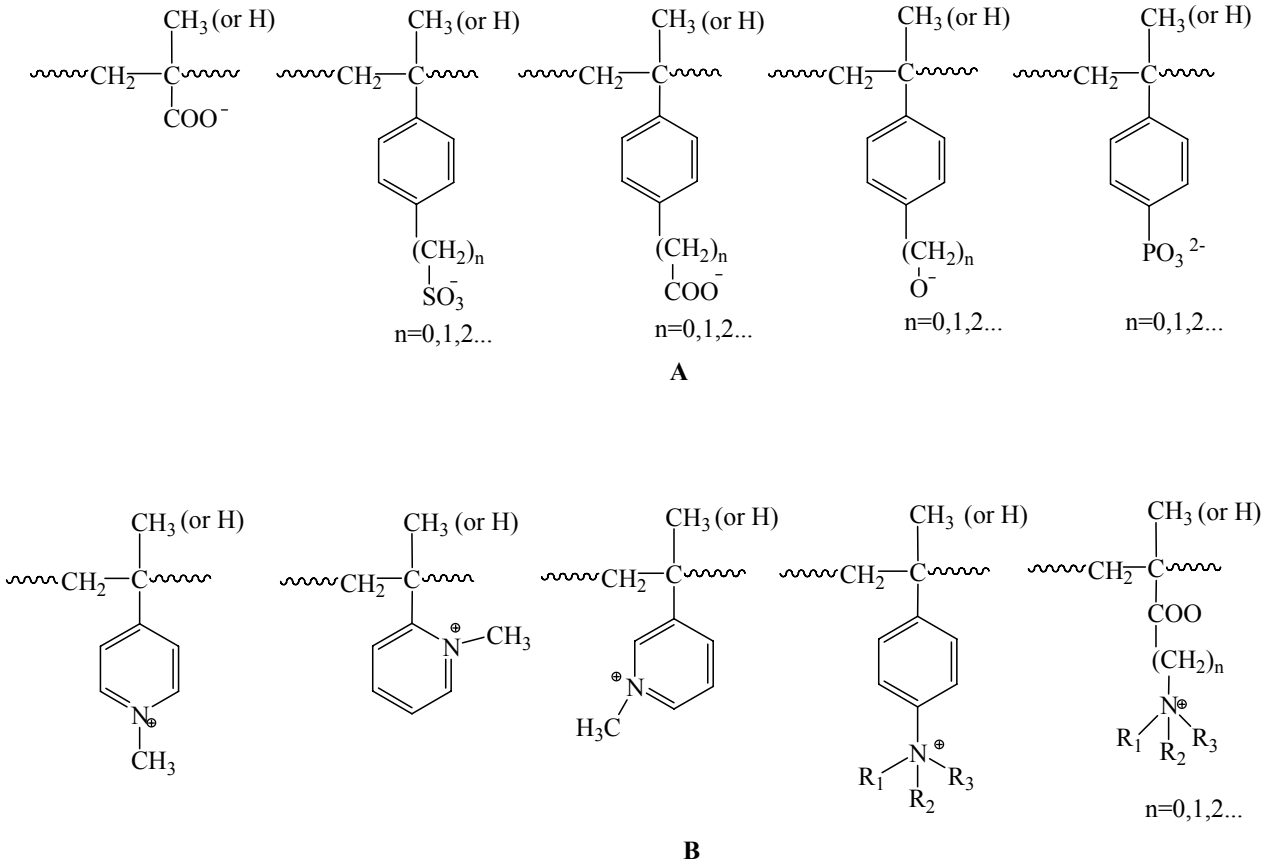

Fig 2.5. Examples of (A) pendent anions and (B) pendent cations for ionomers.[104-112]

2.4.3. Morphology of random ionomers

Over the past two decades, a number of models for the morphology of random ionomers have been proposed based on experimental observations.[104] As early as in 1968, Wilson et al. first published a small angle x-ray scattering (SAXS) profile of an ethylene-based ionomer and proposed a morphological model suggesting ion aggregation.[105] It is generally accepted that the ionic groups associate to form aggregates in the ionomers. The association of ionic groups determines the solid-state property of the ionomers. The size, the shape and even the distribution of the aggregates need to be extensively investigated.

Hard-Sphere Model

In an early study, Delf and MacKnight assigned the SAXS peak [106] and suggested that the peak arises from interparticle scattering from the ionic aggregates, which were taken to be small particles located on a paracrystalline lattice.[107] At the same time, a similar model was advanced by Binsbergen and Kroon,[108] in which the scattering moieties were pointed at the centers of randomly

packed spheres. Later, Yarusso and Cooper[109] proposed a modified hard-sphere model (Scheme 2.12), in which the multiplets have a liquidlike order at a distance of closest approach around 30 Å, somewhat larger than that of the multiplet itself, determined by the hydrocarbon layer attached to and surrounding each multiplet. The model was in good agreement with the experimental SAXS profiles and assumed the existence of multiplets of high electron density surrounded by a layer of hydrocarbon material of much lower electron density immersed in a medium of intermediate ion content.

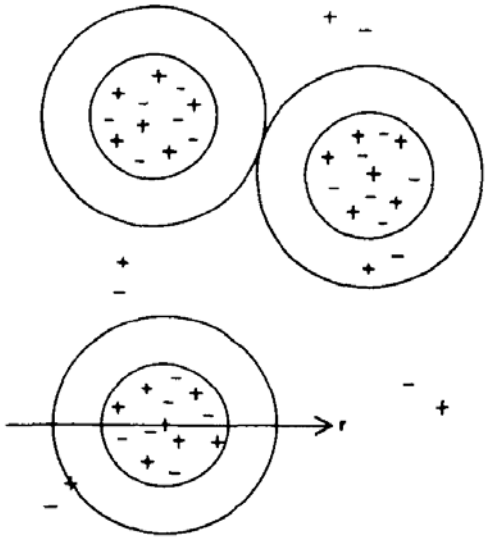

Scheme 2.12. Hard sphere model of Yarusso and Cooper based on SAXS analysis of various ionomers; the dimension of the ionic sphere portion is of the order of 3 nm.[125]

Core-Shell Model

Based on the radial distribution function of scattered x-rays for ionomer, MacKnight et al.[110] developed a core-shell model (Scheme 2.13), assuming that the ion pairs form a core that is surrounded by a shell of material of low electron density. The central core is taken to have a radius of 3-13 Å and to contain ~50 ion pairs. The hydrocarbon shell is in the order of 20 Å. The major difference between this model and the hard-sphere model is the assignment of the ionic peak to intraparticle interference rather than interparticle interference. A modification is made by Roche,[111] who suggested that the geometry of the ion-rich phase is lamellar. The central lamella of high electron density material (high ion content) is sandwiched between lamellae of low electron density hydrocarbon material, which is, in turn, sandwiched between layers of intermediated electron

density. Interlamellar distances are taken to be responsible for the peak.

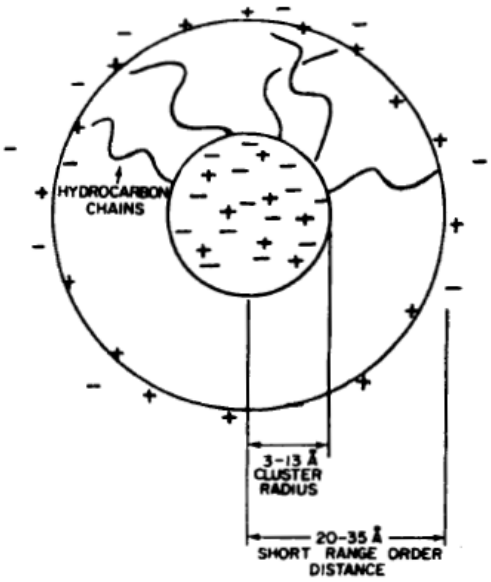

Scheme 2.13. Core shell model of MacKnight et al. based on scattering experiments, with dimensions as shown.[126]

While the hard-sphere and core-shell model were successful in modeling the SAXS profiles, they failed to clearly explain the mechanical properties of the materials: two glass transition temperatures were detected from dynamic mechanical thermo-analysis demonstrating a new region with a dimension greater than 50-100 Å in the monomer, which can neither be fitted into a 30 Å lattice from the hard-sphere model, nor to the core-shell model.[112]

Multiplet-Cluster Concept

Among a number of models for ionomers, the most widely accepted one is the "Multiplet-Cluster" Concept. The concept of a multiplet was proposed and developed by Eisenberg. According to him, the formation of multiplets, which means aggregates consisting of several ion pairs and containing only ionic materials, is a crucial element in ionomers (Scheme 2.14).[113] The driving force for the multiplet formation is the strength of the electrostatic energy between the ion pairs, which is determined by the sizes of the ions, the partial covalent character of the ionic bond and the ion content.[112] If the electrostatic interactions between ion pairs are too weak to overcome the elastic forces of the nonionic chains to which they are attached, no multiplets will be formed. Small highly polar ion pairs interact more strongly and thus tend to be more firmly held together than larger groups. The nature of the matrix polymer, including the dielectric constant of the polymer and the

rigidity of the chains,[114] is also a very important factor for the formation of aggregates. If the dielectric constant is too high, as it is in the polyphosphates, multiplet formation would not be expected because the ion pair is soluble in the polymer.[115] In a random ionomer, low dielectric constant and low T_g of the host polymer tend to favor ionic aggregation formation.

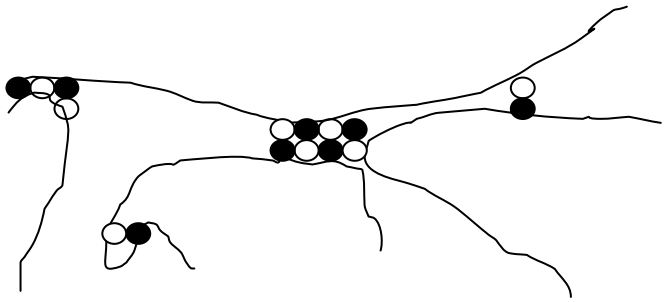

Scheme 2.14. Formation of ionic multiplets, write and black dots present the single cationic and anionic groups.[129]

Both inter and intra molecular ionic multiplets can be form. The form of the multiplets is assumed to be like a spherical liquid drop consisting of ionic groups.[116] The general size of the multiplets is claimed by Eisenberg to be 6-8 Å (around 2-10 ion pairs).[117] Each multiplet is surrounded by nonionic polymer "skin", whose mobility is greatly restricted by multiplets. The distance of the restricted polymer segments is difficult to ascertain exactly but is assumed to be in the order of the persistence length of the bulk polymer (Scheme 2.15).

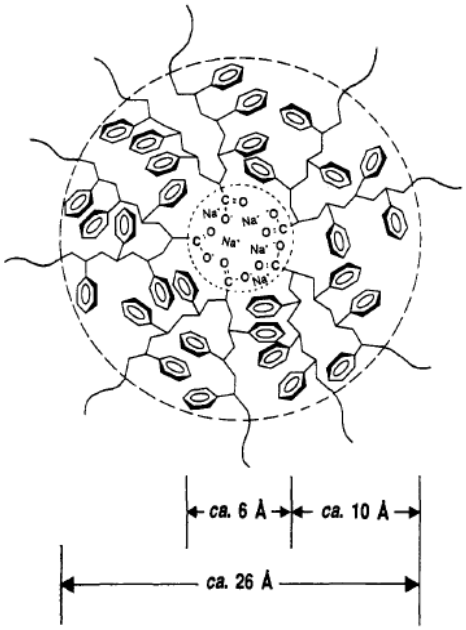

Scheme 2.15. Demonstration of a multiplet and its surroundings in poly(S-co-MANa).[112]

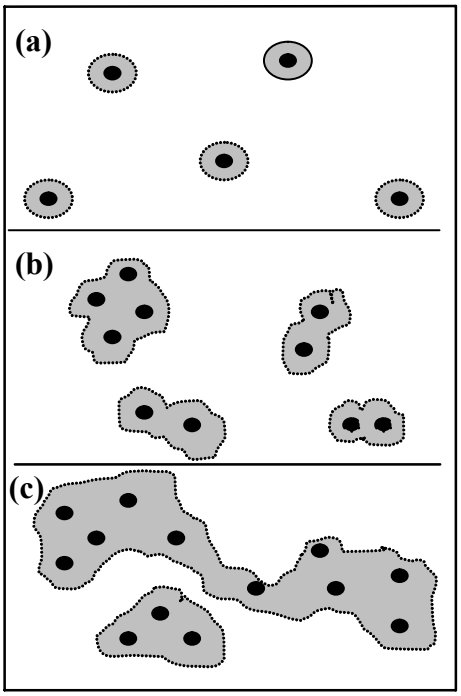

Scheme 2.16. Demonstration of the morphologies of random ionomers at (a) low ion content; (b) intermediate ion content; (c) high ion content. The black shaded areas indicate multiplets and the gray shaded areas indicate regions of restricted mobility.[134]

A multiplet containing only two ion pairs, i.e., a quartet, is expected to behave in a similar manner to a conventional crosslink and hence influences the properties of the material. In general, the restricted mobility region surrounding an isolated multiplet would be too small to have its own T_g. But the multiplet itself would increase the T_g o f the polymer by acting as a large cross-link.

As the ion content is increased, the average distance between multiplets decreases. Eventually some overlap is encountered among the regions of restricted mobility surrounding each multiplet (Scheme 2.16b). As this overlap becomes more frequent, relatively large contiguous regions of restricted mobility are formed (Scheme 2.16c). When such a region is large enough (greater than 5-10 nm) to have its own T_g, detected by dynamic mechanical thermo-analysis, it is defined as a "cluster" exhibiting behavior characteristic of a phase-separated region.[134]

The electrostatic interactions between multiplets are actually week. The presence of clusters is determined by the existence of sufficiently large regions of material with restricted mobility. There is no thermodynamic driving force for phase separation of the clusters. Thus, from a thermodynamic point of view, the term "phase" may not be entirely appropriate to describe the

clustered domains. However, the clusters exhibit their own well-defined mechanical characteristics, which are quite reproducible and thus clearly demonstrate phase separated behavior.

The shape of the clusters is assumed to be irregular. The numbers of multiplets contained in a cluster and the size of a cluster are uncertain, but highly dependent on the ion content.

3. Results and Discussions

3.1. Thermo-sensitive degradable poly(ester-co-NIPAAm)

Reference: Ren, Liqun; Agarwal, Seema; Macromolecular Chemistry and Physics; 2007, 208, 245.

3.1.1. Introduction

Poly(N-isopropyl acylamide) (PNIPAAm) is one of the widely investigated smart polymer having a lower critical solution temperature (LCST) of about 31^{o}C.[118] The solubility of the polymer in cold water can be attributed to its ability to form hydrogen bonds with water via the amide groups while inducing considerable ordering of water through the apolar isopropyl group. This water structuring brings large negative contributions to both the enthalpy $\triangle$H and the entropy $\triangle$S of mixing. At a sufficiently high temperature the entropic term will overcome the negative enthalpy of solution, resulting in a positive free energy. Thus at this temperature phase separation occurs. Due to the thermo-sensitivity PNIPAAm has been designed for applications in the biomedical field.[119,120,121] It is also well-known that the copolymerization of other hydrophobic or hydrophilic monomers with NIPAAm would decrease or increase the LCST, respectively.[122,123,124]

The introduction of ester linkages here is expected to generate new materials with a range of lower critical solution temperatures (LCSTs) besides making them degradable thereby increasing their utility areas for various biomedical applications. Therefore, an attempt has been made to study the copolymerization behavior of N-isopropyl acrylamide (NIPAAm) with BMDO under conventional radical polymerization conditions. The reactivity parameters, the structural characterization using 1D and 2D NMR techniques, the thermal properties, the thermo-sensitivities and the degradability of the new materials poly (NIPA-co-ester)s were investigated.

3.1.2. Copolymerization behavior of BMDO and NIPAAm

Various copolymers of BMDO with NIPAAm were synthesized as shown in Scheme 3.1.1 by changing the molar ratio of two monomers in the initial feed.

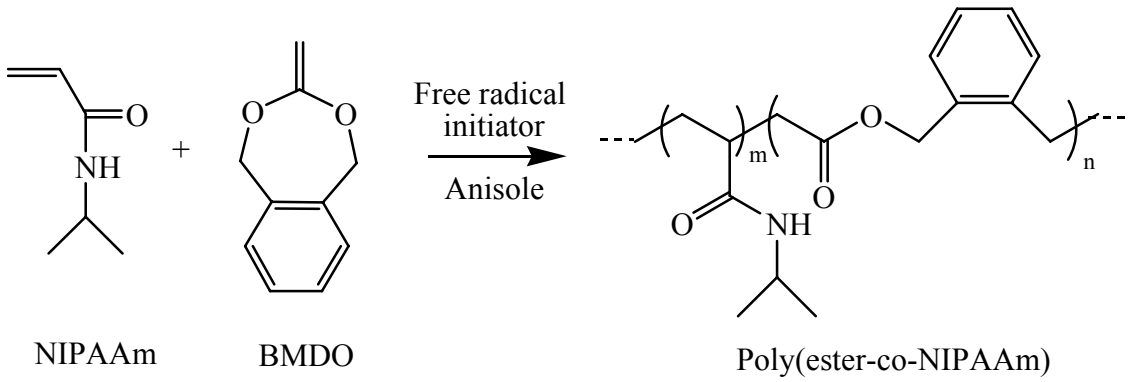

NIPAAm BMDO Poly(ester-co-NIPAAm)

Scheme 3.1.1. Free radical copolymerization of BMDO and NIPAAm.

3.1.2.1. Structure characterization

Various random copolymers were made by changing the molar ration of BMDO and NIPAAm in the feed. The structural characterization of the copolymers is done using 1D and 2D NMR techniques.

The representative ^{1}H-NMR of the copolymer sample with 40% BMDO in the initial feed was shown in the Fig 3.1.1. The characteristic peaks of both BMDO and NIPAAm were seen in the obtained polymers. The ^{1}H-NMR peak assignments were done by comparing it with that of the homopolymers ((BMDO)[125] and PNIPAAm[126]. Protons –OC*H*$_2$– (1) of BMDO, –C$_6$H$_5$C*H*$_2$– (3), (CH$_3$)$_2$C*H*NH– (9), (CH$_3$)$_2$CHN*H*– (8), (C*H*$_3$)$_2$CHNH– (10), –C*H*$_2$–CH(CONH–)– (5), and –CH$_2$–C*H*(CONH–)– (6) of NIPAAm were assigned without ambiguity. The other proton peaks [protons 2 –C*H*$_2$C(O)– and the protons 2′ and 3′ from the linking BMDO units] of BMDO and NIPAAm linking units (5′,6′,5″,6″) in the lower ppm region between 1.2 and 2.9 ppm came as overlapping and not very well resolved peaks. Also, the conformational and configurational sequencing in the copolymers are responsible for the overlapping peaks in this region. Furthermore, an attempt has been made to analyze the overlapping peaks and to establish a chemical link between the two monomeric units, i.e., BMDO and NIPAAm in the copolymers by 2D ^{1}H-^{13}C HMBC-NMR technique, described in the later part of the work.

2D ^{1}H–^{13}C HMQC-NMR technique is used to assign peak positions in the ^{13}C-NMR spectrum (Fig 3.1.2). The correlations are: proton 1with carbon at ppm 64.5 (A), proton 9 with carbon at ppm 41

(B), proton 3 with carbon at ppm 26.7 (C), proton 10 with carbon at ppm 23.5 (D), proton 6 with carbon at ppm 42 (E) and proton 5 with carbon at ppm 32 (F). The broad peak between 2.4 and 3.0 ppm showed three clear correlations in HMQC-NMR spectrum with ^{13}C carbons at ppm 30 (G), 35 (H), and 37 (I) thereby, showing the presence of at least three different types of hydrogen atoms at this position. 2D HMBC-NMR spectrum (Fig 3.1.3) provided further clarity in the peak assignments and peak confirmations.

In HMBC-NMR spectrum, the peak 3 in ^{1}H-NMR spectrum showed 5 very clear cross peaks with one peak at ppm 37 (A), three peaks in the aromatic region (B, C, D), and a peak in the carbonyl carbon region (E). This confirms the correct assignment of peak 3 in the copolymers, as it is expected to show three correlations in the aromatic region (with ar1, ar2, and ar3 by 2 and 3 bond correlations, respectively) and also suggests that the undecided peak marked at ppm 37 (corresponding peak in ^{1}H-NMR at ppm 2.5) in the ^{13}C-NMR spectrum is the carbon 2 peak of BMDO. The cross peak A in HMBC is therefore produced by 2 bond correlations with the protons attached to the carbon 3 of BMDO and its neighboring carbon 2. Further confirmation comes from careful observation of the correlations of this peak (2 of BMDO) at ppm 2.5 in the ^{1}H-NMR spectrum. This showed three strong correlations with the peaks in the ^{13}C-NMR at ppm 26.7 (F), one aromatic peak (G), and one carbonyl carbon (H). This shows that it is from the protons 2 of BMDO, as it expects to show such three correlations with the carbon 3 (2 bond correlation), only one aromatic carbon ar1 (3 bond correlation), and with carbonyl carbon (2 bond correlation). Furthermore, careful examination of the HMBC-NMR spectrum showed the presence of some weak correlations of the peak at ppm 2.47 with carbons at ppm 32 (carbon 5 of NIPAAm) (I) and three aromatic carbons (J), (K), and overlapping (G). This shows the presence of the protons 3′ (at ppm 2.47), i.e. from the linking unit of BMDO to NIPAAm. Again a very clear correlation of the shoulder of the overlapping peaks between ppm 2.4 and 3.0 (around ppm 2.7) were seen, both with carbons of NIPAAm at ppm 32 (L) (carbon 5 of NIPAAm), ppm 42 (M) (carbon 6 of NIPAAm), and carbonyl carbon of BMDO (N) and therefore shows it to be from the protons 2′, i.e. the linking units of BMDO with NIPAAm. The carbon peak of the linking 3′ carbon of BMDO shows weak correlations with the protons in the lower ppm region, 1.5 (P) and 1.8 (O), thereby showing the presence of the protons 5′ and 6′ of the linking NIPAAm units present as overlapping signals with the corresponding proton 5 and proton 6.

HMBC-NMR technique is a powerful tool in the assignment of some overlapping peaks in the ^{1}H-NMR spectrum and also gave a hint of the random copolymer structure with plenty of chemical linkages between the comonomeric units in the copolymers. Also, ^{13}C-NMR spectra showed the absence of any peak in the ppm range 100-110, showing the formation of predominantly ester linkages by ring-opening polymerization reaction of BMDO during copolymerization.

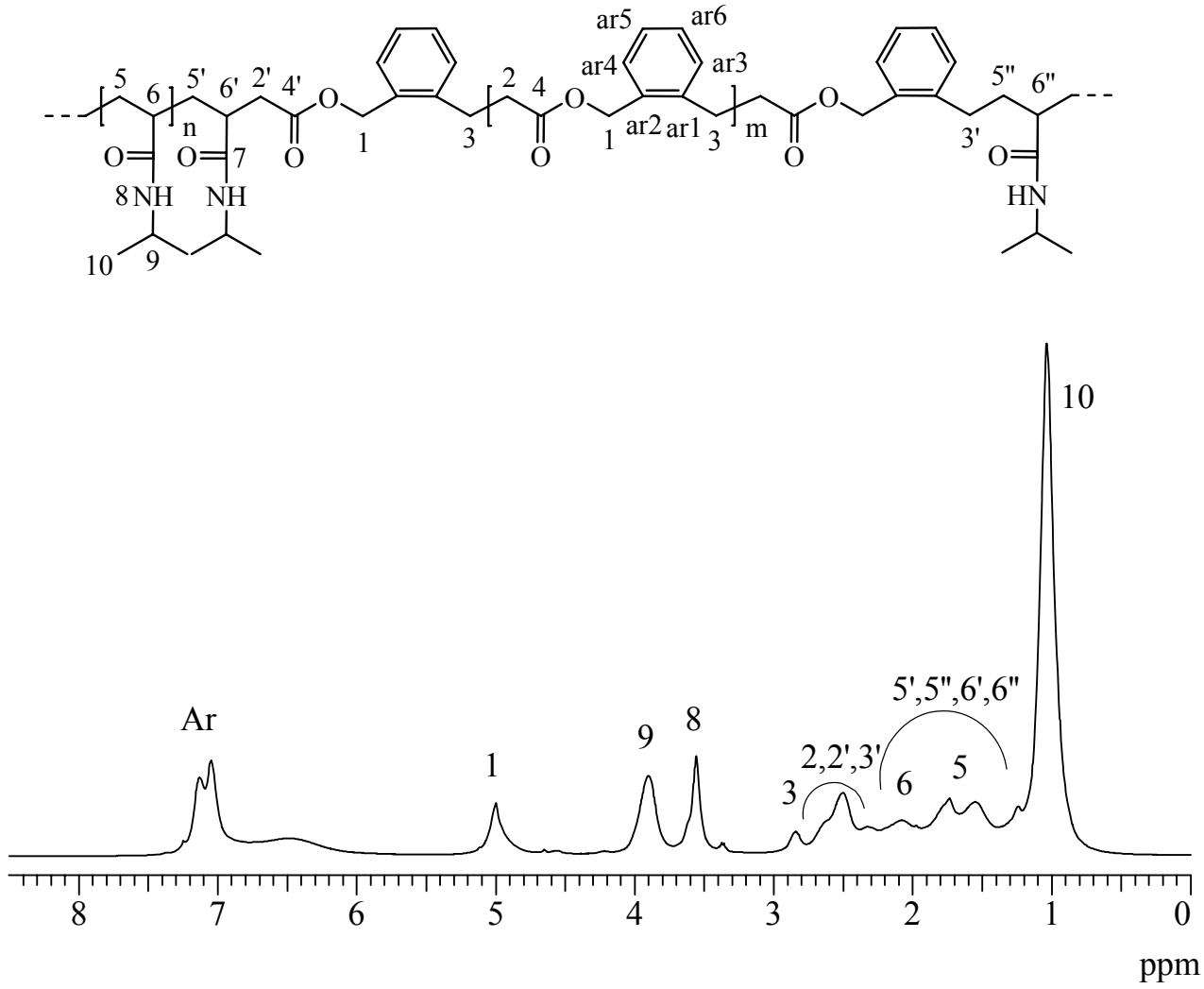

Fig 3.1.1. ^{1}H-NMR spectrum of poly(BMDO-co-NIPAAm) with 40% BMDO in the feed.

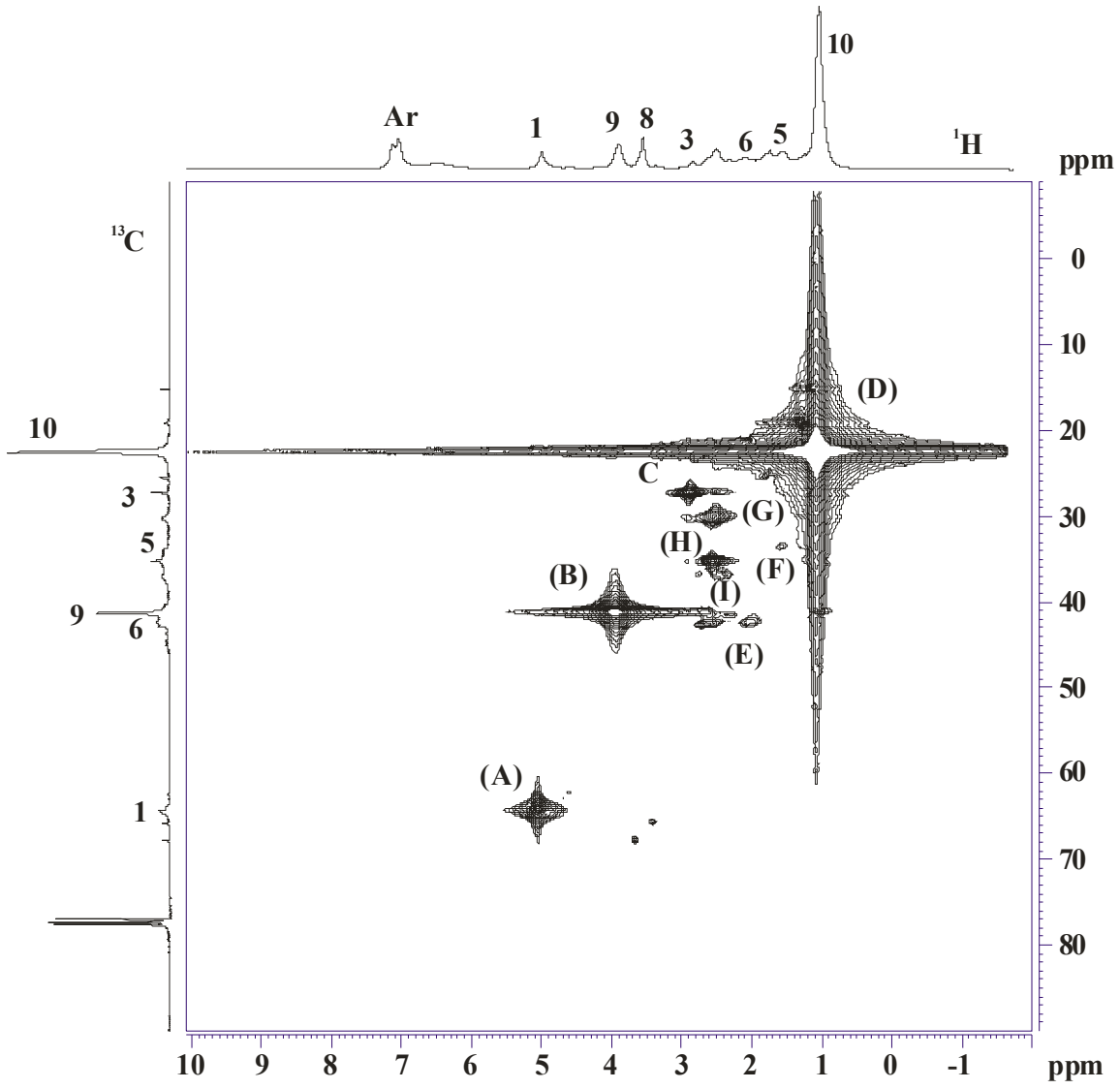

Fig 3.1.2. 2D ^{1}H-^{13}C HMQC-NMR spectrum of poly(BMDO-co-NIPAAm) with 40% BMDO in the feed.

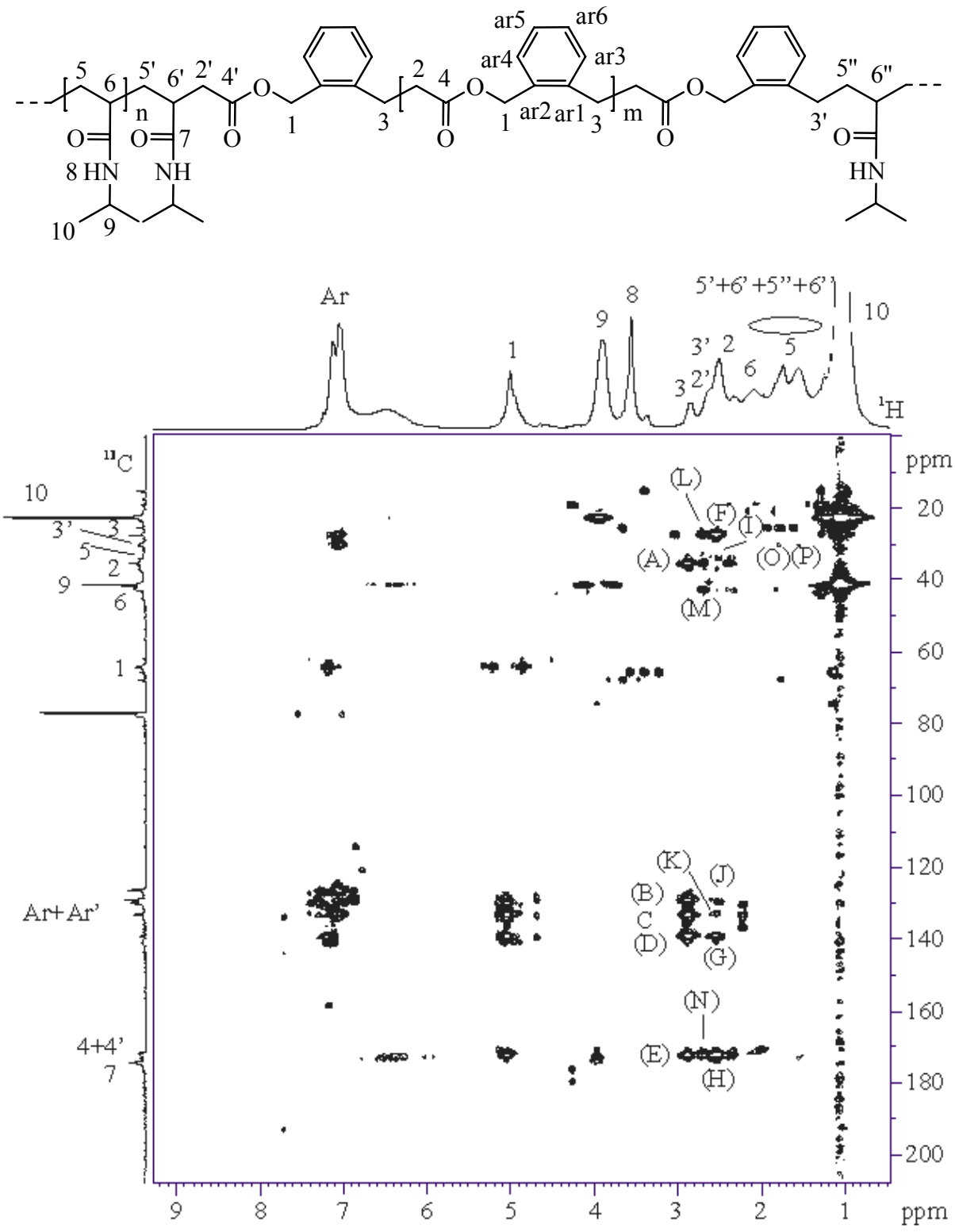

Fig 3.1.3. 2D ^{1}H-^{13}C HMBC-NMR spectrum of poly(BMDO-co-NIPAAm) with 40% BMDO in the feed.

3.1.2.2. Influence of initial feeds on copolymer structures

Copolymers of BMDO with NIPAAm with varied copolymer compositions and molecular weights

were synthesized by changing the molar ratio of two monomers in the initial feed (Table 3.1.1).

Table 3.1.1. Copolymerization of BMDO and NIPAAm at 120°C using dtBp initiator for 8 hrs in anisole [monomer : In = 100 : 2 (molar ratio)]; a) Reaction time: 30 hrs; M_n measured by Group THF GPC

Run	Initial Feed (molar ratio)		Yield (%)	Copolym. Composition (molar ratio)		M_n	PDI
	BMDO	NIPAAm		BMDO	NIPAAm		
1[a)]	100	0	56	100	0	3500	2.7
2	70	30	42	35	65	6600	2.8
3	30	70	73	13	87	36000	3.0
4	20	80	82	8	92	24000	3.1
5	10	90	86	4	96	34000	3.0
6	0	100	95	0	100	26000	3.2

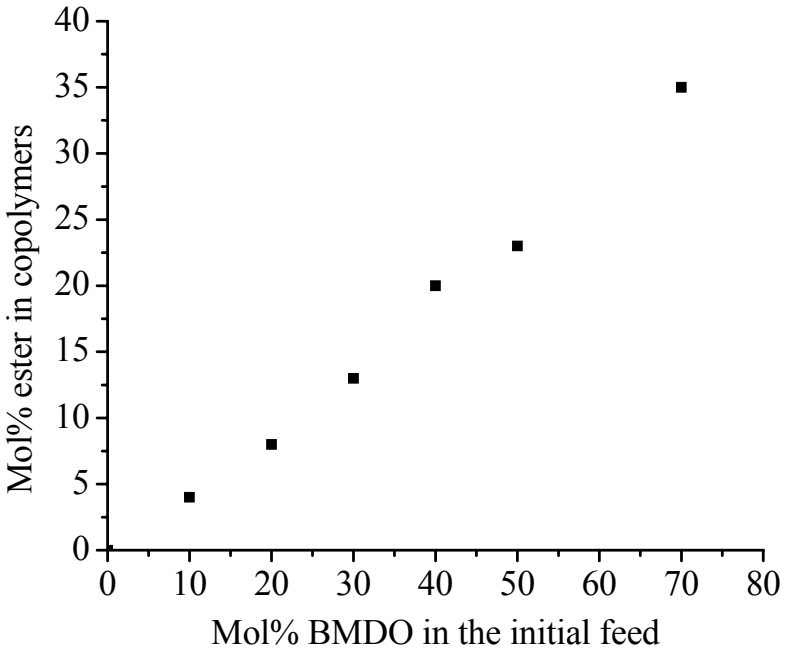

Fig 3.1.4. Mol% of BMDO in initial feeds versus mol% of ester in copolymers.

In general, varied molecular weight copolymers with uni-modal broad GPC curves were obtained. The molecular weight of the polymers increased with the increase in the amount of NIPAAm in the copolymers. There was an increase in the molecular weight from 6600 to 36000 on increasing the

molar ratio of NIPAAm : BMDO from 65 : 35 to 87 : 13. The copolymer composition was determined by using the peak intensities at ppm 4.8-5.1 [I_{BMDO} (–OC*H*$_2$–C_6H_5–)] and ppm 3.9 [I_{NIPAAm} ($(CH_3)_2$C*H*NH–)] in ^{1}H-NMR. The molar ratio of NIPAAm : BMDO in the copolymers was always found to be higher as compared to that in the feed (Table 3.1.1), but different copolymers could be made to have increasing amount of BMDO units just by changing the molar ratio of the two comonomers in the initial feed and this increase was found to be almost linear (Fig 3.1.4).

3.1.2.3. Influence of time on copolymer structures

In order to have an insight into the copolymerization behavior and the microstructure of the copolymers, for one specific initial feed (BMDO : NIPAAm = 50 : 50, molar ratio), the polymerization was followed at different intervals of time. Copolymer composition is determined from ^{1}H-NMR spectra and is followed with respect to the time/progress of the polymerization (Table 3.1.2). There was a continuous increase in both BMDO and NIPAAm content in the copolymers with time, indicating the constant random polymerization within the reaction time. The rate of consumption of NIPAAm was much more than that of the BMDO (Fig 3.1.5). This indicates the preference of both NIPAAm and BMDO radicals for the NIPAAm monomer during copolymerization and, therefore, most probably resulting in diads of the type BMDO–NIPAAm, NIPAAm–BMDO, and NIPAAm–NIPAAm in the copolymer chains with isolated or rather very short BMDO sequences of the type BMDO–BMDO. This is also qualitatively supported by the comparison of the peak areas of proton 3 and that of the peak between ppm 2.3 and 2.7 (from 2, 2′, 3′) in ^{1}H-NMR (Fig 3.1.1). Although the peaks are not very well resolved, they clearly show the presence of more linking 2′and 3′ units than 2 and 3 from BMDO–BMDO type sequences.

The molecular weight of polymers at different intervals of time did not change too much, with relative stable polydispersity around 4.5.

Table 3.1.2. Copolymerization of BMDO (B) and NIPAAm (N) [BMDO : NIPAAm = 50 : 50 (molar ratio)] at 120°C using dtBp initiator for different time intervals in anisole [monomer : In = 100 : 2 (molar ratio)]; M_n measured by Praktikum THF GPC in the group; a) Calculated using the copolymer composition and the yield

Run	Reaction Time (h)	Yield (%)	Copolym. Composition (molar ratio) B : N	Wt.-% of the monomer reacted[a)] B	N	M_n	PDI
1	0.25	18	10 : 90	4.3	38	44000	4.5
2	0.5	27	12 : 88	7.4	55	37000	4.7
3	1	37	17 : 83	14	70	40000	4.9
4	4	44	21 : 79	20	78	/	/
5	8	51	21 : 79	24	89	/	/

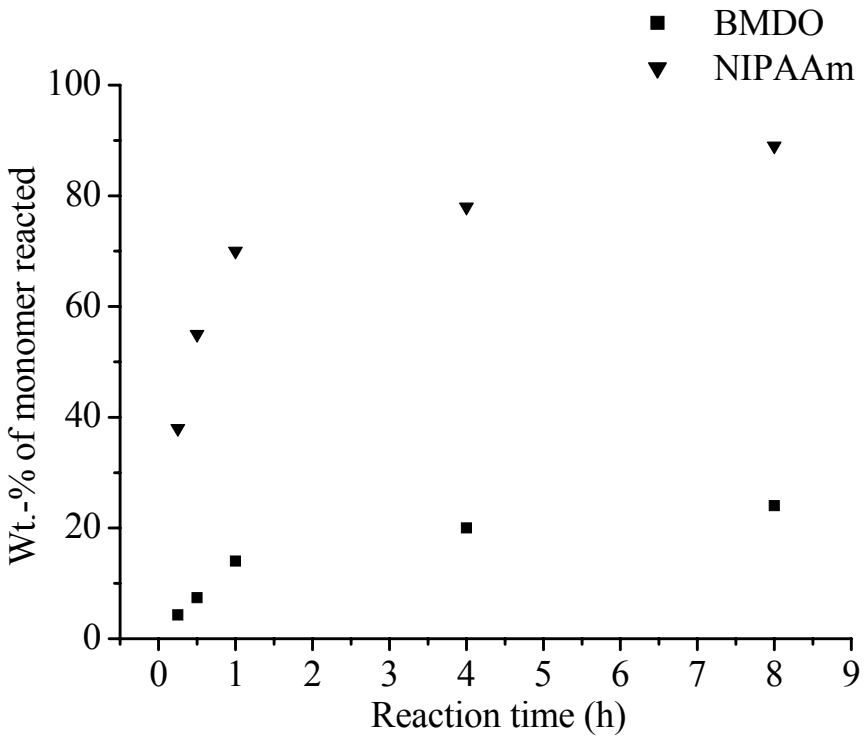

Fig 3.1.5. Wt.-% of the monomers reacted versus time (values from Table 3.1.2).

3.1.2.4. Reactivity ratios

The reactivity ratios were determined using the Kelen-Tüdõs method.[127] Six copolymerizations (Table 3.1.3) were carried out till low-medium percent conversions (between 9 and 34%) for the calculation of reactivity ratios (Fig 3.1.6), and the reactivity ratios were determined to be r_{BMDO} =

0.11 and r_{NIPAAm} = 7.31. Although it is acknowledged that the small error is involved in this calculation because of the compositional drift with the conversion, this gives a hint about the random copolymer microstructure to be having relatively long NIPAAm blocks, well separated by rather short BMDO sequences.

Table 3.1.3.Copolymerization of BMDO and NIPAAm at low concentrations at 120°C using dtBp initiator in anisole [monomer : In = 100 : 2 (molar ratio)]

Run	Feed Ratio (molar ratio)		Reaction Time (min)	Yield (%)	Copolym. Composition (molar ratio)	
	BMDO	NIPAAm			BMDO	NIPAAm
1	10	90	5	38	1	59.89
2	20	80	5	33	1	29.39
3	30	70	5	9	1	18.07
4	40	60	10	13	1	10.74
5	50	50	15	18	1	7.73
6	60	40	20	26	1	4.32

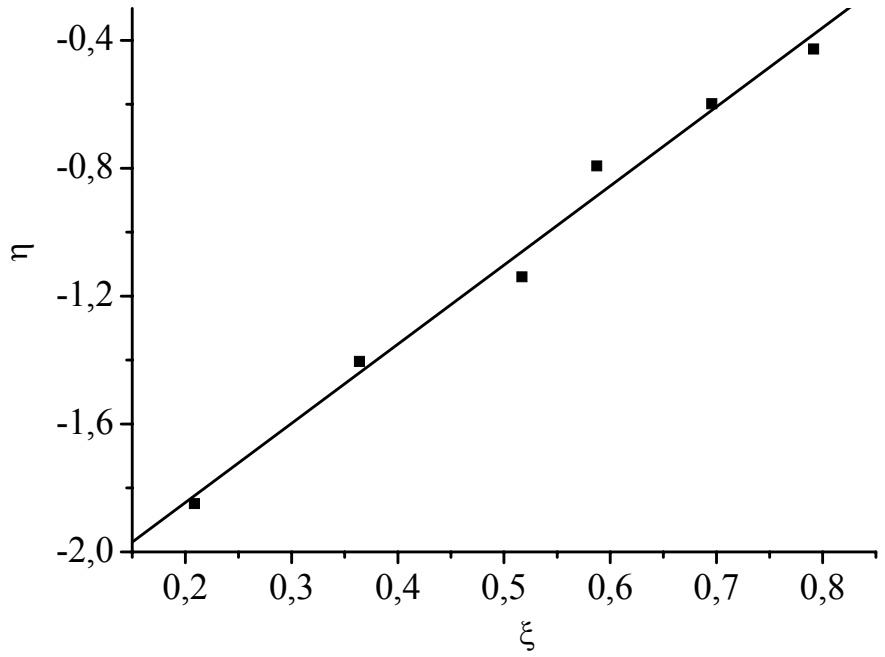

Fig 3.1.6. Kelen-Tüdõs plot for BMDO-NIPAAm copolymers. (values based on Table 3.1.3)

$\eta = (r_{BMDO} + r_{NIPAAm}/\alpha) \cdot \xi - r_{NIPAAm}/\alpha$ ($\eta = 2.457\xi - 2.3408$; $\alpha = 3.1220$)

$$\eta=[(F/f)(f-1)]/(\alpha+F^2/f); \quad \xi=(F^2/f)/(\alpha+F^2/f);$$

where $F= M_{BMDO}/M_{NIPAAm}$ (monomer feed); $f=m_{BMDO}/m_{NIPAAm}$ (copolymer composition);

$$\alpha= [(F^2/f)_{max} (F^2/f)_{min}]^{1/2}.$$

3.1.3. Thermal analysis of poly(BMDO-co-NIPAAm)

Thermal characterization of copolymers was done using TGA and DSC techniques. Poly(NIPAAm-co- ester)s showed a range of glass transition temperatures depending on the amount of BMDO in the copolymers. The glass transition temperatures for the copolymers were listed in Table 3.1.4. Homo-poly BMDO showed a glass transition around 20^{o}C, while PNIPAAm obtained a high glass transition temperature at 143^{o}C. Single glass transition temperature was obtained for copolymers, which is accordance with the random structure of the copolymers. The glass transition temperatures of the copolymers are between that of two homopolymers and increase with an increase in the amount of NIPAAm. Thermal stability of copolymers was studied using thermo gravimetric analyzer. PBMDO, PNIPAAm and poly(BMDO-co-NIPAAm) are thermo stable until 300^{o}C. In the temperature range of 310^{o}C to 500^{o}C, PBMDO, PNIPAAm and the copolymers showed one-step degradation. The 5% degradation temperatures were shown in Table 3.1.4. In general, the temperature, at which 5% degradation takes place, increases slightly as increase the amount of NIPAAm.

Table 3.1.4. Glass transition temperature (T_g) and the temperature at which 5% degradation takes place ($T_{5\%}$) of BMDO-NIPAAm copolymers

Run	Copolymer Composition (molar ratio)		T_g (^{o}C)	$T_{5\%}$ (^{o}C)
	BMDO	NIPAAm		
1	100	0	20	353
3	20	80	95	323
4	13	87	112	333
5	8	92	120	340
6	4	96	131	348
7	0	100	143	356

3.1.4. Thermo-sensitivity of poly(BMDO-co-NIPAAm)

Since PNIPAAm is a water-soluble polymer, it would be of interest to modify its LCST for various biomedical applications besides introducing degradability to the system. For LCST determination, PNIPAAm or copolymers with different contents of BMDO in the polymer chains were added to distilled water and stirred in an ice bath. It was found that copolymers with up to 8mol% of BMDO were soluble in water and the solutions stay transparent when the concentrations of the polymers are below 1 wt.%, 0.5 wt.%, or 0.05 wt.% for poly(NIPAAm-co-BMDO) containing 0 mol%, 3.9 mol%, 5.7 mol% and 8.3 mol% of BMDO, respectively. When BMDO in the copolymer increased to 13mol%, copolymers were not completely soluble in water, although they were highly soluble in other organic solvents like THF, and chloroform. Fig 3.1.7 shows the % transmittance of UV light versus temperature curves for different copolymer solutions in water. The LCST was defined as the onset of the slope of the turbidity curves. The molecular weight (M_n) of these copolymers tested for LCST behavior was in the range of 24000 to 50000.

A decrease in the LCSTs from 31.5^{o}C (pure PNIPAAm) to 13^{o}C was observed when increasing the amount of BMDO to 8.3 mol% in the copolymer. The decrease in the LCST was almost linear with change in the amount of the BMDO in the content (Fig 3.1.8). It is also noted from these curves that the phase separation of an aqueous solution of PNIPAAm occurred fairly sharp, while the copolymers with increased BMDO content exhibited a rather slow and unsharp phase separations. Tirrell et al.[128] have shown broad cloud point transitions for low molecular weight (M_n = 5400) and two broad cloud points for low molecular weight (M_n = 11000) bimodal homo-PNIPAAm samples. On the other hand, Fujishige et al.[129] reported chain-length independent cloud points for PNIPAAm having molecular weights more than 50000. In the present study, the copolymers have relative moderate molecular weights (M_n = 24000 to 34000). Moreover, the microstructure of the copolymers was seen to be long blocks of PNIPAAm separated by BMDO units. Based on the similar cross peak density of the linking section of BMDO-NIPAAm and from the homopolyester blocks of PBMDO in the 2D HMBC-NMR spectrum, supposing the average P_n of short BMDO block is 3, the average chain length (or molecular weight Mn) of the PNIPAAm blocks in these copolymers would decrease upon increasing the BMDO content in the copolymers and were around 8500, 6000, and 4500 for the samples with 3.8, 5.7, and 8.3 mol-% of BMDO units, respectively. The low molecular weight blocks of PNIPAAm might be acting as independent units, thereby

leading to the broad and unsharp phase transitions during LCST measurements.

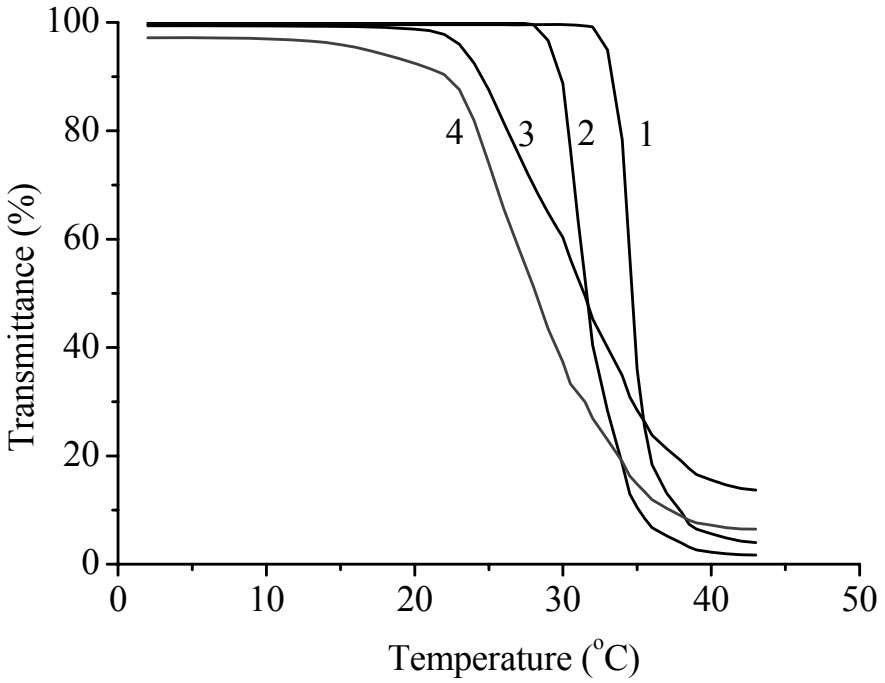

Fig 3.1.7. Transmittance versus temperature curves (535 nm, heating rate 1 $Kmin^{-1}$, 0.01 wt.% solutions of polymers in water): (1) PNIPAAm; (2) Poly(BMDO-co-NIPAAm) with 3.9 mol% BMDO; (3) Poly(BMDO-co-NIPAAm) with 5.7 mol% BMDO; (4) Poly(BMDO-co-NIPAAm) with 8.3 mol% BMDO.

Table 3.1.5. LCST of poly(BMDO-co-NIPAAm)s; values based on Fig 3.1.7; M_n measured by Group THF GPC

Run	Copolym. Composition (molar ratio)		LCST (°C)	M_n	PDI
	BMDO	NIPAAm			
1	0	100	31.5	26000	3.2
2	3.9	96.1	26.8	34000	3.0
3	5.7	94.3	19.8	30000	3.4
4	8.3	91.7	13	24000	3.1
5	13.0	87.0	/	36000	3.0

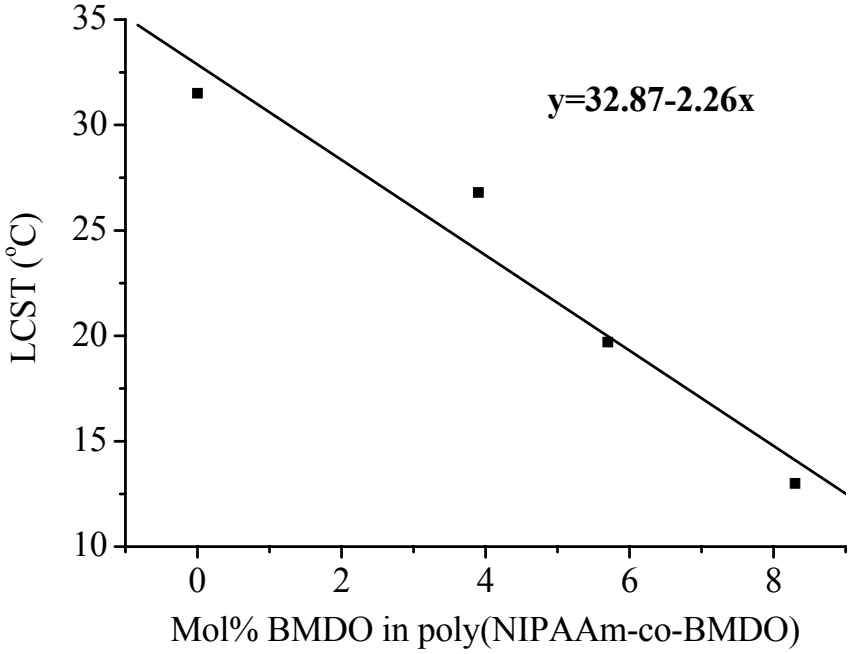

Fig 3.1.8. Variation of LCST with the amount of BMDO in poly(NIPAAm-co-BMDO) copolymers (values based on Table 3.1.5).

3.1.5. Degradability of poly(BMDO-co-NIPAAm)

The hydrolytic degradation behavior of the copolymers containing small amount of BMDO was also studied. The hydrolysis was carried out at very extreme basic conditions for poly(BMDO-co-NIPAAm). The representative GPC curves of the water soluble copolymer sample having LCST of 26.8°C [BMDO : NIPAAm = 4 : 96 (molar ratio)] before and after basic hydrolysis are shown in Fig 3.1.9. The high molecular weight peak (M_n = 49000, PDI = 3.7) disappeared after hydrolysis and shifted to a low molecular weight region (M_n = 1473, PDI = 3.9), thereby showing the hydrolytic degradation capability of new synthesized polymers, i.e., poly(NIPAAm-co-ester)s. This reconfirmed the random incorporation of very short ring-opened BMDO units into the PNIPAAm backbone to insure degradability even with small amount of BMDO in the copolymers. From the GPC curve we can see some amount of polymers with low molecular weights (with an eluent volume around 45 ml) remained before and after hydrolysis. From this point of view, they may be homo oligo (NIPAAm) generated during polymerizations. After hydrolysis in the same condition, the molecular weight of copolymer containing 8 mol% of BMDO was reduced from M_n = 31000 (PDI = 3.2) to M_n = 980 (PDI = 2.6).

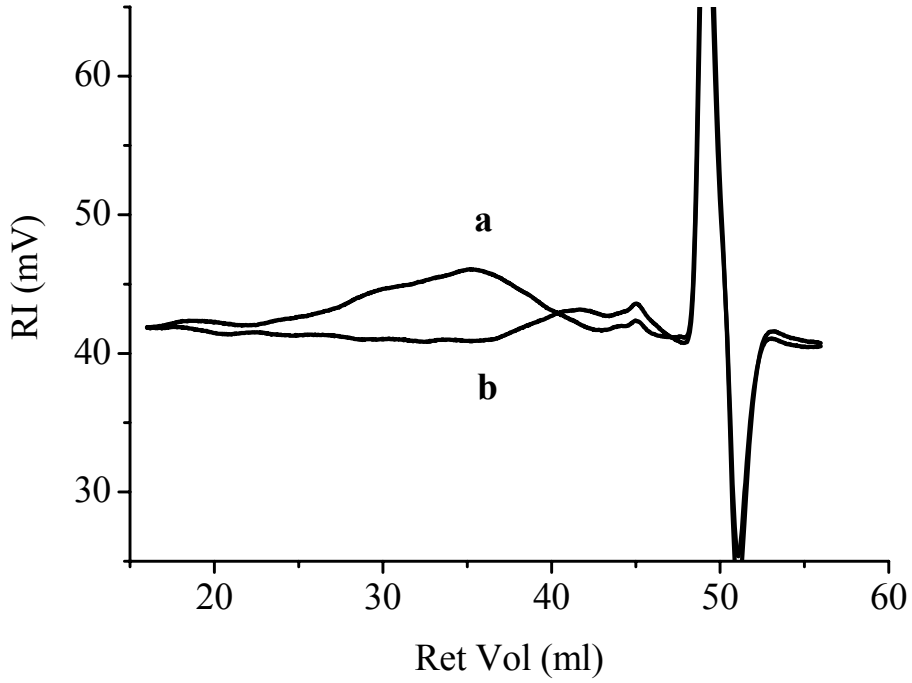

Fig 3.1.9. GPC traces of BMDO–NIPAAm copolymer (BMDO : NIPAAm = 4 : 96 molar ratio): (a) before hydrolytic degradation; (b) after hydrolytic degradation.

3.1.6. Conclusion

Degradable ester linkages are successfully introduced randomly onto the water soluble vinyl polymer PNIPAAm backbone by a combination of radical ring-opening polymerization and vinyl polymerization techniques. BMDO showed quantitative ring-opening during the copolymerization reactions and the amount of ester linkages could be increased by increasing the amount of the BMDO in the initial feed. The copolymers were found to be hydrolytically degradable and their properties like glass transition temperature and LCST can be controlled by controlling the amount of BMDO incorporated in the copolymers. Copolymers with low mol-% of BMDO (till about 9 mol%) were found to be soluble in water and showed hydrolytic degradability also. This behavior could be of great interest for many different biomedical applications.

3.2. Copolymerization behavior of CKAs with vinyl acid monomers

Reference: Ren, Liqun; Agarwal, Seema; Macromolecules; 2007, 40, 7834.

3.2.1. Introduction

Cyclic ketene acetals can be randomly copolymerized with a variety of neutral vinyl monomers to synthesize degradable vinyl polymers. It is possible to combine degradability and other functionalities of vinyl polymers to generate a new class of materials. As is shown in the previous chapter, degradable thermo-responsive polymer was successfully synthesized with varied lower critical solution temperatures (LCST)s by copolymerization of BMDO with N-isopropylacrylamide. Now in an attempt to synthesize water soluble degradable polymers, free radical copolymerization behavior of BMDO with methacrylic acid (MAA) was studied. The copolymerization was done by changing the molar ratio of two monomers in the feed.

Generally, copolymerization of cyclic ketene acetals with vinyl monomers under free radical polymerization conditions leads to any of the four pathways shown in the Scheme 3.2.1 depending on the reaction conditions, i.e. the type of the initiator, its amount, temperature of the reaction, monomer feed radio etc. However for the system of BMDO and methacrylic acid (MAA), unexpected results were observed. The resulting copolymers were not in accordance with the four paths shown in the Scheme 3.2.1. In order to explore the real copolymerization route and establish the structure of the new polymer obtained, the properties of the monomers were intensively investigated. The detailed characterization of the resulting polymers is presented using 1D and 2D NMR techniques.

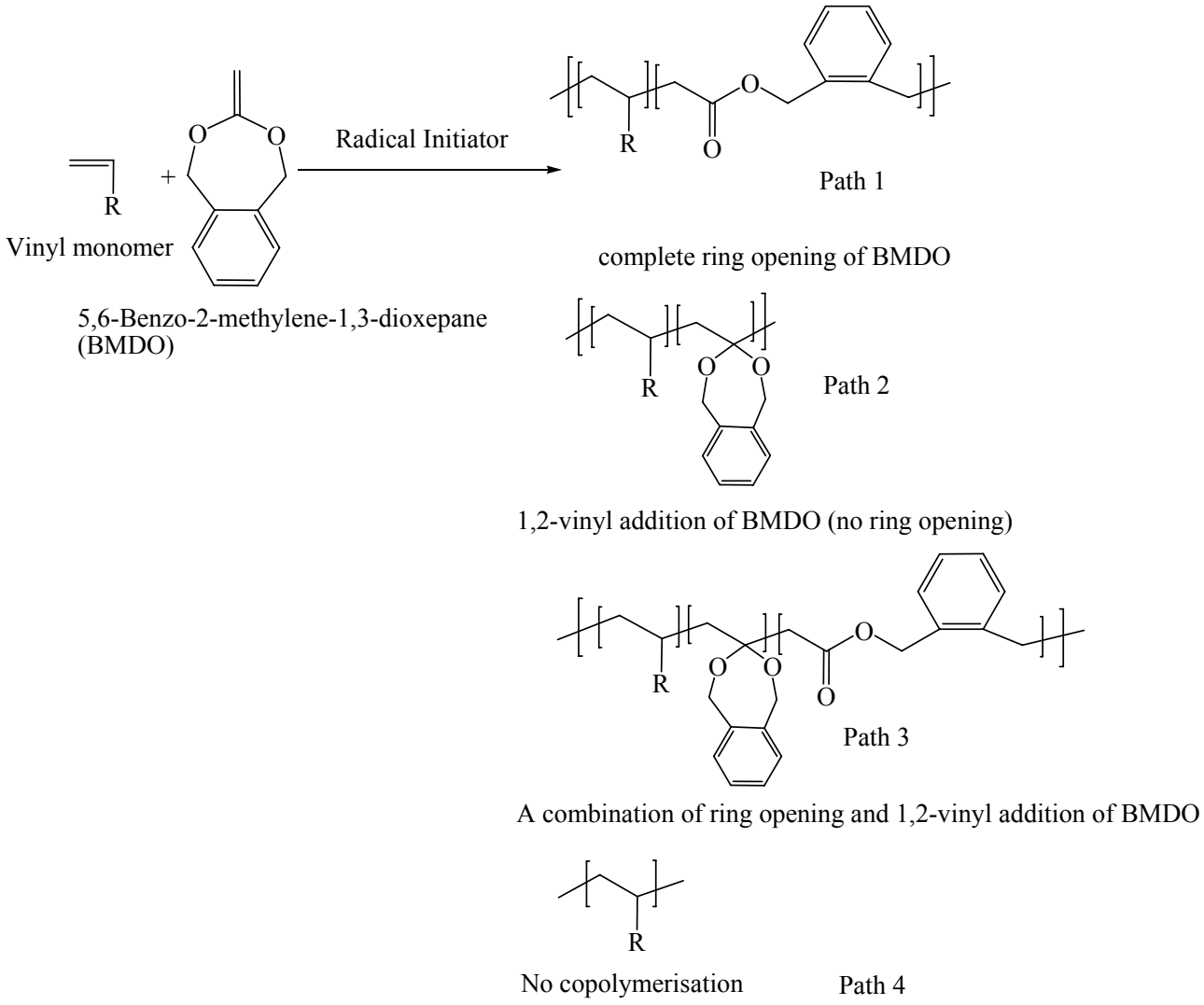

Scheme 3.2.1. General copolymerization routes of cyclic ketene acetals and vinyl monomers.

3.2.2. Reaction of BMDO with Brönsted acids.

Considering the structure of one of the most common cyclic ketene acetals, 5,6-benzo-2-methylene-1,3-dioxepane (BMDO), the double bond is highly electron rich due to donation of two oxygen atoms. It is found that the double bond of BMDO can be easily protonated at room temperature by Brönsted acids, including organic acids, water or some types of alcohols. The possibility of protonation and the reaction rate are determined by the strength of Brönsted acids, which can be compared by acid dissociation constant (Ka) or the pKa values ($pKa = -\log_{10}Ka$)

3.2.2.1. Reaction of BMDO with methacrylic acid (MAA)

3.2.2.1.1. Instantaneous reaction at room temperature

Instantaneous quantitative addition of acidic vinyl monomer, MAA (pKa = 4.66), to the double bond of BMDO took place at room temperature, generating a new vinyl monomer 3-methyl-1, 5-dihydrobenzo[e] [1,3]dioxepin-3-yl methacrylate (A) keeping the seven membered ring of BMDO intact, as shown in the Scheme 3.2.2. The new material A was obtained as a colorless highly viscous liquid, stable at room temperature with protection of Argon and was characterized using different NMR spectroscopic techniques. The representative ^{1}H and ^{13}C-NMR of the new vinyl monomer A formed after 5 mins of mixing MAA and BMDO (mol 1 : 1) at room temperature (25^{o}C) is shown in Fig 3.2.1 and 3.2.2, respectively.

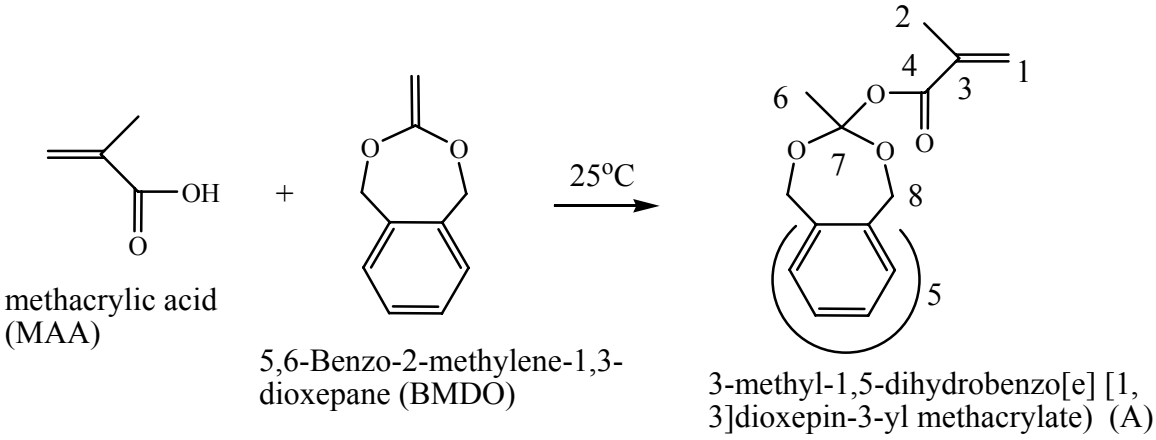

Scheme 3.2.2. Instantaneous reaction of BMDO with MMA at room temperature.

Compared to ^{1}H-NMR spectrum of BMDO, the double bond protons of the starting BMDO disappears at ppm 3.4 (6′), a signature of its structure change on mixing with MAA. In the lower ppm region between ppm 1.75-1.9 two overlapping peaks are assigned to the two methyl groups, i.e. methyl group of MAA and methyl group generated by addition MAA to the double bond of BMDO (protons 2 and 6). The ratio of the peak areas of the protons 8 : 5 : 1 : 2+6 as determined from the ^{1}H-NMR spectrum is in accordance with the structure A (3-methyl-1,5-dihydrobenzo[e] [1, 3]dioxepin-3-yl methacrylate). A very negligible peak at around ppm 11 from the acidic proton (–COO*H*) (marked x in the Fig 3.2.1) from methacrylic acid is found. This may from the unreacted MAA. The purity of the new material A is as much as 99%, which is determined from ^{1}H-NMR from the ratio of peak intensities at ppm 5.45-6.05 (2s, 2H, CH_2=C(CH_3)COO–) of structure 1 and

ppm 10.89 (s, 1H, –COO*H*) from unreacted MAA.

In the ^{13}C-NMR spectrum (Fig 3.2.2), (–$CH_2C_6H_4CH_2$–; 5), (–$CH_2C_6H_4CH_2$–; 8), and (CH_2=C(CH_3)–; 1) are assigned using 2D ^{1}H-^{13}C HMQC-NMR correlation studies (Fig 3.2.3), which has cross peaks A, B and C, respectively. The methyl proton peaks (2 and 6) shows unambiguous correlations (D) and (E) with two carbon peaks between ppm 17-20 respectively. The peak at ppm 117.2 without correlation in the HMQC-NMR spectrum is assigned to the quaternary carbon 7.

The correctness of the assignment is confirmed by ^{1}H-^{13}C HMBC-NMR correlation technique (Fig 3.2.4). The methyl proton at ppm 1.82 produces correlation peaks with signals from carbon 1 (A), 3 (B) and 4(C). While the methyl proton at ppm 1.84 produces correlation peaks with signals from carbon atom at ppm 117.24 (7) (D) and carbon atom at ppm 64.7 (8) (E). This clearly shows the peak at ppm 1.82 to be from carbon 2 and the one at ppm 1.87 from the carbon 6. The peak at ppm 117.2 besides showing correlation with the carbon 6 (D) also shows two more correlation peaks with signals from protons 8 (F and G) thereby showing the correctness of assignment of this peak as quaternary carbon 7. Carbon 3 shows no correlation in 2D HMQC-NMR spectrum but showes correlations with proton 1 (J) and proton 2 (B) in 2D HMBC-NMR spectrum. There is only one carbonyl peak around 163.18 ppm (a minor negligible signal is seen at ppm 179.55 from unreacted MAA impurity), in ^{13}C-NMR (shown in Fig 3.2.2) having three-bond correlations in ^{1}H-^{13}C HMBC-NMR with protons at 6.05/5.45 ppm (CH_2=C(CH_3)–) (cross-peaks H and I) and at 1.82 ppm (CH_2=C(CH_3)–) (cross-peak C), which also speaks in favor of the correct characterization of the new vinyl monomer formed with only one ester group and with intact seven membered ring of BMDO (structure A; Scheme 4.2).

Fig 3.2.5 shows the ^{1}H-NMR spectra of the product formed after mixing BMDO and MAA for different intervals of time at 25^{o}C. The reaction is in fact instantaneous. From 5 mins till 24 hrs after mixing BMDO and MAA, the ratio of peak intensities of the protons 8 : 5 : 1 : 2+6 remains the same and matched with that of structure A. The new vinyl monomer is stable at room temperature (25^{o}C) under Argon.

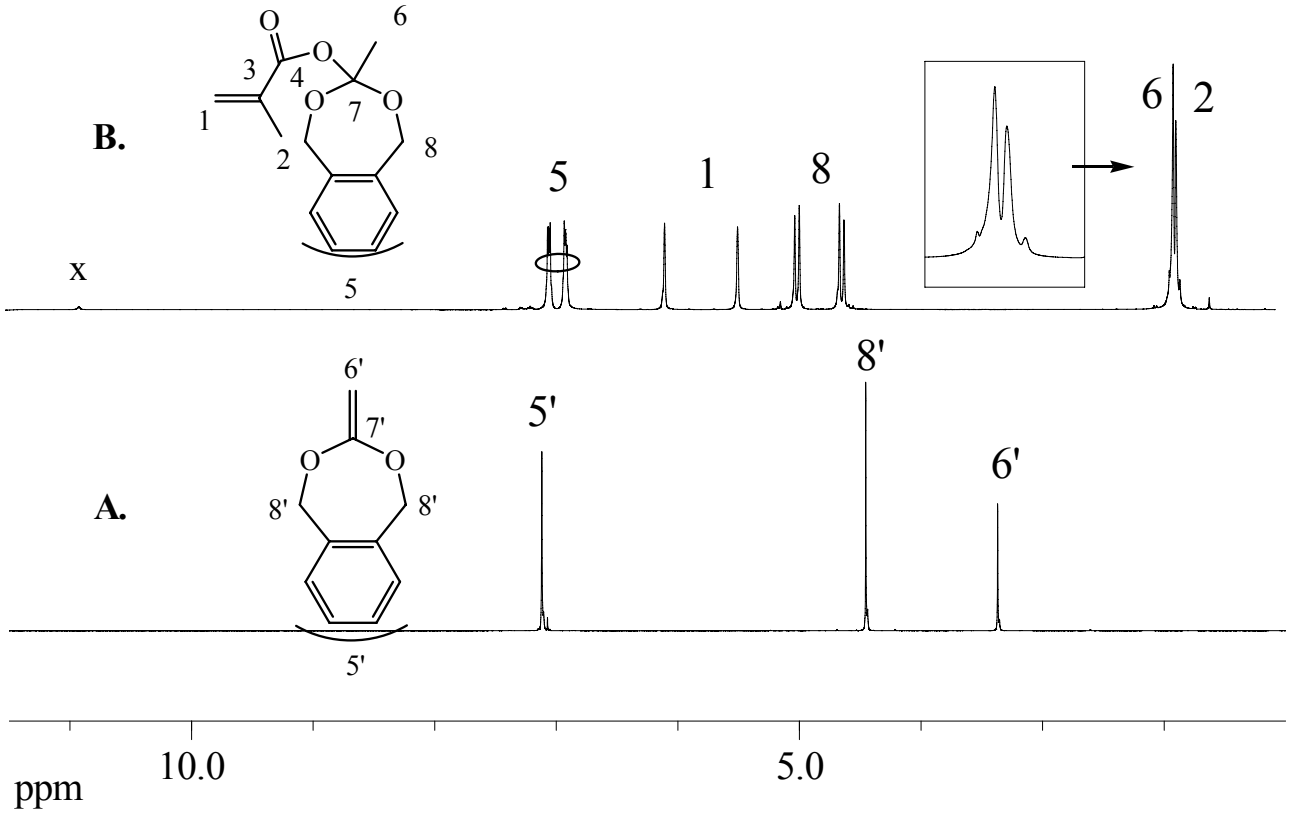

Fig 3.2.1. ^{1}H-NMR spectrum of (A) BMDO; (B) the product formed after 5 mins of mixing MAA and BMDO (1 : 1 in molar ratio） at room temperature.

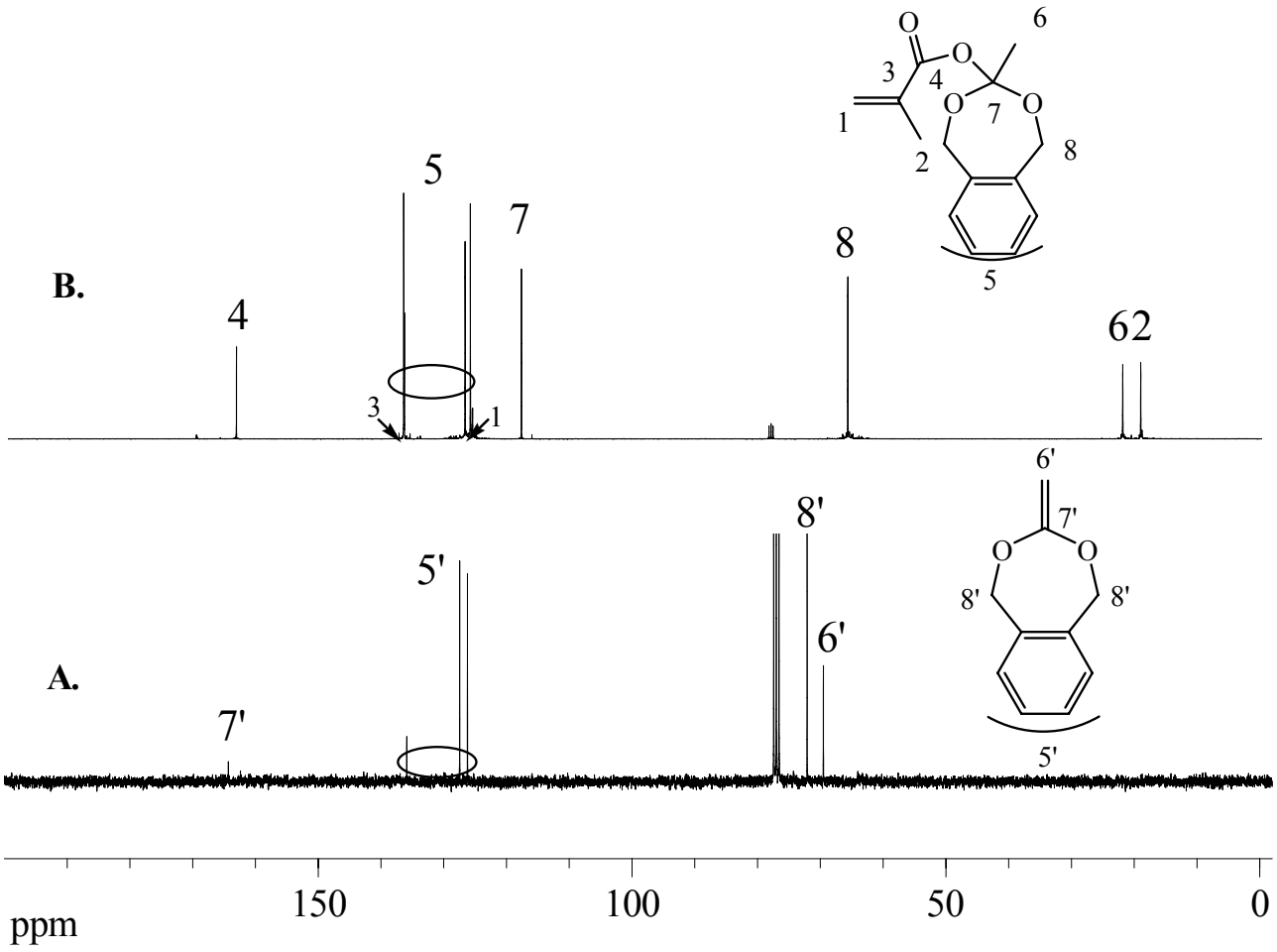

Fig 3.2.2. ^{13}C-NMR spectrum of (A) BMDO and (B) the product formed after 5 mins of mixing BMDO and MAA (1 : 1 in molar ratio) at room temperature.

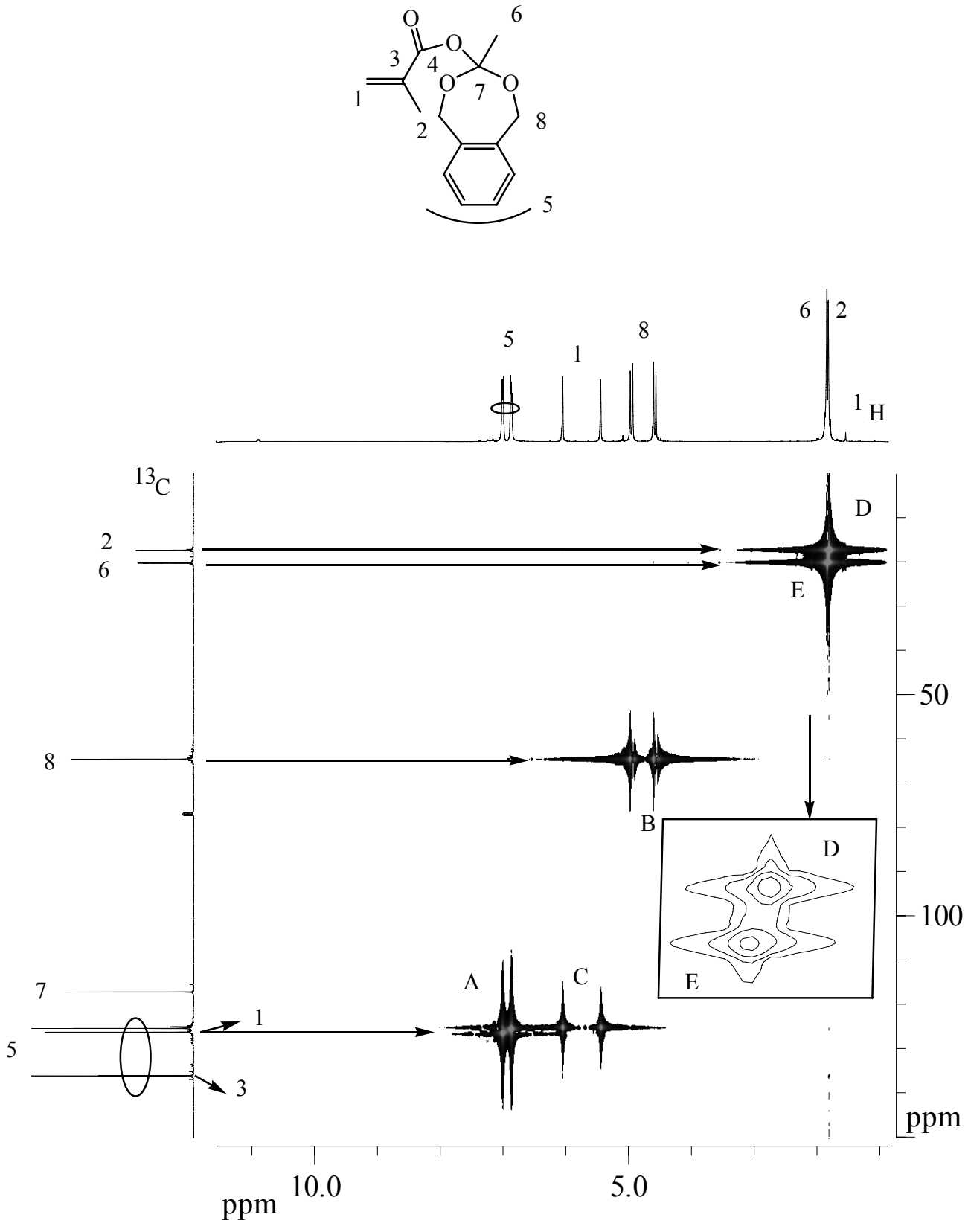

Fig 3.2.3. 2D ^{1}H-^{13}C HMQC-NMR spectrum of structure A.

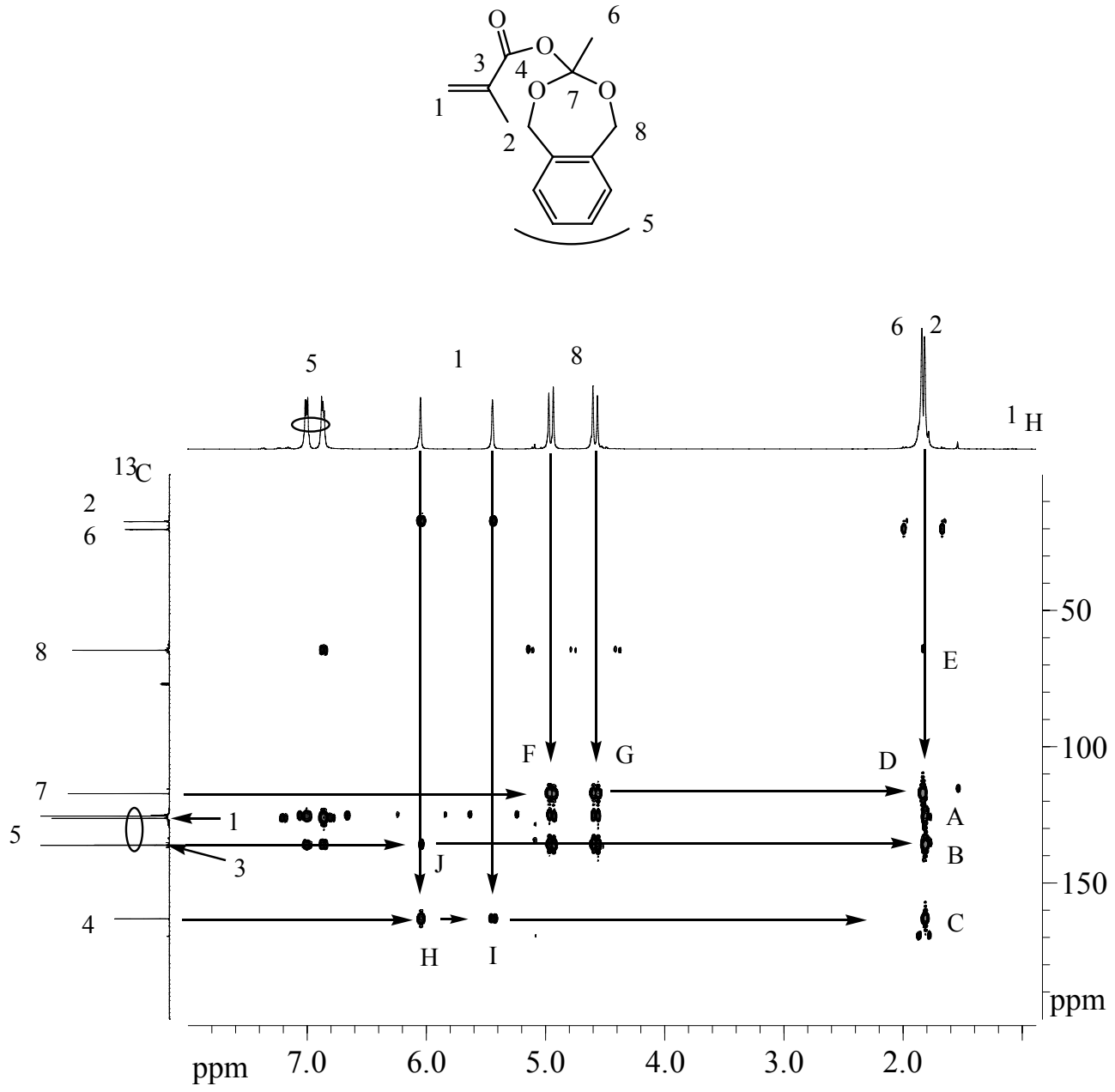

Fig 3.2.4. 2D ^{1}H-^{13}C HMBC-NMR spectrum of structure A.

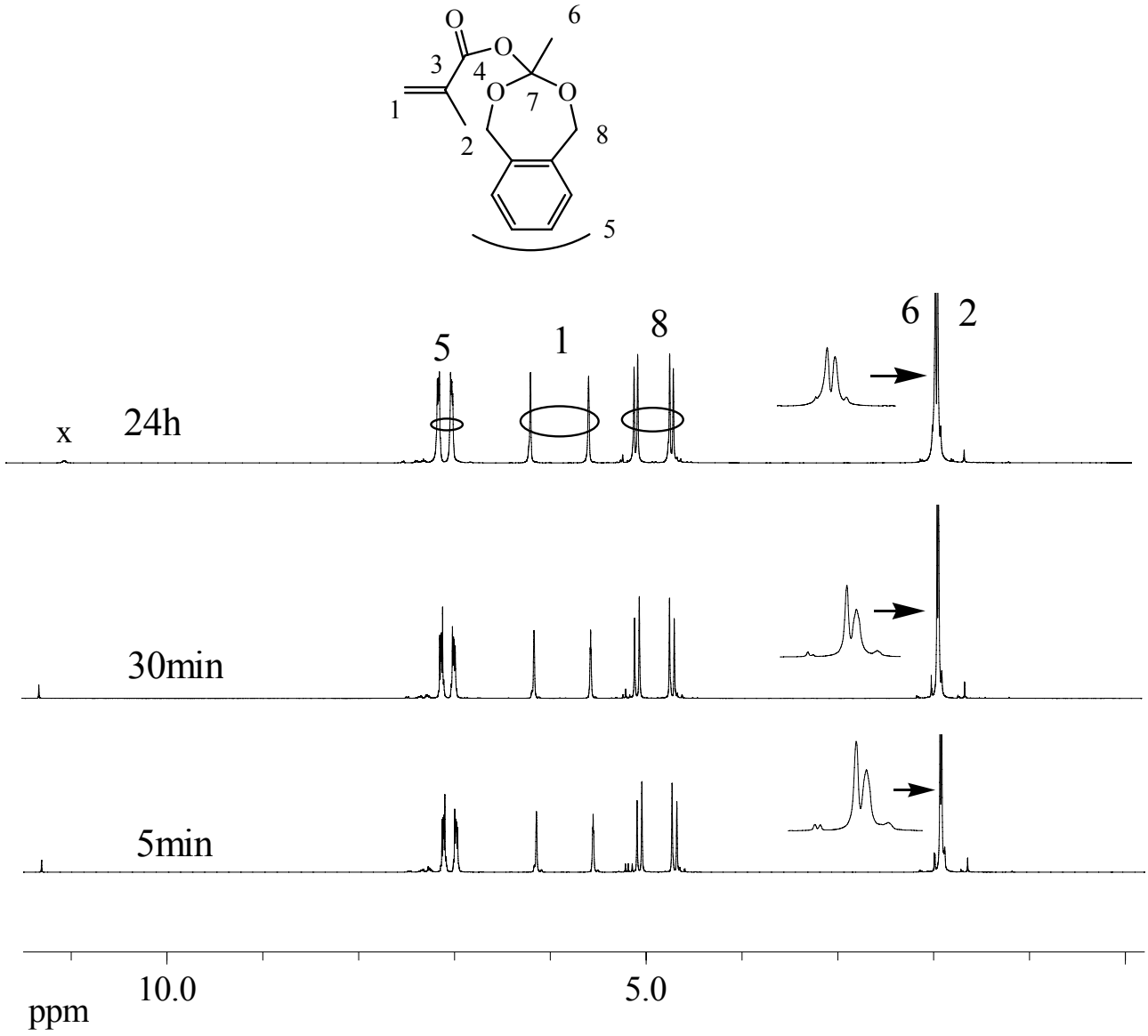

Fig 3.2.5. ^{1}H-NMR spectrum of the product formed after mixing MAA and BMDO (1 : 1 in molar ratio) at different intervals of time.

3.2.2.1.2. Structural changes at higher temperatures

The resulting product of BMDO and MAA, (A) in Scheme 3.2.2, is sensitive to heating, even protected under Argon. The seven-membered ring has the tendency to open up by rearrangement and a new ester group is formed. The new structure B is shown in Scheme 3.2.3. The possibility and the rate of ring-opening reaction of A was dependent upon temperature. At higher temperature (120^{o}C) which is general used for radical ring-opening polymerization of BMDO or its copolymerization with other vinyl monomers, the complete ring opening of structure A was observed after 15 minutes to give another new vinyl monomer having structure B (Scheme 3.2.3). At lower temperature of 60^{o}C, the ring opening was a slow process and gave a mixture of opened

and unopened structures after 30 minutes.

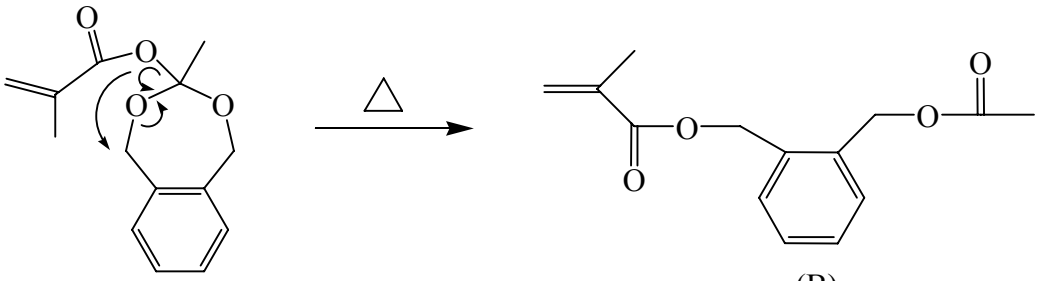

(A) (B)

Scheme 3.2.3. Structural rearrangement of product A under higher temperatures.

^{1}H-NMR spectrum (Fig 3.2.6) shows 75 mol% of the opened structures at 60^{o}C after 30 minutes. Due to the ring-opening, in ^{13}C-NMR spectrum (Fig 3.2.7) two new ester peaks around ppm 170.46 and ppm 166.76 are found, which are assigned to the carbon atoms 7″ and 4″ respectively of the new structure B. The complete disappearance of the quaternary carbon peak (7) at 120^{o}C signifies the opened structure B.

3.2.2.2. Reaction of BMDO with other Brönsted acids.

Not only methacrylic acid (MAA), the double bond of BMDO can be protonated by other organic acids, some of alcohols and water.

3.2.2.2.1. Acetic acid

It is found out that the double bond of BMDO also can be immediately protonated by acetic acid (pKa = 4.78). ^{1}H-NMR spectrum and ^{13}C-NMR spectrum are shown in Fig 3.2.8 and Fig 3.2.9, respectively. The integrations of the peaks in ^{1}H-NMR spectrum are in agreement with the peak assignments. Fig 3.2.8 shows the instantaneous 100% acid addition of BMDO with acetic acid at room temperature. The peak at 117.6 ppm in the ^{13}C-NMR spectrum (Fig 3.2.9) shows the existence of the quaternary carbon atom and, therefore, indicated the ring-structure of the product.

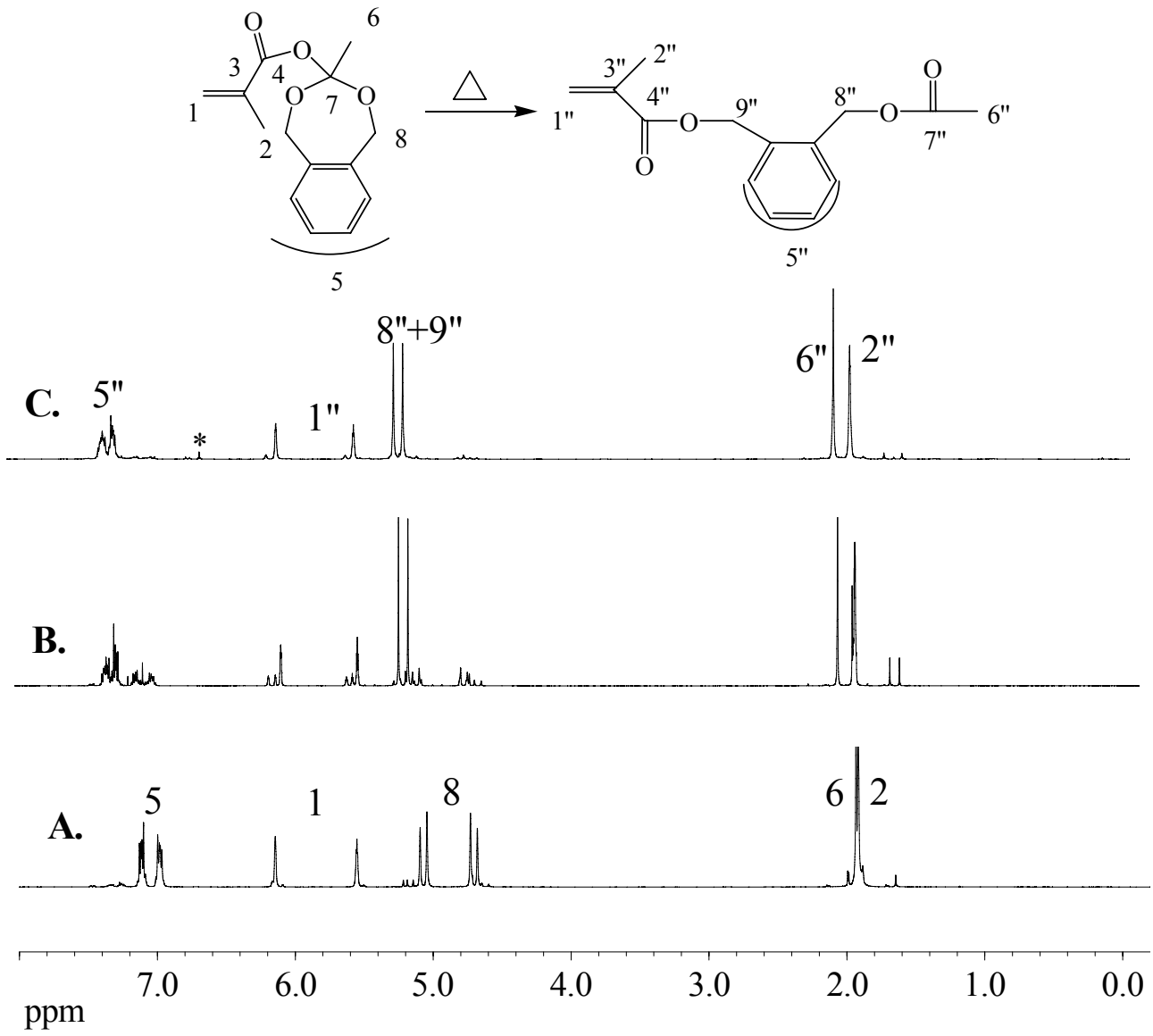

Fig 3.2.6. ^{1}H-NMR spectrum of the new vinyl monomer A (A) overnight under RT;
(B) 30 mins after heating at 60^{o}C; (C) 15 mins after heating at 120^{o}C; *: signal from hydroquinone.

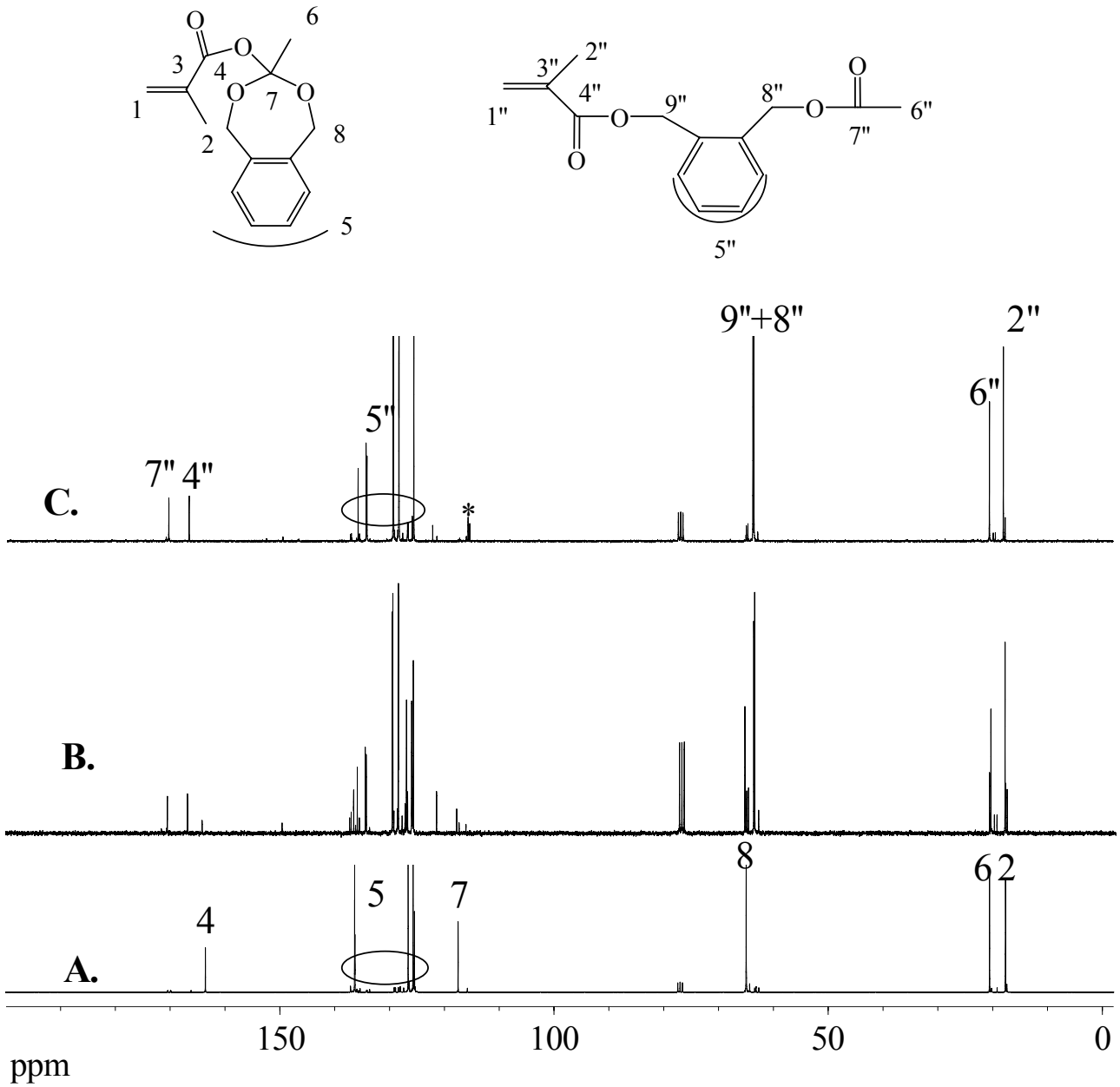

Fig 3.2.7. ^{13}C-NMR spectrum of the new vinyl monomer A (A) overnight at RT;
(B) after 30 mins of heating at 60^{o}C; (C) after 15 mins of heating at 120^{o}C; *: signal from hydroquinone.

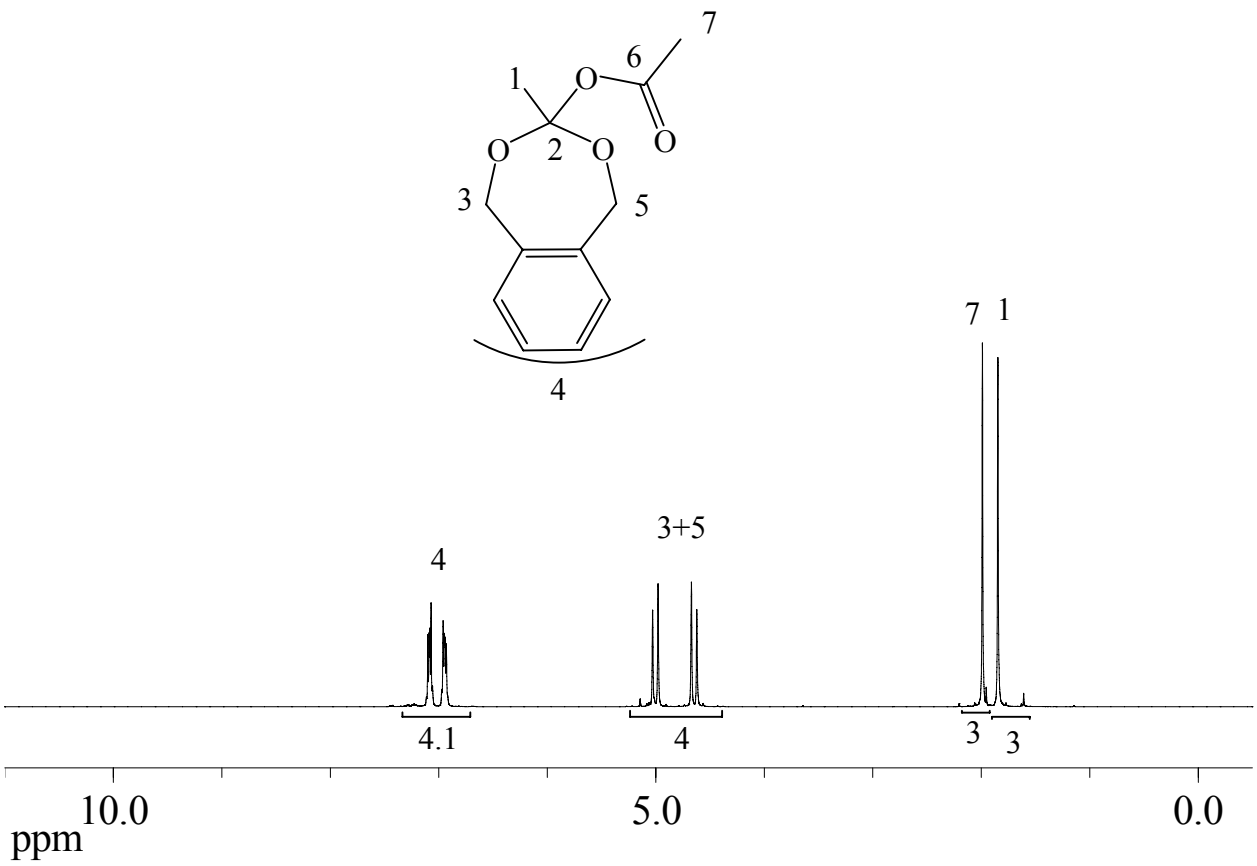

Fig 3.2.8. ^{1}H-NMR spectrum of the product formed after 10 mins of mixing BMDO and acetic acid (1 : 1 molar ratio) at room temperature ($CDCl_3$ as solvent).

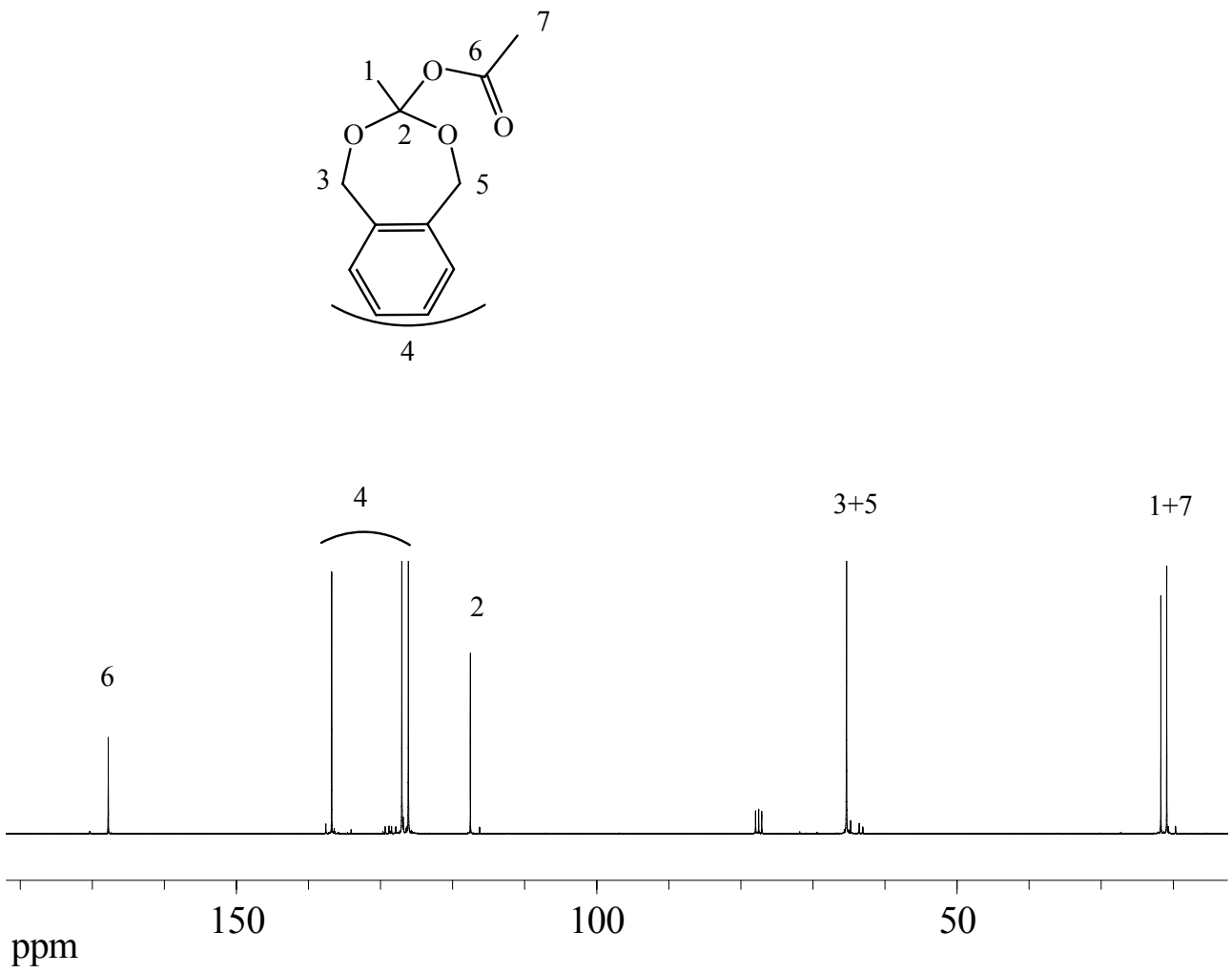

Fig 3.2.9. ^{13}C-NMR spectrum of the product formed after 10 mins of mixing BMDO and acetic acid (1 : 1 molar ratio) at room temperature.

3.2.2.2.2. Water

Comparing to methacrylic acid or acetic acid, water has a relative high pKa of 15.7. It is found out that BMDO reacted with water relatively slowly. 100% acid addition to the double bond of BMDO was achieved after 24 hrs in the presence of water at RT under Argon. Different from the product of BMDO with methacrylic acid, ^{1}H-NMR spectrum in Fig 3.2.10 shows the existence of 3-methyl-1,5-dihydrobenzo-[e][1,3]dioxepin-3-ol (structure C) and 2-(hydroxymethyl)benzyl acetate (structure D) after 24 hrs of mixing at RT. Based on the integrations of the peaks at 2.0 ppm (proton 5) and 1.6 ppm (proton 1), the molar ratio of C : D is roughly found to be 43 : 57.

The acid addition to the double bond of BMDO proceeds relatively faster at 70^{o}C compared to that at room temperature. Fig 3.2.11 shows the ^{1}H-NMR spectrum after mixing BMDO and water at

70°C. Based on the integrations of the peaks at 3.65 ppm (proton 1′) and 7.49-6.97 ppm (aromatic protons 3′, 3, 7), it is roughly found out that 25% of BMDO is protonated after 1 hr and 75% of BMDO is protonated after 2 hrs. Higher temperature also leads to faster structural transition of C to D. The molar ratio of C : D is found to be 27 : 73 after 1 hr and 19 : 81 after 2 hrs at 70°C by mixing BMDO and water.

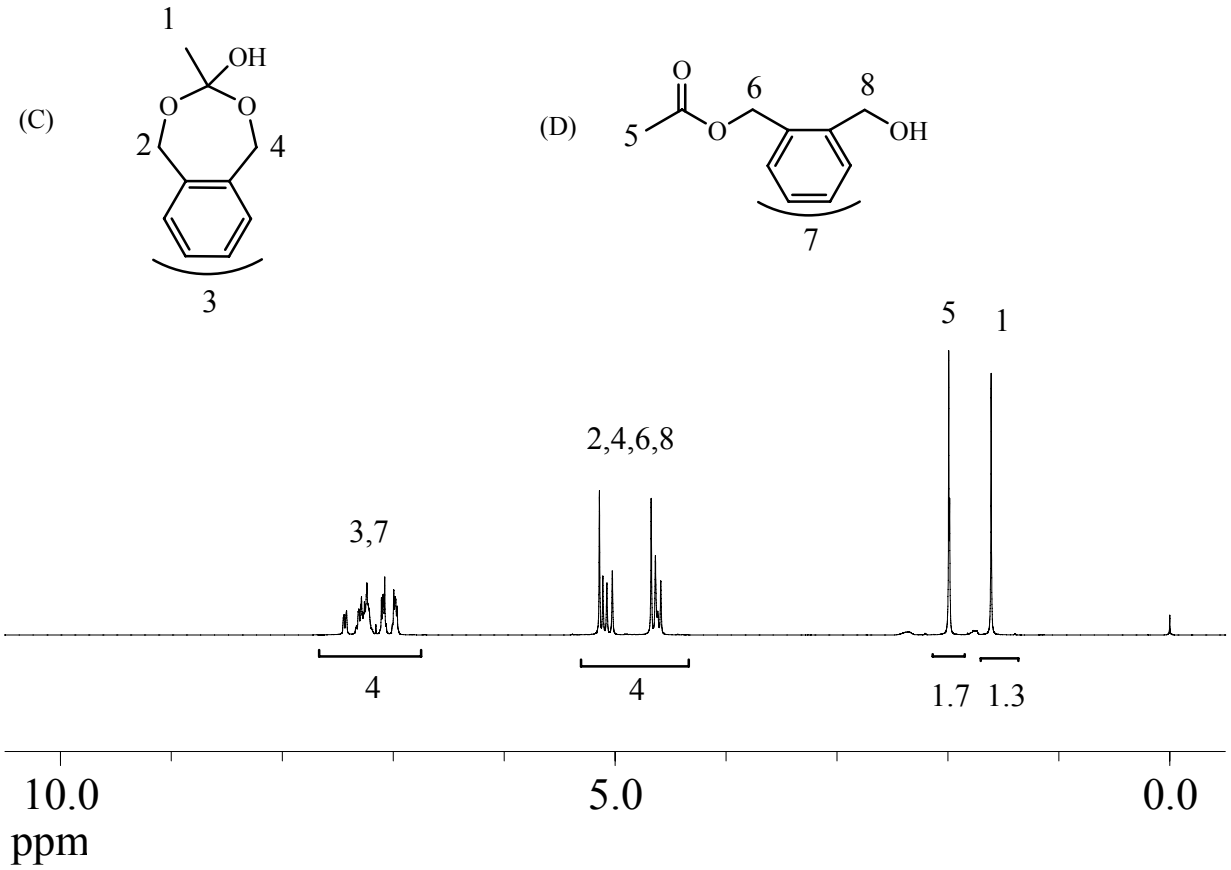

Fig 3.2.10. ^{1}H-NMR spectrum of the product formed after 24 hrs of mixing BMDO and H_2O (1 : 1 molar ratio) ($CDCl_3$ as solvent).

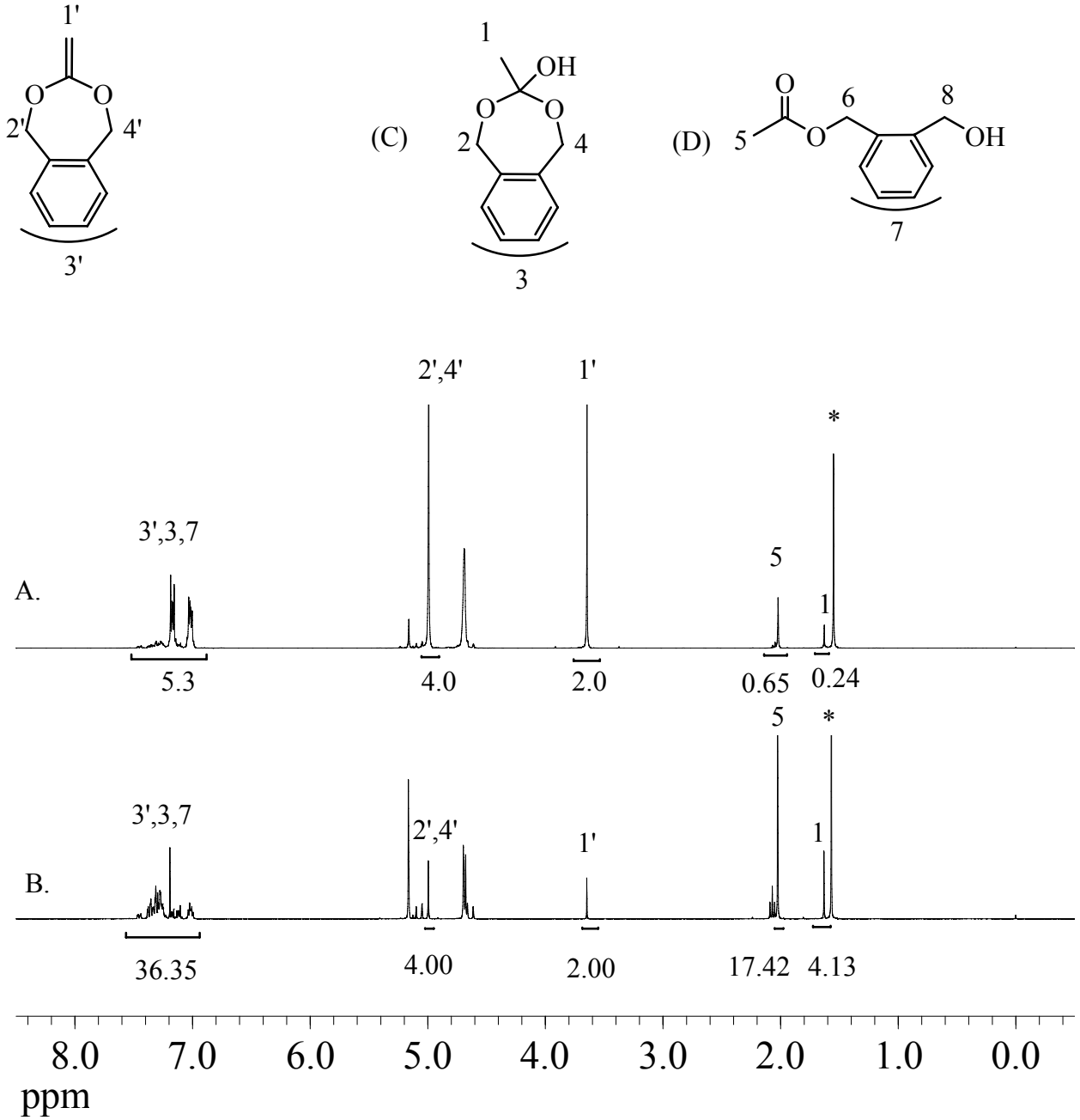

Fig 3.2.11. ^{1}H-NMR spectrum of the product formed after (A) 1 hr and (B) 2 hrs of mixing BMDO and H_2O at 70^{o}C (H_2O in excess, $CDCl_3$ as solvent, *: signal from water).

3.2.2.2.3. Alcohols

BMDO also reacts with some types of alcohols, which has a relatively low pKa. Methanol (pKa = 15.5) was found to be able to protonate the double bond of BMDO in the similar way as water. When pKa increased to 18, e.g. t-butanol, BMDO turned to be very stable with the presence of alcohols. Considering the error with handling the experiment, Fig 3.2.12 showed almost 100% stability of BMDO after 48 hrs with the presence of t-butanol. Therefore, only Brönsted acids with a pKa less than 18 can protonate BMDO.

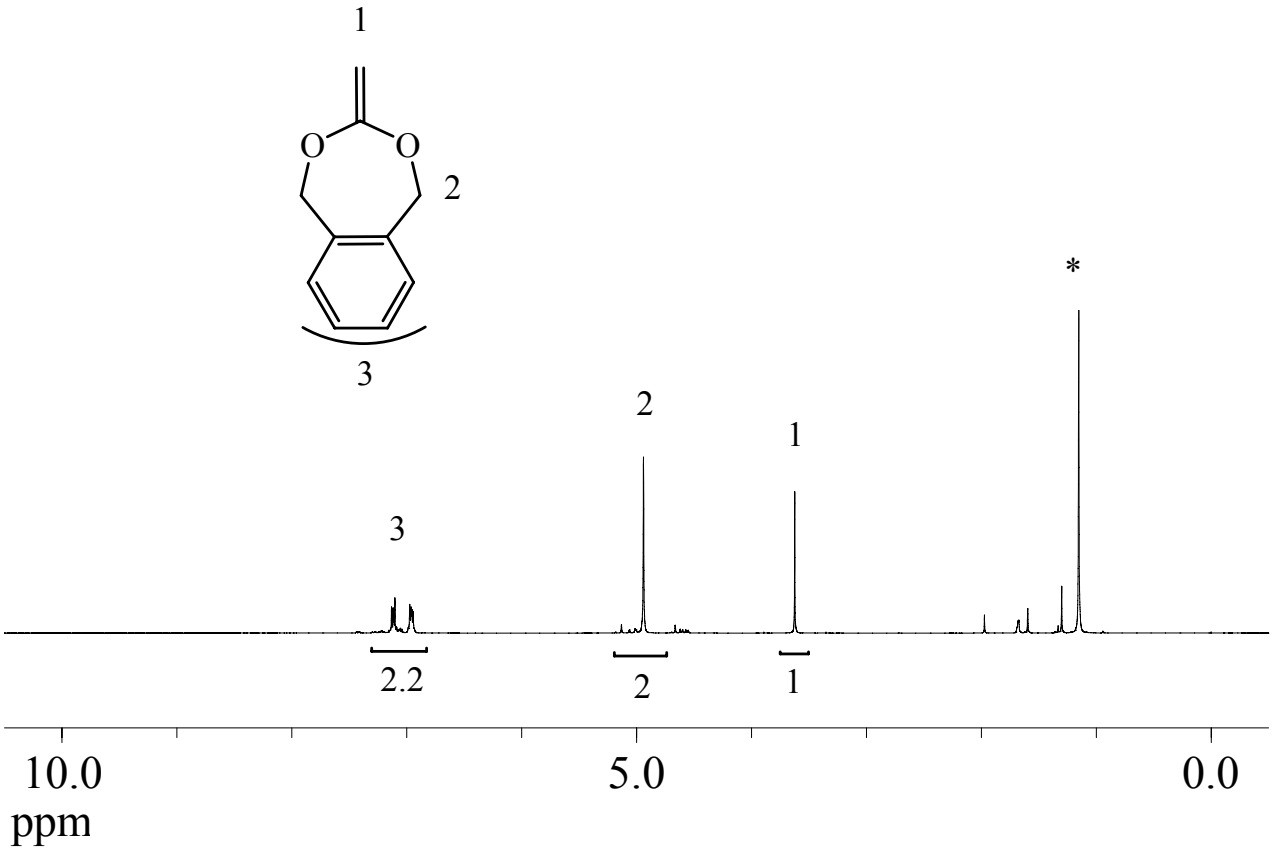

Fig 3.2.12. ^{1}H-NMR spectrum of BMDO after 48 hrs of mixing it and excess t-butanol ($CDCl_3$ as solvent ∗: signal from excess t-butanol).

3.2.3. Copolymerization behavior of BMDO and MAA

3.2.3.1. Copolymerization routes

After establishing the behavior of a simple reaction mixture of BMDO and MAA at different temperatures (25^{o}C and 120^{o}C), the copolymerization behavior of the two monomers BMDO and MAA was studied using radical initiator like dtBp. The reactions of BMDO and MAA with different molar ratios were carried out for 6hrs using 50 : 1 molar ratio of total monomers: initiator at 120^{o}C. The characterization using 1D and 2D NMR techniques shows that the copolymerization of BMDO with MAA does not follow any of the conventional routes given in the literature till now but followed via in situ formation of structure A and afterwards simultaneous ring opening of the seven membered ring with the formation of structure B and its further copolymerization with remaining MAA or BMDO giving copolymer structures with ester linkages in the side chain (Scheme 3.2.4).

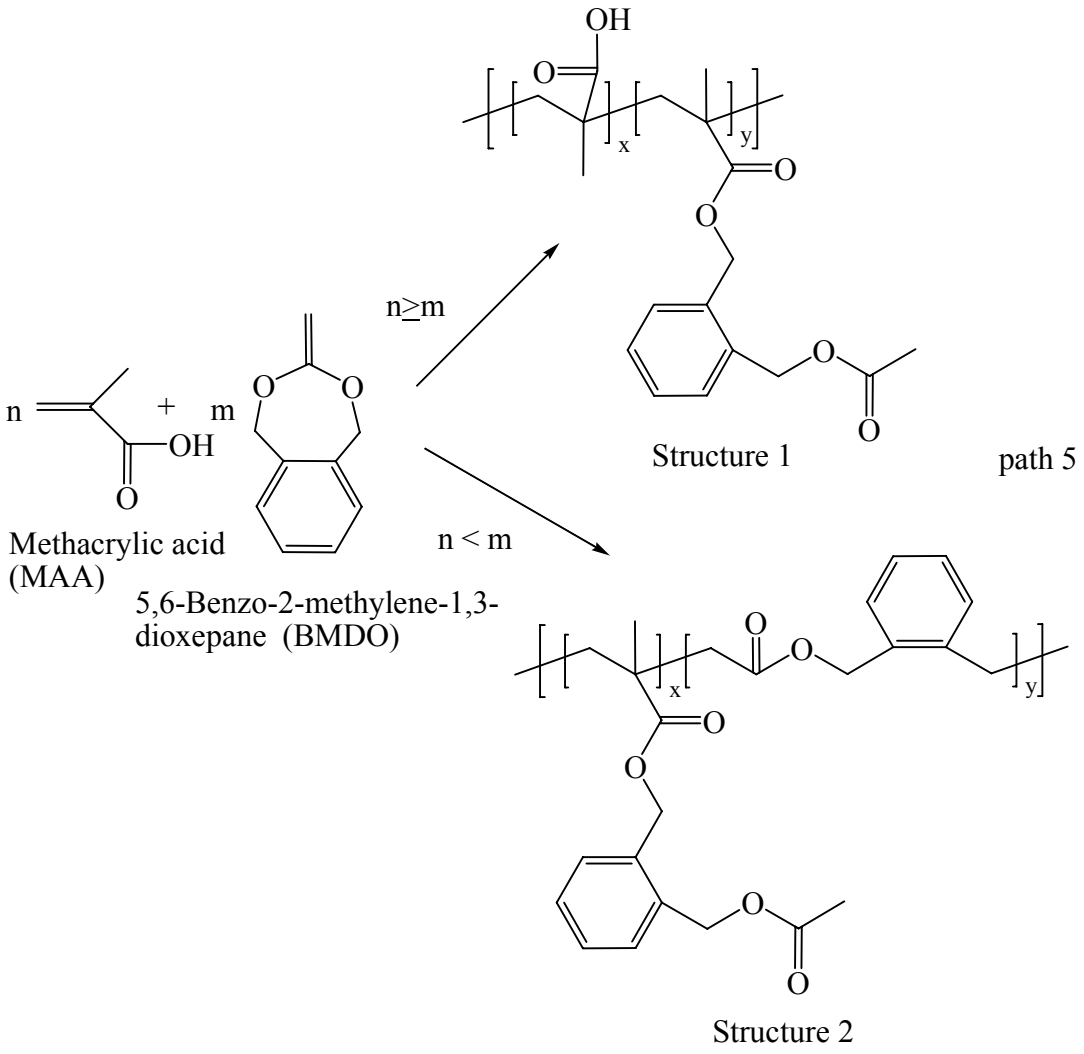

Scheme 3.2.4. Unconventional copolymerization routes of BMDO and MAA.

3.2.3.2. Structure characterization of poly(B-co-MAA)

First, polymerization of BMDO and MAA with the molar ratio of 1 : 1 was carried out for 6 hrs using 50 : 1 molar ratio of total monomers: initiator at 120°C. The ^{1}H-NMR and ^{13}C-NMR spectra are shown in the Fig 3.2.13.

The proton peaks in ^{1}H-NMR spectrum are assigned as shown in the Fig 3.2.13A. The two overlapping methylene proton peaks (–C*H*$_2$C$_6$H$_4$C*H*$_2$–; (8, 9)) between ppm 5-5.4 and the methyl proton peak (–OCOC*H*$_3$; 6) indicate the existence of B sequences in the product. The proton peaks of (–C*H*$_2$COOCH$_2$C$_6$H$_4$C*H*$_2$–) between ppm 2 to 3 are not shown up in the spectrum, demonstrating

the absence of ester groups in the backbones. The peak at ppm 12.5 shows the presence of free –COOH groups (marked X) of MAA sequences in the polymer.

The peaks in ^{13}C-NMR spectrum (Fig 3.2.13B) are assigned using 2D HMQC technique and the corresponding correlations are shown in the Fig 3.2.14. No peak is seen around 100-120 ppm, clearly ruling out the paths 2 and 3 of scheme 3.2.1 and also ruling out the formation of corresponding polymer from structure A with retainment of the BMDO ring. Besides one peak from DMF in the carbonyl carbon region, a single sharp peak at ppm 169.8 (–*C*OOCH$_3$ from B; 7) and a multiplet in the region around ppm 175-178 (–*C*OOH from MAA; 4) are observed.

The further confirmation of the structure of poly(B-co-MAA) was done using HMBC technique (Fig 3.2.15). In HMBC spectrum, proton 6 in the ^{1}H-NMR spectrum shows two clear cross peaks with carbon 8 at ppm 63.4 (A) and one signal in the carbonyl carbon region at ppm 169.8 (B). This suggests that the carbonyl carbon peak at ppm 169.8 is from the new ester group (7) from BMDO after ring-opening of the protonated structure A. The carbon peaks in the region around ppm 175.5-177 shows correlations with the proton peak 9 (C) and with the peaks in the ppm region 0.6-1.2 (D) and therefore is assigned to the carbonyl carbon (4) attached to the polymer backbone. The carbon peaks in the region around ppm 181-183 show ^{1}H-^{13}C correlations with proton peaks in the lower ppm region i.e. ppm 0.8-1.2 (E) in HMBC-NMR spectrum (Fig 3.2.15), demonstrating again the presence of some amount of methacrylic acid units also in the copolymer. This also shows that the lower ppm region 0.8-1.2 besides having protons from structure B (i.e. protons 1, 2 and 6) should also have contribution from aliphatic protons –CH$_2$– and –CH$_3$– of MAA unit in the copolymer.

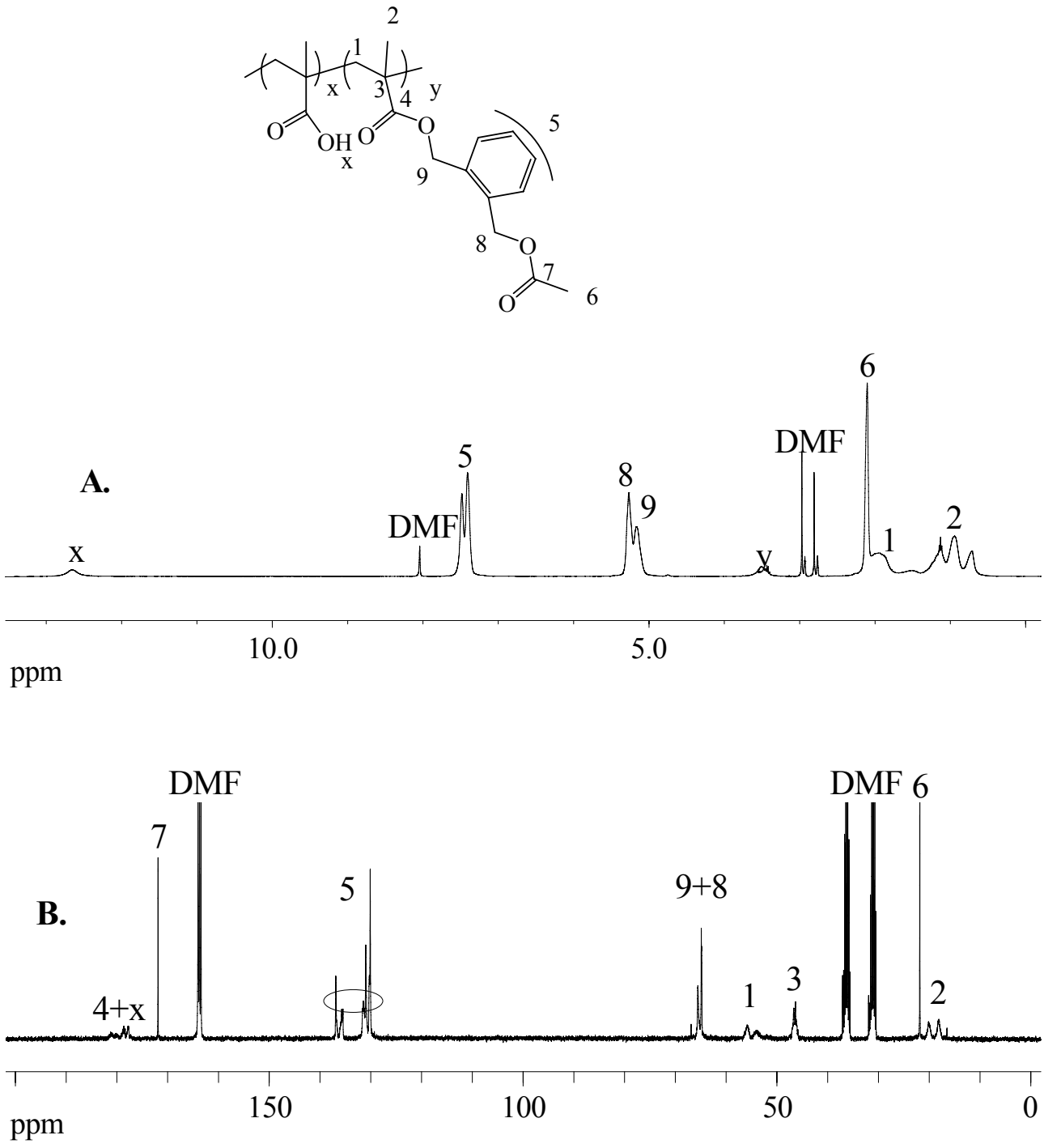

Fig 3.2.13. (A) ^{1}H-NMR spectrum and (B) ^{13}C-NMR spectrum in deuterated dimethylformamide (DMF) of poly (B-co-MAA) made using 1 : 1 molar ratio of 5,6-benzo-2-methylene-1,3-dioxepane (BMDO) : methacrylic acid (MAA) in the feed at 120^{o}C for 6 hrs.

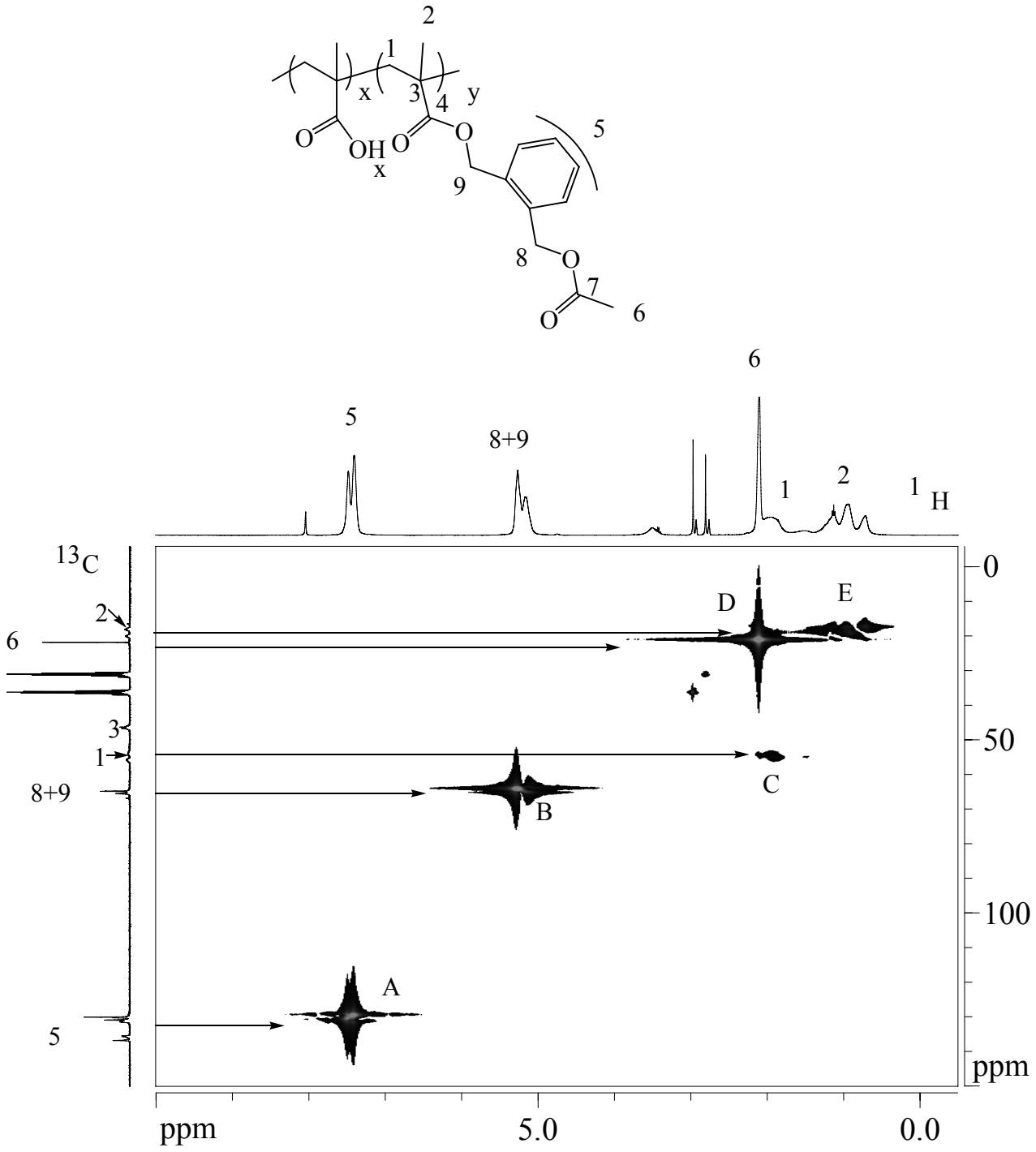

Fig 3.2.14. 2D ^{1}H-^{13}C HMQC-NMR spectrum of poly(B-co-MAA) made using 1 : 1 molar ratio of BMDO : MAA in the feed at 120^{o}C for 6 hrs in DMF.

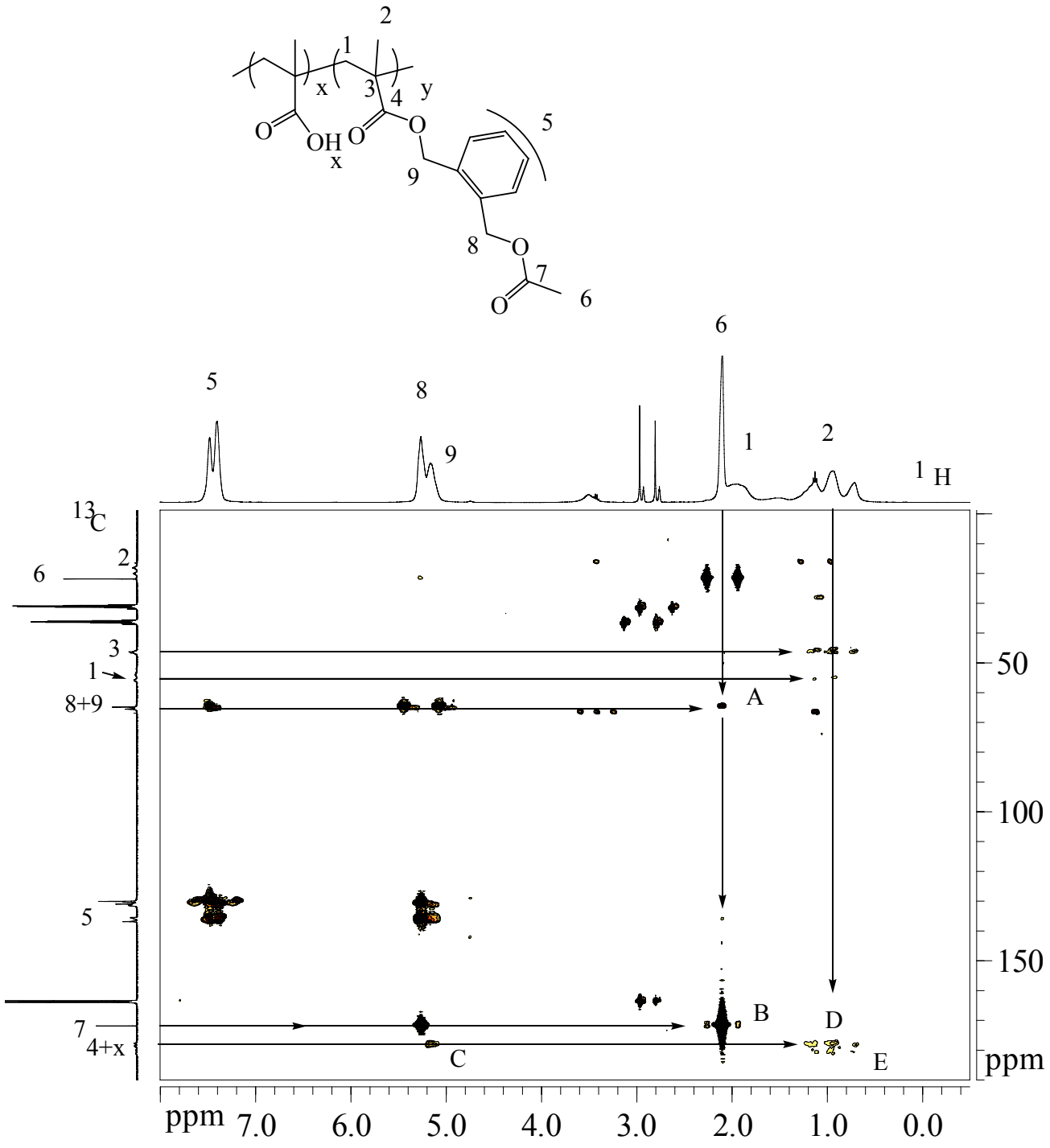

Fig 3.2.15. 2D ^{1}H-^{13}C HMBC-NMR spectrum of poly (B-co-MAA) made using 1 : 1 molar ratio of BMDO : MAA in the feed at 120^{o}C for 6 hrs.

3.2.3.3. Structure characterization of poly(B-co-BMDO)

Changing the molar ratio of BMDO and MAA in the initial feed, the copolymer structure changes. ^{1}H-NMR spectrum of the copolymer with monomer feed ratio 80 : 20 of BMDO : MAA, made in 6

hrs (yield 37%) is shown in the Fig 3.2.16. It is found that the addition of MAA to the double bond of BMDO has precedence over copolymerization and the resulting new monomer B can copolymerize with the remaining BMDO. Besides the aromatic protons around ppm 7, two characteristic multiplet peaks at ppm 2-3 (–C*H*$_2$COOCH$_2$C$_6$H$_4$C*H*$_2$–) of BMDO by ring-opening polymerization are clearly found in the spectrum. The proton 11 from BMDO is attached to an asymmetric carbon in the copolymer and the random nature of the copolymers might have led to the splitting of these peaks in the region around ppm 2-3. The protons (–OC*H*$_2$C$_6$H$_4$C*H*$_2$O–) from structure B + –OCH$_2$– from ring-opening polymerization of BMDO) around ppm 5 also show multiplet peaks. No –COOH peak is seen in the NMR spectra, ruling out the presence of MAA type of units in the copolymer.

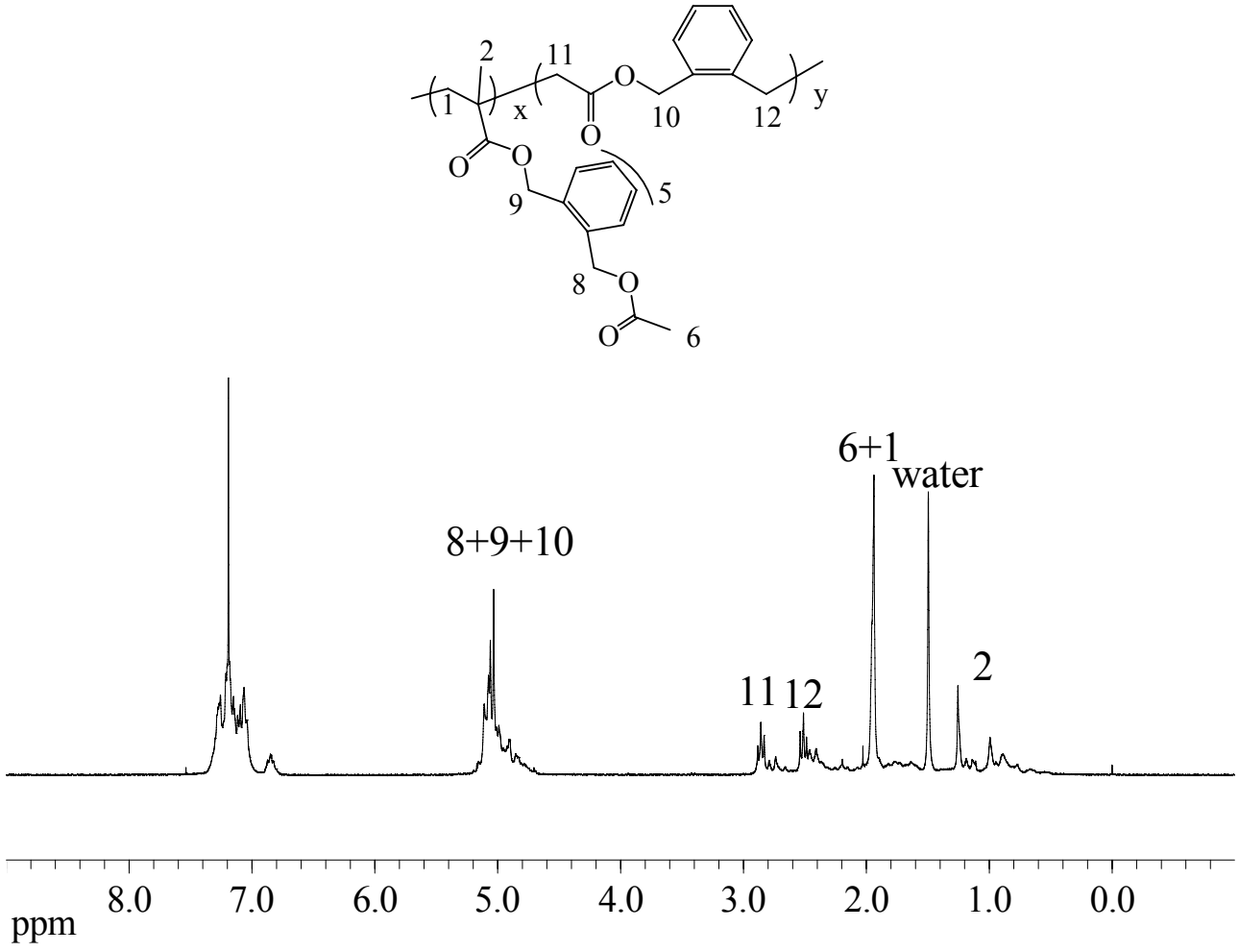

Fig 3.2.16. ^{1}H-NMR spectrum in methanol of poly (B-co-MAA) made using 20 : 80 molar ratio of BMDO : MAA in the feed at 120^{o}C for 6 hrs.

3.2.3.4. Influence of initial feeds on copolymer structures

Changing the molar ratio of BMDO and MAA in the initial feed, changes the copolymer structure. It is found that the addition of MAA to the double bond of BMDO has precedence over copolymerization and the resulting new monomer B can copolymerize with both MAA and BMDO. The molar ratios of B : MAA or B : BMDO are calculated based on the ^{1}H-NMR spectra. The results of copolymer compositions are shown in Table 3.2.1.

The copolymer composition of poly(B-co-MAA) is determined based on integrations of the peak at ppm 12.5 (–COO*H* from MAA) and the peaks at ppm 5.0-5.2 (–OCH_2– from B). From the result of run 1 we can see that the molar ratio of B : MAA in the copolymer (22 : 78) is somehow lower than that in the feed(1 : 3), suggesting the reactivity of MAA is a little higher than B. The copolymer composition of poly(BMDO-co-B) is determined by using the peak intensities at ppm 2.6-3 [I_{BMDO} (–C*H*$_2$COOCH$_2$C$_6$H$_4$– of BMDO)] and ppm 4.6-5.2 [I_{BMDO}(–CH$_2$COOC*H*$_2$C$_6$H$_4$–) + I_B(–COOC*H*$_2$C$_6$H$_4$C*H*$_2$OCO–)] in ^{1}H-NMR. The molar ratio of B : BMDO in the copolymer (44 : 56) is found to be higher as compared to that in the feed (3 : 1), which suggests the much higher reactivity of B than BMDO during copolymerization.

For polymerization of B and MAA, the conversion decreases with increasing the amount of B in the initial feed. For polymerization of B and BMDO, the conversion decreases compared to that of the polymerization of B and MAA.

The molecular weight of poly(B-co-MAA) decreases with increasing the amount of B in the initial feed, demonstrated by the intrinsic viscosities. The GPC curve of poly(B-co-BMDO) showes one modal peak with M_n of 37,000 and polydispersity of 1.7 (Fig 3.2.17).

Table 3.2.1. Copolymerization of 5,6-benzo-2-methylene-1,3-dioxepane (BMDO) and methacrylic acid (MAA) at 120°C for 6 hrs (copolymer composition is determined using ^{1}H-NMR)

Run	Feed Ratio (molar ratio)		Yield (%)	Copolymer Composition (molar ratio)			M_n	[η] (dl/g)
	BMDO	MAA		BMDO	B	MAA		
1	20	80	98	0	22	78	/	0.84
2	50	50	66	0	70	30	/	0.34
3	80	20	37	44	56	0	37,000	/

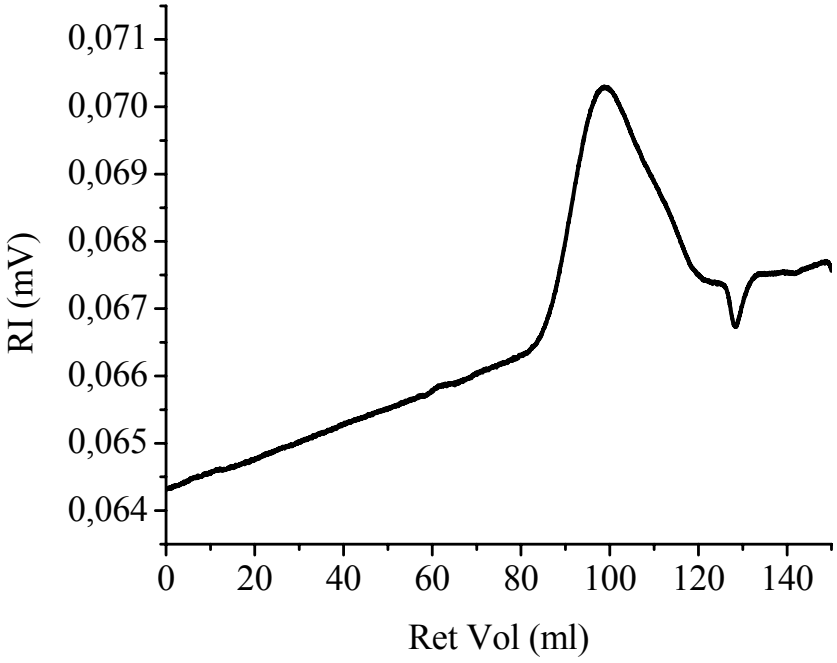

Fig 3.2.17. GPC curve of poly(B-co-BMDO) with 44 mol% of BMDO.

3.2.3.5. Solubility of copolymers

Poly(B-co-MAA) containing higher amount of MAA tend to be soluble in alcohol and water. Increasing the amount of B, polymers tend to be soluble in organic solvent. While poly(B-co-BMDO) are soluble in normal organic solvents like DMF, $CHCl_3$ and THF (Table 3.2.2).

Table 3.2.2. Solubility of poly(B-co-MAA) and poly(B-co-BMDO): + means soluble; – means non-soluble

Copolymer Composition (molar ratio)			DMF	$CHCl_3$	THF	Methanol	Water
BMDO	B	MAA					
0	22	78	–	–	–	+	+
0	70	30	+	–	–	–	–
44	56	0	+	+	+	–	–

3.2.3.6. Thermo-stability of copolymers

The thermo-stability of the resulting polymer was checked by thermogravimetric analyzer, shown in Fig 3.2.18. The glass transition temperature was checked by differential scanning Calorimetry analyzer, shown in Fig 3.2.19. Poly(B-co-BMDO) with higher content of structure B (44%) and no MAA units is found to be highly thermally stable (up to 300^{o}C), as shown in Fig 3.2.18c. The glass transition temperature is 29^{o}C. Poly(B-co-MAA) with 30% of MAA is found to be stable till 200^{o}C and thereafter shows two-step degradation as shown in the Fig 3.2.18b. The glass transition temperature is noted from the second heating cycle and is found to be 36^{o}C. Poly(B-co-MAA) with 78% of MAA shows weight loss at low temperatures starting from 150^{o}C in thermogravimetric analysis (Fig 3.2.18a). No clear glass transition can be seen in the DSC until 150^{o}C for this sample. The results indicate that BMDO sequences help increase the thermo-stability of the copolymers greatly, and MAA sequences lead to a relative fast multi-step thermo-degradation of the polymers. The glass transition temperature decreases with increasing the amount of BMDO in the chains and increases with increasing the amount of MAA in the chains.

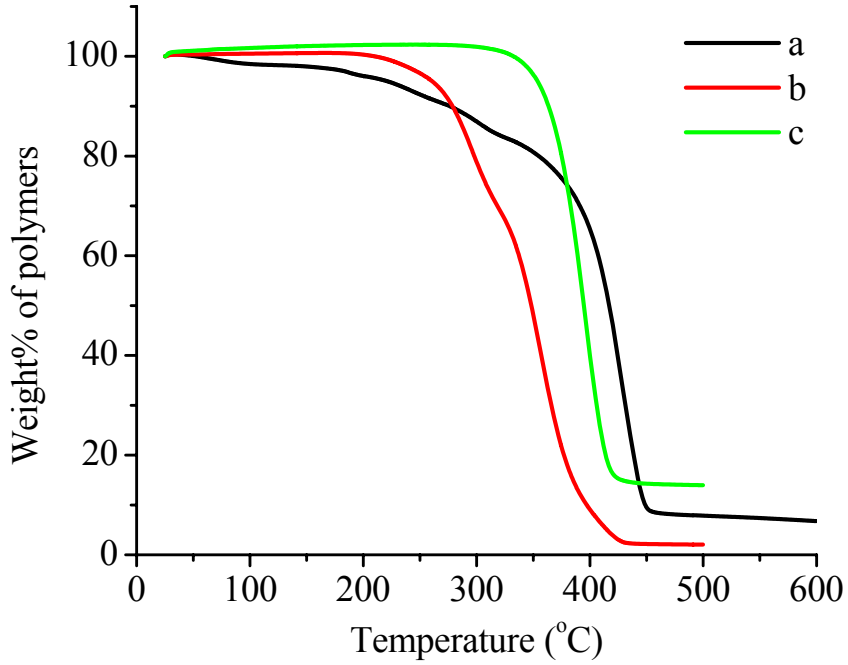

Fig 3.2.18. Thermogravimetric analysis (TGA) thermograms of copolymers with (a) B : MAA = 70 : 30 (molar ratio); (b) B : MAA = 22 : 78 (molar ratio); (c) B : BMDO = 56 : 44 (molar ratio).

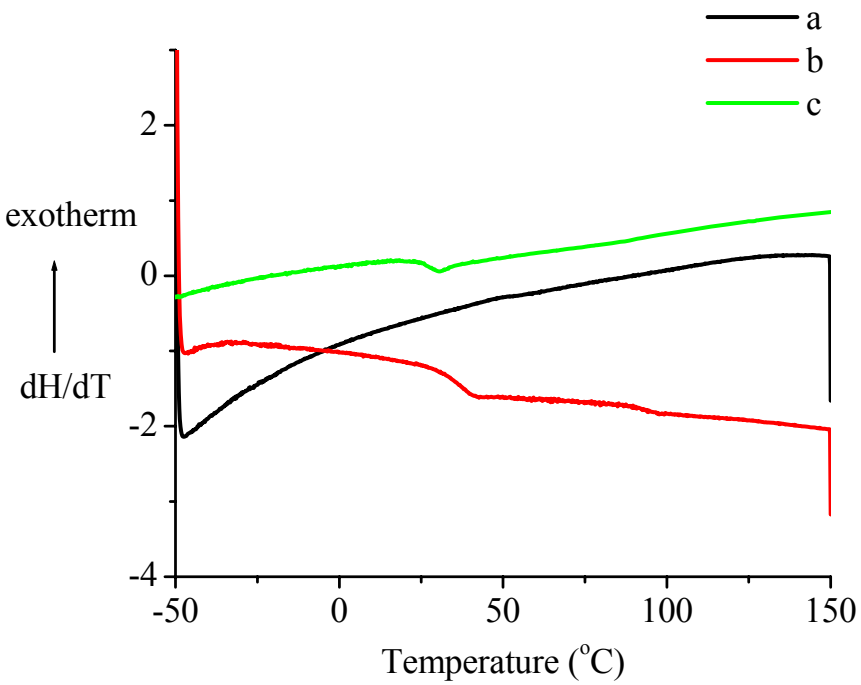

Fig 3.2.19. Differential Scanning Calorimetry (DSC) thermograms of copolymers with (a) B : MAA = 22 : 78 (molar ratio); (b) B : MAA = 70 : 30 (molar ratio); (c) B : BMDO = 56 : 44 (molar ratio).

3.2.3.7. Degradability of the copolymer

The hydrolytic degradation behavior of the sample made with more BMDO in the feed (BMDO : MAA = 80 : 20) with copolymer structures giving ester linkages in the backbone (structure 2; Scheme 3.2.4) was studied under basic conditions as described in the experimental part. The GPC curves of the copolymer samples before and after hydrolysis are shown in the Fig 3.2.20. The high molecular weight peak of poly(B-co-BMDO) disappears after hydrolysis and shifts to a low molecular weight region, thereby showing the hydrolytic degradation capability of new copolymer synthesized and the presence of ester linkages on the polymer backbone.

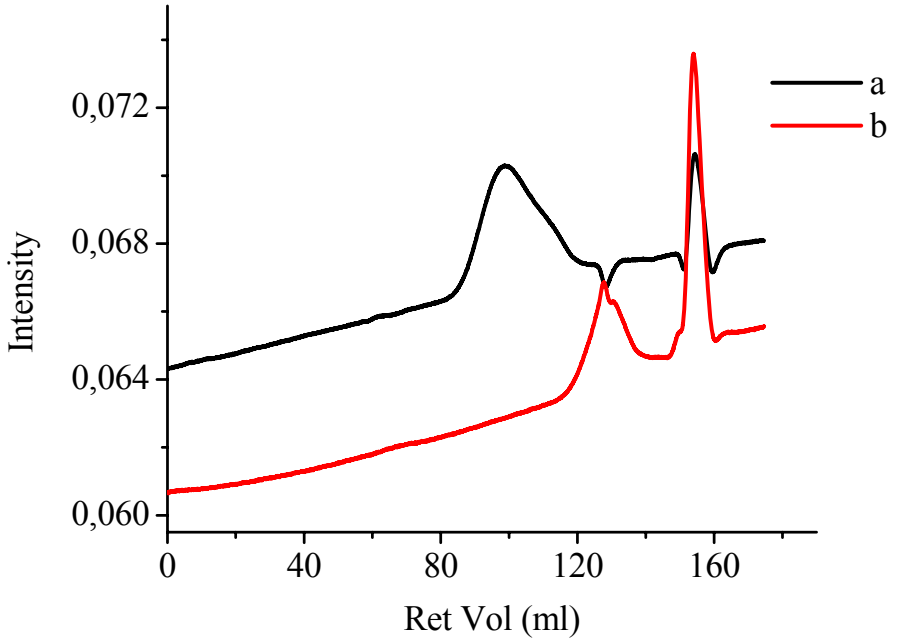

Fig 3.2.20. Gel permeation chromatography (GPC) curves of poly(B-co-BMDO) made using 80 : 20 molar ratio of BMDO : MAA in the feed at 120^{o}C for 6 hrs:
(a) before hydrolysis; (b) after hydrolysis showing the degradability of the copolymers.

3.2.4. Conclusions

The copolymerization of BMDO with MAA does not follow any of the conventional routes of copolymerization of cyclic ketene acetals with vinyl monomers known till now i.e. 1,2 vinyl addition at the double bond of BMDO giving poly acetal rings and /or free-radical ring-opening polymerization generating ester linkages in the backbone. Instead, this work showed a new route to copolymerization by first addition of MAA to the double bond of BMDO generating a new vinyl monomer (3-methyl-1,5-dihydrobenzo[e] [1,3]dioxepin-3-yl methacrylate) which is unstable at higher temperatures like 120^{o}C and rearranged into a new structure (2-(acetoxymethyl)benzyl methacrylate) with vinylic double bond and ester linkages in the side chain. Different monomer ratios in the feed generate different structures with ester linkages either in the backbone or as the side chain. The new polymers depending on their structure could be potential for pH sensitive functional materials. The possibility of protonation of the double bond of cyclic ketene acetals by Brönsted acid is influenced by the strength of the acidity. Material with a pKa higher than 18 does not protonate BMDO any more.

3.3. Degradable cation containing copolymers

Reference: S. Agarwal, L. Ren, T. Kissel, A. Greiner, DE 10 2008 028 146.8

3.3.1. Introduction

Generally, polyelectrolytes are polymers whose repeating units bear an electrolyte group. Charged molecular chains can play a fundamental role in determining structure, stability and the interactions of various molecular assemblies. Their unique properties are being exploited in a wide range of technological and industrial fields. For example, cationic polyelectrolytes are used as emulsifiers or flocculatants for wastewater treatment.[130] Polyelectrolytes containing quaternary ammonium groups are excellent antimicrobial agents.[131] More recently, cationic polyelectrolytes were explored as vectors for gene delivery due to efficient DNA complexation.[132]

An attempt here is made to introduce ester linkage into cationic polyelectrolyte to generate a new class of degradable cationic ion containing polymers.

Synthesis of degradable cationic polymers was done according to two steps as shown in Scheme 3.3.1. First, poly(DMAEMA-co-ester) was synthesized as precursors by free radical polymerization of 5-6-benzo-2-methylene-1,3-dioxepane (BMDO) or 2-methylene-1,3-dioxepane (MDO) and N,N-dimethylaminoethyl methacrylate (DMAEMA). Later, the resulting copolymers were quaternized with alkyl bromide (BrC_nH_{2n+1}) to yield degradable cationic polymers. The synthesis of degradable cationic polymers and the structure-property correlation of the new materials were intensively investigated.

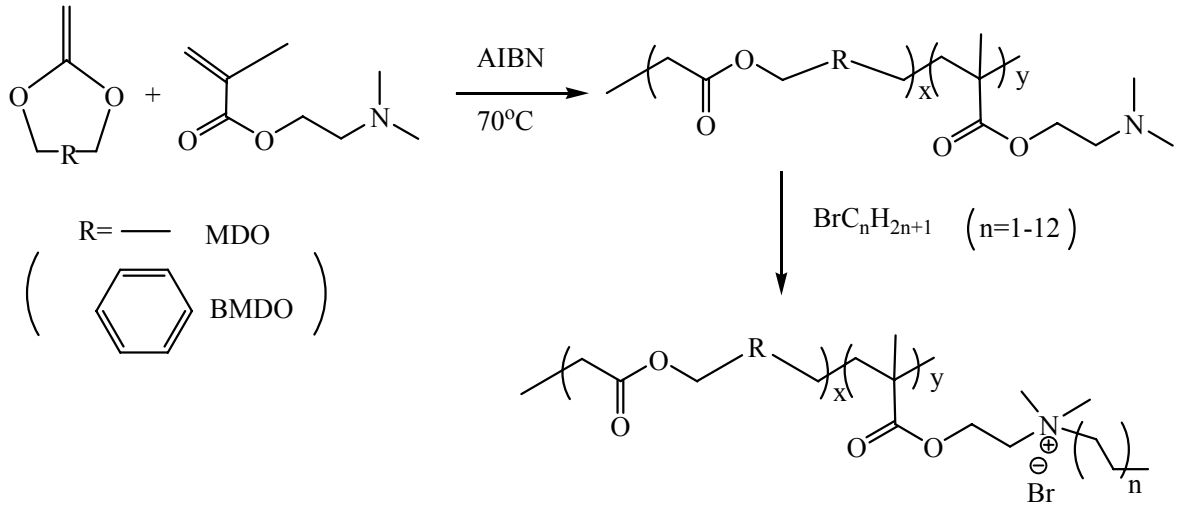

Scheme 3.3.1. Synthesis of degradable cation containing polymers.

3.3.2. Copolymerization behavior of BMDO and DMAEMA

Various random copolymers of BMDO with DMAEMA were synthesized as shown in Scheme 3.3.1 by changing the molar ratio of two monomers in the initial feed. The structural characterization of the copolymers is done by using 1D and 2D NMR techniques.

3.3.2.1. Structure characterization of random copolymers

The representative ^{1}H-NMR of the copolymer product with 65% of BMDO in the initial feed is shown in Fig 3.3.1. Compared to the ^{1}H-NMR spectra of PBMDO and PDMAEMA, the characteristic peaks of both BMDO and DMAEMA are seen in the obtained copolymer. The protons – OC*H*$_2$– (1), –C$_6$*H*$_5$CH$_2$– (5) of BMDO and –COOC*H*$_2$– (10), –N(C*H*$_3$)$_2$ (8), –C*H*$_2$C– (7), –CH$_2$C(C*H*$_3$)– (6) of DMAEMA are assigned without ambiguity. The other proton peaks [–C$_6$H$_5$C*H*$_2$– (2), –C*H*$_2$COO– (3) of BMDO and –C*H*$_2$N– (9) of DMAEMA in the lower ppm region between 2.3 and 3.2 ppm come as overlapping and not very well resolved peaks. Comparing with ^{13}C-NMR spectra (Fig 3.3.2) of PBMDO and PDMAEMA, the carbons –C$_6$H$_5$*C*H$_2$– (2) and –*C*H$_2$COO– (3) of BMDO and –*C*H$_2$N– (9) of DMAEMA are assigned without ambiguity. Between 168.50 and 177.68 ppm there seems to be two main ester peaks splitted into several small peaks, which also gives us a hint of ring-opening polymerization of BMDO and the existence of the linking unit of BMDO and DMAEMA. ^{13}C-NMR spectra shows the absence of any peak in the ppm range 100-110, confirming the formation of predominantly ester linkages by ring-opening polymerization reaction of BMDO during copolymerization.

2D ^{1}H-^{13}C HMQC-NMR technique is used to assign peak positions in the ^{13}C-NMR spectrum and also in the overlapping regions in the ^{1}H-NMR spectrum (Fig 3.3.3).

The correlations seen in ^{1}H-^{13}C HMQC are: proton 1 at 5.09 ppm with carbon at 64.1 ppm (A), proton 10 at 4.1 ppm with carbon at 62.7 ppm (B), proton 8 at 2.27 ppm with carbon at 45.53 ppm (C), proton 7 between 1.90 and 1.72 ppm with carbon at 40.28 (D), proton 6 between 1.41 and 0.98 ppm with carbon between 21.67 and 16.90 ppm (E). The broad peak between 2.3 and 3.2 ppm shows three clear correlations in HMQC-NMR spectrum with carbon 2 at 27.39 ppm (F), carbon 3

at 35.02 ppm (G), and carbon 9 at 57.46 ppm (I), respectively, showing the presence of three types of hydrogen atoms from BMDO and DMAEMA at this position.

2D ^{1}H-^{13}C HMBC-NMR spectrum (Fig 3.3.4) provides further clarity in the peak assignments and peak confirmations. An attempt has been made to analyze the ester linkages, the overlapping peaks and to establish a chemical linkage between the two monomeric units, i.e., BMDO and DMAEMA in the copolymers.

In HMBC-NMR spectrum, the proton 1 showed 4 clear cross peaks, i.e. three in the aromatic region (A) and one in the carbonyl carbon region at 171.73 ppm (B). This confirms the correct assignment of proton 1 in the copolymers and also suggests that the undecided carbonyl carbon peak marked at 171.73 ppm is from carbon 4 of BMDO after ring-opening. While the proton 10 in ^{1}H-NMR spectrum shows 2 cross peaks with carbon 9 (C) and another cross peak in the carbonyl carbon region at 175.51 ppm (D). It demonstrates the carbon peak at 175.51 ppm is from carbon 11 of the ester group in DMAEMA. Furthermore, careful examination of the HMBC-NMR spectrum shows the presence of clear correlations of proton at 2.85 ppm with carbons at 170.73 ppm in the carbonyl carbon region (carbon 4′ of BMDO) (E) and another at 175.56 ppm in the carbonyl region (carbon 11′ of DMAEMA) (F), at 44.4 ppm (carbon 12′ of DMAEMA) (G), at 40.78 ppm (carbon 7′ of DMAEMA) (H) and at 21.44 ppm(carbon 6′ of DMAEMA) (I). This shows the presence of the protons 3′ (at ppm 2.85), i.e., from the linking unit of BMDO to DMAEMA. The split of peaks in the carbonyl carbon region in the ^{13}C-NMR spectrum is attributed to the chemical linkage of BMDO and DMAEMA in the random copolymers. Again some weak correlations of the carbon around 40.78 ppm (carbon 7, 7′, 7″ of DMAEMA) with protons at 2.85 ppm (proton 3′ of BMDO) (H), at 1.33 ppm (proton 6′ of DMAEMA) and at 2.54 ppm (J) are seen. Therefore it confirms the existence of the carbon 7′ from the linking unit of DMAEMA-BMDO. It suggests further that the proton at 2.54 ppm is from proton 2″ of BMDO, i.e., from the linking unit of BMDO–DMAEMA. HMBC-NMR spectrum has helped us in the assignment of some overlapping peaks and demonstration of the chemical linkage between the comonomeric units in the copolymers.

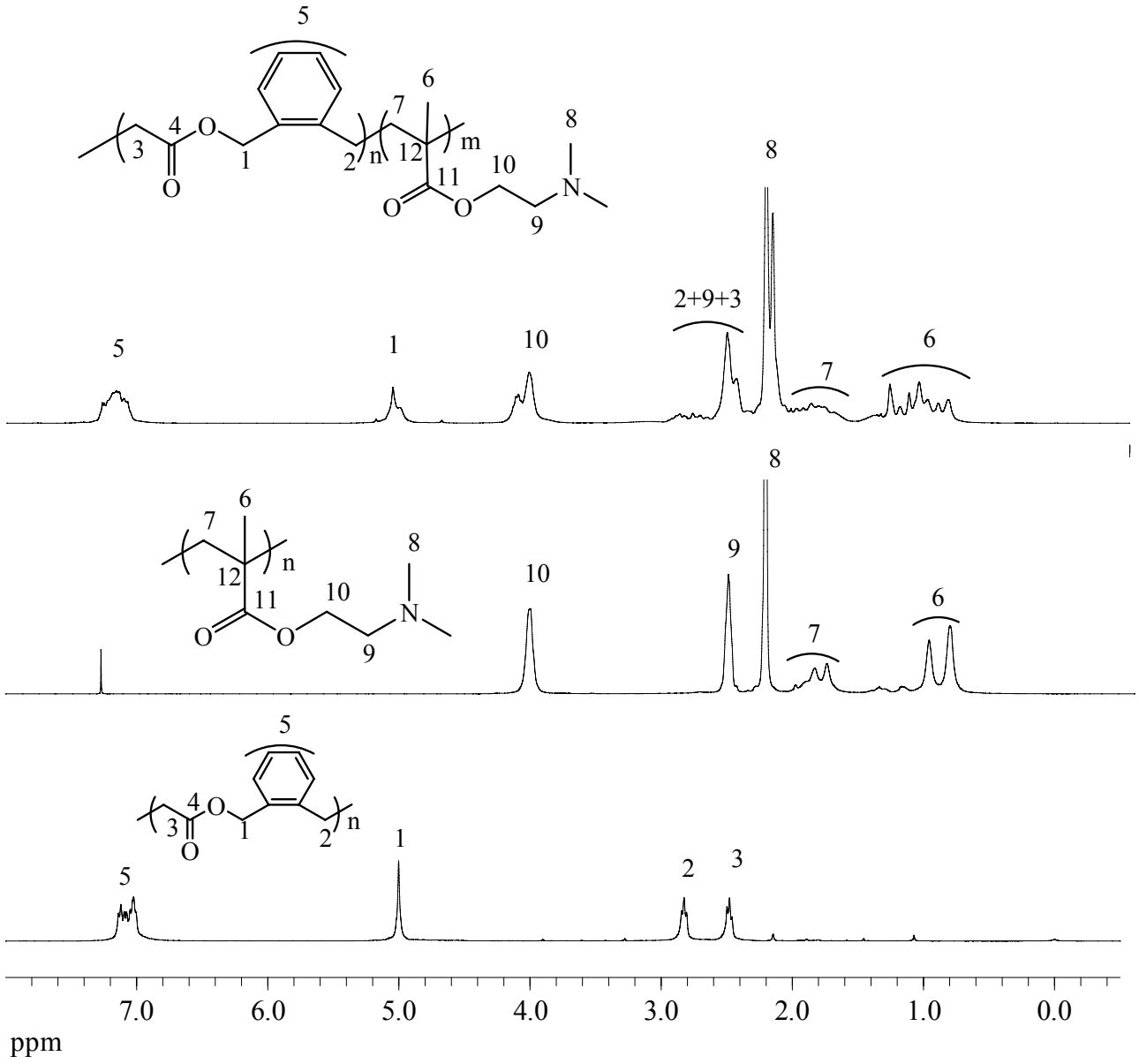

Fig 3.3.1. ^{1}H-NMR spectrum of poly(DMAEMA-co-BMDO) with 65% BMDO in the feed.

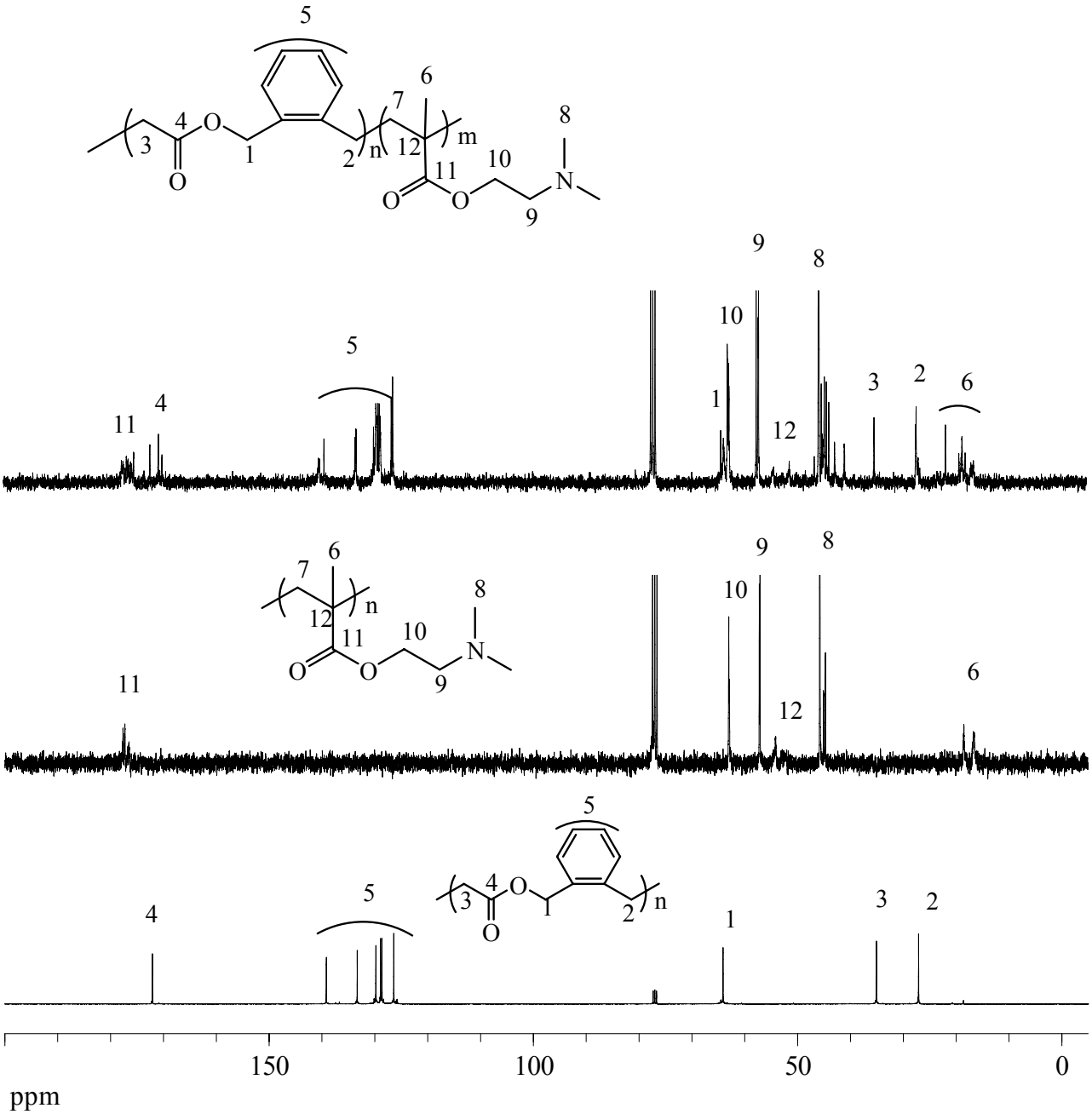

Fig 3.3.2. ^{13}C-NMR spectrum of poly(DMAEMA-co-BMDO) with 65% BMDO in the feed.

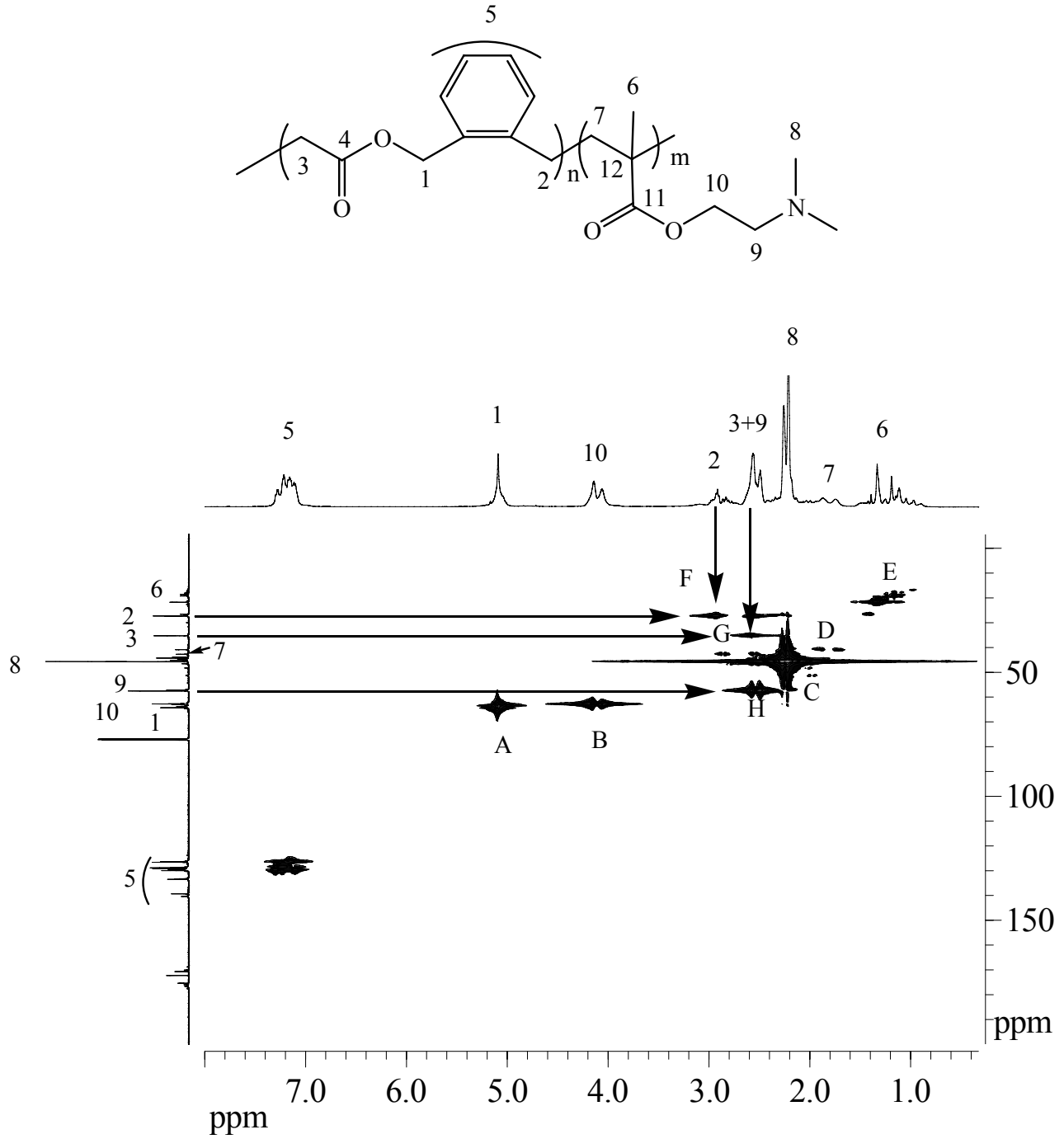

Fig 3.3.3. 2D ^{1}H-^{13}C HMQC-NMR spectrum of poly(DMAEMA-co-BMDO) with 65% BMDO in the feed.

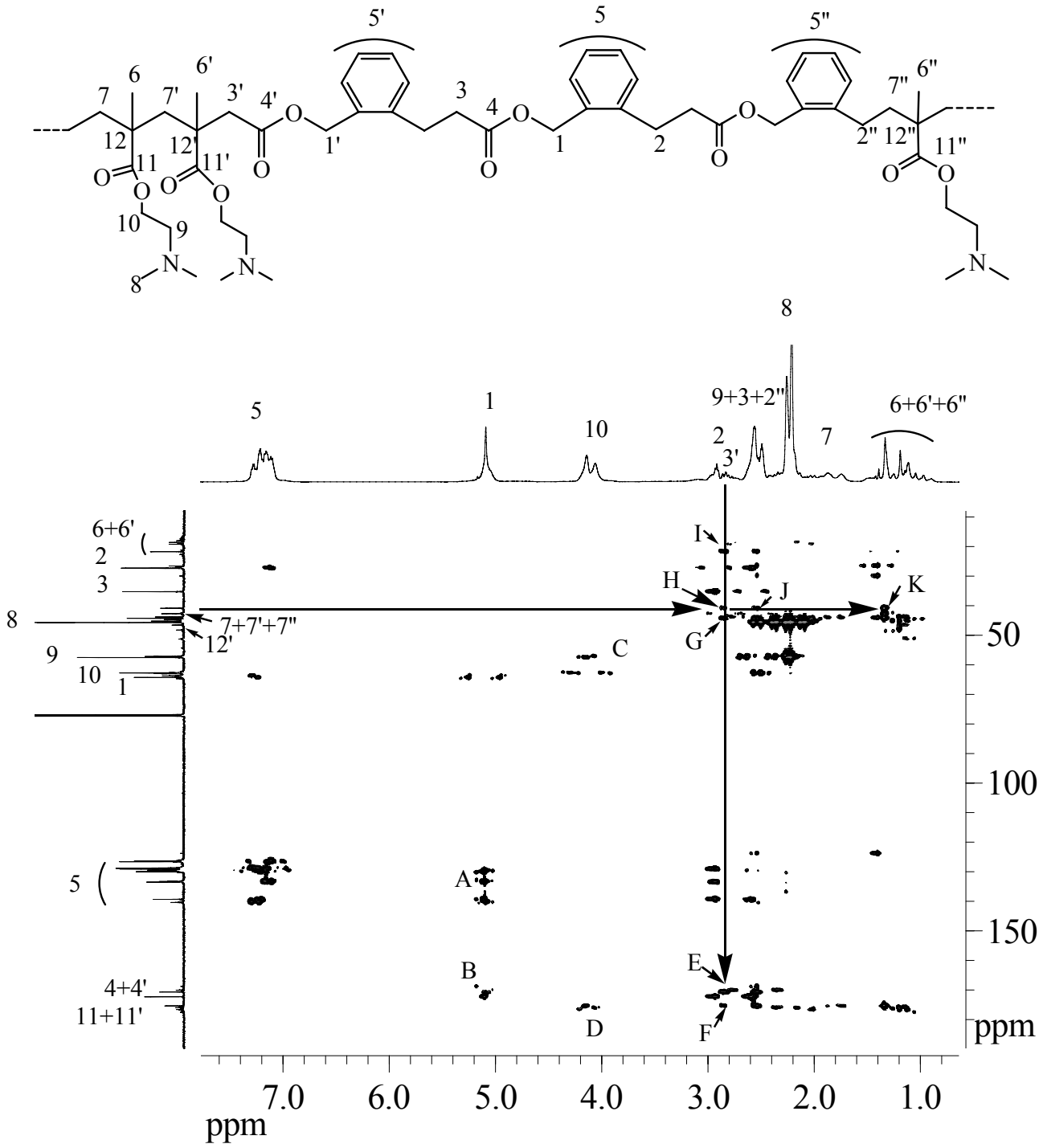

Fig 3.3.4. 2D ^{1}H-^{13}C HMBC-NMR spectrum of poly(DMAEMA-co-BMDO) with 65% BMDO in the feed.

3.3.2.2. Influence of initial feeds on copolymer structures

In general, moderate molecular weight copolymers poly(DMAEMA-co-BMDO) with uni-modal GPC curves were obtained. The molecular weights of the polymers are similar, which, according to the similarity of the molecular weights of the comonomers, indicates the degree of polymerization

(DP) did not change too much with different initial feeds (Table 3.3.1). The copolymer composition is determined by using the peak intensities at 4.8-5.1 ppm I_{BMDO} (–OC*H*$_2$–C_6H_5– of BMDO) and 3.7-4.2 ppm I_{DMAEMA} (–COOC*H*$_2$– of DMAEMA) in ^{1}H-NMR spectrum. The molar ratio of DMAEMA : BMDO in the copolymer was always found to be higher than that in the initial feed, indicating the relative low reactivity of BMDO comparing to DMAEMA. Copolymers with increasing amount of BMDO units were made by changing the molar ratio of the two comonomers in the initial feed and this increase was found to be almost linear to that in the initial feed (Fig 3.3.5). The conversion and therefore the reaction rate decreases with increasing the amount of BMDO in the initial feed, even polymerization was carried for 20 hrs to achieve more conversion, indicating the chain propagation of BMDO unit is much slower than that of DMAEMA.

Table 3.3.1. Synthesis of degradable poly(BMDO-co-DMAEMA) with AIBN as initiator, polymerization temperature: 70^{o}C, polymerization time: 4 hrs; a) polymerization time: 20 hrs.

Run	Feed Ratio (molar ratio)		Yield (%)	Copolym. Composition (molar ratio)		M_n	PDI
	B	D		B	D		
1	0	100	76	0	98	16,000	1.3
2	25	75	74	10	90	11,000	1.3
3	45	55	64	21	79	13,800	1.4
4[a)]	50	50	56	24	76	15,900	1.4
5[a)]	65	35	45	30	70	11,500	1.4
6[a)]	85	15	28	48	52	11,000	1.3

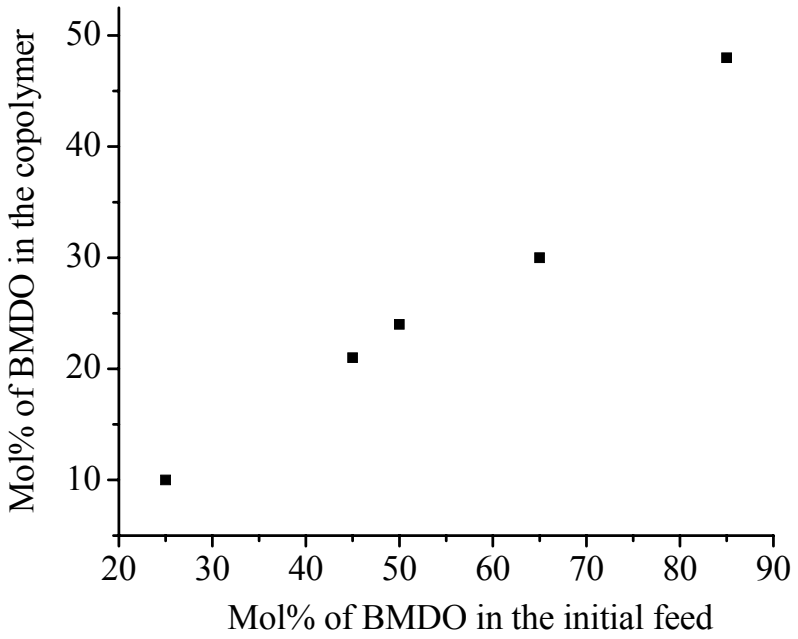

Fig 3.3.5.Mol% of BMDO in the feed versus mol% of BMDO in the copolymer (data from Table 3.3.1).

3.3.2.3. Influence of reaction time on copolymer structures

Furthermore, to have an insight into the copolymerization behavior and the microstructure of the copolymers, for one specific initial feed (BMDO : DMAEMA = 50 : 50 molar ratio), the polymerization was followed at different intervals of time (Table 3.3.2). Comparing the conversion at 4 hrs and 20 hrs, it is assumed that copolymerization of BMDO and DMAEMA almost finished after 4 hrs. Through out the polymerization time there was a continuous increase in reacted BMDO and DMAEMA. However the rate of consumption of DMAEMA was much faster than that of BMDO (Fig 3.3.6). This indicates the preference of both DMAEMA and BMDO radicals for the DMAEMA monomer during copolymerization and, therefore, most probably resulting in diads of the type BMDO–NIPAAm, NIPAAm–NIPAAm and NIPAAm–BMDO in the copolymer chains with isolated or very short BMDO sequences of the type BMDO–BMDO.

Poly(DMAEMA-co-BMDO) with uni-modal GPC curves were obtained at different intervals of time, indicating the constant random copolymerization behavior throughout the reaction time. The molecular weight of the polymers generated did not change too much at different intervals of time.

Table 3.3.2. Kinetic information of copolymerization of DMAEMA and BMDO (50 : 50 in the initial feed), with AIBN as initiator, copolymerization temperature: 70°C; a) calculated using the copolymer composition and the yield

Run	Reaction Time (h)	Copolym. Composition (molar ratio) B	D	Conversion (%)	Wt.-% of the Monomer reacted[a)] B	D	M_n	PDI
1	1/6	13	87	15	4	26	/	/
2	1	14	86	46	13	80	15,760	1.3
3	2	19	81	52	20	85	/	/
4	4	21	79	55	22	83	15,870	1.4
5	20	24	76	56	27	86	16,070	1.4

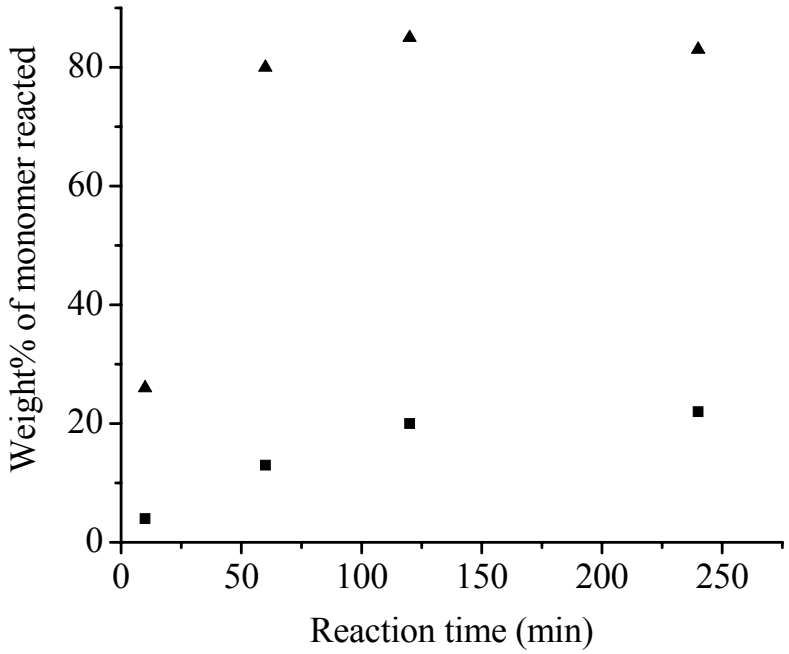

Fig 3.3.6. Weight% of reacted monomers versus reaction time: ▲ DMAEMA; ♦ BMDO (values from Table 3.3.2).

3.3.2.4. Reactivity ratios

Further, the reactivity ratios were determined using the Kelen-Tüdõs method. Five copolymerizations (Table 3.3.3) were carried out at 70°C till low-medium percent conversions (between 10% and 20%) for the calculation of reactivity ratios, and the reactivity ratios were determined to be $r_{BMDO} = 0.14$ and $r_{DMAEMA} = 6.96$ (Fig 3.3.7). Although we acknowledge the small

error involved in this calculation because of the compositional drift with the conversion, the reactivity ratios give us a hint about the random copolymer microstructure having relatively long DMAEMA blocks, well separated by rather short BMDO sequences.

Table 3.3.3. Copolymerization of BMDO and DMAEMA in low conversions, AIBN as initiator, temperature: 70°C

Run	Feed Ratio (molar ratio)		Yield (%)	Copolym. Composition (molar ratio)	
	B	D		B	D
1	70	30	10	23.3	76.7
2	60	40	17	18.0	82.1
3	50	50	15	12.8	87.2
4	40	60	13	8.9	91.1
5	30	70	15	5.3	95.7

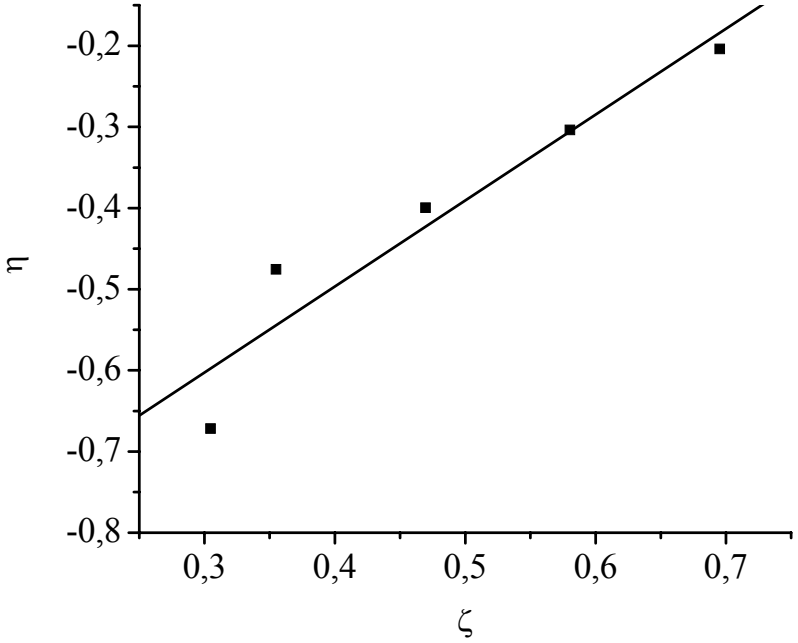

Fig 3.3.7. Kelen-Tüdõs plot for BMDO-DMAEMA copolymers. (values based on Table 3.3.3)

$\eta = (r_{BMDO} + r_{DMAEMA}/\alpha) \cdot\xi - r_{DMAEMA}/\alpha$ ($\eta = 1.059 \cdot\xi - 0.920$); $\eta = [(F/f)(f-1)]/(\alpha+F^2/f)$; $\xi = (F^2/f)/(\alpha+F^2/f)$;

where $F = M_{BMDO}/M_{DMAEMA}$ (monomer feed); $f = m_{BMDO}/m_{DMAEMA}$(copolymer composition);

$\alpha = [(F^2/f)_{max} (F^2/f)_{min}]^{1/2}$.

3.3.3. Quaternization behavior of poly(BMDO-co-DMAEMA)

Generally quaternization of polymers is much slower than that of organic small molecules, especially when the chain of the alkyl bromide is relative long, like 1-bromododecane. In order to loose the polymer coils in the solvent, to provide high chain mobility and to achieve high reaction conversion, it is necessary to have a medium dilute polymer solution (around 10 mg/ml) to avoid high viscosities and therefore to have a high excess of alkyl bromide to insure enough interaction of reagents. In this work, quaternization of poly(BMDO-co-DMAEMA)s was investigated with different reaction time, copolymer compositions and the types of alkyl bromide. Quaternization conversion is determined by elemental analysis, comparing the amount of bromine and nitrogen in the quaternary polymers (Table 3.3.4). It shows that the quaternary conversion can be controlled by changing the reaction time (run1, 2, 3). A relative high quaternization conversion can be achieved with increased reaction time. The copolymer composition also plays a role for the quaternization rate. For copolymers with very small amount of DMAEMA, quaternization becomes more difficult and slower (run 3, 4, 5). Quaternization with short alkyl bromide is relative easier, even when copolymer contains small amount of DMAEMA. The quaternization conversion increases from 60% to 90% when decreasing the length of the alkyl group from 1-bromododecane to bromoethane (run 5, 6).

Table 3.3.4. Quaternization behavior of poly(BMDO-co-DMAEMA)

Run	Copolym.Composition (molar ratio)		Quaternary Agent BrC_nH_{2n+1};	Quaternization Time (day)	Conversion (%)
	B	D	n		
1	0	100	12	0.75	64
2	0	100	12	2	71
3	0	100	12	3	88
4	30	70	12	3	89
5	88	12	12	3	59
6	88	12	2	3	93

3.3.4. Copolymerization behavior of MDO and DMAEMA

MDO showed similar copolymerization behavior as that of BMDO with DMAEMA. ^{1}H-NMR spectrum of the copolymer generated from an initial feed of MDO : DMAEMA as 85 : 15 shows all the characteristic peaks from MDO and DMAEMA, indicating the existence of the comonomers (Fig 3.4.8). The copolymer composition is determined by using the peak intensities at 2.3 ppm [I_{DMAEMA} (–CH_2CH_2*N*–, proton 2 of PDMAEMA)] and 4.2 to 3.8 ppm [I_{MDO} + I_{DMAEMA} (–OCH_2CH_2–, proton 10 of PMDO + –CH_2CH_2N–, proton 1 of PDMAEMA)] and found to be MDO : DMAEMA = 60 : 40. Considering some overlapping of the peaks in the spectrum and the fact that several side reactions including backbiting of MDO may take place during polymerization (–$CH_2CH_2CH_3$, proton 14 of MDO), slight error is acknowledged during determination of the copolymer compositions. Copolymers with increasing amount of MDO units were made by changing the molar ratio of the two comonomers in the initial feed and this increase was found to be almost linear to that in the initial feed (Table 3.3.5). The molar ratio of DMAEMA : MDO in the copolymer was always found to be higher than that in the initial feed, indicating the relative low reactivity of MDO compared to DMAEMA.

Table. 3.3.5. Bulk copolymerization of MDO (M) and DMAEMA (D) with 1(mol) % of AIBN as initiator, reaction temperature: 70^{o}C, reaction time: 5 hrs; a) reaction time: 20 hrs

Run	Feed Ratio (molar ratio)		Yield (%)	Copolym. Composition (molar ratio)	
	D	M		D	M
1	70	30	73	87	13
2	60	40	72	80	20
3[a)]	40	60	55	70	30
4[a)]	30	70	49	65	35

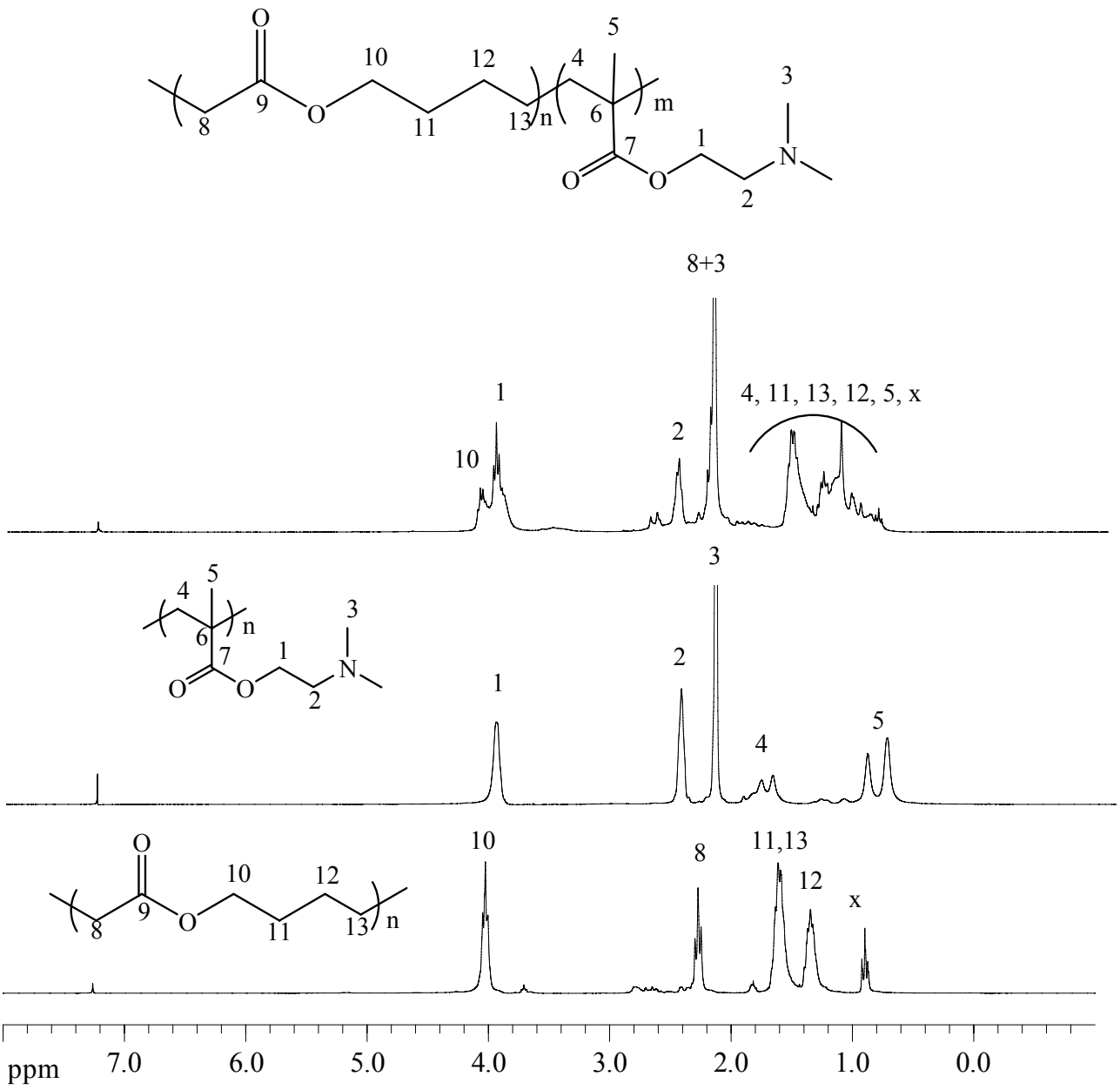

Fig 3.3.8. ^{1}H-NMR spectrum of poly(MDO-co-DMAEMA) with the initial feed of MDO : DMAEMA = 85 : 15.

3.3.5. Quaternization of poly(MDO-co-DMAEMA)

Polymerization was followed by quaternization of amines with BrC_2H_5 to generate degradable water soluble polymers. After 3 days of reaction, relative high quaternization degree was achieved (Table 3.3.6). Quaternized polymers containing up to 30 mol% of MDO were found to be soluble in water.

Table 3.3.6. Quaternization of P(MDO- DMAEMA) with BrC_2H_5, reaction time: 3 days (Ion content was calculated by "mol% of DMAEMA in polymer" x "quaternization conversion")

Run	Copolym. Composition (molar ratio)		Quaternization Conversion (%)	Ion Content (mol%)
	MDO	DMAEMA		
1	20	80	93	74
2	25	75	95	71
3	30	70	93	65

3.3.6. Solubility of quaternized poly(ester-co-DMAEMA)

The length of alkyl bromide plays a very important role in determining the properties of the final degradable cationic polymers. Changing from bromoethane to 1-bromododecane, the final polymer could be tuned from hydrophilic to hydrophobic (Table 3.3.7). Decreasing the length of alkyl bromide, the solubility of cationic polymers in alcohols and in water increased and the solubility in $CHCl_3$ decreased. DMF is a relative common proper solvent for all the cationic polymers quaternized with different length of alkyl bromides. The amount of ester group in the copolymers influences the degradation degree and the solubility. Therefore cation containing polymer with targeting degradation degree and solubility was synthesized by controlling the copolymer composition and the quaternary behavior.

Table 3.3.7. Solubility of quaternized poly(ester-co-DMAEMA) in water and common organic solvents, quaternization conversion: around 85 to 95%; + : clear solution; +*: cloudy suspension; −: precipitate

BrC_nH_{2n+1}	Mol% of ester				Mol% of ester				Mol% of ester				Mol% of ester			
n	10	30	80	100	10	30	80	100	10	30	80	100	10	30	80	100
	water				ethanol				$CHCl_3$				DMF			
2	+	+	+*	−	+	+	+*	−	−	−	−	+	+	+	+	+
4	+	−	−	−	+	+	−	−	−	−	+*	+	+	+	+	+
8	+	−	−	−	+	+	−	−	−	+*	+	+	+	+	+	+
12	−	−	−	−	+	+	−	−	+	+	+	+	+	+	+	+

3.3.7. Hydrophobic cationic electro-spun fibers

Quaternized poly(BMDO-co-DMAEMA) was electrospun in proper solvents. For example, 1-bromododecane quaternized poly(BMDO-co-DMAEMA) with different BMDO compositions (10 mol% and 20 mol%) was electrospun in ethanol, which is much less toxic than other organic solvents, like $CHCl_3$ to the human body. Due to the moderate molecular weight, the concentration of the polymer was as high as 20% in order to generate fibers. The diameter of the resulting beaded fibers (Fig 3.3.9) was around 500 nm. Diameter of the bead is around 3 μm. The amount of beads is decreased by increasing the amount of ester in the copolymers from 10 mol% to 20 mol%.

Interesting is that the fiber mats we got here by electrospinning were highly hydrophobic. The contact angle was observed to be as much as 135^o (Fig 3.3.10). Comparing to the results of around 78^o by film coating of polymers containing 10-20 mol% of BMDO on glass or 93^o by spin coating on glass, the hydrophobility of the material was dramatically increased by electrospinning. It is proposed that the electric force or even the rotating force induces the rearrangement of the polymer chains, so that the hydrophilic ions tend to be lower layer and the hydrophobic neutral chains tend to be the upper layer.

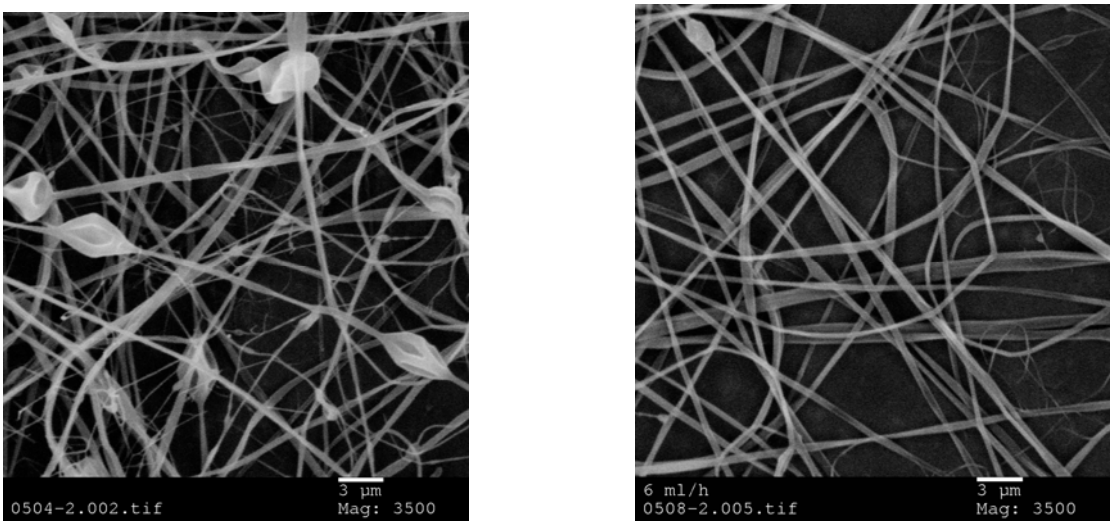

Fig 3.3.9. Electrospun fibers of the quaternized poly(DMAEMA-co-BMDO) (20 wt% of the quaternized copolymer in ethanol, 25 kv, 6 ml/h, distance: 20 cm); left: polymer with10 mol% of BMDO; 88 mol% of ion; right: polymer with 20 mol% of BMDO, 63 mol% of ion; quaternary reagent: $BrC_{12}H_{25}$.

Fig 3.3.10. Contact angle of the fiber mat (polymer with10 mol% of BMDO, 88 mol% of ion, quaternary reagent: $BrC_{12}H_{25}$) by electrospinning.

3.3.8. Thermo-analysis

Thermal properties of quaternized poly(BMDO-co-DMAEMA) were analyzed by TGA and DSC. Fig 3.3.11 shows that PBMDO was relatively highly thermal stable until 300^{o}C and had one-step degradation from 300^{o}C to 450^{o}C. Homo cation containing polymer P(DMAEMA•$BrC_{12}H_{25}$) shows a much earlier three steps thermo-degradation, starting from 160^{o}C till 500^{o}C. While quaternized copolymer P(DMAEMA-co-BMDO)•$BrC_{12}H_{25}$ shows two steps early thermo-degradation, starting from around 180^{o}C and proceeding until 500^{o}C.

The DSC curves of quaternized poly(DMAEMA-co-BMDO) with similar quaternization degree and varied copolymer compositions are shown in Fig 3.3.12. The glass transition temperatures (T_g) of the polymers are listed in Table 3.3.8. PBMDO has a T_g around 20^{o}C. Before quaternization, poly(DMAEMA-co-BMDO) containing 10% BMDO is observed to have a glass transition temperature at 19^{o}C. After quaternization, T_g increases greatly to 123^{o}C. Increasing the amount of BMDO in the chains, the glass transition temperature of quaternized poly(DMAEMA-co-BMDO) decreases. (PDMAEMA)•$BrC_{12}H_{25}$ did not show any T_g within the measuring temperature, i.e. from -100^{o}C to 150^{o}C.

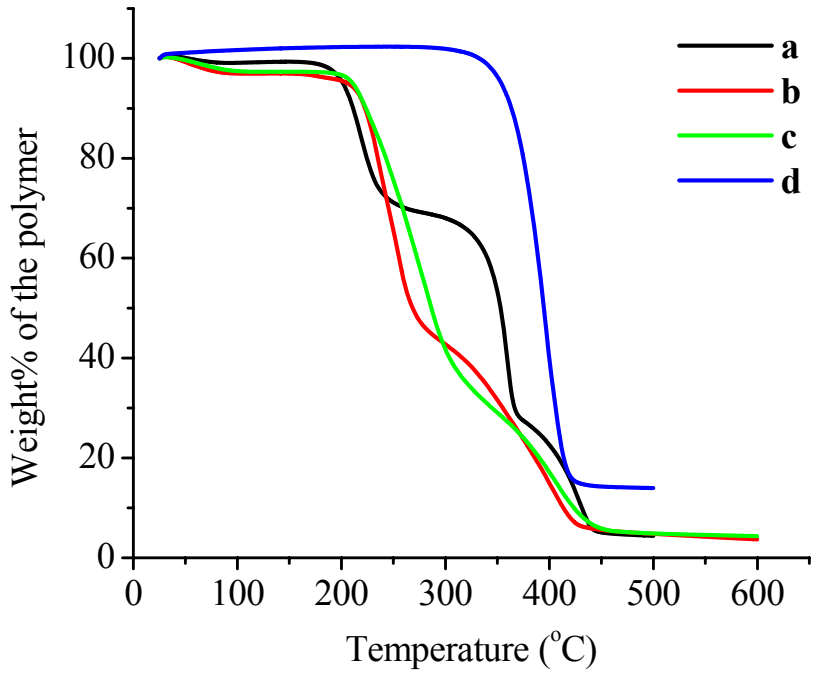

Fig 3.3.11. Thermogravimetric analysis (TGA) of polymers: (a) P(DMAEMA•$BrC_{12}H_{25}$); (b) P(BMAEMA-co-BMDO)•$BrC_{12}H_{25}$ (21% BMDO, quarternization degree 80%); (c) P(BMAEMA-co-BMDO)•$BrC_{12}H_{25}$ (48% BMDO, quarternization degree 83%); (d)PBMDO.

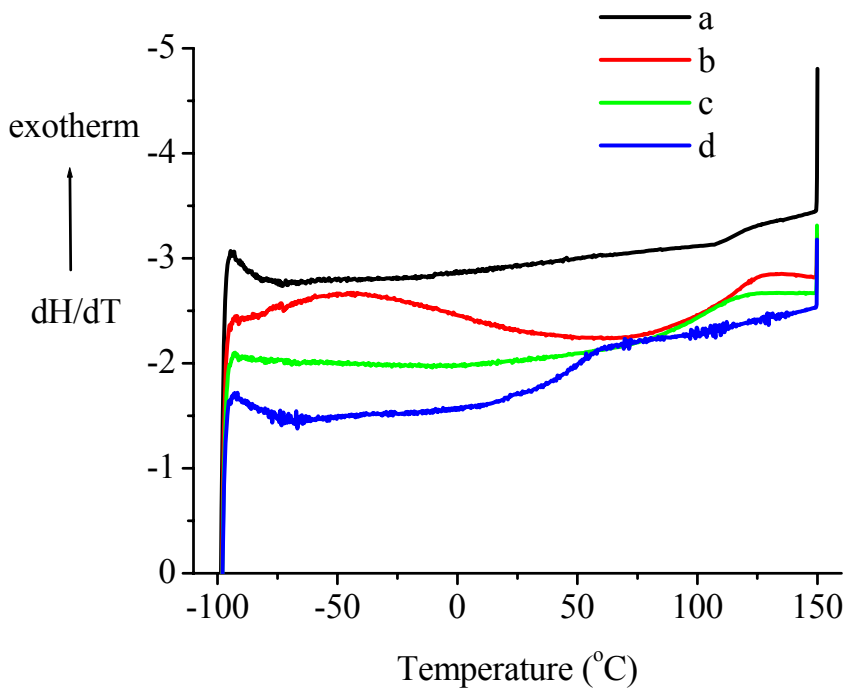

Fig 3.3.12. Differential Scanning Calorimetry (DSC) of polymers quaternated by $BrC_{12}H_{25}$, the second heating cycle: (a) run 2, Table.3.35; (b) run 3, Table 3.3.5; (c) run 4, Table 3.3.5; (d) run 5, Table 3.3.5.

Table 3.3.8. Glass transition temperature of quaternized poly(BMDO-co-DMAEMA), quaternary reagent: $BrC_{12}H_{25}$

Run	Copolym. Composition (molar ratio)		Quaternization Conversion (%)	T_g (After quarternization) (^oC)
	B	D		
1	0	100	88	>150
2	10	90	98	123
3	21	79	80	112
4	30	70	89	98
5	48	52	83	46

3.3.9. Antimicrobial behavior

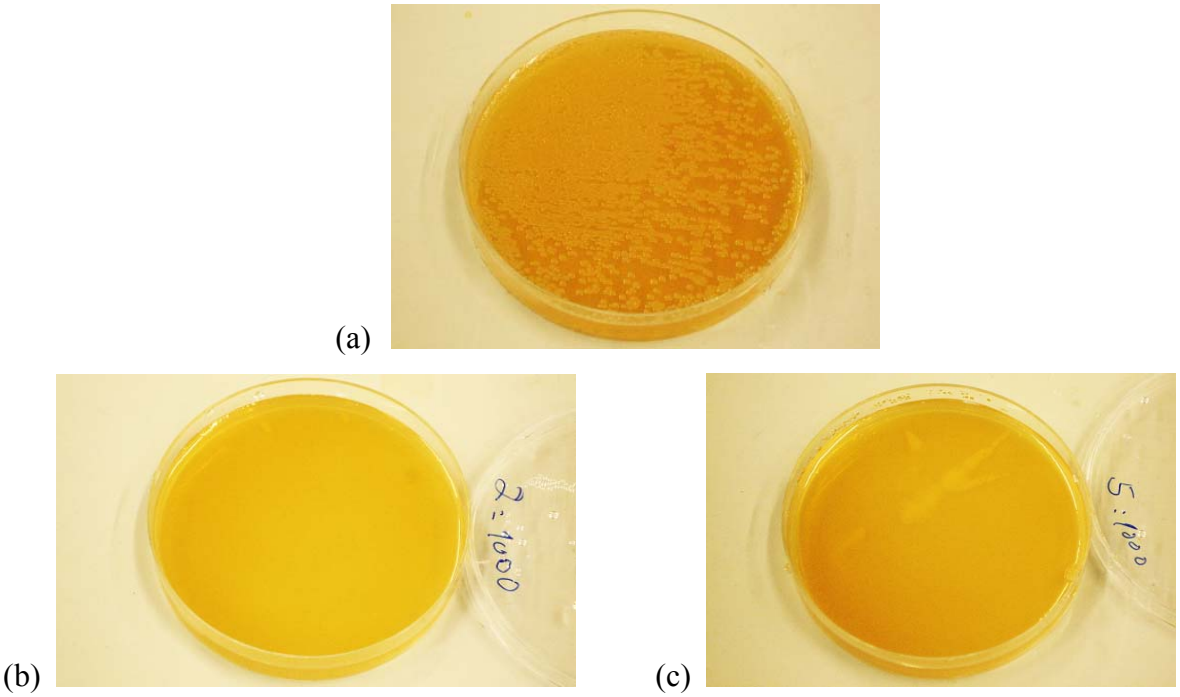

Fig 3.3.13. Impact of quaternized P(BMDO-co-DMAEMA) on bacterial *Escherichia (E.) coli* growthq (a) blank suspension without polymer; (b) P(BMDO-co-DMAEMA)•$BrC_{12}H_{25}$ (10 mol% BMDO, 88 mol% ion); (c)P(BMDO-co-DMAEMA) •$BrC_{12}H_{25}$ (48 mol% BMDO, 43 mol% ion).

As is known, polyelectrolytes containing quaternary ammonium groups are excellent antimicrobial agents. Homopolyelectrolyte P(DMAEMA•BrC_nH_{2n+1}) were found to be antibacterial independent of hydrophilicity.[133] Therefore the antimicrobial activity of quaternized poly(BMDO-co-DMAEMA) containing different copolymer compositions was also tested in the work. It was found that copolymers containing a high amount of quaternary amine, i.e. at least 43 mol%, showed

antimicrobial effect against *E.coli*. Fig 3.3.13 shows that bacterial *E.coli* generated a high amount of colony after incubated without polymers (a). While *E.coli* incubated with poly(BMDO-co-DMAEMA)•$BrC_{12}H_{25}$ containing more than 43 mol% of ion did not show any bacterial colony, indicating that bacterial *E.coli* has been killed by the polymers (b, c). Due to the antibacterial effect and the hydrophobicity, quaternized copolymer poly(BMDO-co-DMAEMA)•$BrC_{12}H_{25}$ could be a potential coating material for wood, papers and medical products.

3.3.10. Hydrolytic degradability

The hydrolytic degradation behavior of the quaternized copolymers was also studied under extreme conditions. Due to the ion effect, the molecular weight of quaternized copolymer before and after hydrolysis could not be measured by GPC. However, the representative ^{1}H-NMR spectra of the quaternized copolymer having 10% of BMDO before and after basic hydrolysis, are shown in Fig 3.3.14. The characteristic proton peak (proton 1) around 5 ppm from PBMDO, which was clearly seen before hydrolysis of the quaternized copolymer, was gone after hydrolysis, thereby showing the hydrolytic degradation capability of polymers quaternized poly(BMDO-co-DMAEMA)s containing as small as 10 mol% of ester in the backbones.

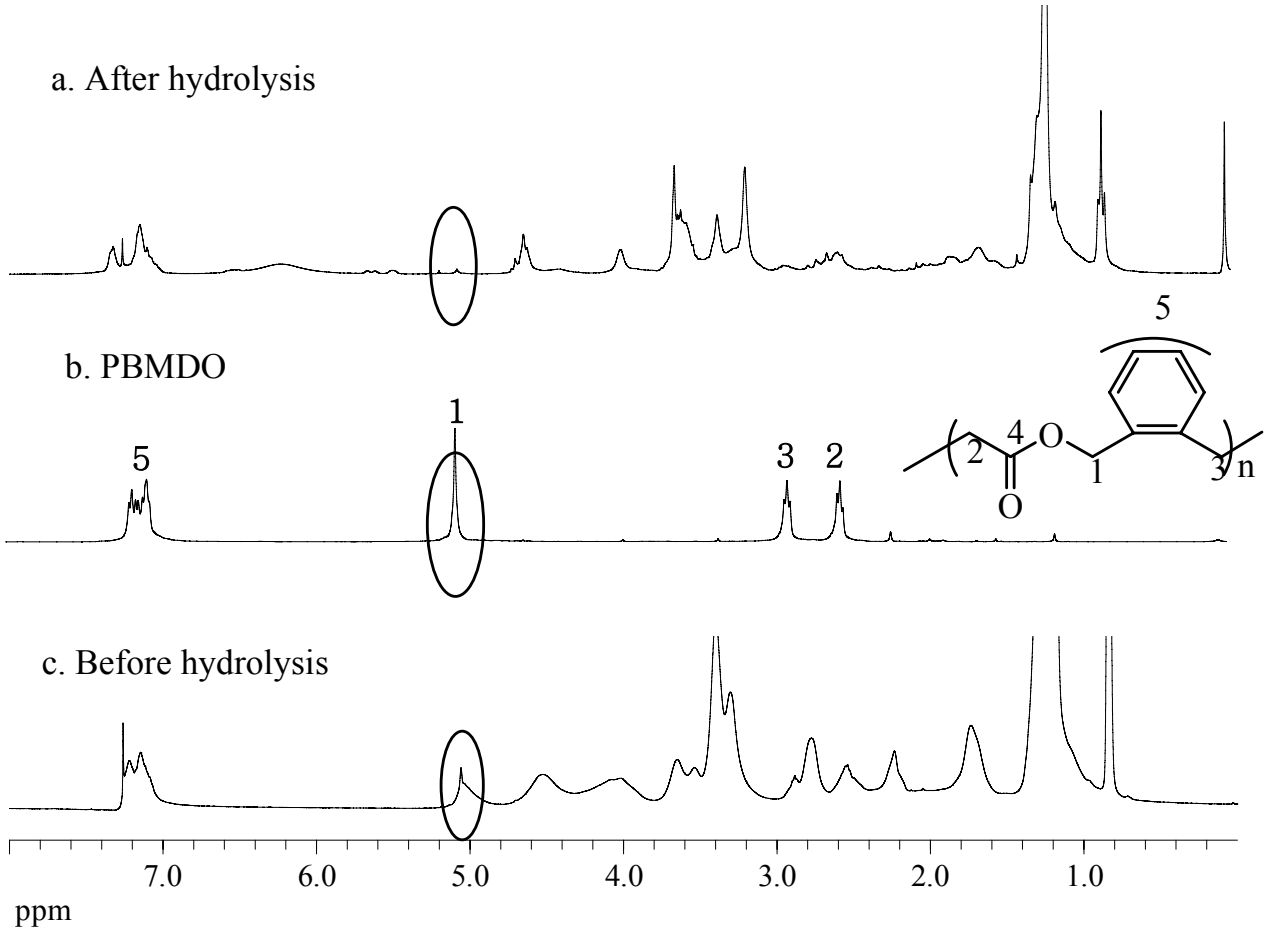

Fig 3.3.14. ^{1}H-NMR spectrum before and after hydrolysis of quaternized poly(DMAEMA-co-BMDO): (a) after hydrolysis of poly(DMAEMA-co-BMDO) •$BrC_{12}H_{25}$ with 10mol% of BMDO; (b) PBMDO; (c) before hydrolysis of poly(DMAEMA-co-BMDO)•$BrC_{12}H_{25}$ with 10mol% of BMDO.

3.3.11. Cytotoxicity test

The degradable water soluble cationic polyelectrolyte P(MDO-co-DMAEMA)•BrC_2H_5 was potential for treatment of highly anionic furnish, like proteins in the biomedical field. The cation could bind proteins and the degradable ester linkages could provide target releasing of the proteins. In order to apply the polymer in this field, the cytotoxicity was tested. The influence of the polymers on the metabolic activity of L929 cells during the incubation period of 24 hrs in a concentration-dependent manner ranging from 0-1 mg/ml is shown in Fig 3.3.15. Corresponding median lethal concentration (IC_{50}) values are summarized in Table 3.3.9. The negative control poly(ethylene glycol) PEG 6 kDa and 35 kDa showed a much higher LC_{50} value, which was more than 1mg/ml, indicating the biocompatibility of the material. As compared to that, cell viability at a concentration of 1 mg/ml was significantly reduced by polymers P(MDO-co-DMAEMA)•BrC_2H_5, which showed a LC_{50} value around 14 x 10^{-3} mg/ml. In fact, cell viability after treatment with P(MDO-co-DMAEMA)•BrC_2H_5 was similar as that with the positive control, namely PEI 25 kDa,

indicating the similar cytotoxicity of P(MDO-co-DMAEMA)•BrC_2H_5 with PEI. By varying the amount of MDO in polymer from 20 mol% to 30 mol%, the cell viability did not change too much. Since poly(caprolactone) is a widely used biocompatible material, the toxicity of P(MDO-co-DMAEMA)•BrC_2H_5 to the cells may result from the ammonium cations in the polymer chains.

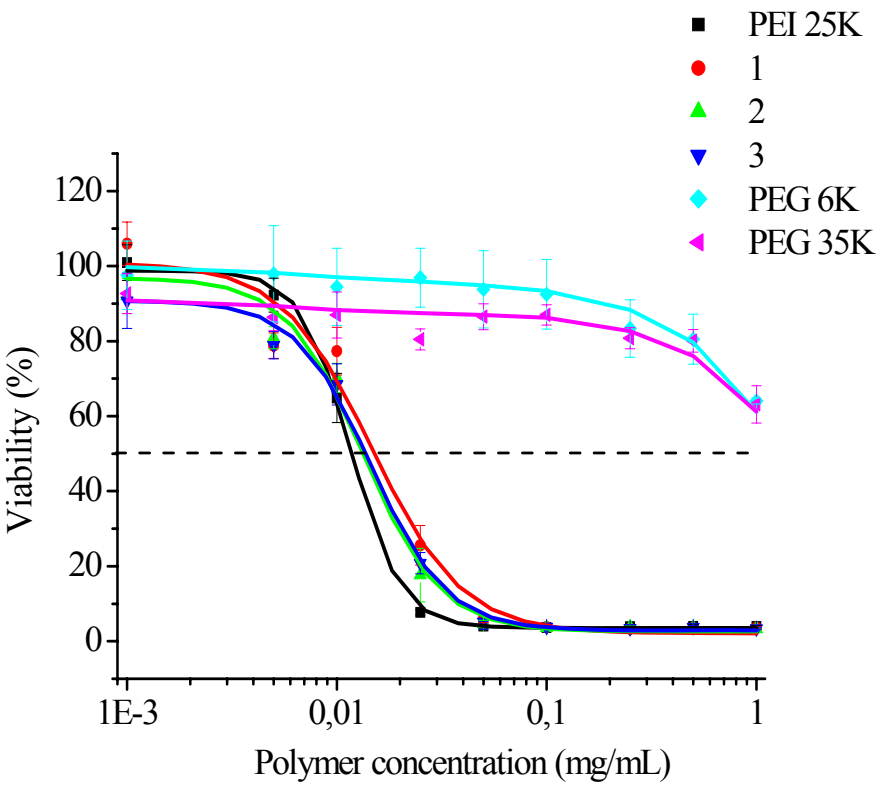

Fig 3.3.15. Cell viability measured by MTT assay after 24 hrs of incubation with serial dilutions of poly(MDO-co-DMAEMA)•BrC_2H_5 (Mn ≈ 50k) as compared to PEG 6 kDa and 35 kDa (negative control) and PEI 25 kDa (positive control): (1) polymer with 20% of MDO and 76% ion; (2) polymer with 30% of MDO and 66% of ion; (3) polymer with 25% of MDO and 72% ion.

Table 3.3.9. Median lethal concentration (LC_{50}) of polymers, values based on Figure 3.3.15

Polymer	LC_{50} (10^{-3} mg/ml)
PEG 6 kDa	>1000
PEG 35 kDa	>1000
PEI 25 kDa	11.6
1	14.7
3	14.6
2	13.4

3.3.12. Conclusion

Degradable ester linkages are successfully introduced randomly onto the vinyl polymer P(DMAEMA) backbone by a combination of radical ring-opening polymerization of BMDO and conventional vinyl polymerization of DMAEMA. BMDO showed quantitative ring-opening during the copolymerization reactions and the amount of ester linkages could be increased by increasing the amount of the BMDO in the initial feed. The copolymers were quaternized with different alkyl bromides to generate degradable cation containing polymers. Water solubility, glass transition temperature could be easily tuned by controlling the amount of BMDO incorporated in the copolymers and the length of quaternary reagent. P(BMDO-co-DMAEMA)•$BrC_{12}H_{25}$ with low-moderate mol% of BMDO (10-40 mol%) showed antibacterial activity, hydrolytic degradability and is potential material for electrospinning and hydrophobic coating. This behavior could be of great interest for many different biomedical applications. MDO showed similar polymerization behavior with DMAEMA. The resulting water soluble P(MDO-co-DMAEMA)•BrC_2H_5 obtained similar cytotoxicity as that of poly(ethylene imine) PEI.

3.4. Biodegradable cationic ionomers

3.4.1. Introduction

Interest in ionomer field has been continuing and growing since 1970s. Ionic association of the ionomers leads to their unique properties, which permits a wide range of applications in the academic and in the industrial world. In order to improve the mechanical properties of biodegradable poly(vinyl-co-ester)s, which has been intensively investigated in our lab,[134] an attempt has been made to incorporate cationic groups into the degradable vinyl polymers to create a new class of degradable cationic ionomers. Degradable cationic ionomers were synthesized by random radical terpolymerization of 2-methylene-1,5-dioxepane (MDO), methyl methacrylate (MMA) and proper amount of N,N-dimethylaminoethyl methacrylate (DMAEMA), followed by quaternization of DMAEMA with different types of alkyl bromides (Scheme 3.4.1).

The length of alkyl group was supposed to influence the strength of ionic association greatly. Different types of ionic aggregates were supposed to generate with different lengths of alkyl bromides, leading to materials with varied mechanical properties.

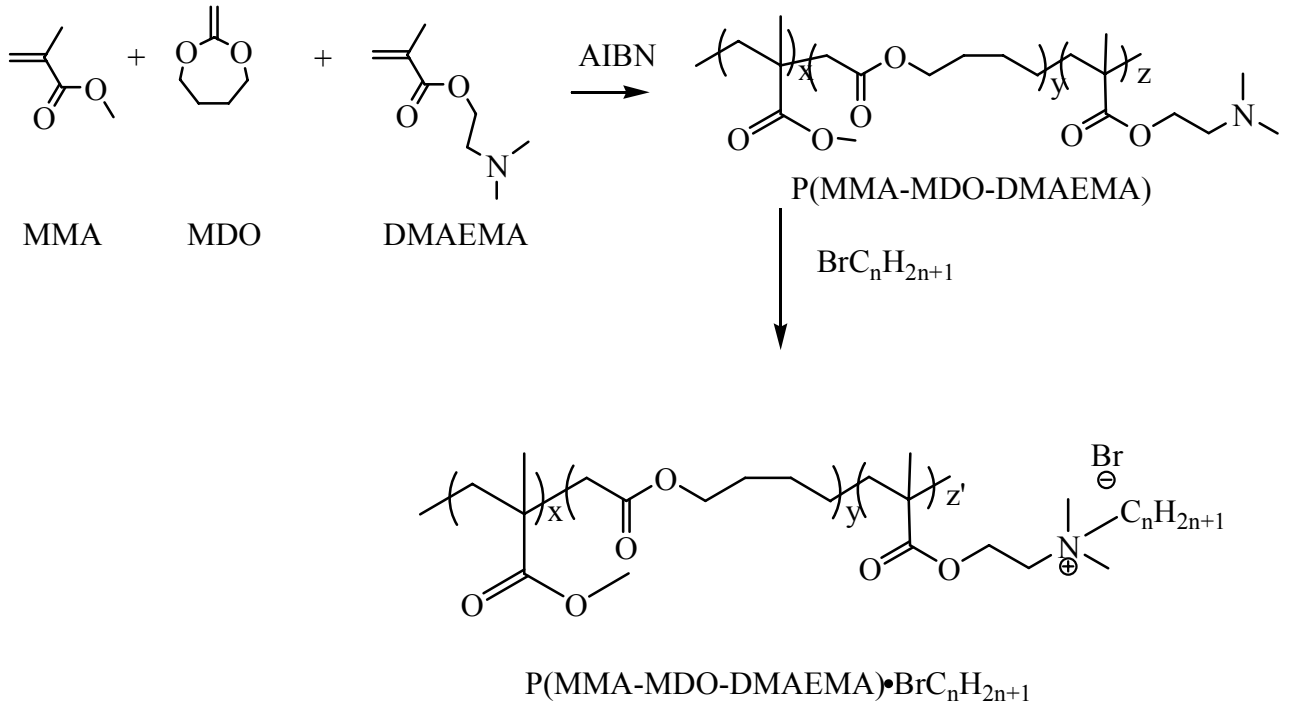

Scheme 3.4.1. Synthesis of degradable cationic ionomers.

3.4.2. Terpolymerization of MDO, MMA and DMAEMA

Based on the previous work on polymerization of cyclic ketene acetal with methyl methacrylate (MMA) and N,N-dimethylaminoethyl methacrylate (DMAEMA), various amounts of MDO, MMA and DMAEMA were terpolymerized.

3.4.2.1. Structure characterization

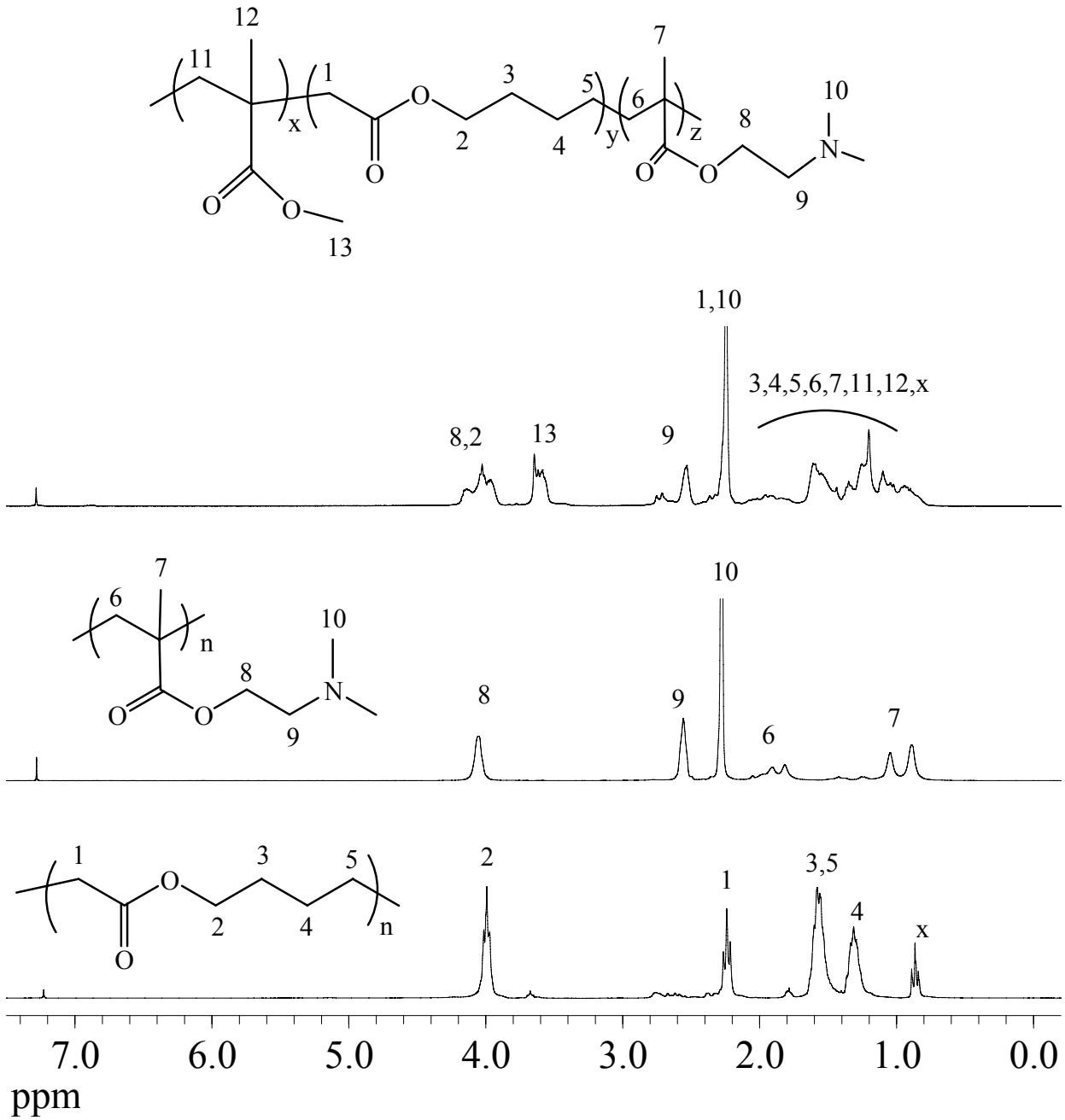

Fig 3.4.1. ^{1}H-NMR spectrum of P(MDO-MMA-DMAEMA) with the initial feed of MDO : MMA : DMAEMA = 1 : 1 : 1.

^{1}H NMR spectrum of the polymers generated from an initial feed of MDO : MMA : DMAEMA as 1 : 1 : 1 showed all the characteristic peaks from MDO, MMA and DMAEMA, indicating the existence of the termonomers (Fig 3.4.1). The terpolymer composition was determined by using the peak intensities at 3.7 ppm [I_{MMA} (–COOC*H*$_3$, proton 13 of PMMA)], 2.3 ppm [I_{DMAEMA} (–CH_2CH_2N–, proton 9 of PDMAEMA)] and 4.2 to 3.8 ppm [$I_{MDO} + I_{DMAEMA}$ (–C*H*$_2CH_2$N–, proton 8 of PDMAEMA + –OC*H*$_2CH_2$–, proton 2 of PMDO)] and was found to be MDO : MMA : DMAEMA = 12 : 43 : 45. Considering some overlapping of the peaks in the spectrum and the fact that several side reactions including backbiting of MDO may take place during terpolymerization, slight error was acknowledged during the determination of terpolymer compositions.

3.4.2.2. Influence of initial feed on terpolymerization

Terpolymers with varied compositions were synthesized by changing the initial feeds (Table 3.4.1). Increasing the amount of MDO and keeping the same small amount of DMAEMA in the initial feeds lead to an increase of ester amount and a slight increase of DMAEMA in the terpolymers. Terpolymers with same amount of ester and different amounts of DMAEMA were synthesized by varying the amount of DMAEMA and keeping the amount of MDO to be constant in the initial feeds. The amount of MMA and DMAEMA in the terpolymers was found to be always higher than that in the initial feed. It indicates that the reactivities of both MMA and DMAEMA were higher than that of MDO. The amount of MDO in the terpolymers was found to be around 40% to 60% of that in the initial feed. This ratio increases by increasing the amount of MDO in the initial feed. The polymerization rate was found to be decreasing by increasing the amount of MDO and DMAEMA in the initial feed, indicating the relative slower chain propagation of MDO and DMAEMA than MMA.

Molecular weights of terpolymers were measured by GPC (Table 3.4.1). Generally, terpolymers showed uni-modal peak with a molecular weight around 30,000 to 60,000 and a typical polydispersity around 2.0. Fig 3.4.2 shows an example of GPC curve with a uni-modal peak, which helps to indicate the random terpolymerization of the monomers. Some of the samples of terpolymers did not generate visible signals in the GPC curves (DMF as solvent). Problem may result from the interaction of terpolymers with the column. The reason of this is not clearly known.

Table. 3.4.1. Bulk terpolymerization of MDO, MMA and DMAEMA (D) with 1 mol% of AIBN as initiator, reaction temperature: 70°C, reaction time: 20 hrs; /: no signal generated by GPC

Run	Feed Ratio (molar ratio)			Yield (%)	Terpolym. Composition (molar ratio)			M_n	PDI
	MDO	MMA	D		MDO	MMA	D		
1	30	65	5	81	12	81	7	37000	2
2	50	45	5	70	21	69	10	55000	2
3	70	25	5	64	40	50	10	/	/
4	70	20	10	52	40	40	20	/	/
5	70	15	15	49	40	32	28	/	/

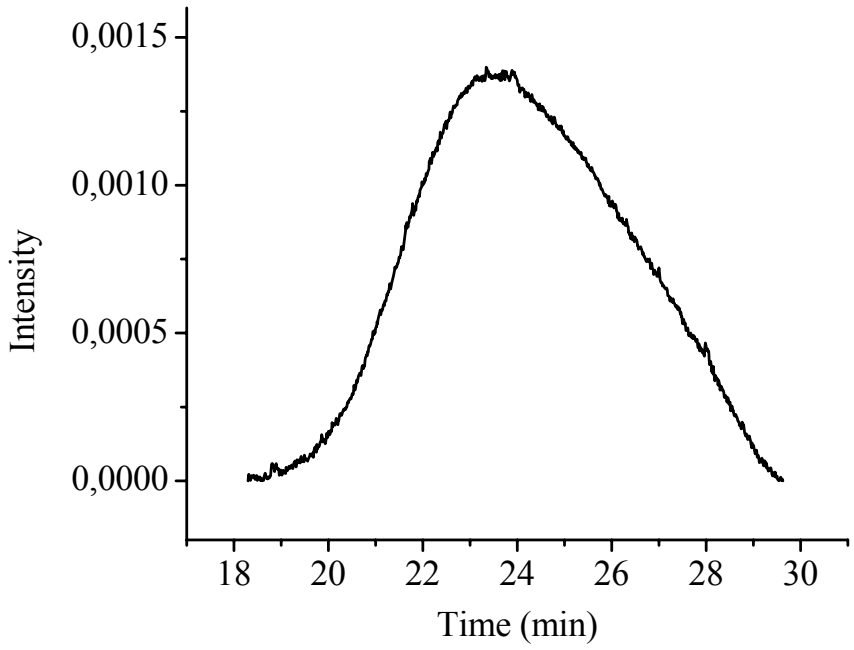

Fig 3.4.2. GPC curve of P(MDO-MMA-DMAEMA) (run 1, Table 3.4.1).

3.4.2.3. Influence of reaction time on terpolymer structure

In order to have an insight into the copolymerization behavior and the microstructure of the copolymers, for one specific initial feed (MDO : MMA : DMAEMA = 50 : 25 : 25 molar ratio), the polymerization was followed at different intervals of time (Table 3.4.2). There was a continuous increase of reacted MDO, MMA and DMAEMA with time, indicating a constant incorporation of

all the monomers during the random polymerization (Fig 3.4.3). The rates of consumptions of MMA and DMAEMA were almost similar and much faster than that of the MDO. This indicates the preference of monomer radicals for the DMAEMA and MMA monomers compared to MDO during copolymerization and therefore, most probably resulting in MMA-DMAEMA, MMA-MMA, DMAEMA-DMAEMA and DMAEMA-MMA in the terpolymer chains with isolated or very short MDO sequences. After 1.5h, the monomers MMA and DMAEMA were completely consumed but MDO was kept almost constant and did not increase further. It gives us a hint that as conversion and the viscosity increase to some extent, propagation of MDO-MDO would be very difficult to take place. Therefore after total consumption of MMA and DMAEMA, homopolymerization of MDO goes extremely slowly within the reaction time.

Table 3.4.2. Kinetic information of copolymerization of MDO, MMA and DMAEMA (50 : 25 : 25 mol% in the initial feed), AIBN : Monomers = 1 : 100 (in molar ratio), copolymerization temperature: 70^{o}C

Run	Reaction Time (h)	Terpolym. Composition (molar ratio)			Conversion (%)
		MDO	MMA	DMAEMA	
1	1/6	9	45	46	12
2	2/3	12	44	44	46
3	1.5	20	42	38	70
4	4	21	43	36	73
5	15	21	38	41	74

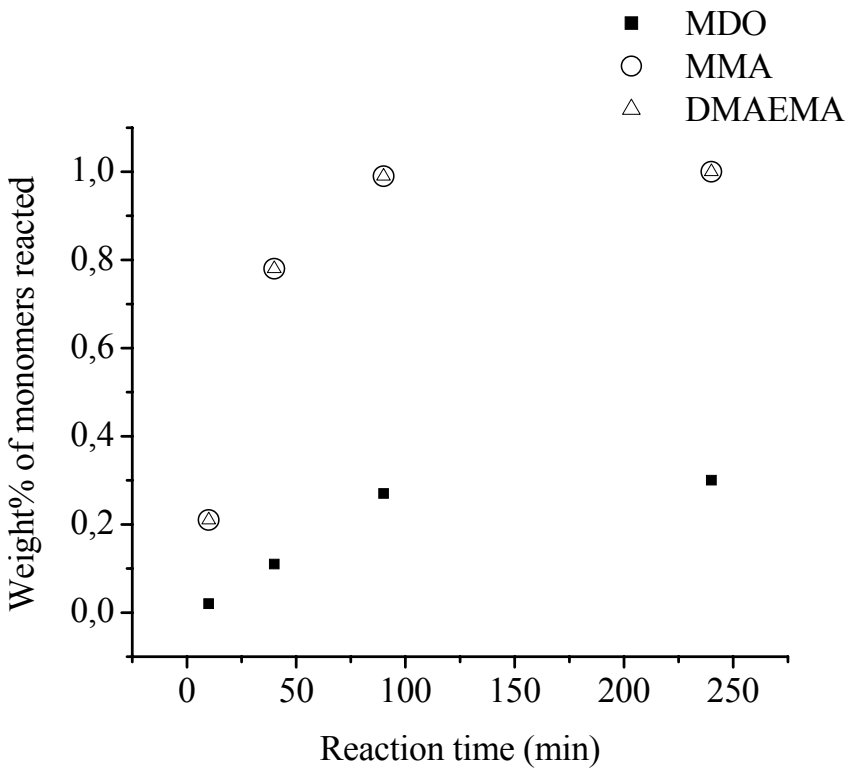

Fig 3.4.3. Weight% of reacted monomers versus reaction time: monomers in initial feed: MDO : MMA : DMAEMA = 50 : 25 : 25 (mol%), AIBN : Monomers = 1 : 100 (mol%), reaction temperature: 70^{o}C.

3.4.3. Quaternization of poly(MDO-MMA-DMAEMA)

Polymerization was followed by quaternization of amines with different types of alkyl bromides (Table 3.4.3). Quaternization was carried for 3 days to get a relative high conversion，which was determined by elemental analysis by comparing the mol% of bromine and nitrogen in the samples (conversion = mol% Br / mol% N). Even though possible error could happen during the measurement, it gives us relatively reliable data on the total ionic content in the final product. Polymers with 40 mol% of ester groups and different amount of quaternary amine based on $BrC_{12}H_{25}$ and BrC_2H_5 were generated. It is clearly seen that the quaternization rate of polymer with BrC_2H_5 is much easier than that with $BrC_{12}H_{25}$, due to the short ethyl group.

Table 3.4.3. Quaternization of P(MDO-MMA-DMAEMA), reaction time: 3 days (Ion content was calculated by "mol% of DMAEMA in polymer" x "quaternization conversion")

Run	Terpolym. Composition (molar ratio)			Quaternization		Ion Content (mol%)
	MDO	M	D	BrC_nH_{2n+1} n	Conversion (%)	
1	40	50	10	12	43	4.3
2	40	50	10	12	70	7
3	40	40	20	12	59	12
4	40	32	28	12	74	21
5	40	50	10	2	91	9
6	40	40	20	2	95	19
7	40	32	28	2	96	27

3.4.4. Ionic aggregation

For most of the widely investigated anionic ionomers, like poly(styrene-co-sodium methacrylate), two kinds of ionic environments (primary and higher aggregates) were detected in ionomers by several spectroscopic experiments.[135, 136] Several models have been proposed for this phenomena, including the core-shell model, the hard sphere model and the most popular multiplet-cluster model. Based on Eisenberg, the formation of primary ionic aggregates, known as multiplets, is the fundamental element in ionomers. Due to the dramatic difference of the solubility and the size between the ion pairs(such as $-COO^{\ominus}\ Na^{\oplus}$, or $-SO_3^{\ominus}\ Na^{\oplus}$) and the nonionic polymer segments, only several (no more than 10) ion pairs can possibly associate together to form a multiplet, which is tightly attached and separated with each other by the long neutral polymer chains. At higher ionic content, several multiplets together with their nonionic surrounding will overlap to form higher aggregate regions, which are called clusters (Chapter 2.4.3). The characteristic anionic ionomer SAXS peaks, centered at q values ranging from 1.5 to 2.5 nm^{-1}, result from scattering of the primary multiplets. The scattering spaces ranging from 4 to 2.5 nm, based on Bragg's law ($d = \lambda/2\sin\Theta$), are assigned to be the distances between multiplets. However, the cationic ionomers, which were studied here, are found to be a different system from the well known anionic ionomers.

3.4.4.1. Ionomers quaternized by BrC_2H_5

3.4.4.1.1. Electron microscopic analysis

Due to the big molecular mass of Bromine, the high ionic aggregate regions in the ionomers can be directly observed by TEM. Fig 3.4.4 and 3.4.5 clearly show the visible ionic aggregates with a diameter concentrated around 30 nm. Precisely, there seems to be an amount of finely small aggregates and, therefore, a broad distribution of the sizes, which could not be seen very clearly due to the limited resolution of the techniques. The sizes of the visible aggregates in TEM pictures showed similar when the total ionic amount increases to twice. The form of the observed aggregates is irregular from the first sight. However, Fig 3.4.5 shows that the aggregates tend to grow to be spherical. TEM pictures can not give a clue of distances between the aggregates or the density of the aggregates in the ionomers since the thicknesses of the films prepared for TEM are not identical and the resolution of TEM is limited. More detailed information about the morphology, including the distance of the aggregates, the formation of the aggregates and the possibility of the existence of the two kinds of ionic aggregates, and etc. needs to be investigated with the help of other experimental technologies.

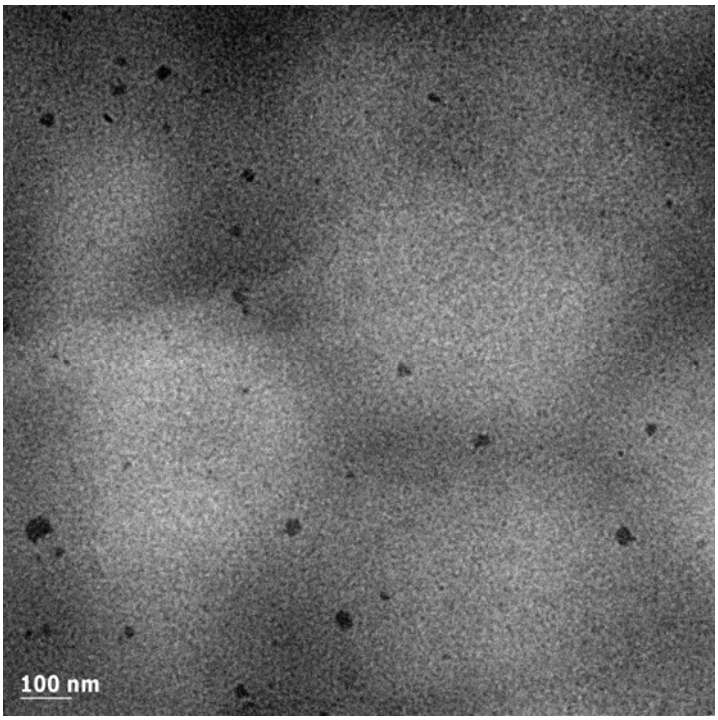

Fig 3.4.4.TEM pictures of P(MDO-MMA-DMAEMA)•BrC_2H_5 containing 9% ion (40-50-10), sample prepared by film casting on the TEM grid.

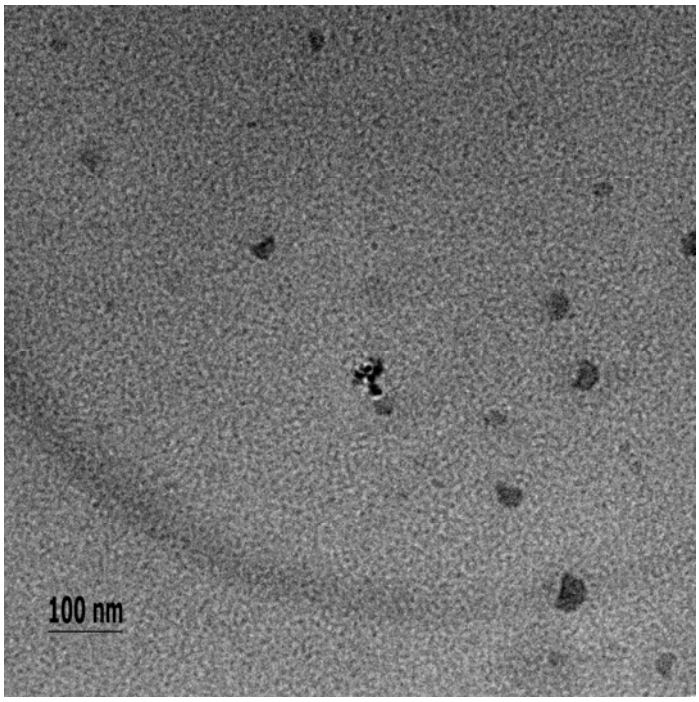

Fig 3.4.5. TEM pictures of P(MDO-MMA-DMAEMA)•BrC_2H_5 containing 18% ion (40-40-20), sample prepared by film casting on the TEM grid.

3.4.4.1.2. Small Angle X-Ray Scattering (SAXS) analysis

SAXS analysis has been actually the most reliable and the most available evidence for the existence of the ionic aggregates in ionomers. A peak was shown in SAXS profile (Fig 3.4.6 and Fig 3.4.7) for polymers with 9% and 18% ionic groups, resulting from the scattering of ionic aggregates. The scattering peak is much broad and centered at q = 0.16 nm^{-1}. Based on Bragg's law ($d = \lambda/2\sin\Theta$), there is a broad distribution of the scattering spaces, ranging from 5 nm to 45 nm and centered at 36 nm and 40 nm for 9% and 18% of ion, respectively. This average space is in the order of the size of the aggregates, which is around 30 nm, observed by TEM techniques. Since there is no possibility to put a 40 nm scattering lattice into a 30 nm ionic aggregate. It is proposed that the characteristic SAXS peak with a q value centered at 0.16 nm^{-1} does not derive from the scattering of primary multiplets, but direct from higher ionic aggregates (30 nm), called clusters, and the scattering spaces were assigned to be the distances between clusters. When increasing the amount of the total ion content from 9% to 18%, the intensity of the scattering peaks increases, which indicates an increase of the surface area of the clusters.

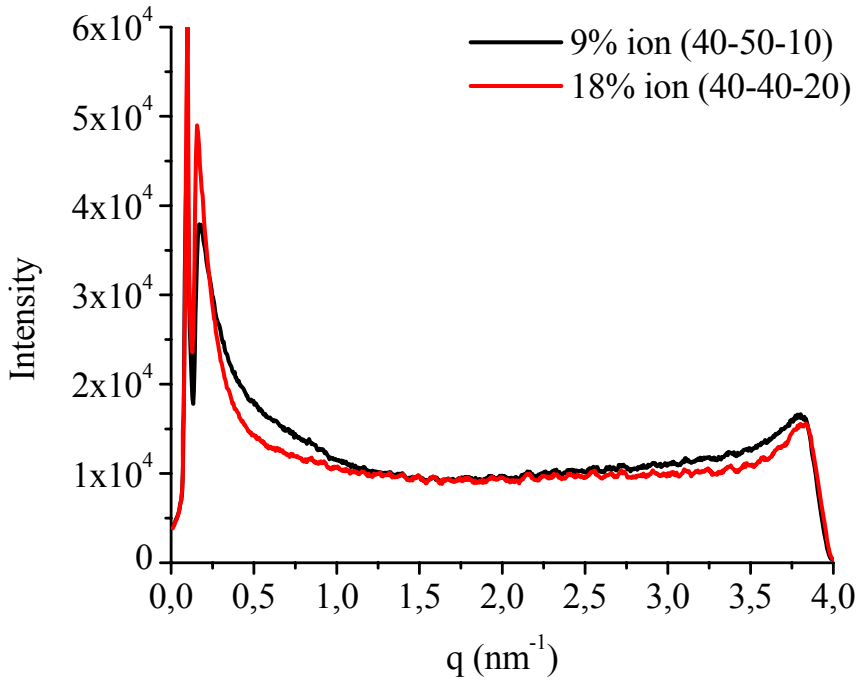

Fig 3.4.6. SAXS profile of P(MDO-MMA-DMAEMA)•BrC_2H_5 , (40-50-10) is the terpolymer composition of MDO : MMA : DMAEMA in molar ratio.

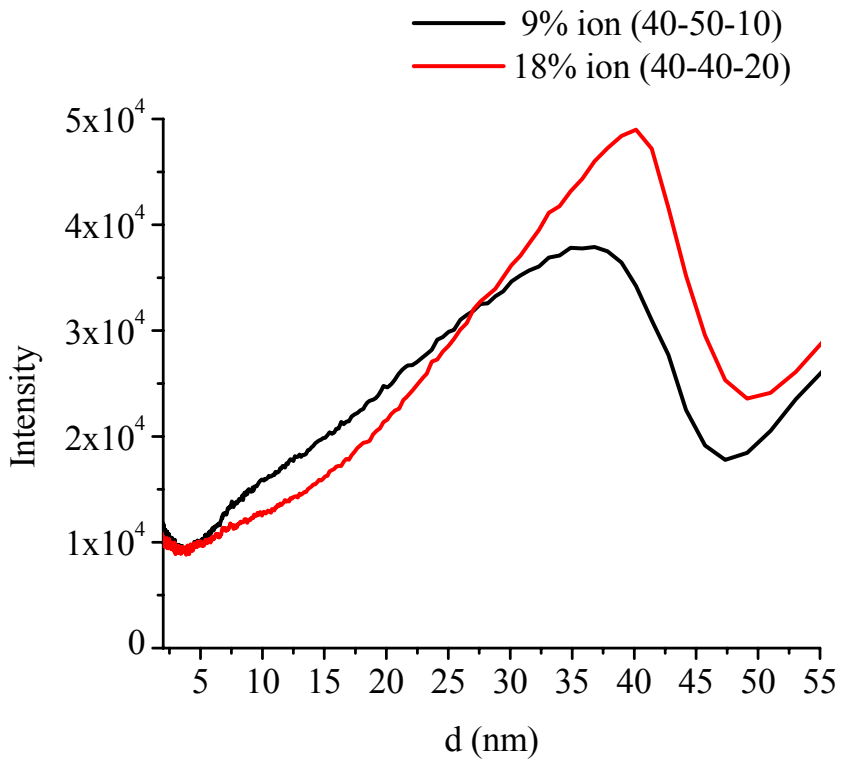

Fig 3.4.7. SAXS profile of P(MDO-MMA-DMAEMA)•BrC_2H_5 after calculation according to Bragg's law: d = λ/(2sinΘ), (40-50-10) is the terpolymer composition MDO : MMA : DMAEMA in molar ratio.

3.4.4.1.3. New model on ionic aggregations

A new model is proposed here to explain the formation of the aggregates in cationic ionomers quaternized by BrC_2H_5.

The driving force of the firm and even spherical primary ionic aggregates, known as multiplet, is the high ion-counter ion electrostatic association energy and the dramatical difference of the solubility of the ionic groups from the polymer chains. Considering the structural characteristic of this quaternary amine cationic ionomer system, the strength of ionic association energy and the difference of the solubility between ionic groups and the polymer backbones are highly decreased by the alkyl groups (including two methyl groups and one ethyl group) on the quaternary amines. It is, therefore, not possible to form a sharp interface between ionic groups and nonionic polymer chains. Due to the relative weak ionic association energy, the primary multiplets may contain less number of ionic groups than that in anionic ionomers. At a higher ionic content, the distances between multiplets decreases. Once overlapping of the restricted polymer covers surrounding the multiplets take place, primary multiplets tend to form higher aggregates, called clusters. When the quaternization takes place it is not perfectly random, there is supposed to be a broad distribution of the sizes of the multiplets and also clusters. If the weak multiplets intra cluster can scatter X-ray, the q value may be too high and beyond the experimental range, which is 0 to 4 nm^{-1}. The scattering ionic peak with a q value centered at 0.16 nm^{-1} results from the scattering of higher aggregates, called clusters. The scattering spaces were assigned to be the distances between the clusters. TEM could not show a clear difference between the sizes of the aggregates with increasing the ionic content from 9% to 18%, partly due to the resolution of the techniques. Another reason could be a balance between electrostatic energy of the ionic association and the elastic energy of the nonionic polymer chains was achieved for the size of aggregates at such high ionic contents. Therefore, the size of the ionic aggregate is limited. In fact, the intensity of the scattering peak increased greatly. It indicates that the concentration of the aggregates increases with increasing the ionic content. From X-Ray profile we can also see that the scattering intensity from the short scattering distances (around 5 nm to 15 nm) decreases somehow, which may indicate that the very small aggregates grow to bigger ones.

3.4.4.1.4. Differential Scanning Calorimetry (DSC)

DSC showed one glass transition temperature for P(MDO-MMA-DMAEMA), before and after quaternization with BrC_2H_5 (Fig 3.4.8 and Table 3.4.4). P(MDO-co-MMA) and P(MDO-MMA-DMAEMA) containing similar amount of MDO and MMA showed similar glass transition temperature i.e. around -8°C (run 1, 2. Table 3.4.4). After quaternization with BrC_2H_5, the glass transition temperature was clearly increased, which was assigned to be one of the neutral matrix polymer chains (run 3, 4. Table 3.4.4). More ionic aggregates lead to more restricted matrix polymer chains, therefore, increasing the ionic amount in the polymer, the glass transition temperature of the matrix increased. However, the ionic aggregates were too small to show a separate T_g for DSC analysis.

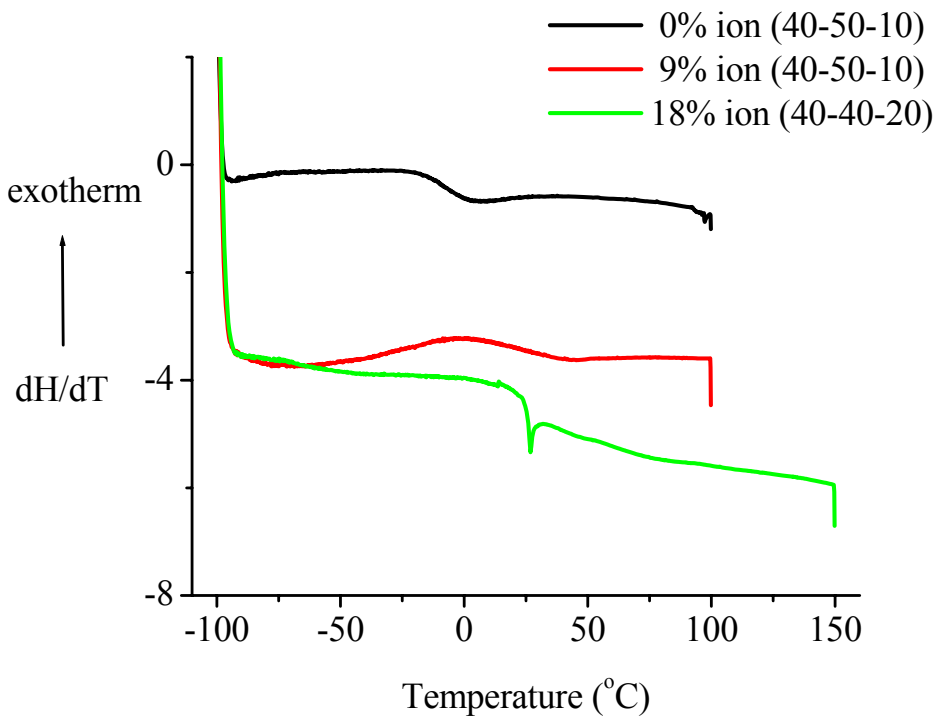

Fig 3.4.8. Differential Scanning Calorimetry (DSC) curve of P(MDO-MMA-DMAEMA)•BrC_2H_5 (the second heating cycle), (40-50-10) is the terpolymer composition MDO : MMA : DMAEMA in molar ratio.

Table 3.4.4. Glass transition temperature (T_g) of P(MDO-MMA-DMAEMA) before and after quaternization, values measured by DSC

Run	Polymer Composition (mol %)			Ion Content (mol %)	T_g (^oC)
	MDO	MMA	DMAEMA	Br_2H_5	
1	44	56	0	---	-9[134]
2	40	50	10	---	-8
3	40	50	10	9	19
4	40	50	20	18	25

3.4.4.1.5. Dynamic Mechanical Analysis (DMA)

DMA is a very useful method to further explore the properties of the ionic aggregates and the nonionic polymer backbones, including the sizes, the volume fraction of the aggregates and the restricted mobility of the chains of ionomers.

The dynamic properties of ionomers quaternized with BrC_2H_5 are shown in Fig 3.4.9. Nonionic poly(MMA-co-MDO) obtained one peak centered at 41^{o}C to show the glass transition of the nonionic polymer chains. In ionomers quaternized with BrC_2H_5 with 9% of ionic groups, there is one peak for glass transition at 51^{o}C and a clear shoulder around 80^{o}C. Comparing with the glass transition temperature of the matrix polymer chains determined by DSC (Chapter 4.4.1.4), the peak centered at 51^{o}C by DMA analysis was assigned to be the glass transition of the nonionic polymer chains. Due to ionic aggregates, the mobility of the nonionic polymer backbones inter aggregates were also restricted. Therefore, the glass transition temperature increased 10 degrees. The shoulder at 80^{o}C resulted from the glass transition temperature of the ionic aggregates with highly restricted mobility. As is known, once a region can show a separated glass transition, the size of it should be at least 5-10 nm. Therefore, the majority of the sizes of the ionic aggregates should be more than 5-10 nm, which is in agreement with the proposals according to TEM and SAXS analysis. These aggregates are what we called clusters.

When ionic content increases to 18%, the shoulder increased further to 97^{o}C and became a clear peak. As is known, the areas of the peaks indicate the volume fractions of the non-ionic polymer

regions between aggregates and ionic aggregates regions. Even though the quantitative data could not be calculated due to the peak overlapping, it can be seen that the volume fraction of the ionic aggregates increases greatly when increasing the total ionic content from 9% to 18%. The increasing ionic content increases the glass transition of both the matrix polymer chains and also the ionic aggregate regions. However, the dielectric constant of the matrix polymer chains influences the formation of ionic aggregates. When the total ionic content further increases to 27%, the higher glass transition temperature disappeared and there is again one peak around 51^{o}C. Clearly there is no big ionic aggregate existing in this polymer. It indicates that there is a limit of ionic content for ionomers quaternized with BrC_2H_5 to generate higher ionic aggregates, which are more than 5 to 10 nm. When the ionic content exceeds the limit leading to a high dielectric constant of the whole polymers, the ionic groups tend to be solved in the whole polymer, probably leading to only multiplets or even no aggregations.

Due to the formation of ionic aggregates, the shapes of storage modulus versus temperature for different polymers changed (Fig 3.4.10). The storage moduli of different polymers at low temperatures up to 0^{o}C are similar, without visible influence from the ionic aggregates. When temperature increases close the glass transition of the matrix polymer around 30^{o}C to 40^{o}C, due to the formation of the ionic aggregates, the storage modulus of ionomers becomes higher than nonionic poly(MMA-co-MDO). Increasing the ionic amount from 9% to 18%, the storage modulus increases to some extent, indicating the increase of ionic aggregates. The storage modulus of P(MDO-MMA-DMAEMA)•BrC_2H_5 with 27% of ion decreases compared to ionomers with 9% and 18% of ion, indicating again the decrease of ionic aggregates.

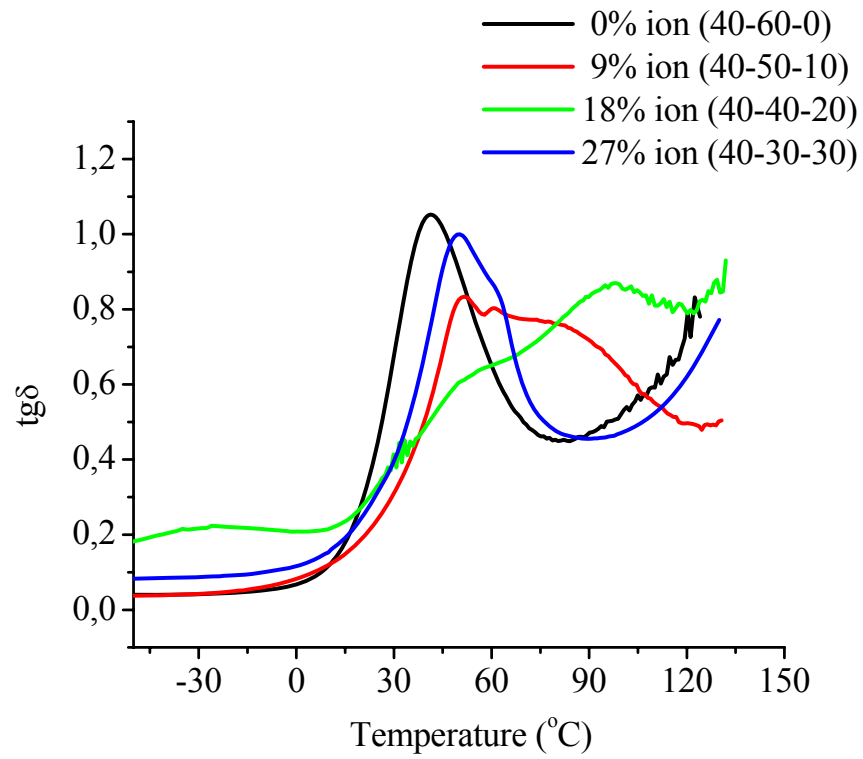

Fig 3.4.9. Los tangent (tgδ) versus temperature of P(MDO-MMA-DMAEMA)•BrC_2H_5, (40-50-10) is the terpolymer composition MDO : MMA : DMAEMA in molar ratio.

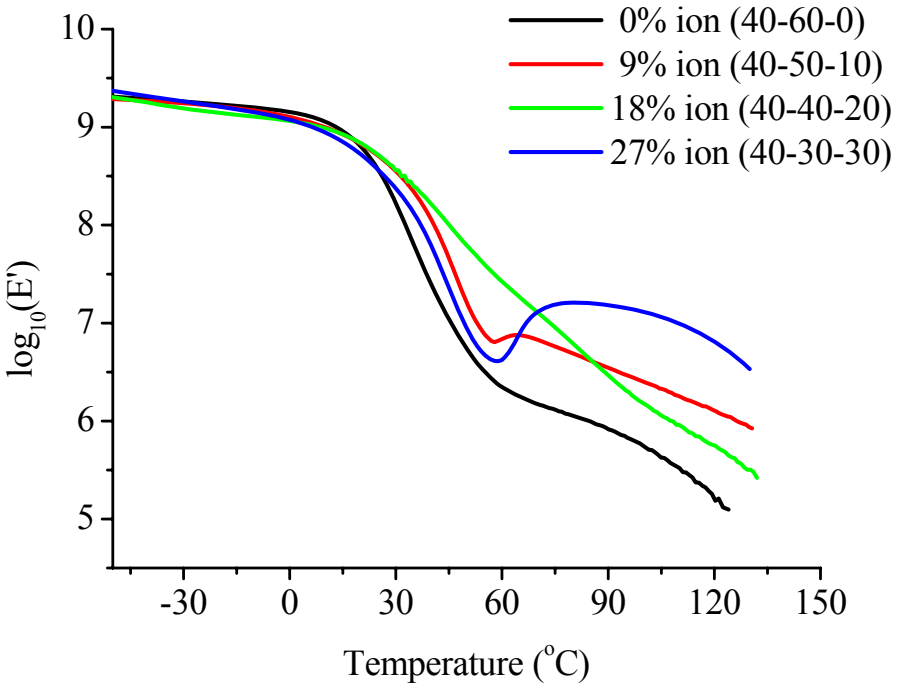

Fig 3.4.10. Log_{10}(E') versus temperature for P(MDO-MMA-DMAEMA)•BrC_2H_5. (40-50-10) is the terpolymer composition MDO : MMA : DMAEMA in molar ratio.

3.4.4.2. Ionomers quaternized with $BrC_{12}H_{25}$

3.4.4.2.1. Small Angle X-Ray Scattering (SAXS) Analysis

SAXS profiles for ionomers quaternized with $BrC_{12}H_{25}$ also showed ionic peaks (Fig 3.4.11 and Fig 3.4.12), which demonstrate the existence of ionic aggregates. When comparing with that for ionomers quaternized with BrC_2H_5, the scattering intensities are greatly decreased, indicating the concentration of ionic aggregates is relative small. Another difference is that there are two peaks shown in the profile. It shows that there are two different distances, centered at 5 nm and more than 30 nm, respectively, according to the Bragg's law, between ionic aggregates. The reason of two scattering peaks is not that clear. Probably it is due to the non-random quaternization of the amines. Since $BrC_{12}H_{25}$ has a long alkyl group, it is not very easy for the quaternization to take place. In the region with relatively high ionic concentration, there is a short distance between aggregates. While in the region with relatively low ionic concentrations, there is a relatively long distance between aggregates. When increasing the amount of the total ion content in ionomers, the scattering intensity at lower q value decreases and that at higher q value increases, which indicates an increase of the amount of aggregates with short distances.

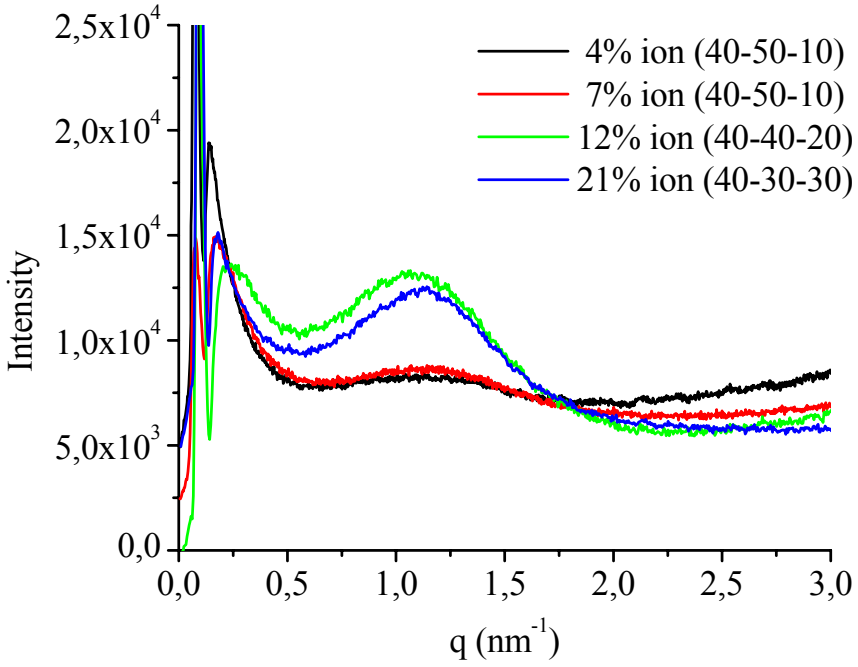

Fig 3.4.11. SAXS profile of P(MDO-MMA-DMAEMA)•$BrC_{12}H_{25}$, (40-50-10) is the terpolymer composition MDO : MMA : DMAEMA in molar ratio.

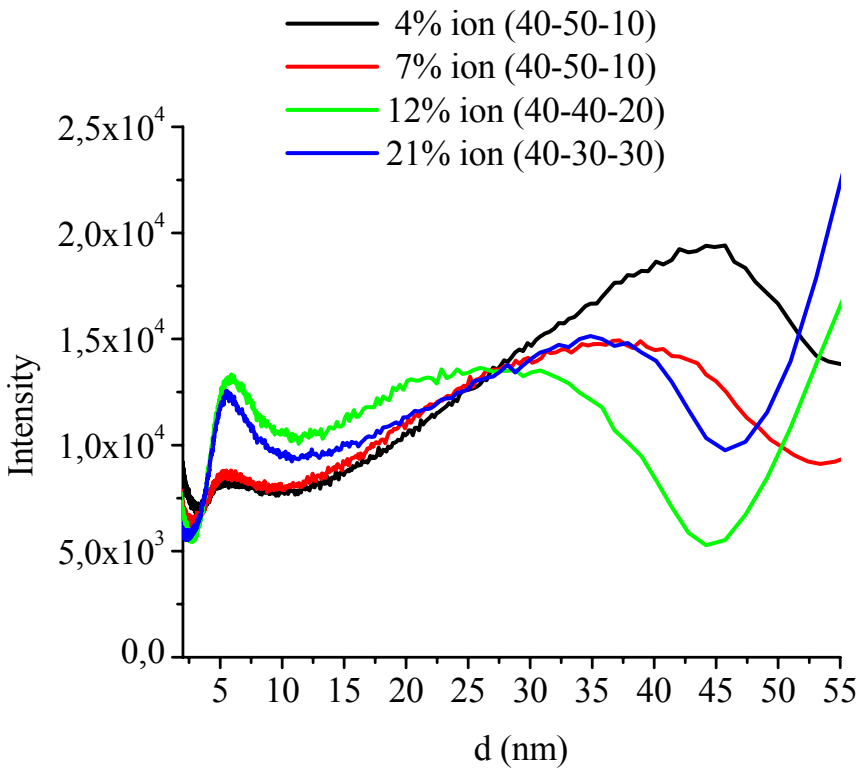

Fig 3.4.12. SAXS profile of P(MDO-MMA-DMAEMA)•$BrC_{12}H_{25}$ after calculation according to Bragg's law: $d = \lambda/(2\sin\Theta)$, (40-50-10) is the terpolymer composition MDO : MMA : DMAEMA in molar ratio.

Compared to ionomers quaternized by BrC_2H_5, it is not that easy to observe clear visible aggregates by TEM.

3.4.4.2.2. Differential Scanning Calorimetry (DSC)

DSC showed one glass transition of P(MDO-MMA-DMAEMA) before and after quaternization with $BrC_{12}H_{25}$ (Fig 3.4.13 and Table 3.4.5). After quaternization, the glass transition temperature increased and became very broad. More ionic aggregates lead to more restricted matrix polymer chains, therefore, increasing the ionic amount in the polymer, the glass transition temperature increased. However, the ionic aggregates were too small to show a separate glass transition for DSC analysis.

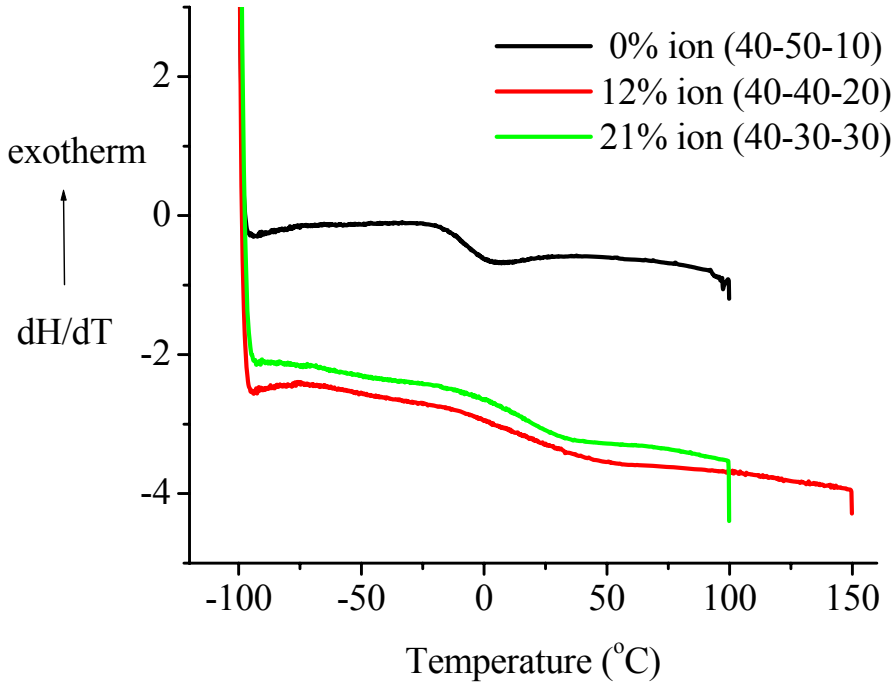

Fig 3.4.13. Differential Scanning Calorimetry (DSC) curve of P(MDO-MMA-DMAEMA)•$BrC_{12}H_{25}$ (the second heating cycle), (40-50-10) is the terpolymer composition MDO : MMA : DMAEMA in molar ratio.

Table 3.4.5. Glass transition temperature (T_g) of P(MDO-MMA-DMAEMA) before and after quaternization with $BrC_{12}H_{25}$, values measured by DSC

Run	Polymer Composition (mol %)			Ion Content (mol %)	T_g (°C)
	MDO	MMA	DMAEMA	$Br_{12}H_{25}$	
1	44	56	0	---	-9[155]
2	44	50	10	---	-8
3	40	50	10	4	13
4	40	50	10	7	18
5	40	40	20	12	25
6	40	30	20	21	21

3.4.4.2.3. Dynamic Mechanical Analysis (DMA)

Further, dynamic mechanical property of ionomers with different quaternization behavior was investigated (Fig 3.4.14). Non ionic poly(MMA-co-MDO) showed one T_g at 41°C. Ionomers with 18% of ion, quaternized with BrC_2H_5, showed two glass transitions and, therefore, demonstrate that the major size of the ionic aggregates should be more than 5 to 10 nm, according to chapter 3.4.1.3.

However, ionomers quaternized with $BrC_{12}H_{25}$ have only one glass transition. This glass transition is broad and centered at 64°C, which is 23°C higher than that for the nonionic polymer regions. The ionic aggregates should be too small to show a separated glass transition. It is proposed that the small ionic aggregates (smaller than 5nm) can act as crosslinkings to broaden the glass transition of the polymers.

Due to the formation of ionic aggregates, the storage modulus of ionomers quaternized with $BrC_{12}H_{25}$ increase in the temperature range of 30°C to 75°C, compared to the nonionic polymer (Fig 3.4.15). The storage modulus of ionomers quaternized with $BrC_{12}H_{25}$ is smaller than that of ionomers quaternized with BrC_2H_5, resulting from the relative weak ionic association.

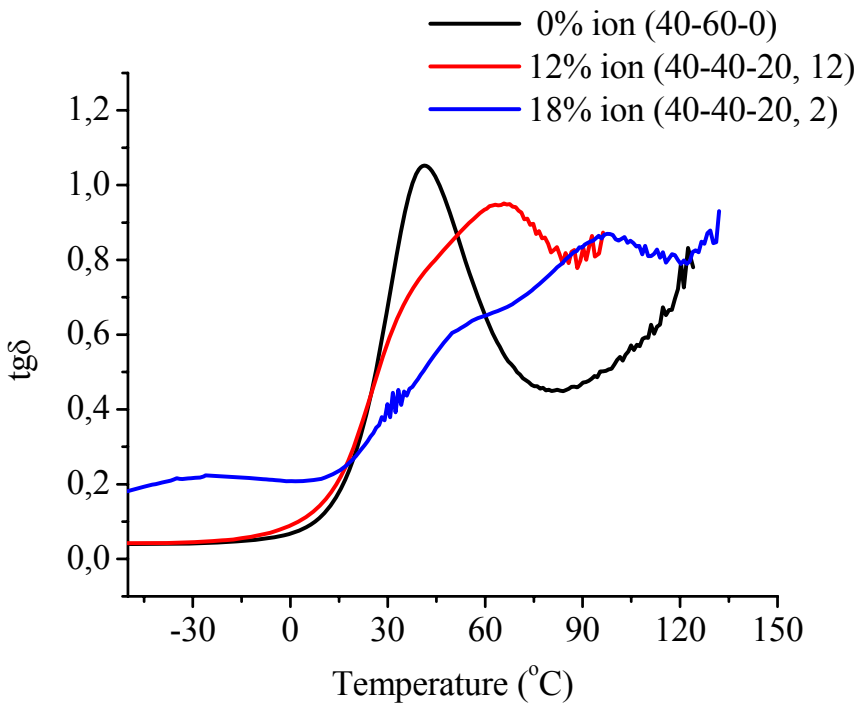

Fig 3.4.14. Loss tangent (tgδ) versus temperature for quaternized P(MDO-MMA-DMAEMA), (40-50-20, 12) means polymer quaternized with $BrC_{12}H_{25}$ with MDO : MMA : DMAEMA = 40 : 50 : 20 in molar ratio.

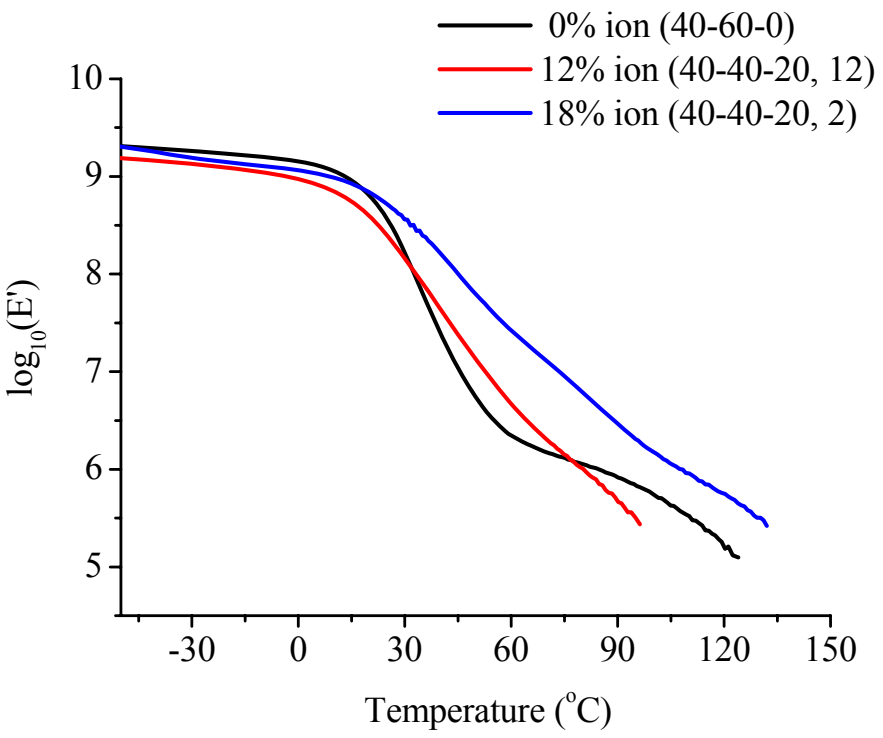

Fig 3.4.15. $Log_{10}(E')$ versus Temperature of quaternized poly(MDO-MMA-DMAEMA), (40-40-20, 12) means polymer quaternized with $BrC_{12}H_{25}$ with MDO : MMA : DMAEMA = 40 : 40 : 20.

3.4.5. Influence of temperature on ionic aggregation

The effect of temperatures on the formation of ionic aggregates was also investigated. Fig 3.4.16 shows scattering peaks in SAXS profiles throughout the temperature range from 20°C to 140°C, demonstrating the existence of the ionic aggregates under heating. However, the scattering intensity of ionic aggregates with a q value centered at 0.14 nm^{-1} tends to increase and takes more majority when increasing the temperatures from 20°C to 100°C, probably resulting from the dissociation of higher aggregates formed by overlapping of multiplets to small ones. After 100°C, there is no change of the scattering profiles. The ionic aggregates existing in the system are proposed to be only primary multiplets, which are stable until under high temperature until 140°C.

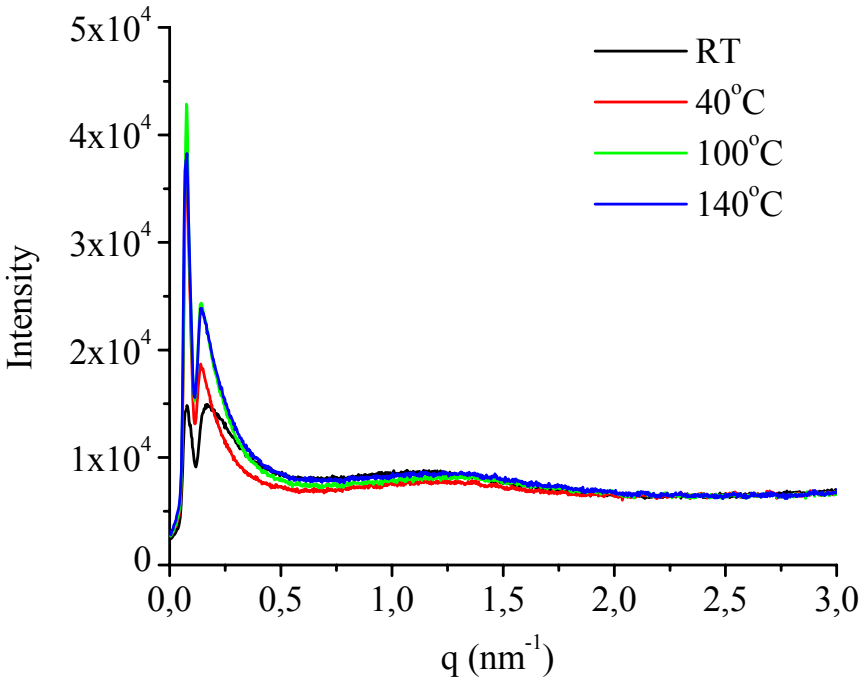

Fig 3.4.16. SAXS of P(MDO-MMA-DMAEMA)•Br$C_{12}H_{25}$ (40-50-10) at different temperatures.

3.4.6. Influence of the matrix composition on ionic aggregations

An attempt to investigate the ionic aggregation behavior of quaternized poly(MDO-MMA-DMAEMA) containing similar amount of ionic groups and different matrix compositions was tried. SAXS analysis could not determine the existence of ionic aggregates due to the broad peak from penetrated primary beams, which covered the range of the possible scattering peaks. In DSC thermograms (Fig 3.4.17), no T_g could be observed for quaternized polymer containing 9% MDO, 83% MMA and 8% DMAEMA. Increasing the amount of MDO to 21%, one wide broad glass transition region was slightly observed. Further increasing the amount of MDO to 40%, one glass transition temperature at 19°C was clearly observed. DMA (Fig 3.4.18) showed two peaks or/and shoulder for the samples with a composition of MDO : MMA = 9 : 83, 21 : 69 and 40 : 50. The first peak at lower temperature region in the DMA curve was assigned to be the glass transition of the matrix polymer chains. The second peak on DMA curve is supposed to be the glass transition temperature of the ionic aggregates, which remained the same with different matrix compositions, indicating that the restrictions of the aggregates were not influenced by the matrix compositions. However, the matrix composition apparently influenced the amount of the aggregates, or/and the size of the aggregates, and for sure influenced the mobility of the matrix region.

Increasing the MDO amount from 9% to 21%, the glass transition temperature of the matrix polymer chains decreased. Further increasing the amount of MDO to 40%, the matrix polymer chains become more flexible. More ionic aggregates are supposed to generate, which in turn leads to an increase of the restriction of the matrix polymer chains. Therefore, a higher glass transition at 51^{o}C was observed for the matrix polymer chains.

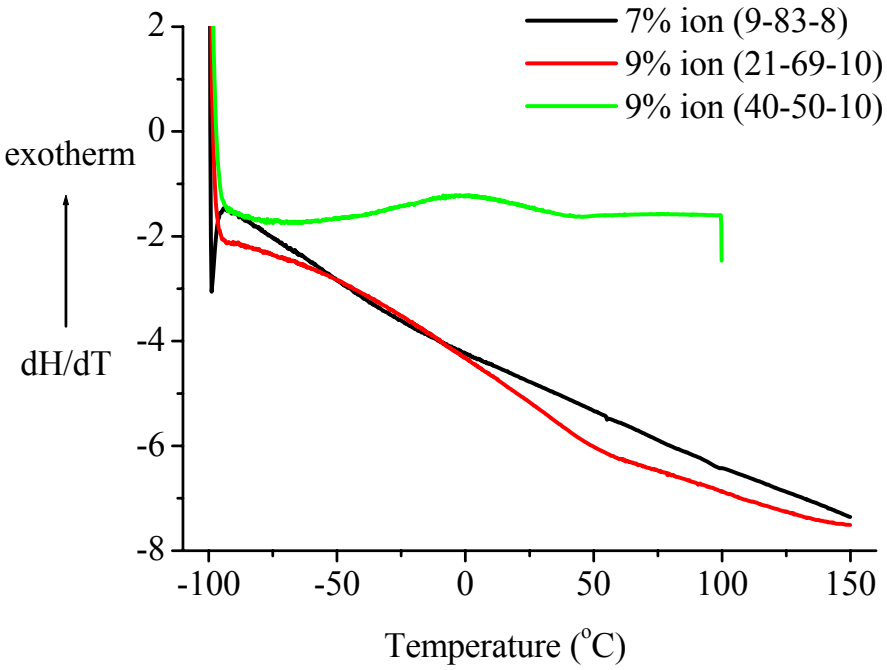

Fig 3.4.17. Differential Scanning Calorimetry (DSC) of P(MDO-MMA-DMAEMA)•BrC_2H_5, (9-83-8) is the terpolymer composition MDO : MMA : DMAEMA in molar ratio.

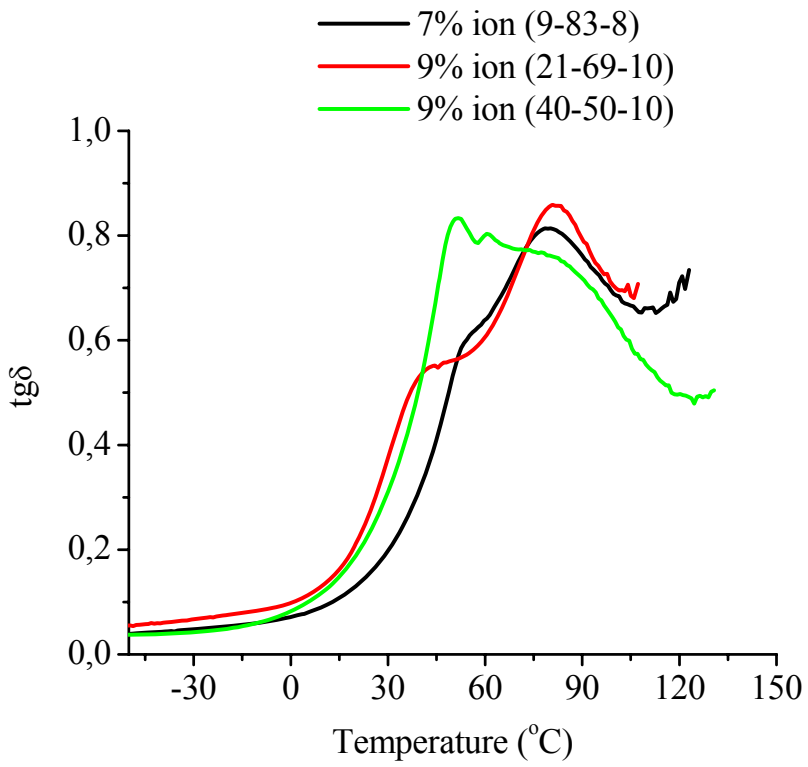

Fig 3.4.18. Loss tangent (tgδ) versus temperature for P(MDO-MMA-DMAEMA)•BrC_2H_5, (9-83-8) is the terpolymer composition of MDO : MMA : DMAEMA in molar ratio.

3.4.7. Morphology of polyelectrolytes P(DMAEMA•BrC_nH_{2n+1})

Chapter 3.4.4.1.4 has already shown that the higher ionic aggregates tend to dissociate into lower ones in ionomers quaternized by BrC_2H_5, which contain more than 27% ionic groups, due to the high dielectric constant of the whole polymers. The morphology of poly(DMAEMA•BrC_nH_{2n+1}) containing 100 mol% of ionic groups was further explored by SAXS analysis (Fig 3.4.19). Poly(DMAEMA•BrC_6H_{13}) does not generate scattering peak, therefore, ruling out the existence of ionic aggregates. While Poly(DMAEMA•$BrC_{12}H_{25}$) shows one scattering peak with a q value centered at 0.9 nm^{-1}, which indicates the existence of ionic aggregates in homopolyelectrolyte P(DMAEMA•$BrC_{12}H_{25}$) containing 100 mol% of ionic groups. The difference of the morphology between (DMAEMA•BrC_6H_{13}) and P(DMAEMA•$BrC_{12}H_{25}$) results from the different types of the alkyl groups, which lead to surroundings of ionic groups with different dielectric constants. The dielectric constant of the homopolyelectrolyte poly(DMAEMA•BrC_6H_{13}) has exceeded the limit for ionic association. The SAXS profiles of the well known polyelectrolyte poly(sodium methacrylate) P(NaMA) and neutral armorph poly(methyl methacrylate) P(MMA) as standard are also shown in Fig 3.4.20. Besides the primary beam, no ionic scattering peak was generated from both of the

polymers.

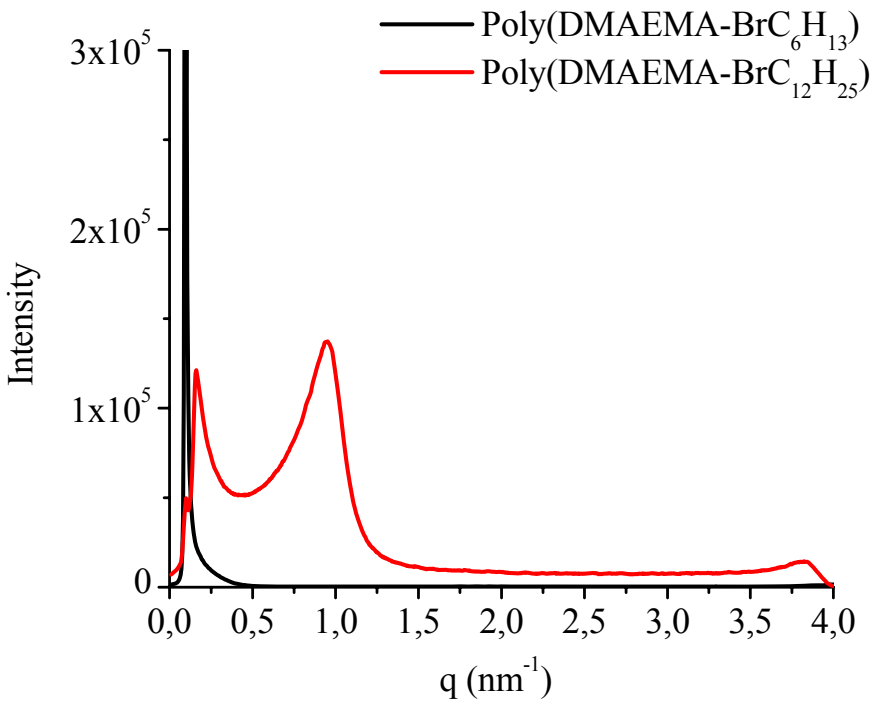

Fig 3.4.19. SAXS profile of different homo cationic polymers.

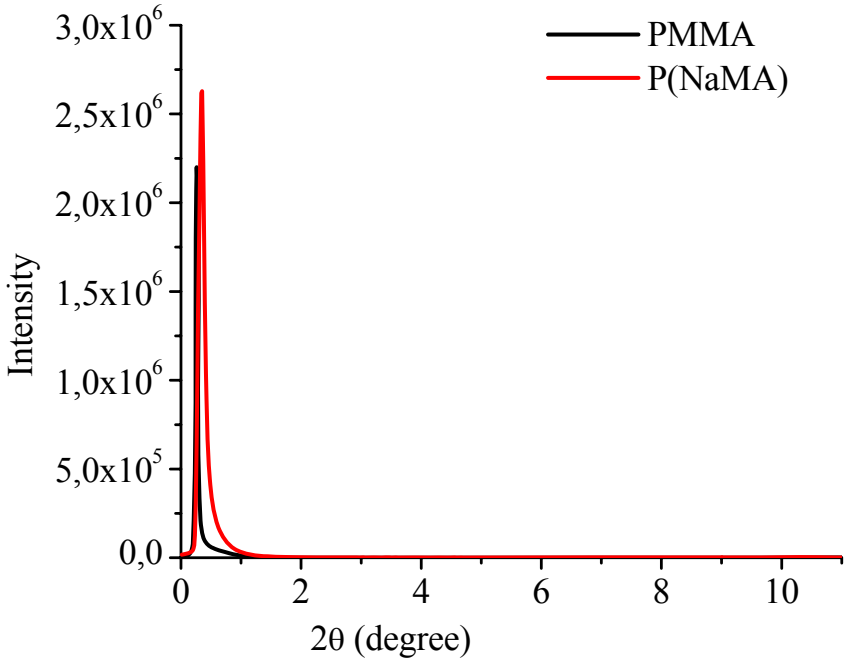

Fig 3.4.20. SAXS profile of PMMA and P(NaMA).

3.4.8. Mechanical properties of cationic ionomers

The tensile testing mechanical properties of ionomers with different types of ionic groups were measured by Instron (Table 3.4.6).

The ionic aggregates in ionomers quaternized with BrC_2H_5, which can show a separated glass transition, increase the Young's modulus and the maximum stress dramatically and decrease the elongation of the polymers. When increasing the amount of ion from 9% to 18%, the young's modulus increases and the elongation and the maximum stress does not change much considering the experimental errors. Supposing the ionic aggregates mainly act as fillers in the ionomers quaternized with BrC_2H_5, according to the equation for the filler systems $E^* = E(1+ 2.5V_f + 14.1V_f^2)$,[137] where E* stands for Young's modulus of filled system, E stands for Young's modulus of unfilled system and V_f stands for the volume fraction of the filler，it is possible to calculate the volume fraction of the ionic aggregates in ionomers (Table 3.4.6). Increasing the ionic amount from 9% to 18%, the calculated volume fraction of ionic aggregates increased from 47% to 61%. Ionomer with 27 mol% of ionic groups showed a decrease in the volume fraction of ionic aggregates from 61% to 40%, indicating the tendency of dissociation of ionic aggregates by high ionic amount for polymers quaternized with bromoethane.

The ionic aggregates in ionomers quaternized with $BrC_{12}H_{25}$, which are too small to show a separated glass transition, act more like a physical cross-linking and increase the elongation of the film. The filler theory does not fit this system well. The maximum stress and the modulus decrease when increasing the ionic content, while the elongation increases slightly. The ionomers quaternized with $BrC_{12}H_{25}$ tend to show the behavior of thermo-elastomers. After being stretched to 5 times of the original length, the ionomers shrink almost to the original size. However, different from the permanent chemical cross-linking, there is a possibility of collapse of the ionic aggregates under stress, which leads to the permanent shift of the polymer chains. Therefore, the ionomers could not shrink exactly to the original size.

Table 3.4.6. Mechanical properties of quaternized P(MDO-MMA-DMAEMA) containing 40% of MDO and different types of ionic groups; (40-50-10, 2) means polymer with MDO : MMA : DMAEMA = 40 : 50 : 20 in molar ratio quaternized with BrC_2H_5; V_f: volume fraction of ionic aggregates, calculated based on filler theory

Polymer	Max. STR (MPa)	Max. STN (mm/mm)	Modulus (MPa)	V_f (%)
(40-60-0), 0% ion	15.7	4.5	74.1	0
(40-50-10, 2), 9% ion	16.6	2.3	390.9	47
(40-40-20, 2), 18% ion	15.4	2.0	577.3	61
(40-30-30, 2), 27% ion	13.32	1.7	312.8	40
(40-50-10, 12), 7% ion	18.2	3.5	168.6	22
(40-40-20, 12), 12% ion	8.8	4.7	40.1	/
(40-30-30, 12), 21% ion	8.3	4.6	46.2	/

3.4.9. Polyelectrolyte behavior in polar solvent

Cation containing polymers P(MDO-MMA-DMAEMA)•$BrC_{12}H_{25}$ containing different mol% of ions were soluble in polar solvent N, N-dimethyl formamide (DMF). Fig 3.4.21 shows solution property of polymers in DMF. The reduced viscosity (η_{sp}/c) of non-ionic P(MDO-MMA-DMAEMA) decreases slightly with decreasing the concentration of polymer. While P(MDO-MMA-DMAEMA)•$BrC_{12}H_{25}$ containing small amount of ions, i.e. from 4.3% to 21%, showed an increase of reduced viscosity with decreasing the concentration of polymer, which is a typical characteristic of polyelectrolyte. It indicates that the pendent ions in P(MDO-MMA-DMAEMA)•$BrC_{12}H_{25}$ were delocalized in the polar solvent DMF. No ionic association could take place. Polymer chains with pendent ions repel each other and show polyelectrolyte behavior.

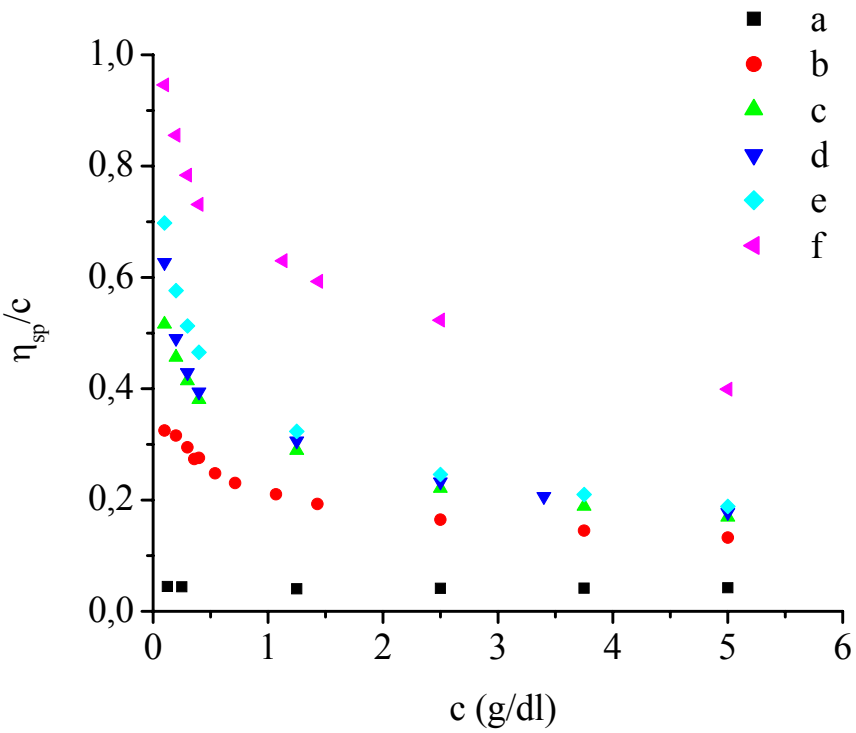

Fig 3.4.21. Reduced viscosity (η_{sp}/c) versus concentration of P(MDO-MMA-DMAEMA)•$BrC_{12}H_{25}$ in DMF; a: 0% ion (40-50-10); b: 4.3% ion (40-50-10); c: 7% of ion (40-50-10); d: 12% ion (40-40-20); e: 21% ion (40-30-30); f: P(DMAEMA •$BrC_{12}H_{25}$); (40-50-10) is the polymer composition MDO : MMA : DMAEMA in molar ratio.

3.4.10. Biodegradability

It has been reported by Agarwal et al. that Poly(MDO-co-MMA)s containing at least 40 mol% of ester group are degradable in compost.[138] Since polymers P(ester-co-DMAEMA)•$BrC_{12}H_{25}$ containing high amount of quaternary amine have been found to be antimicrobial in Chapter 3.3.7, the effect of small amount of quaternary amine on the biodegradability of P(MDO-MMA-DMAEMA)•$BrC_{12}H_{25}$ ionomers was also investigated. 0.1 mm thick ionomer P(MDO-MMA-DMAEMA)•$BrC_{12}H_{25}$ film containing 40 mol% of MDO and 12 mol% of ion was buried in compost under proper humidity at 60°C. Visible degradated holes were found out after 2 weeks, demonstrating the biodegradability of the ionomers (Fig 3.4.22). Further, antimicrobial testing was carried out for ionomers P(MDO-MMA-DMAEMA)•$BrC_{12}H_{25}$ containing up to 20 mol% of ion. After contact with ionomers, bacterial *E.coli* showed the same growth as that in the blank TS Broth in absence of polymer (Fig 3.4.23), indicating that ionomers containing up to 20 mol% of quaternary amine are not antimicrobial.

Fig 3.4.22. P(MDO-MMA-DMAEMA)•$BrC_{12}H_{25}$ containing 40 mol% of MDO and 12 mol% of ion, two weeks after buried in compost.

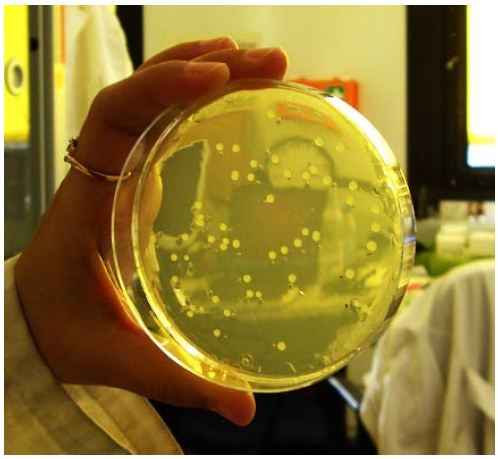

Fig 3.4.23. Bacterial *E.coli.* grows with contact with P(MDO-MMA-DMAEMA)•$BrC_{12}H_{25}$ containing 40 mol% of MDO and 20 mol% of ion.

3.4.11. Conclusion

Degradable ionomers P(MDO-MMA-DMAEMA)•BrC_nH_{2n+1} were synthesized by random radical terpolymerization of MDO, MMA and DMAEMA and subsequent quaternization. The strength of ionic association differs with different lengths of alkyl bromides. Ionomers quaternized with BrC_2H_5 generate ionic aggregates with a diameter around 30 nm, while ionomers quaternized with $BrC_{12}H_{25}$ only show very small aggregates with a diameter less than 5 nm. The higher ionic aggregates act in polymer rather as fillers to increase the Young's modulus dramatically while the small aggregates act rather as cross-linking to increase the elongation of polymers greatly. Ionomers with at least 40 mol% of MDO, up to 20 mol% of quaternary amine showed biodegradability in

compost. Polymers with small amount of quaternary amine do not show antimicrobial activity against Bacterial *E.coli.*

4. Experimental Part

4.1. Materials

azobisisobutyronitrile (AIBN)	Recrystallized from methanol
5,6-benzo-2-methylene-1,3-dioxepane (BMDO)	Synthesized in the laboratory according to our previously reported method.[9]
1-bromododecane	Acros, used after received
bromoethane	Acros, used after received
1-bromohexane	Acros, used after received
diethyl ether	BASF, distilled before use
dimethyl formamide (DMF)	BASF, distilled before use
di-tert-butyl peroxide (dtBp)	Aldrich, used as received
ethanol	BASF, distilled before use
hexane	BASF, distilled before use
methacrylic acid (MAA)	Acros, used after purification by distillation
methanol	BASF, distilled before use
2-methylene-1,3-dioxepane (MDO)	Used as received
methyl methacrylate (MMA)	BASF, distilled before use
methyl t-butyl ether	BASF, distilled before use
N-isopropylacrylamide (NIPAAm)	Acros, used as received
N, N-dimethylaminoethyl methacrylate (DMAEMA)	Acros, distilled before use
tetrahydrofuran (THF)	BASF, purified by distillation over potassium

4.2. Characterization

Contact angle measurement

The contact angle measurement was performed in the group of Prof. Dr. Joachim Wendorff in the Department of Macromolecular Chemistry at the Philipps-University Marburg with a Contact Angle measuring system G10 from Kruess equipped with a syringe (1ml) and a hypodermic needle (0.45 mm x 25 mm). One drop of water from the syringe was expressed onto the surface of the sample films to measure the contact angle.

Electrospinning

10-20 weight% (wt%) of quaternized poly(DMAEMA-co-ester)s in ethanol solution was prepared for electrospinning. The electrospinning setup was previously described in the literature.[139] The utilized electrical potential amounted to be 25 kV, the distance between the capillary and the substrate electrode was 20 cm, and the feed rate of the solution was 6 ml/h. The electrospinning was performed at 20^{o}C. The resulting fibers were collected on aluminum foils.

Elemental analysis

Elemental analysis was performed in the Department of Analytic Chemistry at the Philipps-University Marburg. The weight% of the carbon (C), hydrogen (H), nitrogen (N) and bromine (Br) element was given as result.

Gel permeation chromatography (GPC)

The molecular weights of P(NIPAAm-co-ester)s were measured by GPC at 25^{o}C equipped with 2 columns, PSS-SDV (linear,10 µm, 60 cm x 0.8 cm), a UV photometer, and a differential refractive index detector. THF was used as eluent at a flow rate of 0.8 ml/min. 200 µl of a solution containing ~1.0 mg/ml toluene was applied as internal standard. A poly(methyl methacrylate) conventional calibration was used.

The molecular weights of P(DMAEMA-co-ester)s were measured by GPC at 25 ^{o}C equipped with 3

linear columns, PSS-SDV (the size of the bead is 10 μm, the pore sizes of the beads are 10^6 Å, 10^4 Å and 10^3 Å respectively, the sizes of the columns are 0.8 cm x 60 cm, 0.8 cm x 60 cm and 0.8 cm x 30 cm, respectively), an UV photometer and a differential refractive index detector. Dimethylformamide (DMF) was used as eluent at a flow rate of 0.24 ml/min at 25°C. 200 μl of a solution containing ~1.0 mg/ml toluene was applied as internal standard. A poly(methyl methacrylate) conventional calibration was used.

Mechanical analysis

Dynamic Mechanical Analysis (DMA) was performed by Ping Hu in the group of Prof. Haoqing Hou in the Department of Macromolecular Chemistry at Jiangxi Normal University using a Perkin-Elmer Pyris diamond analyzer with a heating rate at 5 °C min^{-1} in nitrogen atmosphere. The applied frequency and amplitude were respectively 1 Hz and 20 μm. The storage modulus (E′), loss modulus (E″) and loss tangent (tan δ) of the polymer film were recorded in the temperature range from -100°C to 150°C.

The tensile testing was performed using Instron. The extension was applied at 30 cm/min at room temperature. The curve of stress versus strain was recorded.

Nuclear magnetic resonance (NMR)

1D and 2D NMR measurement was done in the NMR Department at the Philipps-University Marburg. ^{1}H (400.13 MHz) and ^{13}C (100.21 MHz) NMR spectra were recorded on a Bruker DRX-300 spectrometer. Tetramethylsilane (TMS) was used as an internal standard. ^{1}H-^{13}C correlation experiments were performed on a Bruker DRX-400 spectrometer. Typical experiment time was about 1.5 and 3.0 hrs for HMQC and HMBC, respectively.

Small angle X-ray scattering (SAXS)

SAXS measurement was performed by Dr. Dieter Schollmeyer in the Institute of Organic Chemistry at the University Mainz with a compact Kratky camera from Anton Paar and a detector PSD 50 from Firma Braun. The distance between the sample and the detector is 25 cm. The wave length of the primary X-ray beam is 0.3 nm. The scattering angle (2θ) was performed from 0° to 10°. The

average measuring time was set to be 1 hr. Sample films were wrapped with aluminum and measured at certain temperature. Besides the scattering peaks, most of the measurements generated one peak from the penetrated primary beam with q value around 0.1 nm^{-1}.

Spin coating

Spin coating of P(BMDO-co-DMAEMA)•$BrC_{12}H_{25}$ was carried in the group of Prof. Dr. Joachim Wendorff in the Department of Macromolecular Chemistry at the Philipps-University Marburg using a spin coater. Polymer sample was prepared with a concentration of 20 wt% in $CHCl_3$ and spin coated square glass plates. The spin rate was around 1000 rpm for 5-10 seconds. After spin-coating, the film was tried at room temperature for several hours before contact angle measurement.

Thermal analysis

Thermal analysis was done using Mettler thermal analyzers having 851 Thermogravimetric (TG) and 821 Differential Scanning Calorimetry (DSC) modules. DSC scans were recorded in nitrogen atmosphere at a heating rate of 10 ^{o}C/min. Thermal stability was determined by recording TG traces in nitrogen atmosphere (flow rate = 50 ml/min). A heating rate of 10^{o} C/min and sample size of 10±1 mg was used in each experiment.

Transmission electron microscopy (TEM)

TEM pictures were taken by Michael Hellwig and Dr. Andreas Schaper in the Electron Microscopy Lab with a high resolution-Transmission-Electron Microscope of Type JEM 3010 from Company JEOL equipped with a digital camera of 2000×2000 pixels under acceleration-voltage of 300 kV. The thin film of polymer was made first by solving ionomer in $CHCl_3$ with a dilute concentration, then dipping the TEM grid once fast in the solution, followed by drying the grid under air.

Turbidity test

LCSTs were determined by turbidity measurements by Oliver Happel in the group of Prof. Dr. Andreas Seubert in the Department of Analytic Chemistry at the Philipps-University Marburg. The turbidity test was performed with a UV spectrometer with a temperature controlling system. 1 mg of

polymer was dissolved in 10 ml of distilled water in an ice bath. The solution was than heated from around 0°C to 40°C at the rate of 1 K•min^{-1}. The percentage of transmission of UV light at 535 nm through the polymer solution/suspension was recorded.

4.3. Polymer film preparation

Sample films of P(MDO-MMA-DMAEAM)•BrC_2H_5 for SAXS, DMA and Tensile Testing were prepared by solvent casting. The residues of solvents were continuously dried in the vacuum oven for 2 days at room temperature before the measurements.

Sample films of P(MDO-MMA-DMAEMA)•$BrC_{12}H_{25}$ for SAXS, DMA, Tensile Testing and compostability testing were prepared by compression molding machine. Polymer samples were heated to around 110°C, compressed and then cooled down to room temperature.

4.4. Degradability test

Hydrolytic degradability

Hydrolytic degradability was tested in extreme basic conditions. Generally, 200 mg of copolymer was dissolved in a bottle containing 20 ml of 5% KOH in distilled water and was stirred for 24 hrs at room temperature. After this, 10 ml of 10% HCl was added. The mixture was extracted with chloroform, washed with water, and dried over Na_2SO_4. After filtration, the solvent was evaporated under reduced pressure. The remaining solid was dried in a vacuum oven at 40°C and analyzed by NMR and GPC further.

Biodegradability

Biodegradability was tested in compost material. Cationic ionomers film (10 cm x 2 cm x 0.1 mm) with at least 40 mol% of MDO and up to 20 mol% of quaternary amine were made by compression molding machine. Such polymer film was buried then in compost (BASF) containing proper humidity under 60°C for weeks/months. In between, small amount of water may be added to the soil in order to keep certain humidity. The appearance of holes in the polymer film indicates the biodegradation of polymers by a variety of micro-organisms in the compost.

4.5. Antibacterial test

Antibacterial activity of water insoluble quaternized poly(DMAEMA-co-ester) was evaluated by quantifying the viability of bacterial *Escherichia (E.) coli* after contact with polymer in Tryptic Soy Broth (TS Broth). Briefly, 2 mg Polymers were put into the sterile polypropylene tube. 1 mL of a solution containing approximately 5×10^5 cfu/mL of *E. coli* in TS Broth was then added. Negative control tube containing only *E.coli* inoculated in TS Broth was also prepared. The tubes were incubated at 37°C with shaking at 200 rpm for 18-20 hrs. After incubation, the mixture was well shaken before 100 µL of the solution was withdrawn and then diluted by sodium phosphate buffer (c = 50 mmol/L, pH = 7) by 1000 times. Aliquots from the final diluted solution, i.e. 100 µL/1ml, were then plated on LB agar plates and incubated at 37°C for 16-20 hrs. The colonies were quantified and compared according to CFU-method to evaluate the antibacterial activity of the quaterternized polymers.

4.6. Cytotoxicity determination by MTT Assay

Cytotoxicity test of P(MDO-co-DMAEMA)•BrC_2H_5 was done with the help of Prof. Dr. Thomas Kissel in the Department of Pharmaceutics at the Philipps-University Marburg.

Cell viability was evaluated using the MTT assay as described previously.[140] Briefly, L929 cells were seeded into 96-well microtiter plates (NunclonTM, Nunc, Germany) at a density of 8000 cells/well. After 24 hrs the culture medium was replaced with serial dilutions of polymer stock solutions in antibiotic-free DMEM (n = 8). After an incubation period of 24 hrs, 20 l MTT (Sigma, Deisenhofen, Germany) (5 mg/ml in PBS) were added. After an incubation time of 4 hrs unreacted dye was removed by aspiration and the purple formazan product was dissolved in 200 ml/well dimethylsulfoxide (Merck, Darmstadt, Germany) and quantified by a plate reader (Titertek Plus MS 212, ICN, Germany) at wavelengths of 570 and 690 nm.

The relative cell viability [%] related to control wells containing cell culture medium without polymer was calculated by absorbance test/absorbance control x 100. Poly(ethylene imine) 25 kDa (BASF, Germany), a water-soluble polycationic polymer whidely used as gene transfer reagent was used as a positive control. The IC_{50} was calculated as polymer concentration which inhibits growth

of 50% of cells relative to non treated control cells.[141] Data are presented as a mean of three measurements. IC_{50} was calculated using the Boltzman sigmoidal function from Microcal Origin® v 7.0 (OriginLab, Northampton, USA).

4.7. Synthesis and polymerization

4.7.1. Homo- and copolymerization of BMDO and NIPAAm

In general, all homo- and copolymerization reactions were carried out under argon in predried Schlenk tubes by free radical polymerizations. In a typical polymerization reaction, 4 mmol of BMDO, 4 mmol of NIPAAm, 2 mol-% of the initiator (dtBp), and 2 ml of the solvent (anisole) were polymerized in an oil bath at 120°C. After 8 hrs polymerization, the reaction mixture was dissolved in THF and precipitated in diethyl ether. Purification of the polymers was done by dissolving in THF and re-precipitation in diethyl ether. Drying of polymers was done in a vacuum oven at 40°C until a constant weight is attained. The conversion of the polymerization was estimated by gravimetry.

^{1}H-NMR(300 MHz, $CDCl_3$):

δ/ppm = 1.05(s, 24.4H, $(C\mathit{H}_3)_2CHNH$– von NIPAAm), 1.38-3.00(m, 16.4H), 3.57(s, 3.1H, $(CH_3)_2CHN\mathit{H}$– von NIPAAm), 3.92(s, 3.8H, $(CH_3)_2C\mathit{H}NH$– von NIPAAm), 5.01(s, 2H, –$COOC\mathit{H}_2C_6H_5$– von BMDO)

^{13}C-NMR （100 MHz, $CDCl_3$):

δ/ppm = 22.28(–$\mathit{C}H_3$ von NIPAAm), 26.99(–$COOCH_2C_6H_5\mathit{C}H_2$– von BMDO), 33.52(–$\mathit{C}H_2CH$– von NIPAAm), 34.98(–$\mathit{C}H_2COOCH_2C_6H_5$– von BMDO), 41.00(–$NH\mathit{C}H$– von NIPAAm), 42.18(–$CH_2\mathit{C}H$– von NIPAAm), 64.06(–$COO\mathit{C}H_2C_6H_5$– von BMDO), 124.95-141.59 (–$COOCH_2\mathit{C}_6H_5$– von BMDO), 171.82(–$\mathit{C}OOCH_2C_6H_5$– von BMDO), 174.22(–$\mathit{C}ONH$– von NIPAAm)

Various copolymers were made by changing the molar ratio of the two comonomers (NIPAAm and BMDO) in the feed. Details of characterization are given in Chapter 3.1.

4.7.2. Reaction of BMDO with MAA

4.7.2.1. At room temperature

In a representative example, two monomers BMDO and MAA in 1 : 1 molar ratio (BMDO (324 mg; 2mmol) and MAA (172 mg; 2 mmol)) are simply mixed under Argon without any initiator , in a predried Schlenk tube. The mixture was stirred at 25^{o}C for different intervals of time and analyzed as such without any purification, by 1D and 2D NMR techniques. The double bond of BMDO underwent electrophilic addition by acidic vinyl monomer MAA (PKa = 4.66) under study, generating a new vinyl monomer 3-methyl-1, 5-dihydrobenzo[e] [1, 3]dioxepin-3-yl methacrylate (A) keeping the seven membered ring of BMDO intact, as shown in the Scheme 4.2. The product obtained after 30 minutes, contained structure A and unreacted MAA in the molar ratio 99 : 1. This was determined from ^{1}H-NMR from the ratio of peak intensities at ppm 5.45-6.05 (2s, 2H, C*H*$_2$=C(CH$_3$)COO–) of structure A and ppm 10.89 (s, 1H, –COO*H*) from unreacted MAA.

^{1}H-NMR (300 MHz, $CDCl_3$):

δ/ppm = 1.82 (s, 3H, CH_2=C(C*H*$_3$)–), 1.84 (s, 3H, –(C*H*$_3$)C(OCH$_2$–)$_2$(OC(O)–), 4.60 – 4.97 (2d, 4H, –OC*H*$_2$C$_6$H$_4$C*H*$_2$O–), 5.45-6.05 (2s, 2H, C*H*$_2$=C(CH$_3$)COO–)，6.87-7.02 (2m, 4H, –OCH$_2$ C$_6$*H*$_4$CH$_2$O–), 10.89 (s, 1H, –COO*H*).

^{13}C-NMR (100 MHz, $CDCl_3$):

δ/ppm = 17.40 (CH_2=C(*C*H$_3$)–), 20.31 (–(*C*H$_3$)C(OCH$_2$)$_2$(OC(O)–), 64.62 (–O*C*H$_2$C$_6$H$_4$*C*H$_2$O–), 117.24 (–(CH$_3$)*C*(OCH$_2$)$_2$(OC(O)–)，125.16 (*C*H$_2$=C(CH$_3$)–), 125.47-136.21 (–OCH$_2$*C*$_6$H$_4$CH$_2$O–), 136.11 (CH_2=*C*(CH$_3$)–), 163.18 (–*C*OOCCH$_3$(OCH$_2$)$_2$O(C(O)), 169.55 (–*C*OOH).

The details of characterization part are given in the text and as Figs in Chapter 3.2.2.

4.7.2.2. At higher temperature

The resulting product of BMDO and MAA i.e. the new vinyl monomer A is heated at 120^{o}C for 15 minutes under Argon. The seven-membered ring of BMDO has the tendency to open up by rearrangement and a new ester group (structure B; 2-(acetoxymethyl)benzyl methacrylate) is formed as shown in the Scheme 4.3. The product was analyzed as such, without any purification,

using various NMR techniques. The product contained 92 mol% of structure B as determined from the ^{1}H-NMR spectrum.

^{1}H-NMR (400 MHz, $CDCl_3$):

δ/ppm = 1.84(s, 3H, CH_2=C(C*H*$_3$)–), 1.96(s, 3H, –$C_6H_4CH_2OCOCH_3$), 5.10 (s, 2H, –$C_6H_4CH_2$ $OCOCH_3$), 5.17(s, 2H, –$CH_2C_6H_4CH_2OCOCH_3$), 5.46-6.03(2s, 2H, C*H*$_2$=C(CH_3)–), 7.2-7.33 (2m, 4H, –$CH_2C_6H_4CH_2OCOCH_3$ + C*H*Cl_3).

^{13}C-NMR (100 MHz, $CDCl_3$):

δ/ppm = 18.07(CH_2=C(*C*H_3)–), 20.62(–$C_6H_4CH_2OCOCH_3$), 63.62(–$C_6H_4CH_2OCOCH_3$), 63.81 (–$CH_2C_6H_4CH_2OCOCH_3$), 125.73-135.90 (–$CH_2C_6H_4CH_2OCOCH_3$), 166.76 (CH_2=C(CH_3)*C*OO CH_2–), 170.46 (–$CH_2C_6H_4CH_2OCOCH_3$).

Other details of characterization of B are given in the text and as Figs in Chapter 3.2.2.

4.7.3. Copolymerization behavior of BMDO with methacrylic acid

In general, all homo- and copolymerization reactions were carried out under Argon in predried Schlenk tubes using free radical initiator (Di-tert-butyl peroxide (dtBp)). In a typical polymerization reaction, 649 mg (4 mmol) of BMDO and 344 mg (4 mmol) of methacrylic acid, 2 mol% of the total monomers of t-butyl peroxide initiator (dtBp) were placed in a Schlenk tube under Argon. The reaction was started by placing the reaction contents in a preheated oil bath at 120^{o}C. After 6 hrs of reaction time, the reaction mixture was diluted with DMF and precipitated in about 200 ml of diethyl ether. The polymers were purified by dissolving in DMF and reprecipitation in diethyl ether. The copolymers were dried in vacuum at 40^{o}C until constant weight. The product was obtained as white powder (655 mg; 66 %), intrinsic viscosity (0.34 dL/g; DMF; 25^{o}C), copolymer composition structure B : MAA 70 : 30 (molar ratio). The homo- and different copolymers of BMDO and MAA were made by changing the molar ratio of the two monomers in the feed, under similar reaction conditions as described above. The feed compositions, the yields and the copolymer compositions obtained by ^{1}H-NMR technique are shown here. Detailed characterisation is shown in Chapter 3.2.3.

4.7.4. Copolymerization of BMDO and DMAEMA

In general, all polymerization reactions were carried out under Argon in predried Schlenk tubes using free radical initiator AIBN. In a typical polymerization reaction, BMDO (811 mg, 5 mmol) and DMAEMA (790 mg, 5 mmol), in a molar ratio of 1 : 1 and 1 mol% of the total monomers of the initiator AIBN were placed in a Schlenk tube under Argon. Small residual O_2 was removed from the tube by once of the freeze-cooling-thaw cycle. Then the reaction was started by placing the reaction tube in a preheated oil bath at 70^{o}C. After 20 hrs polymerization, the reaction mixture was diluted with $CHCl_3$ and precipitated in about 200 ml of n-hexane. Purification of the polymers was done by dissolving in $CHCl_3$ and re-precipitation in n-hexane. The copolymers were dried in vacuum at 40^{o}C until constant weight. The microstructure of the polymer was characterized by 1D and 2D NMR techniques.

^{1}H-NMR (400 MHz, $CDCl_3$):

δ/ppm = 0.75-1.35(m, 12.6H, –CH_2–C(CH_3)– von DMAEMA), 1.58-2.06(m, 8.1H, –CH_2C– von DMAEMA), 2.08-2.27(m, 23.4H, –N(CH_3)$_2$ von DMAEMA), 2.34-2.85(m, 10.3H, –CH_2COOC$H_2$$C_6H_5$– von BMDO + –COOC$H_2CH_2$– von DMAEMA), 4.20(m, 7.5H, –COOCH_2CH_2– von DMAEMA), 4.99(m, 2H, –COOC$H_2$$C_6H_5$– von BMDO), 6.91-7.26(m, 5H, –C_6H_5– von BMDO + C$H$$Cl_3$)

^{13}C-NMR (100 MHz, $CDCl_3$):

δ/ppm = 17.53-21.76(–$C$$H_3$ von DMAEMA), 27.30(–COO$C$$H_2$$C_6H_5$– von BMDO), 35.28 (–$C$$H_2$COOC$H_2$$C_6H_5$– von BMDO), 44.30(–$C$$H_2$C– von DMAEMA), 45.69(-N($C$$H_3$)$_2$ von DMAEMA), 46.42(–CH_2C– von DMAEMA), 57.56(–COOC$H_2$$C$$H_2$– von DMAEMA), 62.78(–COO$C$$H_2CH_2$– von DMAEMA), 64.11(–COO$C$$H_2$$C_6H_5$– von BMDO), 126.37-140.82 (–C_6H_5– von BMDO), 169.13-172.29(–COO– von BMDO), 174.88-177.48(–COO– von DMAEMA)

Different copolymers of BMDO and DMAEMA were made by changing the molar ratio of the comonomers in the initial feeds under similar reaction conditions as described above. Details of characterization were given in Chapter 3.3.3

4.7.5. Copolymerization of MDO and DMAEMA

In general, all polymerization reactions were carried out under Argon in predried Schlenk tubes using free radical initiator AIBN. In a typical polymerization reaction, MDO (660 mg, 6 mmol) and DMAEMA (632 mg, 4 mmol), in a molar ratio of 6 : 4 and 1 mol% of the total monomers of the initiator AIBN were placed in a Schlenk tube under Argon. Small residual O_2 was removed from the tube by once of the freeze-cooling-thaw cycle. Then the reaction was started by placing the reaction tube in a preheated oil bath at 70°C. After 20 hrs polymerization, the reaction mixture was diluted with $CHCl_3$ and precipitated in about 200 ml of n-hexane. Purification of the polymers was done by dissolving in $CHCl_3$ and re-precipitation in n-hexane. The copolymers were dried in vacuum at 40°C until constant weight. The microstructure of the polymer was characterized by 1D NMR techniques. Details are given in Chapter 3.3.4.

^{1}H-NMR (400 MHz, $CDCl_3$):

δ/ppm = 2.22(m, –N(C*H*$_3$)$_2$ von DMAEMA + C*H*$_2$COO– von MDO), 2.50(m, –CH$_2$C*H*$_2$N– von DMAEMA), 4.01(m, –COOC*H*$_2$CH$_2$N– von DMAEMA), 4.12(m, –COOC*H*$_2$CH$_2$CH$_2$– von MDO).

4.7.6.Terpolymerization of MDO，MMA and DMAEMA

In general, all terpolymerization reactions were carried out under Argon in predried Schlenk tubes using free radical initiator AIBN. In a typical polymerization reaction, MDO (770 mg, 7 mmol), MMA (250 mg, 2.5 mmol) and DMAEMA (79 mg, 0.5 mmol) and 1mol% of the total monomers of the initiator AIBN were placed in a Schlenk tube under Argon. Small residual O_2 was removed from the tube by once of the freeze-cooling-thaw cycle. Then the reaction was started by placing the reaction tube in a preheated oil bath at 70°C. After 20 hrs polymerization, the reaction mixture was diluted with $CHCl_3$ and precipitated in about 200 ml of n-hexane. Purification of the polymers was done by dissolving in $CHCl_3$ and re-precipitation in n-hexane. The terpolymers were dried in vacuum at 40°C until constant weight. The microstructure of the terpolymer was characterized by ^{1}H-NMR techniques. Different terpolymers of MDO, MMA and DMAEMA were made by changing the molar ratio of the monomers in the initial feeds under similar reaction conditions as described above. Details are given in Chapter 3.4.2

4.7.7. Quaternization

4.7.7.1. Quaternization with $BrC_nH_{2n+1}(n\geq4)$

500 mg of the sample was well solved in 50 ml of chloroform at RT. Around 60 mmol of alkyl bromide (e.g.14 ml of 1-bromododecane or 8.5 ml of 1-bromohexane) was added to the mixture. Quaternization reaction underwent for 3 days under stirring and heating at 40^{o}C in the oil bad. After that, the product was separated by steam-evaporation and washing with n-hexane. Purification was done twice by dissolving the resulting ion-containing polymer in chloroform and re-precipitation in n-hexane. Quaternization degree was quantitatively measured by elemental analysis, by comparing the mol% of bromine and nitrogen. The results of quaternization of poly(BMDO-co-DMAEMA) are given in the text in Chapter 3.3.3. The results of quaternization of poly(MDO-co-DMAEMA) are given in the text in Chapter 3.3.5. The results of quaternization of poly(MDO-MMA-DMAEMA) are given in the text in Chapter 3.4.3. The quaternization conversion was quantitatively determined with elemental analysis by comparing the molar ratio of nitrogen (N) and bromine (Br) (conversion = mol% Br / mol% N).

4.7.7.2. Quaternization with $BrC_nH_{2n+1}(2\leq n<4)$

500 mg of the sample was well solved in 40 ml of chloroform at RT. Around 60 mmol of alkyl bromide (e.g. 4.5 ml of bromoethane) was added to the mixture. Quaternization reaction was carried on under stirring at room temperature. Once the mixture turned to cloudy after some reaction time, proper amount of methanol was added until the mixture became clear. After 3 days of reaction, the product was separated by steam-evaporation and washing with n-hexane. Purification was done twice by dissolving the resulting ion-containing polymer in the mixture of chloroform/methanol and re-precipitation in n-hexane. Quaternization degree was quantitatively measured by elemental analysis, by comparing the mol% of bromine and nitrogen. The results of quaternization of poly(BMDO-co-DMAEMA) are given in the text in Chapter 3.3.3. The results of quaternization of poly(MDO-co-DMAEMA) are given in the text in Chapter 3.3.5. The results of quaternization of poly(MDO-MMA-DMAEMA) are given in the text in Chapter 3.4.3. The quaternization conversion was quantitatively determined with elemental analysis by comparing the molar ratio of nitrogen (N) and bromine (Br) (conversion = mol% Br / mol% N).

5. Zusammenfassung

Die ringöffende radikalische Polymerisation von Cycloketenacetal führte zu einem Polyester, einer Klasse von abbaubaren Polymeren. Im Rahmen dieser Arbeit wurde die Bioabbaubarkeit mit unterschiedlichen Vinylpolymeren kombiniert, indem Cycloketenacetal mit einem Vinylmonomer radikalisch copolymerisiert wurde. Die neuen Materialien behielten zum Teil die Eigenschaften von beiden Polymeren bei oder zeigten neue Eigenschaften, abhaengig von der Copolymerzusammensetzung.

Zu Beginn wurden 5,6-Benzo-2-methylene-1,3-dioxepan (BMDO) und N-isopropylaminoacrylat (NIPAAm) radikalisch copolymerisiert. Die Copolymerisation von BMDO und NIPAAm führte zu einer 100%igen Ringöffnung des BMDO und einer statistischen Struktur des Copolymers – Poly(ester-co-NIPAAm) mit einem Molekulargewicht (M_n) von ca. 25,000. Der Einbau der Estergruppe in das PNIPAAm wurde durch 1D und 2D NMR Techniken gezeigt. Als Copolymerisationsparameter wurden $r_{BMDO} = 0.11$ and $r_{NIPAAm} = 7.31$ festgestellt. Die statistische Struktur zeigte kurze BMDO-Blöcke, die von langen NIPAAm Blöcke abgetrennt waren. Die Zusammensetzung der Copolymere mit einem unterschiedlichem Gehalt an Estergruppen konnte durch eine Änderung der initialen Eingabe von BMDO und NIPAAm kontrolliert werden. Die Thermosensitivitaet des neuen Copolymers – Poly(BMDO-co-NIPAAm) wurde ebenfalls untersucht. Copolymere mit bis zu 8 mol% BMDO lösen sich in Wasser bei niedriegen Tempe raturen und zeigten ein Unlöslichkeit in Wasser bei erhöhter Temperatur. Dieses Phänomen ist bekannt als „lower critical solution temperature“ (LCST). Ein Anteil von 4 mol% bis 8 mol% BMDO im Copolymer fürte zu einer ausreichenden hydrolytischen Abbaubarkeit der Copolymere – Poly(BMDO-co-NIPAAm), was durch GPC-Messungen bewiesen wurde.

Um wasserlösliche abbaubare Vinylpolymere herzustellen, wurde Cylcoketenacetal mit Methacrylsaeure (MAA) radikalisch copolymerisiert. Die Copolymerisation von BMDO und MAA folgte nicht dem erwarteten konventionelen Weg. Durch saeurekatalysierte Addition von MAA an die Doppelbindung des BMDO wurde ein neue Vinylmonomer (3-methyl-1, 5-dihydrobenzo[e] [1, 3]dioxepin-3-yl methacrylat, (A), gebildet. Das neue Monomer (A) mit einem siebenen Ring ging bei der hohen Polymerisierungstemperatur – 120^{o}C schnell eine Umlagerung ein, was zur Bildung eines anderen neuen Vinylmonomers (2-(acetoxymethyl)benzyl methacrylat, B) mit einer neuen

Estergruppe führte. Monomer B kann mit BMDO oder MAA in-situ copolymerisieren, dabei werden die neuen Copolymere Poly(B-co-MAA) oder Poly(B-co-BMDO) gebildet. Nicht nur MAA, sondern auch andere Brönsted Saeuren mit pKa < 18 können die Doppelbindung des BMDO protonieren.

Bei dem Ziel abbaubare ionische Vinylpolymere zu synthetisieren, wurden abbaubare kationische Vinylpolymere durch eine zweistufige Reaktion hergestellt. Zuerst wurde eine radikalische Copolymerisation von 5,6-benzol-2-methylene-1,3-dioxepan (BMDO) und N,N-dimethylaminöthyl methacrylat (DMAEMA) durchgeführt. Im zweiten Schritt wurde das Copolymer – Poly(BMDO-co-DMAEMA) mit Alkylbromid (BrC_nH_{2n+1}) quaternisiert. Die Copolymerisation von BMDO und DMAEMA führte zu einer 100%igen Ringöffnung des BMDO und einer statistischen Struktur des Copolymers – poly(ester-co-DMAEMA) mit einem Molekulargewicht (M_n) von ca. 15,000. Der Einbau der Estergruppe in das PDMAEMA wurde durch 1D und 2D NMR Techniken gezeigt. Als Copolymerisationsparameter wurden $r_{BMDO} = 0.14$ and $r_{NIPAAm} = 6.96$ festgestellt. Die statistische Struktur zeigte kurze BMDO-Blöck, die von langen DMAEMA Blöcke abgetrennt waren. Die Zusammensetzung der Copolymere mit einem unterschiedlichem Gehalt an Estergruppen konnte durch eine Änderung der initialen Eingabe von BMDO und DMAEMA kontrolliert werden. Die Quaternierungsgeschwindigkeit des poly(BMDO-co-DMAEMA) wurde durch die Reaktionszeit, die Copolymerzusammensetzung und die Länge des Alkylbromids stark beeinflusst. Durch Kontrolle der Copolymerzusammensetzung und des Quaternierungsverhaltens wurden neue kationischen Polymere mit unterschiedlicher Wasserlösichkeit, antibakteriellem Verhalten und Abbaubarkeit hergestellt.

In vorhergehenden Arbeiten wurde das bioabbaubare Copolymer – P(MDO-co-MMA) mit 40mol% MDO durch radikalische Polymerisation von MDO und MMA synthetisiert. Um die mechanischen Eigenschaften dieses bioabbaubaren Copolymers zu verbessern, wurde ein Ionomer, dessen Matrix Poly(MDO-co-MMA) ist, hergestellt. Zuerst wurden MDO, MMA und DMAEMA radikalisch terpolymerisiert. Die erfolgreiche Terpolymerisation wurde durch NMR- und GPC-Messungen bewiesen. Als Quaternierungsmaterial wurden Bromethan (BrC_2H_5) und Bromdodecan ($BrC_{12}H_{25}$) ausgewaehlt. Die Messungen der Small Angle X-ray Scattering (SAXS) und der Trans -missionselektronenmikroskopie (TEM) zeigten die ionischen Aggregate in einer neutralen

Polymermatrix. Dabei führten durch Bromdodecan quaternisierte Ionen zu einer schwächeren Assoziation zwischen ionischen Gruppen als durch Bromethan quaternisierte Ionen. Das durch Bromethan quaternisierte Ionomer zeigte c.a. 30 nm groβe ionische Aggregate, die einen eigenen Glassübergang zeigten und ehrer als Füllungsmaterial dienten. Im Gegensatz dazu zeigte das durch Bromdodecan quaternisierte Ionomer die ionische Aggregate mit einem Durchmesser von weniger als 5nm, die keinen eigenen Glassübergang zeigten und ehrer als physikalische Vernetzung in der Matrix dienten. Das Ionomer mit 40 mol% MDO, welches bis zum 20 mol% Ionen enthielt, zeigte keine antibakterielle Aktivitaet und ist immer noch komposterbar.

6. List of symbols and abbreviations

A	3-methyl-1, 5-dihydrobenzo[e] [1, 3] dioxepin-3-yl methacrylate
B	2-(acetoxymethyl)benzyl methacrylate
c	concentration
C	3-methyl-1,5-dihydrobenzo-[e][1,3]dioxepin-3-ol
CKA	cyclic ketene acetal
Copolym.Composition	copolymer composition
d	distance between clusters
D	2-(hydroxymethyl)benzyl acetate
DMA	dynamic mechanical analysis
DMAEMA	N, N-dimethylaminoethyl methacrylate
DMF	dimethyl formamide
DSC	differential scanning calorimetry
dtBp	di-tert-butyl peroxide
E′	storage modulus
E″	loss modulus
GPC	gel permeation chromatography
HMBC	heteronuclear multiple bond coherence
HMQC	heteronuclear multiple quantum coherence
LCST	lower critical solution temperature
MAA	methacrylic acid
MDO	2-methylene-1,3-dioxepane
MMA	methyl methacrylate
Mn	number-average molecular weight(g/mol)
NIPAAm	N-isopropylacrylamide
Pka	acidic association constant, -lg(Ka)
PBMDO	poly(5,6-benzo-2-methylene-1,3-dioxepane)
P(BMDO-co-B)	poly(5,6-benzo-2-methylene-1,3-dioxepane-co-2-(acetoxymethyl)benzyl methacrylate)

P(BMDO-co-NIPAAm)	poly(5,6-benzo-2-methylene-1,3-dioxepane-co- N-isopropylacrylamide)
P(BMDO-co-DMAEMA)	poly(5,6-benzo-2-methylene-1,3-dioxepane-co- N,N-dimethylaminoethyl methacrylate)
P(BMDO-co-DMAEMA) •BrC_nH_{2n+1}	quaternized poly(5,6-benzo-2-methylene-1,3-dioxepane-co-N,N-dimethylaminoethyl methacrylate) with alkyl bromide
PDI	polydispersity index
PDMAEMA	poly(N,N-dimethylaminoethyl methacrylate)
P(DMAEMA•$BrC_{12}H_{25}$)	
(PDMAEMA)•$BrC_{12}H_{25}$	quaternized poly(N,N-dimethylaminoethyl methacrylate) with 1-bromododecane
PMDO	poly(2-methylene-1,3-dioxepane)
P(MDO-MMA-DMAEMA)	poly(2-methylene-1,3-dioxepane-co-methyl methacrylate- co-N,N-dimethylaminoethyl methacrylate)
P(MDO-MMA-DMAEMA) •BrC_nH_{2n+1}	uaternary poly(2-methylene-1,3-dioxepane -co-methyl methacrylate-co-N,N-dimethylaminoethyl methacrylate) with alkyl bromide)
PMMA	poly(methyl methacrylate)
PNIPAAm	poly(N-isopropylacrylamide)
r	reactivity ratio
RI	reflective index
RT	room temperature
SAXS	small angle X-ray scattering
tan δ	loss tangent
TEM	transmission electron microscopy
TGA	thermogravimetric analysis
T_g	glass transition temperature
THF	tetrahydrofuran
$T_{5\%}$	5% thermo-degradation temperature
wt.%	weight percentage
η_{sp}	special viscosity
η_{sp}/c	reduced viscosity
$[\eta]$	Intrinsic viscosity

7. Literature

1. W. J. Bailey, Z. Ni, S. R. Wu, *Macromolecules* **1982**, 15, 711.

2. W. J. Bailey, S. R. Wu, Z. Ni, *Makromol. Chem.* **1982**, 183, 1913.

3. I. Cho, M. S. Gong, *J. Polym. Sci., Polym. Lett. Ed.* **1982**, 20, 361.

4. T. Endo, M. Okawara, W. J. Bailey, K. Azuma, K. Nate, H. Yokono, *J. Polym. Sci. Polym. Lett. Ed.* **1983**, 21, 373.

5. M. H. Acar, Y. Nambu, K. Yamamoto, T. Endo, *J. Polym. Sci. Polym. Chem.* **1989**, 27, 4441.

6. W. J. Bailey, Z. Ni, S. R. Wu, *J. Polym. Sci., Polym. Chem. Ed.* **1982**, 20, 3021.

7. Y. Liu, C. U. Pittman, *Journal of Polymer Science: Part A: Polymer Chemistry* **1997**, 35, 3655.

8. E. Klemm, T. Schulze, *Acta. Polym.* **1999**, 50, 1.

9. H. Wickel, S. Agarwal, *Macromolecules* **2003**, 36, 6152.

10. H.Tsuji, *Macromolecular Bioscience* **2005**, 5, 509.

11. E. Renard, V. Langlois, P. Guerin, *Corrosion Engineering, Science and Technology* **2007**, 42, 300.

12. G. Pitarresi, F. S. Palumbo, R. Calabrese, E. F. Craparo, G. Giammona, *Journal of Biomedical Materials Research, Part A* **2008**, 84A, 413.

13. K. Subramanian, *Journal of Macromolecular Science, Polymer Reviews* **2003**, C43, 323.

14. R. Narayan, C. A. Pettigrew, *ASTM Standardization news*, December **1999**, 36.

15. *[ASTM D 5510-94]* Standard Practice for Heat Aging of Oxidatively Degradable Plastics.

16. *[ASTM D 3826-98]* Practice for Determining Degradation End Point in Degradable Polyolefins Using a Tensile Test; *[ASTM D5071-99]* Standard Practice for Exposure of Photodegradable Plastics in a Xenon Arc Apparatus; *[ASTM D5208-91]* Standard Practice for Fluorescent Ultraviolet UV Exposure of Photodegradable Plastics.

17. *[ASTM D 6118]*Standard Test Method for Determining Hydrolytic Degradation of Plastic Materials in an Aqueous Solution.

18. *[ASTM D5988-96]* Standard Test Method for Determining Aerobic Biodegradation in Soil of Plastic Materials or Residual Plastic Materials After Composting; *[ASTM D5338-98]* Standard Test Method for Determining Aerobic Biodegradation of Plastic Materials Under Controlled Composting Conditions.

19. *[ASTM D6400-04]* Standard Specification for Compostable Plastics.

20. U. Edlund, A. C. Albertsson, *Advances in Polymer Science* **2001**, 157, 67 and the references therein.

21. C. C. Chu, in "*Surfaces and Interfaces for Biomaterials"* **2005**, pp585 and the references therein.

22. A. Liebmann-Vinson, M. Timmins, *PBM Series* **2003**, 2, 329 and the references therein.

23. J. Watanabe, H. Kotera, M. Akashi, *Macromolecules* **2007**, 40, 8731.

24. L. Erdmann, B. Macedo, K.E. Uhrich, *Biomaterials* **2000**, 21, 2507.

25. L. Erdmann, K.E. Uhrich, *Biomaterials* **2000**, 21, 1941.

26. U. Witt, T. Einig, M.Yamamoto, I.Kleeberg, W.-D.Deckwer, R.-J.Mueller, *Chemosphere* **2001**, 44, 289.

27. S. Zhang, H.Yu, X.Ge, R. Zhu, *Industrial & Engineering Chemistry Research* **2005**, 44, 1995.

28. M. Watanabe, F. Kawai, *Polymer Degradation and Stability* **2003**, 81, 393.

29. E. Baimuratov, D. S. Saidov, I. Yu. Kalontarov, *Polymer Degradation and Stability* **1993**, 39, 35.

30. H. Park, Eli M. Pearce, T. K. Kwei, *Macromolecules* **1990**, 23, 434.

31. Y. Y. Chien, Eli M. Pearce, T. K. Kwei, *Journal of Polymer Science, Part A: Polymer Chemistry* **1991**, 29, 849.

32. B. Mailhot, S. Morel, J. Gardette, *Polymer Degradation and Stability* **1998**, 62, 117.

33. M. Mochizuki, M. Hirami, *Polymers for Advanced Technologies* **1997**, 8, 203.

34. A. Lofgren , AC.Albertsson , Ph.Dubois, *Polymer reviews* **1995**, 35, 379.

35. O. Coulembier et al. *Prog. Polym. Sci.* **2006**, 31, 723.

36. Y. Tokiwa, T. Suzuki, *J. Appl. Polym. Sci.* **1981**, 26, 441.

37. M. J. Diamond, B. Freedman, J. A. Garibaldi, *J. A. Int. Biodeg. Bull.* **1975**, 11, 127.

38. R. D. Fields, F. Rodriguez, *in Proceedings of the Third International Biodegradation Symposium, J. M. Sharpley and A. M. Kaplan, eds., Applied Science* **1976**, pp 775.

39. M. M. Bitritto, J. P. Bell, G. M. Brenckle, S. J. Huang, J. R. Knox, *J. Appl. Polym. Sci. Appl. Polym. Symp.* **1979**, 35, 405.

40. K. Mukai, Y. Doi, Y. Sema, K. Tomita, *Biotech. Lett.* **1993**,15, 601.

41. S. J. Huang, Encycl. *Polym. Sci. Eng.* **1985**, 2, 220.

42. M. Mochizuki, M. Hirami, *Polymers for Advanced Technologies* **1997**, 8, 203.

43. Y. Tokiwa, T. Suzuki, *J. Appl. Polym. Sci.* **1981**, 26, 441.

44. U. Witt, R.-J. Mueller, et al, *J. Environ. Degrad.* **1995**, 3, 215.

45. U.Witt, et al, *J. Environ. Degrad.* **1996**, 4, 9.

46. U.Witt, et al, *J. Environ. Degrad.* **1997**, 5, 81.

47. U.Witt, et al, *Angewante Chemie* **1999**, 38, 1438.

48. T. Endo, W. J. Bailey, *J. Polym. Sci., Polym. Lett. Ed.* **1975**, 13, 193.

49. *"Ring-Opening Polymerization"*, Ed. T. Saegusa, E. Goethals, American Chemical Society, Washington, D. C., **1977**, p.38.

50. S. M. Mc Elvain, M. J. Curry, *J. Am. Chem. SOC.* **1948**, 70, 3781.

51. S. Jin, K. E. Gonsalves, *Macromolecules* **1997**, 30, 3104.

52. W. J. Bailey, T. Endo, B. Gapud, Y.-N. Lin, Z. Ni, C.-Y. Pan, S. E. Shaffer, S.-R. Wu, N. Yamazaki, K. Yonezawa, *J. Macromol. Sci., Chem.* **1984**, 21, 979.

53. W. J. Bailey, J. Gu, Y. Lin, Z. Zheng, L. L. Zhou, Makromol. *Chem., Macromol. Symp.* **1991**, 42,195.

54. B. Wu, R. Lenz, W. J. Bailey, *J. Environ. Polym. Degr.* **1998**, 6, 23.

55. L. M. Morris, T. P. Davis, R. P. Chaplin, *Polymer* **2001**, 42, 495.

56. S. Jin, K. E. Gonsalves, *Macromolecules* **1998**, 31, 1010.

57. J. E. Potts, R. A. Clendinning, W. B. Ackart, W. D. Niegisch, *Polym. Sci. Technol.* **1973**, 3, 61.

58. Y. Tokiwa, T. Suzuki, *Nature* **1977**, 270, 76.

59. G. E. Roberts, M. L. Coote, J. P. A. Heuts, L. M. Morris, T. P. Davis, T. Endo, Y. Naoto, K. Azuma, K. Nate, *Macromol. Chem.* **1985**, 186, 1543.

60. L. F. Sun, R. X. Zhuo, Z. L. Liu, *J. Polym. Sci. Polym. Chem.* **2003**, 41, 2898.

61. G. Odian, *Principles of Polymerization*, 3rd ed.; John Wiley & Sons: New York, **1991**, Chapter 3.

62. J. Y. Yuan, C. Y. Pan, *European Polym. J.* **2002**, 38, 1565.

63. Y. Liu, C.E. Keller, C.U. Pittman, *Journal of Polymer Science, Part A: Polymer Chemistry* **1997**, 35, 3707.

64. P. C. Zhu, C.U. Pittman, *Journal of Polymer Science, Part A: Polymer Chemistry* **1996**, 34, 73.

65. K. C. Khemani, F. Wudl, *J. Am. Chem. Soc.* **1989**, 111, 9124.

66. K. Khemani, S. Askari, F. Wudl, *Macromolecules* **1991**, 24, 2156.

67. R.F. Brady, Jr., *J. Macromol. Sci., Rev. Macromol. Chem. Phys.* **1992**, C32, 135.

68. R. J. Statz, *Polym. Prepr. Polym. Chem.* **1989**, 29, 435.

69. E. N. Drake, *Polym. Prepr. Polym. Chem.* **1994**, 35, 14.

70. J. R. Rogers, F. J. Randall, *Polym. Prepr. Polym. Chem.* **1989**, 29, 432.

71. A. Diaz, D. Fenzel-Alexander, D.C.Miller, D.Wollmann, A. Eisenberg, *J. Polym. Sci. C Polym. Lett.* **1990**, 28, 75.

72. R. P. Molitor, *U.S. Patent* **1974**, 3 819 768.

73. W. M. Jr. Risen, *In "Ionomers: Characterization, Theory, and Applications"* S. Schlick, Ed., CRC, Boca Raton, FL, **1996**, Chapter 12.

74. R. D. Lundberg, *in " Structure and Properties of Ionomers"*, M. Pineri, A. Eisenberg, Eds., NATO ASI Series C: Mathematical and Physical Sciences 198, Reidel: Dordrecht **1987**, pp. 429.

75. R.C. Portnoy, R. D. Lundberg, D.G. Peiffer, *Polym. Prepr. Polym. Chem.* **1989**, 29, 433.

76. R. D. Lundberg, *In " Structure and Properties of Ionomers"*, M. Pineri, A. Eisenberg, Eds., NATO ASI Series C: Mathematical and Physical Sciences 198, Reidel: Dordrecht **1987**, pp. 87.

77. A, Eisenberg, M. Rinaudo, *Polymer Bulletin* **1990**, 24, 671.
78. X. F. Zhang, A. Eisenberg, *Macromolecules* **1994**, 27, 1751.
79. G. Broze et al. *Macromolecules* **1982**, 15, 920.
80. J. Horrion, R. Jerome, P. Teyssie, *J. Polym. Sci. C Polym. Lett.* **1986**, 24, 69.
81. P. Vanhoorne, G. Van den Bossche, F. Fontaine, et al. *Macromolecules* **1994**, 27, 838.
82. J. L. Wu, Y. M. Wang, M. Hara, M. Granville, R. J. Jerome *Macromolecules* **1994**, 27, 1195.
83. J. Selb, Y. Gallot, *J. Polym. Sci. Polym. Lett. Ed.* **1975**, 13, 615.
84. D. Wollmann, C.E. Williams, A. Eisenberg, *J. Polym. Sci. Polym. Phys. Ed.* **1990**, 28, 1979.
85. A. Eisenberg, M. Navratil, *J. Polym. Sci. Polym. Lett.* **1972**, 10, 537.
86. J. S. Kim, R. J. Jackman, A. Eisenberg, *Macromolecules* **1994**, 27, 2789.
87. P. Smith, A. Eisenberg, *Macromolecules* **1994**, 27, 545.
88. E. P. Otocka, F. R. Eirich, *J. Polym. Sci. A-2* **1968**, 6, 921.
89. S. B. Vitta, E. P. Stahel, V. T. Stannett, *J. Macromol. Sci. Chem.* **1985**, A22, 579.
90. W. O. Kenyon, G. P. Wangh, *J. Polym.Sci.* **1958**, 32, 83.
91. B. Hird, A. Eisenberg, *J. Polym. Sci. A, Poly. Chem.* **1993**, 31,1377.
92. R. W. Lenz, "*Organic Chemistry of Synthetic High Polymers",* Interscience: New Year, **1967**.
93. R. A. Weiss, R. D. Lundberg, A. Werner, *J. Polym. Sci. Polym. Chem. Ed.* **1980**, 18, 3427.
94. S. Gauthier, A. Eisenberg, *Macromolecules* **1987**, 20, 760.
95. S. Gauthier, D. Duchesne, A. Eisenberg, Macromolecules **1987**, 20, 753.
96. J. P. Gouin, F. Bosse, D. Nguyen, A. Eisenberg, *Macromolecules* **1993**, 26, 7250.
97. B. Atthoff, F. Nederberg, J. Hilborn, T. Bowden, *Macromolecules* **2006***,* 39, 3907.
98. Y. Deng, Z. Yan, N. Yang, *Colloid and Polymer Science* **1999**, 277, 227.
99. J. A. Miller, K. K. S. Hwang, S. L. Cooper, *J. Macromol. Sci. Phys.* **1984**, B23, 153.
100. M. Hara, P. Jar, J. A. Sauer, *Macromolecules* **1990**, 23 , 4465.
101. X. D. Fan, C. G. Bazuin, *Macromolecules* **1995**, 28, 8209.
102. H. A. Al-Salah, K. C. Frisch, H. X. Xiao, J. A. Jr. McLean, *J. Polym. Sci. A Polym.Chem.* **1987**, 25, 2127.
103. T. Ravikumar et al. *Biomacromolecules* **2006**, 7, 2762.
104. K. A. Mauritz, *J. Macromol. Sci., Rev. Macromol. Chem. Phys.* **1988**, C28, 65.
105. F. C. Wilson, R. Longworth, D. J. Vaughan, *Polym. Prepr. Div. Polym.Chem.* **1968**, 9, 505.
106. B.W. Delf, W. J. MacKnight, *Macromolecules* **1969**, 2, 309.
107. C.L. Marx, D.F. Caulfield, S.L. Cooper, *Macromolecules* **1973**, 6, 344.
108. F. L. Binsbergen, G.F. Kroon, *Macromolecules* **1973**, 6, 145.
109. D. J. Yarusso, S.L. Cooper, *Macromolecules* **1983**, 16, 1871.

110. W. J. MacKnight, W. P. Taggart, R.S. Stein, *J. Polym. Sci. Symp.* **1974**, 45, 113.

111. E. J. Roche, R. S. Stein, T. P. Russell, W. J. MacKnight, *Journal of Polymer Science, Polymer Physics Edition* **1980**, 18, 1497.

112. A. Eisenberg, B. Hird, R. B. Moore, *Macromolecules* **1990**, 23, 4098.

113. A. Eisenberg, *Macromolecules* **1970**, 3, 147.

114. A. Eisenberg, J.S. Kim, *in "Introduction to Ionomers"* **1998**, Chapter 3, pp 38.

115. A. Eisenberg, H. Farb, L.G. Cool, *J. Polym. Sci. A-2* **1966**, 4, 855.

116. A. Eisenberg, J.S. Kim, *in "Introduction to Ionomers"* **1998**, Chapter 3, pp 39.

117. A. Eisenberg, J.S. Kim, *in "Introduction to Ionomers"* **1998**, Chapter 3, pp 47.

118. M. Heskins, J.E. Guillet, J. E. *J. Macromol. Sci., Part A* **1968**, 2, 1441.

119. M. Hales, C.B. Kowollik, T. P. Davis, M.H. Stenzel *Langmuir* **2004**, 20, 10809.

120. (a) A. S. Hoffman, *J. Controlled Release* **1986**, 4, 213; (b) T. Okano, Y. H. Bae, S. W. Kim, *J. Controlled Release* **1990**, 11, 255; (c) X. S. Wu, A. S. Hoffman, P. Yager, *J. Intelligent Mater. Sysr. Srruct.* **1993**, 4, 202.

121. (a) H. Feil, Y. H. Bae, J. Feijen, S. W. Kim, J. Membr. Sci. **1991**, 64, 283; (b) I. Y. Galaev, B. Mattiasson, *Enzyme Microb. Technol.* **1993**, 15, 354.

122. H. G. Schild, *Prog. Polym. Sci*. **1992**, 17, 163.

123. H. Feil, Y. H. Bae, J. Feijen, S. W. Kim, *Macromolecules* **1993**, 26, 2496.

124. Y. Weng, Y. Ding, G. Zhang, *J. Phys. Chem. B* **2006**, 110, 11813.

125. H. Wickel, S. Agarwal, A. Greiner, *Macromolecules* **2003**, 36, 2397.

126. F. Zeng, Z. Tong, *Polymer* **1997**, 38, 5539.

127. T. Kelen, F. Tüdõds, *J. Macromol. Sci.-Chem.* **1975**, A9, 1.

128. H. G. Schild, D. A. Tirrell, *J. Phys. Chem.* **1990**, 94, 4352.

129. S. Fujishige, K. Kubota, I. Ando, *J. Phys. Chem.* **1989**, 93, 3311.

130. R. S. Fernandes, G. Gonzalez, E. F. Lucas, *Colloid Polym. Sci.* **2005**, 283, 375.

131. (a) E. R. Kenawy, Y. A. G. Malmoud, *Macromol. Biosci.* **2003**, 3, 107; (b) I. Cakmuk, Z. Ulukanli, M. Tuzcu, S. Karabuga, K. Genctav, *Eur. Polym. J.* **2004**, 40, 2373; (c) J. C. Grunian, J. K. Choi, A. Lin, *Biomacromolecules* **2005**, 6, 1149.

132. S. C. Smedt, J. Demeester, W. E. Hennink, *Pharm. Res.* **2000**, 17,113.

133. B. Dizman, M. O. Elasri, L. J. Mathias, *Polymer Preprints* **2005**, 46, 562.

134. S.Agarwal, *Polymer Journal* **2007**, 39, 163.

135. I. M. Hodge, A. Eisenberg, *Macromolecules*, **1978**, 11, 289.

136. E. D. Andreeva, V. N. Nikitin, Yu. M. Bovartchuk. *Macromolecules* **1976**, 9, 238.

137. Guth, E. J. Appl. Phys. **1945**, 16, 20.
138. S. Agarwal, *Makromolekulares Kolloquium **2007** in Freiburg,* "New class of degradable vinyl polymers poly: synthetic strategies and properties evaluation".
139. M. Bognitzki, H. Hou, M. Ishaque, T. Frese, M. Hellwig, C. Schwarte, et al. *Adv Mater* **2000**, 12, 637.
140. D. Fischer, T. Bieber, Y. Li, H. P. Elsasser, T. Kissel, *Pharm. Res.* **1999**, 16, 1273-1279.
141. T. Minko, P. Kopeckova, V. Pozharov, J. Kopecek. *J Control Release* **1998**, 54, 223.